ISSN 1007-9327 (print)
ISSN 2219-2840 (online)

World Journal of *Gastroenterology*

World J Gastroenterol 2023 March 7; 29(9): 1395-1538

Published by Baishideng Publishing Group Inc

World Journal of Gastroenterology

Contents

Weekly Volume 29 Number 9 March 7, 2023

Contents

ABOUT COVER

AIMS AND SCOPE

The primary aim of *World Journal of Gastroenterology* (*WJG*, *World J Gastroenterol*) is to provide scholars and readers from various fields of gastroenterology and hepatology with a platform to publish high-quality basic and clinical research articles and communicate their research findings online. *WJG* mainly publishes articles reporting research results and findings obtained in the field of gastroenterology and hepatology and covering a wide range of topics including gastroenterology, hepatology, gastrointestinal endoscopy, gastrointestinal surgery, gastrointestinal oncology, and pediatric gastroenterology.

INDEXING/ABSTRACTING

The *WJG* is now abstracted and indexed in Science Citation Index Expanded (SCIE, also known as SciSearch®), Current Contents/Clinical Medicine, Journal Citation Reports, Index Medicus, MEDLINE, PubMed, PubMed Central, Scopus, Reference Citation Analysis, China National Knowledge Infrastructure, China Science and Technology Journal Database, and Superstar Journals Database. The 2022 edition of Journal Citation Reports® cites the 2021 impact factor (IF) for *WJG* as 5.374; IF without journal self cites: 5.187; 5-year IF: 5.715; Journal Citation Indicator: 0.84; Ranking: 31 among 93 journals in gastroenterology and hepatology; and Quartile category: Q2. The *WJG*'s CiteScore for 2021 is 8.1 and Scopus CiteScore rank 2021: Gastroenterology is 18/149.

RESPONSIBLE EDITORS FOR THIS ISSUE

Production Editor: *Ying-Yi Yuan*; **Production Department Director:** *Xiang Li*; **Editorial Office Director:** *Jia-Ru Fan.*

NAME OF JOURNAL
World Journal of Gastroenterology

ISSN
ISSN 1007-9327 (print) ISSN 2219-2840 (online)

LAUNCH DATE
October 1, 1995

FREQUENCY
Weekly

EDITORS-IN-CHIEF
Andrzej S Tarnawski

EDITORIAL BOARD MEMBERS
http://www.wjgnet.com/1007-9327/editorialboard.htm

PUBLICATION DATE
March 7, 2023

INSTRUCTIONS TO AUTHORS
https://www.wjgnet.com/bpg/gerinfo/204

GUIDELINES FOR ETHICS DOCUMENTS
https://www.wjgnet.com/bpg/GerInfo/287

GUIDELINES FOR NON-NATIVE SPEAKERS OF ENGLISH
https://www.wjgnet.com/bpg/gerinfo/240

PUBLICATION ETHICS
https://www.wjgnet.com/bpg/GerInfo/288

PUBLICATION MISCONDUCT
https://www.wjgnet.com/bpg/gerinfo/208

ARTICLE PROCESSING CHARGE
https://www.wjgnet.com/bpg/gerinfo/242

STEPS FOR SUBMITTING MANUSCRIPTS
https://www.wjgnet.com/bpg/GerInfo/239

ONLINE SUBMISSION
https://www.f6publishing.com

World Journal of Gastroenterology

Submit a Manuscript: https://www.f6publishing.com

World J Gastroenterol 2023 March 7; 29(9): 1395-1426

DOI: 10.3748/wjg.v29.i9.1395

ISSN 1007-9327 (print) ISSN 2219-2840 (online)

REVIEW

Molecular mechanisms targeting drug-resistance and metastasis in colorectal cancer: Updates and beyond

Samar Al Bitar, Marwan El-Sabban, Samer Doughan, Wassim Abou-Kheir

Specialty type: Gastroenterology and hepatology

Provenance and peer review: Invited article; Externally peer reviewed.

Peer-review model: Single blind

Peer-review report's scientific quality classification

Grade A (Excellent): 0
Grade B (Very good): B
Grade C (Good): C
Grade D (Fair): D
Grade E (Poor): 0

P-Reviewer: Cheng H, China; Luo Y, China; Peng XC, China

Received: September 13, 2022
Peer-review started: September 13, 2022
First decision: September 29, 2022
Revised: October 12, 2022
Accepted: November 16, 2022
Article in press: November 16, 2022
Published online: March 7, 2023

Samar Al Bitar, Marwan El-Sabban, Wassim Abou-Kheir, Department of Anatomy, Cell Biology and Physiological Sciences, American University of Beirut, Beirut 1107-2020, Lebanon

Samer Doughan, Department of Surgery, American University of Beirut Medical Center, Beirut 1107-2020, Lebanon

Corresponding author: Wassim Abou-Kheir, MSc, PhD, Associate Professor, Department of Anatomy, Cell Biology and Physiological Sciences, American University of Beirut, Bliss St, Beirut 1107-2020, Lebanon. wa12@aub.edu.lb

Abstract

Colorectal cancer (CRC) is the third most diagnosed malignancy and a major leading cause of cancer-related deaths worldwide. Despite advances in therapeutic regimens, the number of patients presenting with metastatic CRC (mCRC) is increasing due to resistance to therapy, conferred by a small population of cancer cells, known as cancer stem cells. Targeted therapies have been highly successful in prolonging the overall survival of patients with mCRC. Agents are being developed to target key molecules involved in drug-resistance and metastasis of CRC, and these include vascular endothelial growth factor, epidermal growth factor receptor, human epidermal growth factor receptor-2, mitogen-activated extracellular signal-regulated kinase, in addition to immune checkpoints. Currently, there are several ongoing clinical trials of newly developed targeted agents, which have shown considerable clinical efficacy and have improved the prognosis of patients who do not benefit from conventional chemotherapy. In this review, we highlight recent developments in the use of existing and novel targeted agents against drug-resistant CRC and mCRC. Furthermore, we discuss limitations and challenges associated with targeted therapy and strategies to combat intrinsic and acquired resistance to these therapies, in addition to the importance of implementing better preclinical models and the application of personalized therapy based on predictive biomarkers for treatment selection.

Key Words: Colorectal cancer; Metastatic colorectal cancer; Targeted therapy; Drug-resistance; Personalized medicine

Core Tip: Efforts in cancer research has yielded significant advances in our understanding of the molecular mechanisms underlying colorectal cancer (CRC) resistance and metastasis. Therapeutic strategies centered on targeted molecules involved in CRC progression have been shown to be highly promising in overcoming resistance to conventional treatments. Targeted agents are currently being evaluated in preclinical and clinical studies to identify novel pharmacological targets and to study the efficacy of personalized medicine-based approaches.

Citation: Al Bitar S, El-Sabban M, Doughan S, Abou-Kheir W. Molecular mechanisms targeting drug-resistance and metastasis in colorectal cancer: Updates and beyond. *World J Gastroenterol* 2023; 29(9): 1395-1426
URL: https://www.wjgnet.com/1007-9327/full/v29/i9/1395.htm
DOI: https://dx.doi.org/10.3748/wjg.v29.i9.1395

INTRODUCTION

Colorectal cancer (CRC) is among the most prevalent malignancies in the world and the third most frequent cause of cancer-related death in the US and Europe[1,2]. Estimates from the American Cancer Society indicate that over 100000 new cases of CRC will be diagnosed in 2022 in the US and 53000 deaths will result from CRC in the same year. In addition to the increased incidence of CRC, the number of patients presenting with advanced, metastatic CRC (mCRC) is increasing[3]. In fact, it has been estimated that 25% of CRC patients have mCRC at the time of diagnosis and 50% of patients subsequently develop mCRC[4].

Lifestyle factors are thought to be a major factor in the increased incidence of CRC, and they include unhealthy diet, lack of physical activity, smoking, and alcohol consumption[3]. Other factors include heredity and family history which contribute to 30% of cases and genetic mutations and variations which contribute to 10% of cases[3]. It is important for health care providers and individuals to understand the causes and risk factors of CRC, in addition to the prevention strategies that could reduce the incidence. Screening can reduce CRC incidence and death through early detection and treatment of disease[3]. Colonoscopy is the standard screening method for CRC[5]. Other imaging-based tests are also available and include computed tomography colonography, colon capsule, and flexible sigmoidoscopy. In addition, screening modalities include stool-based tests, such as fecal immunochemical testing and the multitarget stool DNA test[5].

Conventional therapy for CRC includes surgery, chemotherapy, and radiotherapy[6]. 5-fluorouracil (5-FU) is the standard treatment for mCRC. It is now being combined with other chemotherapeutic drugs to improve patient survival. 5-FU, leucovorin, and irinotecan (FOLFIRI), 5-FU, leucovorin, oxaliplatin, and irinotecan, and 5-FU, oxaliplatin, and leucovorin (FOLFOX4) have been used as multidrug chemotherapy regimens. Although these treatment strategies have improved overall survival (OS), intrinsic and acquired resistance has been a major limitation in the effectiveness of these treatments in 90% of patients with mCRC[6]. Innate resistance is usually noted during early treatment or in early clinical trials. Acquired resistance may occur through different molecular mechanisms, and is specific to each therapy; however, acquired resistance to one drug sometimes results in resistance to other drugs with the same or different mechanism of action. This is known as multidrug resistance and is responsible for multiple cross-resistance towards different drugs[7].

Chemotherapy targets rapidly dividing cells by blocking DNA replication or tubulin assembly, and thus is not specific to cancer cells and is associated with toxicity to healthy tissues[8]. In the last 15 years, major attempts have been made to develop targeted or biological therapies that kill cancer cells by targeting specific pathways implicated in tumor growth. Targeted therapies against cancer cells include mainly monoclonal antibodies (mAbs) that bind membrane growth factor receptors or their ligands, and small molecules that cross the cell membrane and inhibit cell growth and survival[9].

With the development and advancement of next generation sequencing (NGS) and omics technologies[10], it has been possible to determine molecular mechanisms underlying resistance and to develop new strategies to overcome this resistance. Over the past decade, new discoveries in the field of CRC led to the introduction of targeted therapies in clinical practice, which resulted in significant therapeutic efficacy and prolonged survival. New drugs whose action is directed at specific pathways implicated in CRC pathogenesis, including the epidermal growth factor receptor (EGFR) pathway, have been tested in preclinical models and in clinical trials. Yet, the best combination of standard chemotherapy and targeted therapy for the first-line treatment of mCRC has been debated for several years.

Understanding the mechanisms of acquired drug resistance to targeted therapies is critical for the development of novel and effective treatment combinations and will help guide future therapies. In this article, we review mechanisms of resistance to conventional therapy, we discuss the efficacy of novel targeted therapies against drug-resistant and mCRC and challenges associated with them, in addition to

strategies to overcome resistance to targeted therapy. We conclude by highlighting lessons learned from molecular studies and their clinical relevance, as well as the importance of employing novel preclinical models to facilitate the development of effective targeted therapy.

RESISTANCE TO THERAPY

Resistance to conventional treatment is one of the most challenging problems in cancer therapy, resulting in poor prognosis, recurrence, and metastasis. It is attributed to several intrinsic and acquired factors in tumor cells and in the microenvironment they reside in.

Cancer stem cells

CRC treatment requires surgical intervention, which is accompanied by the application of chemotherapy or radiotherapy, before or after surgery, as neoadjuvant or adjuvant treatment to ensure maximum reduction of tumor size[11]. These treatments are effective against cancer cells but spare the more resistant cancer stem cells (CSCs). Mechanisms of resistance are still unclear, but several factors are known to contribute to it. For example, CSCs are quiescent and do not enter the cell cycle, therefore they are not targeted by conventional therapy that kills highly proliferating cells[12]. Different molecular mechanisms are involved in CRC drug-resistance[13], as shown in Figure 1, and are summarized in this paper.

CSCs express high levels of ATP-binding cassette (ABC) transporters that mediate drug efflux and resistance to chemotherapy[14,15]. The first identified ABC member is ABCB1 or P-glycoprotein, which is expressed in normal intestinal cells. The overexpression of ABCB1 has been reported in preclinical and clinical studies of CRC and is associated with resistance to chemotherapy[16,17]. First-, second-, and third-generation inhibitors have been designed against ABCB1 and have been shown to have high affinity; however, their effectiveness is limited and needs further improvement[18]. Other ABC members include ABCC6, ABCC11, ABCF1, and ABCF2 and their upregulation has been documented in CRC tumor tissues[19], suggesting that these transporters may serve as potential targets for reversing drug-resistance in CRC.

The anti-cancer effect of chemotherapeutic drugs can be reduced by impaired drug metabolism. Capecitabine is a chemotherapeutic agent used for the treatment of mCRC. Upon administration, it is converted into 5-FU by thymidine phosphorylase (TP)[20]. It has been shown that methylation of the gene encoding TP inhibits its translation and results in resistance to capecitabine[20]. 5-FU acts by inhibiting thymidylate synthase and incorporating its metabolites into DNA and RNA[21]. Several enzymes, such as orotate phosphoribosyl-transferase and uridine monophosphate synthetase, mediate the conversion of 5-FU into its active metabolites[22]. Interestingly, lower expression of these enzymes is associated with resistance to 5-FU in CRC[23]. Additionally, TP converts 5-FU into 5-fluoro-2′ deoxyuridine and it has been shown to predict good response to 5-FU treatment and is associated with higher progression-free survival (PFS) in patients with high expression of TP[24]. Another enzyme that has been reported to affect response to chemotherapy is carboxylesterase 2. This metabolic enzyme plays a major role in the activation of irinotecan and its high expression and activity improves the efficacy of irinotecan[25]. On the other hand, uridine diphosphate glucuronosyltransferase 1A1 and β-glucuronidase inactivate irinotecan, and their alteration results in reduced irinotecan activity, suggesting that targeting these enzymes may reverse resistance to irinotecan[26,27]. Similarly, dihydropyrimidine dehydrogenase is a metabolic enzyme that mediates the catabolism of 5-FU to its inactive metabolite, and its high expression has been associated with resistance to 5-FU in CRC[28,29].

In cancers, including CRC, the DNA damage response (DDR) is activated and aberrant. This damage response consists of several kinase-dependent signaling pathways and is important for maintaining genome integrity and stability. Damage sensing is usually mediated by DDR sensors, followed by transduction of damage signals to DDR mediators and downstream molecules, leading to either cell cycle arrest, DNA damage repair, or apoptosis[30]. Ataxia telangiectasia mutated and ATM and Rad3-related protein, members of the phosphatidyl-inositol 3-kinase (PI3K) like family of protein kinases, are the main regulators of DDR. They interact with p53 and checkpoint pathways that regulate Cdc25[31]. Several mechanisms attribute to resistance of CSCs to DNA damage and include cell cycle checkpoint alteration and activation of an efficient scavenging system that protects against reactive oxygen species (ROS), which are induced by therapy[32]. Three main pathways that contribute to CRC development are unsensed or repaired by the aberrant DDR. These pathways are chromosomal instability (CIN), CpG island hypermethylation phenotype, and microsatellite instability (MSI) pathways. CIN is common in 80% of CRC cases while MSI results from inactivation of mismatch repair genes (MMR) and is common in sporadic CRC[33]. Notably, DNA repair induced by oxaliplatin is mainly mediated by the nucleotide excision repair pathway[34]. The upregulation of excision repair cross-complementing 1 has been linked to oxaliplatin resistance in CRC[34] and its mRNA expression level is a predictive marker of survival in patients treated with 5-FU and oxaliplatin[35]. These results suggest that the expression levels of DNA repair proteins may serve as treatment response biomarkers, and the reduction of their expression can enhance the effect of DNA-damaging agents, leading to eradication of resistant CSCs.

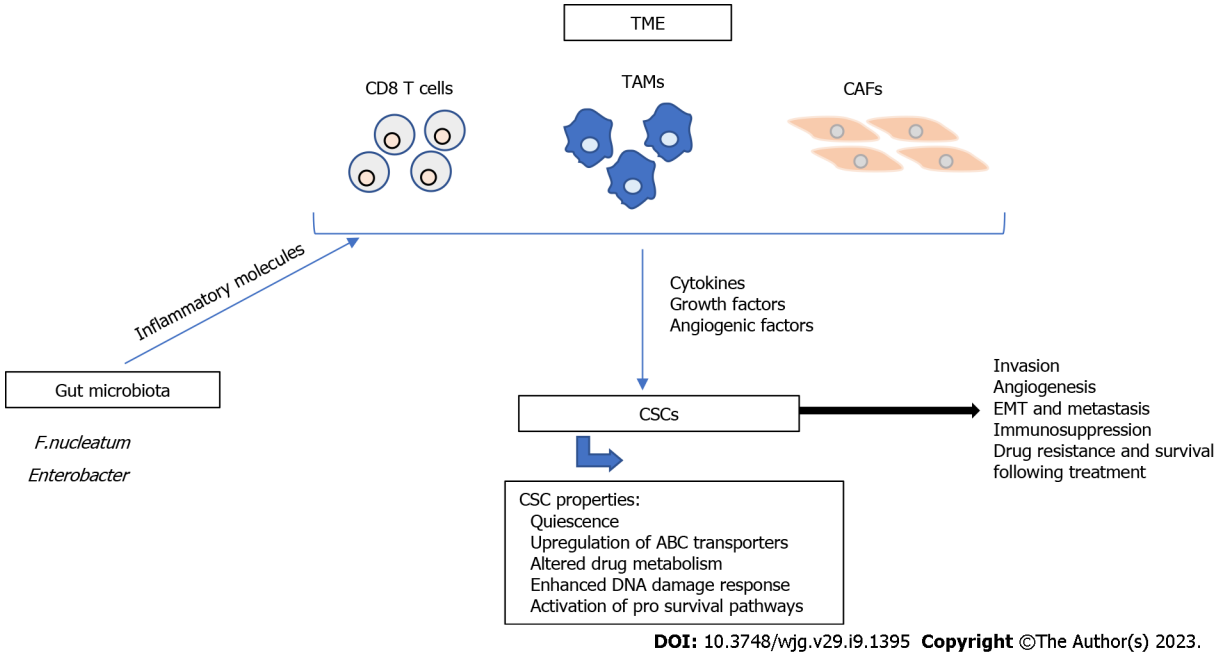

DOI: 10.3748/wjg.v29.i9.1395

Figure 1 Major mechanisms of cancer stem cell resistance. Cancer stem cell (CSC) resistance has been associated with CSC characteristics including quiescence, upregulation of ATP-binding cassette transporters, altered drug metabolism, enhanced DNA damage response, and activation of pro survival pathways. The tumor microenvironment (TME) plays a major role in the resistance of CSCs to therapy. CD8 T cells, tumor associated macrophages, and cancer associated fibroblasts (CAFs) are major components of the TME and contribute to tumor progression and metastasis through the secretion of cytokines, growth factors, and angiogenic factors. Additionally, gut microbiota, such as *Fusobacterium nucleatum* and *Enterobacter* secrete inflammatory molecules that modulate the TME and contribute to therapy resistance. All of these mechanisms contribute to tumor invasion, angiogenesis, epithelial-to-mesenchymal transition, immunosuppression, drug resistance and survival following treatment. TAMs: Tumor associated macrophages; CAFs: Cancer associated fibroblasts; EMT: Epithelial-to-mesenchymal transition.

Intrinsic and acquired resistance to apoptosis is one of the characteristics of CSCs. Apoptosis is regulated by a balance between pro-apoptotic, anti-apoptotic, and pro-survival mechanisms[36], which is frequently altered in cancer, including CRC[34,37]. p53 plays a key role in the induction of apoptosis in response to DNA damage by chemotherapy[34]. However, p53 is mutated in 85% of CRC cases and is linked to resistance to 5-FU and oxaliplatin[38]. In addition, the expression of high levels of anti-apoptotic proteins, including Bcl-2 family members, is a characteristic of CSCs and results in resistance to cell death by apoptosis[39]. Frameshift mutations in the *BAX* gene result in the loss of expression and activity of the anti-apoptotic protein BAX, leading to chemoresistance[34]. Other anti-apoptotic proteins that are implicated in chemoresistance include Bcl-XL and the FLICE-inhibitory protein[40].

Moreover, several pro survival signaling pathways are activated in CRC. One major pathway is the Wnt/β-catenin pathway, which is important for stemness and resistance. Binding of Wnt ligand to the Frizzled receptor results in activation of β catenin, a key effector in this pathway[41]. Activation of the Wnt pathway induces proliferation and differentiation of CSCs, which is partly mediated by activation of several molecules that are recognized as putative CSC markers and include Lgr5, CD44, CD133, and Epcam[42]. All of these markers are associated with CSC resistance to chemo- and radiotherapy. Other pathways that are involved in stemness include the Notch and Hedgehog pathways[42].

Tumor microenvironment

CRC resistance has been also linked to the tumor microenvironment (TME) that is also involved in the multistep process that encompasses the development of adenomatous polyps from normal colonic epithelium, finally leading to invasive CRC[43,44]. The TME consists mainly of immune cells, endothelial cells, stromal cells, extracellular matrix (ECM), and signaling molecules[45]. Solid tumors, including CRC are infiltrated by different cells, such as dendritic cells, monocytes, neutrophils, CD8 and CD4 T cells, cancer-associated fibroblasts (CAFs), tumor-associated macrophages (TAMs), and mesenchymal stem cells. During tumor formation, interactions between tumor and stromal cells and secretion of soluble inflammatory molecules mediate the attraction of immune cells that promote tumor cell survival and metastasis[45,46]. The most important tumor-promoting cells are TAMs and CAFs. These cells facilitate tumor progression through direct contact with other cells or through secretion of cytokines, growth factors, and angiogenic factors, thereby promoting ECM formation, tumor invasion, angiogenesis, epithelial-to-mesenchymal transition (EMT), and immunosuppression[43,45].

Gut microbiota

Strong evidence is emerging to support the role of gut microbiota in the progression and resistance of

CRC and interventions made in this regard may hold promises for improving CRC treatment[47]. *Fusobacterium nucleatum* has been shown to contribute to CRC chemoresistance through activation of innate immune signals that stimulate the autophagy pathway[48]. The use of antibiotics can increase pathogenic bacteria such as *Enterobacter* and has been shown to reduce the anti-cancer effect of oxaliplatin through modulation of cytokine secretion and ROS production in the TME[49]. On the other hand, the effect of immunotherapy has been shown to be enhanced by intestinal microbiota, such as *Faecalibacterium*, *Clostridiales*, and *Bifidobacterium spp*[50,51]. The exact mechanism of action is still unclear but has been attributed to direct interactions between these bacteria and immune cells[52], in addition to a possible role for microbial metabolites, such as butyrate and propionate[53].

TARGETED THERAPY

Targeted agents can directly inhibit the proliferation and migration of cancer cells (Figure 2). They could also target the TME, thereby limiting tumor growth and enhancing immune surveillance. Small molecules play a major role in such treatments, as they can penetrate cells to selectively inactivate specific enzymes involved in tumor proliferation induction and apoptosis inhibition[54].

Targeting EGFR

EGFR belongs to the ErbB family of receptor tyrosine kinases and is involved in cellular proliferation, survival, migration, adhesion, and angiogenesis[55,56]. 80% of CRCs express or upregulate the *EGFR* gene[57,58], and this expression is associated with a risk of metastasis[59], therefore inhibiting EGFR could be a possible strategy to reduce cellular proliferation.

EGFR activation can be blocked by mAbs or tyrosine kinase inhibitors (TKIs). EGFR mAbs include cetuximab and panitumumab, which are currently used in parallel with FOLFOX or FOLFIRI regimens in the treatment of patients with *KRAS* or *NRAS* wild-type (WT) tumors[60]. In RAS-mutant tumors, constitutive activation of signaling pathways downstream of EGFR limits the effectiveness of EGFR inhibitors[61].

Cetuximab is a chimeric murine human IgG1 mAb that binds to the extracellular domain of EGFR and inhibits its pro-oncogenic action in cancer cells[62,63] (Table 1 and Figure 2). It also binds to natural killer cells and induces antibody-dependent cell-mediated cytotoxicity[62]. In a study that involved patients with advanced CRC after treatment with irinotecan, treatment with cetuximab alone or in combination with irinotecan showed significant clinical activity, with an enhanced rate of response and median survival time in the combination groups[64]. Combining cetuximab with FOLFIRI reduced the risk of progression of mCRC by 15% in first-line treatment of patients with *KRAS* WT tumors, when compared to FOLFIRI alone[65]. Complete or partial tumor responses were observed in 46.9% of patients treated with combination therapy and in 38.7% of patients treated with FOLFIRI alone[65]. Another treatment regimen that was tested in the first-line treatment of mCRC included FOLFOX4 and cetuximab[66]. Results from this randomized study showed an increased chance of response and lower risk of disease progression in the combination-treated group when compared to FOLFOX4 alone in *KRAS* WT patients[66]. A more recent randomized phase 3 Medical Research Council COIN trial showed that adding cetuximab to oxaliplatin-based chemotherapy increased the response rate in patients with advanced CRC; yet no enhancement of PFS or OS was shown[67].

Similar to cetuximab, treatment with panitumumab alone or in combination with standard chemotherapy has shown promising results in several clinical trials[60,68]. Panitumumab monotherapy was effective in CRC patients with *KRAS* WT tumors, with a response rate of 17%[69]. In an open-label phase III trial that involved patients with chemotherapy-refractory mCRC, panitumumab plus best supportive care (BSC) significantly prolonged PFS when compared to BSC alone. Response rates were 10% for panitumumab and 0% for BSC, with no difference observed in OS[70]. Several clinical trials were conducted to compare the efficacy of panitumumab and FOLFOX4 in comparison to FOLFOX4 alone[60,68]. Results from a phase III trial showed that combination treatment significantly improved PFS whereas the increase in OS was insignificant when compared to FOLFOX4 alone in *KRAS* WT tumors[60]. Except for the toxicities that are usually associated with EGFR inhibitors, adverse event rates were comparable between these treatments[60]. The very recent PARLIM trial showed that PFS and OS were improved upon the addition of panitumumab to FOLFOX in *KRAS* WT CRC patients with R0/1-resected liver metastases. Importantly, no new adverse events were observed in the combination-treated group[71].

The most common side effects observed in trials of these EGFR mAbs were skin toxicity, abdominal pain, nausea, diarrhea, infusion reactions, fatigue, and hypomagnesemia. Rare adverse events included pulmonary fibrosis, sepsis, severe skin toxicity, and anaphylaxis[72].

EGFR TKIs are small molecules derived from quinazolines that block the tyrosine kinase domain of different receptors, including EGFR. Erlotinib is specific to EGFR alone and is used to block ligand-induced EGFR receptor phosphorylation[73]. Gefitinib is another EGFR TKI that has a similar mechanism of action to erlotinib, but also targets other pathways, such as the extracellular signal-related kinases 1/2 (ERK1/2) pathway in mesothelioma cell lines[73].

Table 1 Agents targeting epidermal growth factor receptors and downstream molecules under clinical investigation for the treatment of drug-resistant and metastatic colorectal cancer

Agent	Targeted molecule	Condition	Study phase	Clinical trial identifier
Erlotinib	EGFR	First-line treatment for mCRC	Phase III	NCT01229813
Futuximab/Modotuximab (Sym-004)	EGFR	mCRC	Phase II	NCT02083653
Gefitinib	EGFR	Refractory CRC	Phase I/II	NCT00242788
Afatinib	EGFR	Refractory mCRC	Phase II	NCT01919879
		Advanced CRC	Phase II	NCT00801294
		mCRC	Phase II	NCT01152437
Dabrafenib (GSK2118436)	BRAF	mCRC	Phase II	NCT03668431
		mCRC	Phase II	NCT03428126
BMS-908662	BRAF	K-RAS/BRAF-mutated CRC	Phase I/II	NCT01086267
Encorafenib	Wild-type and BRAF V600E	Previously untreated BRAF-mutant mCRC	Phase II	NCT03693170
Vemurafenib	Mutated BRAF V600E	BRAF V600E mutated advanced CRC	Phase II	NCT03727763
PX-866	PI3K	mCRC	Phase I/II	NCT01252628
Gedatolisib	PI3K/mTOR	KRAS/NRAS-wild-type mCRC	Phase II	NCT01925274
		mCRC	Phase I/II	NCT01937715
Temsirolimus CCI-770	mTOR	KRAS-mutated mCRC	Phase II	NCT00827684
		Cetuximab-refractory CRC	Phase I	NCT00593060
Everolimus (RAD001)	mTOR	mCRC	Phase II	NCT01387880
		mCRC	Phase I/II	NCT01058655
		Advanced mCRC	Phase I/II	NCT01139138
		Refractory mCRC	Phase I	NCT01154335
MK-2206	AKT	Advanced CRC	Phase II	NCT01333475
Napabucasin (BBI608)	STAT3	Previously treated mCRC	Phase III	NCT03522649
Cobimetinib	MAPK	mCRC	Phase III	NCT02788279
Selumetinib	MEK	mCRC	Phase II	NCT00514761
Binimetinib	MEK	Previously untreated BRAF-mutant mCRC	Phase II	NCT03693170
Neratinib	EGFR/HER2/4	KRAS/NRAS/BRAF/PIK3CA-wild-type mCRC	Phase II	NCT03457896
Sapitinib (AZD-8931)	EGFR/HER2/3	mCRC	Phase II	NCT01862003
Duligotuzumab (MEHD7945A)	EGFR/HER3	KRAS-mutated mCRC	Phase II	NCT01652482
Trastuzumab	HER2	First-line HER2-positive mCRC	Phase III	NCT05253651
Tucatinib	HER2	First-line HER2-positive mCRC	Phase III	NCT05253651
Disitamab Vedotin	HER2	HER2-positive advanced CRC	Phase II	NCT05493683
		HER2-expressing mCRC	Phase II	NCT05333809
Trastuzumab-emtansine	HER2	HER2-positive mCRC progressing after trastuzumab and lapatinib	Phase II	NCT03418558

EGFR: Epidermal growth factor receptor; mCRC: Metastatic colorectal cancer; PI3K: Phosphoinositide 3-kinases; mTOR: Mammalian target of rapamycin; STAT3: Signal transducer and activator of transcription 3; AKT: Protein kinase B; MAPK: Mitogen-activated protein kinases; MEK: Mitogen-activated extracellular signal-regulated kinase; HER2: Human epidermal growth factor receptor 2.

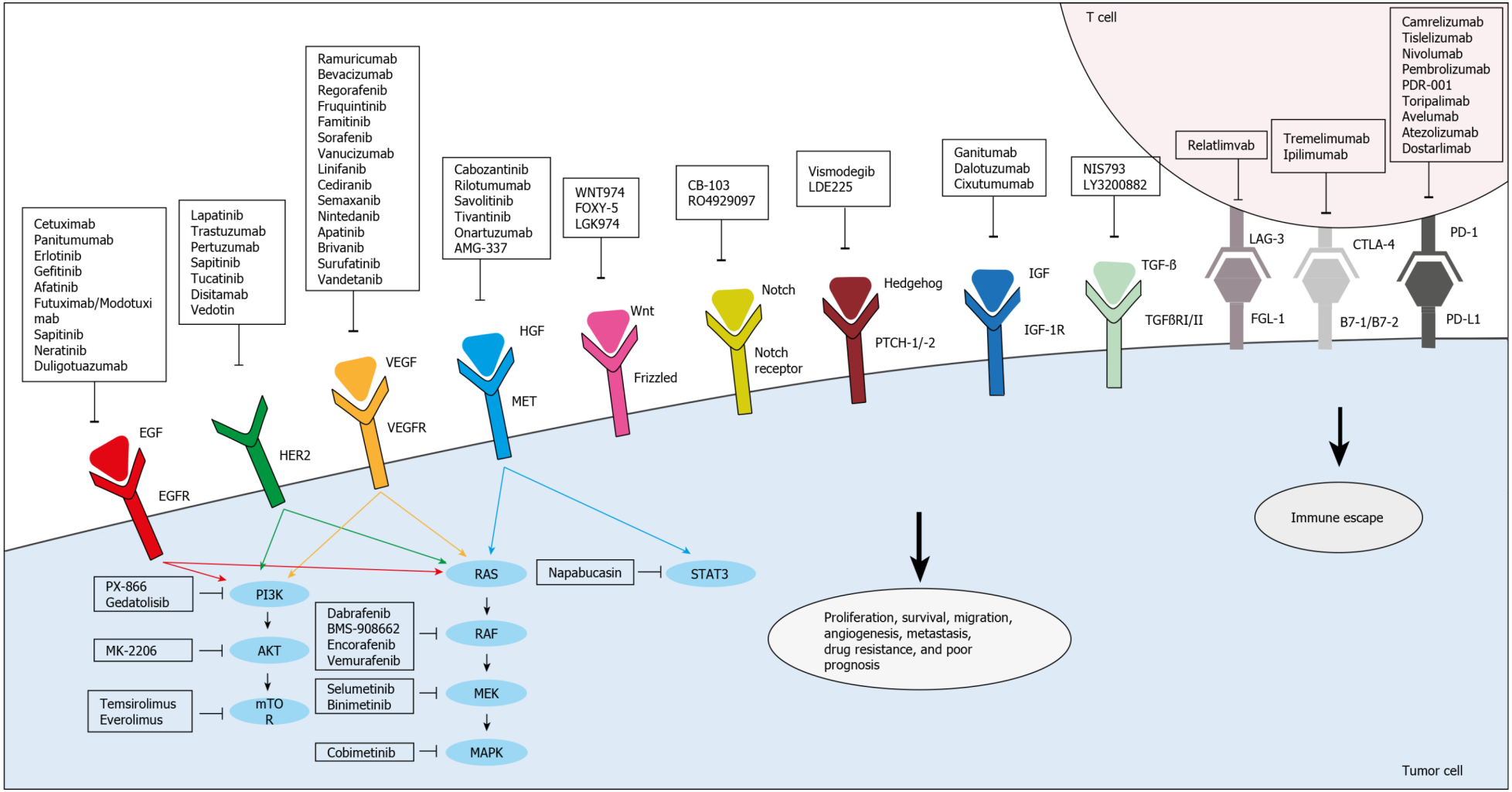

DOI: 10.3748/wjg.v29.i9.1395

Figure 2 Targeted therapies under investigation for the treatment of drug-resistant and metastatic colorectal cancer. Anti-epidermal growth factor receptor, anti-vascular endothelial growth factor/vascular endothelial growth factor receptor, and anti-human epidermal growth factor receptor 2 agents inhibit their respective targets and thus, the downstream effector pathways, PI3K/Akt and RAS/RAF. Other agents directly target and inhibit PI3K, AKT, mammalian target of rapamycin, RAF, mitogen-activated extracellular signal-regulated kinase, or mitogen-activated protein kinases. In addition, anti-hepatocyte growth factor/mesenchymal epithelial transition factor receptor agents target this pathway to inhibit signal transducer and activator of transcription, which is also targeted by Napabucasin. Several novel agents that are aimed at other pathways implicated in colorectal cancer proliferation, survival, resistance, and metastasis are also being evaluated. Targeted pathways include Wnt, Notch, Hedgehog, insulin growth factor/insulin growth factor receptor-1, and transforming growth factor beta. Moreover, immune escape can be hindered through immunotherapy which targets co-inhibitory molecules, mainly programmed

death-1/programmed death ligand-1, cytotoxic T lymphocyte-associated antigen 4, and lymphocyte activation gene 3. EFGR: Epidermal growth factor receptor; VEGF: Vascular endothelial growth factor; VEGFR: Vascular endothelial growth factor receptor; HER2: Human epidermal growth factor receptor 2; mTOR: Mammalian target of rapamycin; MEK: Mitogen-activated extracellular signal-regulated kinase; MAPK: Mitogen-activated protein kinases; HGF: Hepatocyte growth factor; MET: Mesenchymal epithelial transition factor receptor; STAT3: Signal transducer and activator of transcription; CRC: Colorectal cancer; IGF: Insulin growth factor; IGF-1R: Insulin growth factor receptor-1; TGF-β: Transforming growth factor beta; PD-1: Programmed death-1; PD-L1: Programmed death ligand-1; CTLA-4: Cytotoxic T lymphocyte-associated antigen 4; LAG-3: Lymphocyte activation gene 3; EGF: Epidermal growth factor; TGFβRI/II: Transforming growth factor-Beta type I/II.

It is important to note that studies investigating the efficacy of EGFR targeted therapy vary widely in clinical context, and some focus on the effect of EGFR monotherapy while others compare it to a combination of various chemotherapy regimens. One important factor to be taken into consideration is *KRAS* status, which could be used as a biomarker to predict the effectiveness of a treatment. Several inhibitors targeting EGFR or downstream molecules are currently under clinical investigation and are summarized in Table 1.

Targeting HER

Human EGFR 2 (HER2) is emerging as a key driver in CRC. It acts similar to EGFR, as they both share common downstream pathways, such as RAS/RAF/MEK and PI3K/AKT, which explains the link between HER2 overexpression and resistance to EGFR inhibitors[74,75]. The *HER2/neu* oncogene encodes a receptor with intrinsic tyrosine kinase activity[76]. HER2 lacks an endogenous ligand unlike other members of the HER/EGFR/ERBB system[77]. Homodimerization or heterodimerization with other EGFR family receptors, HER3 and EGFR, results in transphosphorylation of tyrosine residues within the cytoplasmic domain of HER2, thus leading to its activation[77,78]. HER2-HER3 heterodimers activate the PI3K/AKT pathway which is implicated in cancer cell growth and survival[79].

Different rates of HER2 amplification have been reported in CRC[80-82], with rates of membranous expression ranging from 2.1% to 11%[80,83,84], and that of cytoplasmic expression ranging from 47.4 to 68.5%[80,85,86]. Several factors may account for this variability, including small sample size, different antibodies used for immunohistochemistry (IHC), and analysis of different subgroups of patients with multiple clinical characteristics[87]. The efficacy of targeted agents against HER2-expressing CRC was determined in several clinical trials. Ramanathan *et al*[88] reported the detection of HER2/neu overexpression in only 8% of screened tumors in patients with advanced CRC and this low overexpression rate limited the study of irinotecan and trastuzumab, a humanized mAb targeting the HER2/neu receptor, in a phase II clinical study. Yet, partial response was observed in some patients, and the response was maintained for approximately six wk[88]. In a proof-of-concept study that exploited patient-derived xenografts (PDX), HER2 was identified as an effective therapeutic target in cetuximab-resistant mCRC [89]. HER2 amplification was detected in clinically unresponsive *KRAS* WT patients, and the combination of lapatinib (a dual EGFR/HER2 TKI) and pertuzumab induced an increase in response rate and tumor regression, in agreement with clinical studies in patients with similar clinicopathological characteristics[89]. The synergic antiproliferative effect of HER2 and EGFR blockade was also demonstrated in cetuximab-resistant CRC cell lines[74,90]. Interestingly, HER2 activating mutations were identified in CRC PDX and were shown to be highly sensitive to HER2/EGFR TKIs neratinib and afatinib and resulted in tumor regression when subjected to dual HER2 targeted therapy with trastuzumab plus TKIs[91]. It was also reported that these mutations cause oncogenic transformation of colon epithelial cells and resistance to anti-EGFR monotherapy[91]. Various clinical trials targeting

HER2 alterations in combination with chemotherapeutic therapies in patients with mCRC have validated findings from preclinical studies. High toxicity[92] and poor accrual[88,93] were the reasons behind halting earlier clinical studies evaluating the addition of HER2 mAbs (trastuzumab or pertuzumab) to cetuximab or chemotherapy (*i.e.*, irinotecan, 5-FU, and oxaliplatin). In a phase I trial involving patients with HER2-positive refractory tumors, none of the CRC patients responded to the combination of trastuzumab, paclitaxel, and interleukin (IL)-12[94]. More recently, a study that followed the stringent HERACLES criteria reported that the combination of trastuzumab and lapatinib achieved an objective response rate of 30% and was well tolerated in *KRAS* codon 12/13 WT, HER2-positive mCRC patients[95]. Within the same project, HERACLES-B phase II trial assessed the efficacy of pertuzumab and trastuzumab emtansine; however, it did not reach its primary endpoint of response rate. Yet, this combination can be considered a potential therapeutic strategy for HER2-positive mCRC, based on the high disease control achieved, in addition to the enhanced PFS and low toxicity[96]. The MyPathway trial assessed the combination of pertuzumab and trastuzumab in pretreated HER2-amplified mCRC patients and further supported the efficacy of the dual blockage of HER2[97,98]. Several agents targeting HER and EGFR are currently under clinical investigation (Table 1).

Targeting VEGF

Angiogenesis is the formation of new blood vessels from endothelial cells. It is mediated by vascular endothelial growth factor (VEGF), together with platelet-derived growth factor (PDGF) and fibroblast growth factor (FGF)[99]. Angiogenesis plays an important role in tumor initiation, growth, and metastasis. The VEGF system consists of six ligands and three receptors known as VEGF receptors (VEGFR). VEGF-A is secreted by multiple cell types, including cancer cells, and plays a major role in survival, growth, differentiation, and migration of endothelial cells[100]. VEGF-A mediates its effect by binding to VEGFR2, which is the major signal transducer of angiogenesis and is expressed by endothelial cells. On the other hand, VEGFR1 is a strong VEGF inhibitor[101]. Hypoxia is a key regulator of angiogenesis in cancer through hypoxia-inducible factors, which induce transcription of several genes, including VEGF-A[102].

VEGF levels and VEGFR activity are elevated in patients with CRC and are associated with poor prognosis[103]. The activation of this system is important both in local sites to support tumor progression and in metastatic sites to support neovascularization and tumor survival; therefore, a targeted therapy against VEGF/VEGFR might be developed at all stages of tumor progression and metastasis. Like EGFR, targeted therapy against angiogenesis consists of mAbs and TKIs. mAbs bind to VEGF-A or block the extracellular domain of its receptor. mAbs that bind VEGF-A include bevacizumab and aflibercept, thereby preventing activation of their receptors. Ramucirumab binds to the VEGFR2 extracellular domain, inhibiting the binding of VEGF ligands, thereby inhibiting receptor activation [104].

Bevacizumab as a monotherapy has a limited effect and is therefore used in combination with chemotherapy in first- and later-lines of mCRC treatment[105]. It is the first Food And Drug Administration (FDA)-approved VEGF-targeted agent for mCRC[105]. The first randomized clinical trial showed that bevacizumab improves response rate, PFS, and OS, thereby enhancing chemotherapy efficacy[106]. Combining bevacizumab (5 mg per kg of body weight every two wk) with irinotecan, 5-FU, and leucovorin (IFL) enhanced median duration of survival and PFS, as compared to IFL treatment alone, corresponding to a hazard ratio for death of 0.66 and for disease progression of 0.54, respectively[106]. The results also showed that median duration of the response to combination treatment was 10.4 mo as compared to 7.1 mo in the group treated with IFL and placebo[106]. A major adverse event was grade 3 hypertension which was more common in the group treated with IFL and bevacizumab but was easily managed. More recent trials showed that modern combination regimens were better substitutes for IFL; however, the efficacy of combining bevacizumab with first-line treatment of mCRC has been controversial. Several recent clinical trials demonstrated the promising efficiency of combining bevacizumab with trifluridine/tipiracil, which is usually better tolerated than capecitabine, especially in elderly patients with mCRC[107-109]. Notably, promising results were reported in the phase II TASCO study that assessed the effectiveness of combining bevacizumab with trifluridine/tipiracil as first-line treatment in untreated patients with unresectable mCRC[110]. This combination treatment achieved better median PFS and OS when compared to patients receiving bevacizumab plus capecitabine. On the other hand, Chen *et al*[111] carried out a meta-analysis that showed no improvement in OS upon the addition of bevacizumab to FOLFOX/FOLFIRI/capecitabine plus oxaliplatin (XELOX) regimens when compared to chemotherapy alone, unless PFS is considered, specifically in capecitabine-based regimens. This exception was established based on two trials, the NO16966 study[112] and ITACA trial[113], which used PFS as an endpoint measurement. These studies showed that adding bevacizumab to oxaliplatin-based therapy (XELOX or FOLFOX4) significantly improved PFS in patients with mCRC [112]. OS and response rate were not changed by the addition of bevacizumab, suggesting that prolonged treatment may be needed for optimal combination efficacy[112]. Interestingly, it has been documented that both patients with *KRAS* mutations and with WT *KRAS* may benefit from adding bevacizumab to chemotherapy[114,115]. The efficacy of the second-line application of bevacizumab has also been validated in several trials that showed longer PFS and OS, and a better response rate, compared with standard chemotherapy alone in the E3200 study[116] and III ML18147 trial[117].

The addition of aflibercept to FOLFIRI enhanced the survival of patients progressing who were previously given oxaliplatin-based regimens[118]. Combination treatment resulted in a 9% increase in response rate, accompanied by an improvement in PFS from 4.7 to 6.9 mo and OS from 12.1 to 13.5 mo [118].

Ramucirumab was approved by the FDA for second-line treatment of mCRC based on the phase III RAISE trial[119]. Data from this study showed that the addition of ramucirumab significantly prolonged PFS and OS but not response rate, following first-line treatment with 5-FU, oxaliplatin, and bevacizumab[119].

Few VEGF TKIs have been proven to be effective in patients with mCRC. These include regorafenib, which was approved by FDA for the treatment of mCRC[120]. Yet, regorafenib has multiple targets, other than VEGF, whereby it also inhibits PDGF receptor, FGF receptor, and BRAF[120]. Notably, treatment of mCRC patients with regorafenib was associated with enhanced OS[121]. A more significant OS benefit was observed when combining regorafenib with its major metabolites, M-2 and M-5, in concentrations ranging between 2.5 and 5.5 mg/L[121]. While no improvement in the response rate was shown upon adding regorafenib to FOLFOX in mCRC patients as compared to chemotherapy alone [120], better median OS and PFS were achieved using regorafenib alone than placebo for refractory mCRC treatment in the phase III CORRECT trial[122]. These results were also validated in an Asian population in the CONCUR trial[123]. Anlotinib, a novel TKI that inhibits VEGFR1/2/3, among other kinases, showed an enhanced overall rate response and PFS when combined with capecitabine and oxaliplatin in the first-line treatment of mCRC[124]. Other TKI agents have been developed in the last few years, these include fruquintinib[125] and famitinib[126], in addition to other agents that are under clinical investigation and are summarized in Table 2.

Targeting MEK and mutant BRAF

BRAF mutations are found in 8% to 12% of mCRC cases, and the V600E-activating mutations, which are the most prevalent mutations, are most commonly located in right-colon tumors, and confer a worse prognosis for mCRC[127,128]. *BRAF* mutations are generally mutually exclusive with *KRAS* and *NRAS* mutations. Notably, BRAF and RAS are the only available biomarkers for advanced CRC that are used in clinical practice[129].

BRAF is a downstream effector of RAS in the EGFR pathway and several preclinical studies have shown that BRAF inhibition may induce EGFR overactivation and that EGFR inhibition is important for sensitizing resistant cell lines to anti-BRAF agents[130]. In fact, BRAF inhibitor monotherapy in CRCs harboring V600E-activating mutations is ineffective with a response rate of only 5%[131]. Capalbo *et al* [132] reported the first clinical evidence that combining anti-EGFR (panitumumab) and an inhibitor of BRAF V600 kinase (vemurafenib) achieves strong disease control and is well tolerated in patients with mCRC that progressed on standard lines of treatment. However, this is only achieved in *RAS* and *BRAF* WT tumors, as *RAS* and *BRAF* mutations lead to the constitutive activation of downstream transducers of EGFR, circumventing EGFR inhibition, resulting in failure of anti-EGFR therapy[133-135]. A very recent randomized trial reported that the addition of vemurafenib to irinotecan combined with cetuximab improved PFS (hazard ratio of 0.50) in patients with *BRAF*-mutated, *RAS* WT mCRC. The response rate was 17% upon addition of vemurafenib and 4% without vemurafenib[136]. Disease control rate was also improved by 44%, suggesting that blocking signaling activity of EGFR using cetuximab prevents its feedback upregulation by vemurafenib. Interestingly, treatment with EGFR and BRAF inhibitors led to a decline in circulating tumor DNA (ctDNA) BRAF V600E variant allele frequency in 87% of the studied population[136]. In the phase III BEACON CRC trial, twenty-nine patients with *BRAF V600E*-mutant mCRC who had experienced treatment failure with chemotherapy were selected to assess the safety of the encorafenib, binimetinib, and cetuximab regimen. The results showed that the tolerability of this treatment regimen was acceptable, with an overall response rate of 48%, median PFS of 8.0 mo, and median OS of 15.3 mo[137].

BRAF V600E mutations result in constitutive activation of BRAF kinase, which results in activation of mitogen-activated protein kinase (MAPK) kinases MEK1 and MEK2. The latter phosphorylates and activates ERK kinases, resulting in phosphorylation and activation of key molecules involved in proliferation and survival[138].

Studies have shown that combination therapies targeting RAF and EGFR or RAF and MEK can inhibit feedback reactivation of the MAPK signaling pathway, resulting in more robust inhibition and improved efficacy of the treatment in *BRAF*-mutant CRC[139,140]. Combining RAF and MEK inhibitors produced a 12% partial response and 2% complete response, with a more than 36 mo duration of response, whereby 56% of the patients achieved stable disease. Interestingly, 9 patients who remained in the study for more than 6 mo had reduced levels of phosphorylated ERK during treatment, relative to pretreatment biopsies[141]. A clinical trial of combined inhibition of BRAF, EGFR, and MEK with dabrafenib, panitumumab, and trametinib, respectively, showed improved efficacy in patients with *BRAF V600E*-mutant CRC[140]. Interestingly, the triplet regimen achieved a response rate of 21% that was higher than dabrafenib and panitumumab (10%) or panitumumab and trametinib (0%)[140]. The BEACON trial reported similar results, whereby a triple treatment consisting of cetuximab, encorafenib, and binimetinib (a MEK inhibitor) significantly prolonged OS and achieved a higher response rate than standard chemotherapy, with a comparable rate of adverse events[142]. Few agents targeting mutant

Table 2 Agents targeting vascular endothelial growth factor/vascular endothelial growth factor receptor under clinical investigation for the treatment of drug-resistant and metastatic colorectal cancer

Agent	Targeted molecule	Condition	Study phase	Clinical trial identifier
Vanucizumab	VEGF-A/angiopoietin-2	mCRC	Phase II	NCT02141295
Sorafenib	VEGFR	mCRC	Phase II	NCT03251612
		Previously treated mCRC	Phase II	NCT01471353
		mCRC	Phase II	NCT00826540
		KRAS-mutated mCRC	Phase II	NCT01715441
Bevacizumab	VEGF	Untreated mCRC	Phase II	NCT02141295
		Advanced CRC	Phase II	NCT02487992
Linifanib ABT-869	VEGFR	Advanced CRC	Phase II	NCT00707889
Vatalanib	VEGFR	mCRC	Phase III	NCT00056446
		mCRC	Phase III	NCT00056459
Famitinib	VEGFR2/3	Advanced CRC	Phase II	NCT01762293
Cediranib	VEGFR2	First-line mCRC	Phase III	NCT00399035
Semaxanib	VEGFR	mCRC	Phase III	NCT00004252
		Advanced CRC	Phase I/II	NCT00005818
Nintedanib	VEGFR	Refractory mCRC	Phase III	NCT02149108
Ramucirumab	VEGFR2	Chemotherapy refractory mCRC	Phase III	NCT03520946
Apatinib	VEGFR2	Refractory CRC	Phase II	NCT03190616
		mCRC	NA	NCT03743428
		End-stage CRC	Phase II	NCT02829385
Brivanib	VEGFR2	KRAS-wild-type mCRC	Phase III	NCT00640471
Regorafenib	VEGFR1/2/3	Later-lines treatment of mCRC	Phase III	NCT05328908
		mCRC	Phase III	NCT05425940
Surufatinib	VEGFR1/2/3	Advanced CRC	Phase II	NCT05372198
Lenvatinib	VEGFR1/2/3	mCRC	Phase III	NCT04776148
Fruquitinib	VEGFR tyrosine kinase	Non-MSI-H/dMMR mCRC	Phase II	NCT04866862
Vandetanib	VEGF/VEGFR	mCRC	Phase I	NCT00532090
		mCRC	Phase II	NCT00500292
		Advanced CRC	Phase I	NCT00496509

VEGF: Vascular endothelial growth factor; VEGFR: Vascular endothelial growth factor receptor; mCRC: Metastatic colorectal cancer; MSI: Microsatellite instability; dMMR: mismatch repair deficient.

BRAF or *MEK* have been tested in clinical settings in the context of mCRC (Table 1).

The most common adverse events associated with BRAF inhibition include rash, fatigue, arthralgia, and diarrhea. When combined with MEK inhibitors, toxicities include pulmonary toxicities and ophthalmic changes[143].

Targeting c-MET and HGF

MET is activated by hepatocyte growth factor (HGF) that is secreted by cells of mesenchymal lineage [144]. The MET pathway is frequently aberrantly activated in CRC, in which its overexpression has been reported in up to 70% of cases[144]. MET has been proposed to be a major contributor to resistance to anti-angiogenic therapy and is associated with progression, metastasis, and poor prognosis[145,146], due to c-MET activation of several proteins, such as surviving and x-linked inhibitor of apoptosis protein[147]. In fact, inhibition of the VEGF pathway results in upregulation of MET. A study reported that resistance to cetuximab was caused by MET locus amplification in CRC PDX and that treatment with a MET inhibitor led to an anti-tumor effect[148].

Various mAbs and small molecules with different mechanisms of action have been developed to target the HGF-MET pathway in mCRC[9]. Some drugs are directed at blocking HGF activation and production, while other drugs inhibit the binding of HGF to MET receptors. Agents that interfere with the binding of HGF to MET can be classified as MET antagonists, which competitively bind to MET receptors or as MET TKIs, which inhibit intracellular tyrosine kinase activity[9].

Cabozantinib is a multi-kinase inhibitor that targets MET and VEGFR2, in addition to other kinases [146]. A study reported a potent growth inhibitory effect of cabozantinib in 80% of tumors treated using a CRC PDX model and this inhibition was mostly observed in tumors with *PIK3CA* mutation. Mechanistically, cabozantinib inhibited Akt activation and decreased the expression of genes involved in the PI3K pathway[146]. Several clinical trials assessed the efficacy of agents that neutralize HGF and block its ability to bind to the MET receptor. A randomized phase Ib/II trial of panitumumab in combination with rilotumumab (a human mAb against HGF), ganitumab (a human mAb against insulin-like growth factor 1 receptor), or placebo in patients with *KRAS* WT mCRC showed a significant increase in overall response rate of 10% when combining panitumumab with rilotumumab[149]. However, the enhancement in response rate did not translate into significant improvement in OS and PFS. Agents, such as onartuzumab, that compete with HGF for binding to MET have been developed and tested in various solid tumors, including CRC. A phase II randomized trial of first-line FOLFOX plus bevacizumab with or without onartuzumab (MET inhibitor) reported an improvement in PFS in the MET IHC-negative population with mCRC, as compared to those receiving treatment without onartuzumab[150]. However, the addition of onartuzumab did not improve OS or response rate in this population[150]. Tivantinib is an oral small molecule allosteric receptor TKI that selectively keeps MET in the inactive state[151]. In the case of mCRC, clinical trials of tivantinib are insufficient to evaluate its efficacy. A phase I/II trial involving CRC patients with WT *KRAS* receiving tivantinib or placebo plus cetuximab and irinotecan found no PFS improvement[152]. A recent phase II trial of tivantinib and cetuximab in patients with MET-high *KRAS* WT mCRC did not meet its primary endpoint; yet, results suggested some efficacy of the combination, with approximately 10% of patients achieving an objective response[153]. Merestinib, an oral multikinase inhibitor, demonstrated an acceptable safety profile and potential anti-tumor effect in a recent first-in-human phase I study involving patients with advanced cancer, including CRC[154]. Findings from this study warrant further investigation to determine the efficacy of this agent in patients with *KRAS* WT mCRC.

Mild adverse events have been reported for the above-mentioned agents, including fatigue, poor appetite, allergic reactions, edema, skin rash, and neutropenia[155,156].

AMG-337, an oral ATP-competitive TKI specific to MET, is being investigated in a CRC phase I trial (Table 3). Crizotinib targets TKIs of MET, in addition to macrophage-stimulating 1 receptor and ROS proto-oncogene[157]. Although there is a lack of clinical evidence for crizotinib in CRC, a series of trials are in progress[158] (Table 3). The use of crizotinib might enhance the response to radiation therapy in *KRAS*-mutant CRC cell lines, and a combination of crizotinib with mitomycin C seemed to have a synergistic effect against CRC in preclinical results, which showed promise for future anti-CRC treatments[159]. Few MET inhibitors are under clinical investigation for the treatment of mCRC, and several new agents are being tested in patients with CRC (Table 3).

Immune checkpoint inhibitors

In addition to developing agents to directly target pathways involved in tumor growth and metastasis, there is great interest in modulating other pathways involved in immune recognition and responses against cancer cells (Table 4). Immune escape has been frequently identified in various cancers, including CRC[160]. Underlying mechanisms include secretion of immunosuppressive cytokines (transforming growth factor beta (TGFβ), IL-6, CXCL3, CXCL4, and high mobility group box-1), recruitment of regulatory T cells, and loss of immunogenicity *via* downregulation of major histocompatibility complex-I (MHC-I)[161,162]. Tumor activation of co-inhibitory receptors, also known as immune checkpoint receptors, on the surface of T cells results in T cell inactivation and exhaustion[163]. These receptors include programmed death-1 (PD-1) and cytotoxic T lymphocyte antigen 4 (CTLA-4)[164]. PD-1 is expressed on peritumoral lymphocytes and is activated by its ligands [programmed death ligand-1 (PD-L1) or PD-L2], which are expressed on tumor cells, to suppress immune functions[165]. mCRC lesions express higher levels of PD-L1 than primary lesions[166], paving the way for promising clinical benefits. Six antibodies against PD-1 or PD-L1 have been approved by the FDA as an anti-cancer treatment, among which some have been evaluated in mCRC patients[167,168]. Metastatic DNA mismatch repair-deficient (dMMR)/MSI-high (MSI-H) CRC has a poor prognosis and is less responsive to conventional chemotherapy, which could be linked to *BRAF* mutation[169,170]. Importantly, patients who have high mutational tumor burden, with dMMR or MSI-H, respond to immune checkpoint targeted therapy[171-173], most probably due to the fact that mutations result in tumor neoantigens that attract T cell infiltration[174]. Pembrolizumab was the first PD-1 inhibitor to be approved by the FDA for the treatment of mCRC. The KEYNOTE-016 study showed that MSI-H mCRC patients responded to pembrolizumab treatment and showed a response rate of 40% and PFS of 78%[168]. The efficacy of pembrolizumab for the treatment of MSI-H mCRC was also validated in another phase I clinical trial [175]. The more recent trial, KEYNOTE-164, showed that when given in the second-line setting, pembrolizumab resulted in an objective response rate of 33%, PFS of 2.3 mo, and OS of 31.4 mo[176].

Table 3 Agents targeting mesenchymal epithelial transition factor receptor under clinical investigation for the treatment of colorectal cancer and metastatic colorectal cancer

Agent	Targeted molecule	Condition	Study phase	Clinical trial identifier
Savolitinib	MET	mCRC	Phase II	NCT03592641
Tivantinib	MET	mCRC	Phase I/II	NCT01075048
Onartuzumab	MET	CRC	Phase II	NCT01418222
Cabozantinib	MET/RET/VEGFR-2	CRC	Phase I	NCT02008383
		mCRC	Phase I	NCT03798626
		Refractory mCRC	Phase II	NCT03542877
Rilotumumab	HGF	KRAS wild-type mCRC	Phase I/II	NCT00788957

MET: Mesenchymal epithelial transition factor receptor; mCRC: Metastatic colorectal cancer; CRC: Colorectal cancer; VEGFR: Vascular endothelial growth factor receptor; HGF: Hepatocyte growth factor; RET: Rearranged during transfection.

The clinical benefit of PD-1 blockade in dMMR mCRC was also documented in the CheckMate 142 phase I trial of nivolumab in patients with refractory solid tumors, 14 of whom had mCRC. A durable complete response was achieved in one patient with mCRC, after receiving five doses of 3 mg/kg nivolumab[177]. This study led to the FDA approval of nivolumab for dMMR or MSI-H mCRC. Combined therapy with nivolumab and the CTLA-4 inhibitor ipilimumab produced durable clinical benefits and helped previously treated patients who had MSI-H or dMMR reach high PFS and OS rates [178,179]. The potential of PD-1 blockade using the single-agent dostarlimab was also evaluated in a very recent phase II study in patients selected for having dMMR stage II or III rectal adenocarcinoma. Administration of dostarlimab every three wk for six mo in twelve patients, who had not received chemoradiotherapy or undergone surgery, resulted in a clinical complete response in all patients with no evidence of progression or recurrence during the six to twenty-five mo follow-up[180]. Several preclinical studies are evaluating other potential immunotherapy agents. A novel antibody (LBL-007), recently characterized by Yu *et al*[181], targets lymphocyte activation gene 3 (LAG-3) expressed on activated T cells, natural killer cells, and B cells, and functions to negatively regulate these cells. This antibody was found to bind activated T cells and prevent LAG-3 binding to MHC class II molecules, blocking downstream signaling induction *in vitro*. *In vivo* results showed that treating mice bearing CRC with LBL-007 significantly delayed tumor growth and combining it with an anti-PD-1 antibody led to a more effective inhibition. Serum LBL-007 levels were high in monkeys injected with LBL-007 at 3, 10, or 30 mg/kg[181]. Another negative regulator of the immune system, T cell immunoglobulin and mucin domain 3, has been shown to be expressed in mCRC and plays an important role in cancer progression [181], and therefore might be a potential target for immunotherapy.

Pathways offering potential for targeted therapy

Several clinical trials have been initiated to evaluate the efficacy of agents targeting other pathways, yet no meaningful results have been presented so far. RO4929097 is a selective inhibitor of γ-secretase, a proteolytic enzyme that produces an activated intracellular Notch[182]. Notch is an attractive drug target as it is involved in CRC progression; however, a study of RO4929097 showed that no objective radiographic responses were observed and only a few mCRC patients had stable disease, although positive staining for intracellular Notch and its receptor was demonstrated in tissues[182]. A randomized phase II trial of vismodegib, a Hedgehog pathway inhibitor, reported no added benefit in combination with FOLFIRI or FOLFOX, and was instead associated with increased toxicity in mCRC patients[183]. The expression of morphogenetic protein 4 (BMP-4) has been shown to be upregulated in human CRC tissue and inhibition of BMP-4 by BMP type I receptor inhibitor, LDN-193189, induced apoptosis and inhibited tumor formation in mice injected with CRC cells[184]. The progress in the development of agents targeting TGF-β, Wnt, and ATP-binding cassette member B5 is still limited and needs further investigation[185-187]. Limitations in targeted therapy against these pathways are attributed to the existence of crosstalk between pathways, in addition to difficulty selecting patients, identifying predictive biomarkers, and specifically blocking targeted molecules. However, several clinical trials are investigating novel agents, which are summarized in Table 5.

BEATING RESISTANCE TO TARGETED THERAPY

Although multiple targeted therapy agents have demonstrated significant potency in mCRC patients, several challenges hinder the effectiveness of these therapies. Such therapies are associated with

Table 4 Agents targeting immune checkpoints under clinical investigation for the treatment of drug-resistant and metastatic colorectal cancer

Agent	Targeted molecule	Condition	Study phase	Clinical trial identifier
Camrelizumab	PD-1	Non-MSI-H/dMMR mCRC	Phase II	NCT04866862
		mCRC	Phase II	NCT03912857
Tislelizumab	PD-1	HER2-Positive Advanced CRC	Phase II	NCT05493683
Nivolumab	PD-1	Later-lines treatment of mCRC	Phase III	NCT05328908
		Advanced CRC	Phase I	NCT02991196
		Metastatic MSS CRC	Phase I	NCT03993626
		mCRC	Phase II	NCT04166383
Pembrolizumab (MK-3475)	PD-1	MSI-H/dMMR CRC	Phase III	NCT05239741
		mCRC	Phase III	NCT04776148
		MMR-proficient mCRC	Phase II	NCT03519412
		HER2-expressing mCRC	Phase II	NCT03631407
		HER2-expressing mCRC	Phase II	NCT05333809
PDR-001	PD-1/PD-L1	mCRC	Phase I	NCT03081494
		First-line mCRC	Phase I	NCT03176264
Toripalimab	PD-1/PD-L1	mCRC	Phase II	NCT03927898
Avelumab	PD-1/PD-L1	mCRC	Phase II	NCT03150706
		mCRC	Phase II	NCT03258398
Atezolizumab	PD-L1	mCRC	Phase III	NCT05425940
		mCRC	Phase III	NCT02788279
		First-line mCRC	Phase II	NCT02291289
		Refractory CRC	Phase II	NCT02873195
Relatlimab	LAG-3	Later-lines treatment of mCRC	Phase III	NCT05328908
Tremelimumab	CTLA-4	mCRC	Phase I/II	NCT03202758
		mCRC	Phase II	NCT03122509
		mCRC	Phase II	NCT03428126
		mCRC	Phase II	NCT03435107

PD-1: Programmed death-1; PD-L1: Programmed death ligand-1; mCRC: metastatic colorectal cancer; MSI-H/dMMR: Microsatellite instability-high/mismatch repair deficient; MSS: Microsatellite stable; HER2: Human epidermal growth factor receptor 2; LAG-3: Lymphocyte activation gene 3; CTLA-4: Cytotoxic T lymphocyte-associated antigen 4.

intrinsic and acquired resistance and a thorough understanding of resistance mechanisms is essential for developing effective drugs (Figure 3). For example, EGFR inhibitors are effective against *KRAS* WT mCRC but not *KRAS* mutated mCRC and there is a need for effective agents in this poor prognosis group. Several clinical trials have assessed the combination of VEGF and chemotherapy, but no attractive results have been shown[9,188].

Overcoming resistance to EGFR

Administration of EGFR antibodies with MEK inhibitors has been tested in preclinical models, but clinical data are still limited[189]. Alterations in ctDNA in the following genes: *KRAS*, *NRAS*, *MET*, *ERBB2*, *FLT3*, *EGFR*, and *MAP2K1* have been identified in patients with primary or secondary resistance to EGFR inhibition[190]. Thus, determining the ctDNA profiles of patients with mCRC might help predict patient response[191]. Güttlein *et al*[192] recently tested *NRAS*, *KRAS*, and *BRAF* mutations in liquid plasma biopsies of patients with mCRC and reported a 12- and 4-mo median PFS of *RAS*/*BRAF* WT and *RAS*/*BRAF* mutated patients, respectively. The frequency of plasma mutations was highest for *KRAS* (34%). This study suggested that analysis of these mutations in the plasma of mCRC patients can be used to predict OS. The REVEAL study identified multiple actionable targets by performing NGS

Table 5 Agents targeting other pathways under clinical investigation for the treatment of drug-resistant and metastatic colorectal cancer

Agent	Targeted molecule	Condition	Study phase	Clinical trial identifier
CB-103	Notch	Resistant to oxaliplatin or irinotecan-based therapy advanced or mCRC	Phase I/II	NCT03422679
RO4929097	Notch	mCRC	Phase II	NCT01116687
WNT974	Wnt	BRAF-mutant mCRC	Phase I/II	NCT02278133
FOXY-5	Wnt	mCRC	Phase I	NCT02020291
LGK974	Wnt	BRAF mutant CRC	Phase I	NCT01351103
Vismodegib (GDC-0449)	Hedgehog	First-line therapy mCRC	Phase II	NCT00636610
		mCRC	Phase II	NCT00959647
LDE225	Hedgehog	mCRC	Phase I	NCT01576666
NIS793	TGF	Advanced CRC	Phase I	NCT02947165
LY3200882	TGF	Advanced chemotherapy -resistant CRC with an activated TGF-beta Signature	Phase I/II	NCT04031872
Ganitumab	IGF-1R	KRAS wild-type mCRC	Phase I/II	NCT00788957
		KRAS-mutant mCRC	Phase II	NCT00813605
Dalotuzumab (MK-0646)	IGF-1R	mCRC	Phase II	NCT00614393
Cixutumumab (IMC-A12)	IGF-1R	mCRC resistant to EGFR therapy	Phase II	NCT00503685

Wnt: Wingless-related integration site; mCRC: Metastatic colorectal cancer; TGF: Transforming growth factor; IGF-1R: Insulin growth factor receptor-1; EGFR: Epidermal growth factor receptor.

and transcriptional analysis of tumor and liquid biopsies during and after standard first-line chemotherapy treatment of patients with mCRC[193]. Differentially identified genes reported by this study were associated with EMT, ECM modulation, metabolism regulation, and several oncogenic pathways, such as PI3K/AKT and MAPK[193]. This study also reported the secreted phosphoprotein 1/osteopontin gene as a potentially druggable target whose inhibition also modulates the previously mentioned oncogenic pathways. Interestingly, the approach devised in this study aids in identifying mutations and transcriptional changes following first-line treatment, and thus can be used to predict novel resistance mechanisms and manage them by administering the appropriate targeted agents. Several clinical studies are underway to determine patient subsets who can benefit from anti-EGFR therapy[194,195]; however, sensitivity thresholds in PCR should be taken into consideration since they can affect the genotyping of *KRAS*, *NRAS*, *BRAF* and *PIK3C*. This would improve the selection of treatment for mCRC with anti-EGFR therapy, as shown by the ULTRA trial[196]. A prospective-retrospective cohort study documented that ctDNA *KRAS* tested using Digital PCR showed consistency with tumor tissues obtained from mCRC patients and predicted responses to EGFR inhibition[197]. Notably, recent studies have demonstrated that while left-sided *KRAS* WT mCRC should be preferentially treated with anti-EGFR agents, right-sided tumors might respond better to bevacizumab plus chemotherapy; however, optimization of treatment for these subsets of tumors is yet to be achieved[198-200]. Reversal strategies have emerged to overcome intrinsic resistance, and these include development of new EGFR inhibitors, combination of anti-EGFR with multitargeted inhibitors, development of small molecules that enhance the effect of anti-EGFR agents, and the implementation of metabolic regulators [201]. The development of EGFR mAbs that bind to mutated extracellular domains may enhance the efficacy of these treatments. A study involving CRC patients showed that MM-151, a mAb that binds to different regions of EGFR, significantly inhibits EGFR signaling and decreases mutations in ctDNA [202]. The FDA-approved anti-EGFR agent, necitumumab, was developed to bind to EGFR that harbors the most common cetuximab-resistant variant[203]. The first-in-class anti-EGFR non-overlapping mAbs mixture Sym004 has been documented to suppress mutant EGFR signaling in cetuximab-resistant cell lines and in xenograft models, contrary to cetuximab and panitumumab[204]. Interestingly, Sym004 is currently under clinical investigation for the treatment of mCRC (Table 1 and Figure 1). Notably, recombinant protein-based therapeutics have become an interesting therapeutic option for the treatment of resistant mCRC. A very recent study showed that $PEPD^{G278D}$, a recombinant human protein that induces the degradation of both EGFR and HER2, exerts strong anti-tumor activity and overcomes resistance to anti-EGFR therapy in CRC PDX[205]. As for patients with *KRAS*-mutant CRC, a fully

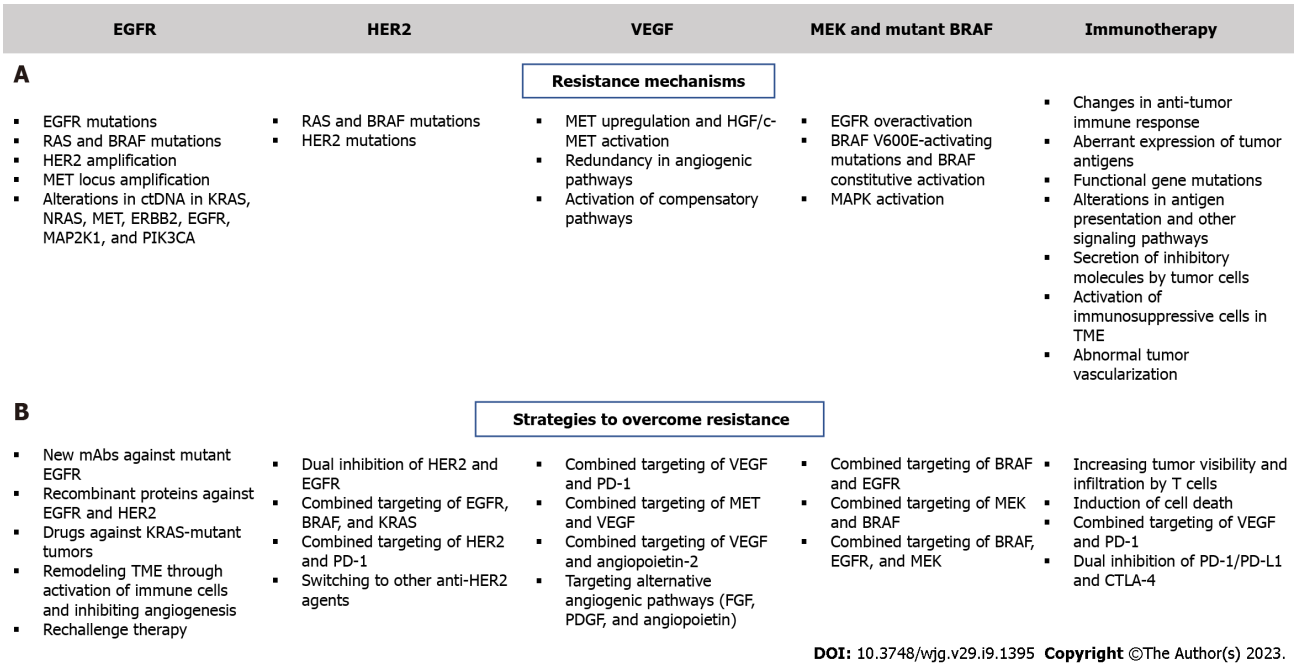

DOI: 10.3748/wjg.v29.i9.1395

Figure 3 Mechanisms of resistance to targeted therapy and strategies to overcome resistance in colorectal cancer. A: Resistance mechanisms; B: Strategies to overcome resistance. EGFR: Epidermal growth factor receptor; HER2: Human epidermal growth factor receptor 2; VEGF: Vascular endothelial growth factor; MEK: Mitogen-activated extracellular signal-regulated kinase; MAP2K1: Mitogen-Activated Protein Kinase 1; PI3KCA: Phosphoinositide 3-kinases catalytic subunit alpha; MAP2K1: Mitogen-activated protein kinase 1; HGF: Hepatocyte growth factor; MET: Mesenchymal epithelial transition; ERBB2: Erb-B2 Receptor Tyrosine Kinase 2; TME: Tumor microenvironment; FGF: Fibroblast growth factor; PDGF: Platelet-derived growth factor; PD-1: Programmed death-1; PD-L1: Programmed death ligand-1; CTLA-4: cytotoxic T lymphocyte-associated antigen 4.

humanized EGFR mAb (GC1118) showed significant inhibitory effects against *KRAS*-mutant CRC PDX [206] and hopes are now placed on the use of this novel compound for better targeting of these tumors.

Extrinsic resistance is mainly mediated by changes in the TME, specifically immune cells and CAFs, in addition to novel development of *KRAS* mutations and activation of angiogenesis[207,208]. Strategies to remodel the TME are usually beneficial to increase the efficacy of anti-EGFR antibodies and they may include activation of T cells and natural killer cells, suppression of CAFs, and inhibition of angiogenesis through VEGF blockade[201].

Interestingly, rechallenge and reintroduction strategies have been implemented in recent years and have been tested on patients with mCRC who have received an anti-EGFR therapy and whose treatment was halted[209]. Rechallenge refers to anti-EGFR re-treatment of *KRAS* WT mCRC patients who have initially received and benefited from first-line anti-EGFR therapy before disease progression and receiving a different treatment. Reintroduction refers to re-exposure after prior discontinuation of anti-EGFR therapy due to toxicity, intolerance, and other factors[209,210]. Very recently, Schulz *et al*[210] reported real-world evidence supporting the benefits of anti-EGFR treatment re-exposure in patients with mCRC, regardless of the reason for discontinuation of anti-EGFR therapy. The reintroduction or rechallenge of this treatment was associated with high OS and PFS[210], suggesting that the administration of more than one-line of treatment with anti-EGFR could be a promising tool to manage disease progression, given the limitations in the current treatment options.

Overcoming resistance to anti-HER2 therapy

Several strategies have been tested to combat resistance to anti-HER2 therapy (Figure 3). These include dual HER2 and EGFR inhibition in the first-line setting and increasing sensitivity to HER2 blockade following resistance to trastuzumab-based therapy[190,211]. Patients with HER2-amplified mCRC that harbor *RAS, BRAF,* or *PIK3CA* mutations show limited response to HER2 inhibitors[211], and therefore require a novel therapeutic strategy that would concomitantly block feedback loops involving *EGFR*, *BRAF*, and *KRAS* in mutated mCRC. In terms of the first strategy, several compounds are currently under clinical investigation and new drugs are being proposed as candidates to inhibit both molecules and improve efficacy of CRC targeted therapy, particularly in HER2-positive mCRC[212,213] (Table 1). In fact, HER2 amplification has been linked with resistance to EGFR inhibition[214] and thus, may serve as a biomarker for these treatment regimens. Moreover, combinations of HER2 and PD-1 inhibitors are also being investigated in HER2 expressing advanced CRC or mCRC (Table 6). As for patients with trastuzumab-refractory disease, a possible strategy would be to switch to another anti-HER2 agent. A novel antibody-drug conjugate (T-DM1) consisting of a mAb covalently linked to the cytotoxic agent DM1 has shown robust activity in patients with trastuzumab-resistant HER2-positive breast cancer

Table 6 Combination of targeted therapies under clinical investigation for the treatment of drug-resistant and metastatic colorectal cancer

Agents	Targeted molecule (s)	Condition	Study phase	Clinical trial identifier
Encorafenib + Binimetinib + Cetuximab	Wild type plus BRAF V600E and MEK, EGFR	Previously untreated BRAF-mutant mCRC	Phase II	NCT03693170
Tucatinib + Trastuzumab	HER2	First-line HER2-positive mCRC	Phase III	NCT05253651
Disitamab + Vedotin + Tislelizumab	HER2 and PD-1	HER2-positive advanced CRC	Phase II	NCT05493683
Vanucizumab + Bevacizumab	VEGF-A/angiopoietin-2 and VEGF	mCRC	Phase II	NCT02141295
Regorafenib + Nivolumab	VEGFR1/2/3 and PD-1	Later-lines treatment of mCRC	Phase III	NCT05328908
Lenvatinib + Pembrolizumab	VEGFR1/2/3 and PD-1	mCRC	Phase III	NCT04776148
Fruquitinib + Camrelizumab	VEGFR tyrosine kinase and PD-1	Non-MSI-H/dMMR mCRC	Phase II	NCT04866862
Disitamab + Vedotin + Pembrolizumab	HER2 and PD-1	HER2-expressing mCRC	Phase II	NCT05333809
Cobimetinib + Atezolizumab	MAPK and PD-L1	mCRC	Phase III	NCT02788279
Cetuximab + Vemurafenib	EGFR and mutated BRAF V600E	BRAF V600E Mutated Advanced CRC	Phase II	NCT03727763
Penpulimab + Anlotinib	PD-1 and VEGFR1/2/3	Refractory mCRC	Phase II	NCT04970914
Favezelimab	LAG-3 and PD-1	Previously treated metastatic PD-L1 positive CRC	Phase III	NCT05064059
MEN1611 + Cetuximab	PI3K and EGFR	mCRC	Phase I/II	NCT04495621
Encorafenib + Cetuximab + Pembrolizumab	BRAF V600E, as well as wild-type BRAF, EGFR, andPD-1	Previously untreated mCRC	Phase II	NCT05217446
RXC004 + Nivolumab	Porcupine (wnt activator) and PD1	RNF43 or RSPO aberrated, metastatic, MSS CRC after progression on SOC	Phase II	NCT04907539
Regorafenib + Pembrolizumab	VEGFR1/2/3PD1	Advanced or mCRC	Phase I/II	NCT03657641
Isatuximab + Atezolizumab	Epitope on CD38, and PD-L1	mCRC	Phase I/II	NCT03555149
Atezolizumab + Selicrelumab + Bevacizumab	PD-L1, CD40 antigen, and VEGF	mCRC	Phase I/II	NCT03555149
Atezolizumab + Idasanutlin	PD-L1 and MDM2	mCRC	Phase I/II	NCT03555149
Atezolizumab + Regorafenib	PD-L1 andVEGFR1/2/3	mCRC	Phase I/II	NCT03555149
Olaparib (MK-7339) + Bevacizumab	PARP and VEGF	Unresectable or mCRC	Phase III	NCT04456699
Nivolumab + Ipilimumab	PD-1 andCTLA-4	dMMR and/or MSI mCRC resistant to anti-PD1 monotherapy	Phase II	NCT05310643
Nivolumab + Ipilimumab	PD-1 and CTLA-4	dMMR and/or MSI mCRC	Phase II	NCT04730544
Surufatinib + Sintilimab	VEGFR1/2/3 and PD-1	Advanced MSS-Type CRC	Phase II	NCT04764006
Camrelizumab + Apatinib	PD-1 and VEGFR-2	Advanced CRC	Phase I/II	NCT04067986
Fruquintinib + Tislelizumab + Stereotactic ablative radiotherapy	VEGFR1/2/3 and PD-1	mCRC	Phase II	NCT04948034
Avelumab + Cetuximab + mFOLFOXIRI	PD-1/PD-L1 and EGFR	Unresectable mCRC	Phase II	NCT04513951
Geptanolimab (GB226) + Fruquintinib	PD-1 and VEGFR1/2/3	mCRC	Phase I	NCT03977090
Selinexor + Pembrolizumab	Exportin 1 and PD-1	Previously treated mCRC with RAS mutations	Phase II	NCT04854434
Panitumumab + Rilotumumab	EGFR and HGF	wild-type KRAS mCRC	Phase I/II	NCT00788957

Panitumumab + Ganitumab	EGFR and IGF-1R	wild-type KRAS mCRC	Phase I/II	NCT00788957

MEK: Mitogen-activated extracellular signal-regulated kinase; EGFR: Epidermal growth factor receptor; mCRC: Metastatic colorectal cancer; HER2: Human epidermal growth factor receptor 2; PD-1: Programmed death-1; PD-L1: Programmed death ligand-1; VEGF-A: Vascular endothelial growth factor-A; VEGFR: Vascular endothelial growth factor receptor; MSI-H/dMMR: Microsatellite instability-high/mismatch repair deficient; MSS: Microsatellite stable; MAPK: mitogen-activated protein kinases; LAG-3 Lymphocyte activation gene 3; PI3K: Phosphoinositide 3-kinases; RNF43: Ring Finger Protein 43; RSPO: R-spondin; SOC: Standard of Care; PARP: Poly ADP ribose polymerase; CTLA-4: Cytotoxic T lymphocyte-associated antigen 4; HGF: Hepatocyte growth factor; IGF-1R: Insulin growth factor receptor-1.

[215]. A clinical trial is currently evaluating the efficacy of this new compound in HER2-positive mCRC progressing after trastuzumab and lapatinib (Table 1).

Overcoming resistance to anti-VEGF therapy

The major mechanisms of resistance to anti-VEGF therapy are still not fully elucidated. Redundancy in angiogenic signaling pathways and compensation through activation of other pathways may contribute to this resistance (Figure 3). Several agents are currently under development for the purpose of improving anti-angiogenic therapy efficacy (Table 2). Importantly, it has recently been shown that the location of the primary tumor affects the choice of targeted therapy for the treatment of mCRC, whereby left-sided tumors benefit more than right-sided tumors from EGFR inhibition[198,200]. As mentioned before, combining anti-angiogenic agents with immune checkpoint inhibitors has been shown to restore vascular-immune crosstalk to establish a strong anti-tumor immune response[216]. In addition to VEGF/VEGFR, targeting alternative angiogenic pathways such as FGF, PDGF, and angiopoietins can inhibit VEGF-independent angiogenic pathways that are activated in response to VEGF blockade[217]. In mCRC patients, increased plasma levels of FGF, PDGF, and placental growth factor were linked to disease progression during bevacizumab-based therapy[217]. The clinical efficacy of the dual inhibition of VEGF-A and angiopoietin-2 using vanucizumab is still under phase II clinical trials, though with promising results[218] (Table 2). It is important to note that additional factors, including hypoxia and the limited blood supply restrict the delivery of drugs to the tumor site, resulting in resistance. In addition, cancer resistance to anti-VEGF therapy has been linked to activation of the HGF/c-MET pathway[219]. The latter activates key pathways involved in CRC metastasis and drug-resistance, including MAPK/ERK, STAT3, NF-κB, and PI3K/Akt[219]. Several MET inhibitors are being evaluated in the clinic for the purpose of blocking MET to overcome resistance to anti-VEGFR treatment (Table 3). This approach has produced effective results in other types of cancer, including advanced renal cell carcinoma[220]. Dual inhibition of MET and VEGFR2 using cabozantinib showed a strong anti-tumor effect in a preclinical CRC PDX model and the effect was greatest in tumors that possessed a mutation in the *PIK3CA* gene[146]. Several trials have been initiated to evaluate the efficacy of this compound in mCRC (Table 3).

Overcoming resistance to immunotherapy

Evading the immune system is an important hallmark of cancer, including CRC and is linked to immunotherapy and targeted therapy resistance[221]. Intrinsic resistance to immunotherapy is mainly conferred by changes in anti-tumor immune response, aberrant expression of tumor antigens, functional gene mutations, alterations in antigen presentation and other signaling pathways in tumor cells, in addition to secretion of inhibitory molecules by tumor cells[222] (Figure 3). Extrinsic mechanisms include activation of immunosuppressive cells in the TME and abnormal tumor vascularization[222]. One of the most effective strategies to deal with resistance to immunotherapy involves increasing tumor visibility and infiltration by T cells, through induction of immunogenic cell death by targeted agents and other therapies. The success of combining anti-angiogenic agents with immunotherapy has been shown in several cancers and is being evaluated in phase III clinical studies involving patients with advanced or metastatic and/or refractory CRC (Table 6). In addition, the efficacy of combining immune checkpoint inhibitors with chemokines that mediate the recruitment of T cells into the TME warrants investigation in mCRC. This could also be achieved by the administration of VEGF inhibitors that would normalize tumor vasculature and permit T-cell infiltration[223].

Enhancing the immune system function is also a good strategy to activate effector T cells and inhibit immunosuppressive immune cells. An emerging approach is the dual or combinatory inhibition of PD-1/PD-L1 and CTLA-4 to concomitantly block immune system inhibitory pathways and has shown promising results in preclinical[224,225] and clinical[226] (Table 6) models of mCRC. Ongoing trials are also addressing genomic and epigenetic alterations by evaluating the efficacy of anti-PD-1 agents in combination with VEGFR or CTLA-4 inhibitors in dMMR and/or MSI mCRC (Table 6).

Implementation of better preclinical models

The importance of preclinical models has been highlighted in the case of mCRC. The rapidly emerging role of patient-derived tumor samples may be considered one of the revolutionizing approaches to improve treatment strategies. Such samples can be propagated in mice to produce PDXs or in three-

dimensional cultures to produce patient-derived organoids (PDOs)[227-230]. These models are important for understanding and predicting treatment responses in drug-resistant CRC and mCRC. Molecular response predictors are usually identified in clinical trials by employing a statistically significant enrichment for a genetic mutation and correlating it with a clinical outcome in responsive and non-responsive patients. A major limitation of this approach is the inability to elucidate the mechanisms underlying this correlation and to validate whether these predictors influence response to treatment. Cancer cell line cultures have made it possible to gain insight into the functional processes; however, they do not recapitulate the *in vivo* structure, in addition to the genomic and functional heterogeneity of mCRC. Therefore, patient-derived models are ideal platforms with clinical fidelity and good reflection of disease diversity. These models are being used for target discovery and for characterization of response biomarkers to combat drug-resistance and to predict treatment response[228]. For example, PDX were used to validate the correlation between *KRAS* mutations in exon 2 and *de novo* resistance to EGFR inhibition and to identify HER2 as a potential target in cetuximab-resistant mCRC[89,231]. Additionally, these models were the first to identify *KRAS* exon 3 and 4 mutations as predictors of resistance to EGFR mAbs[89]. Both PDX and PDOs have clinical relevance; however, PDOs are easier to cultivate and are useful for high-throughput drug screening[232]. Subsequently, PDOs have been used to model CRC and study mechanisms of resistance. In addition, the newly emerging CRISPR/Cas9 genome-editing tool has been applied to introduce mutations in normal human colorectal organoids and has confirmed the role of these mutations in CSC maintenance, in addition to metastasis and resistance to therapy[233,234]. The association between *KRAS* mutation and lack of response to EGFR blockade has been also validated in organoids derived from mCRC[235]. Importantly, results from PDOs have been shown to recapitulate clinical response to targeted therapies, including cetuximab and regorafenib[236]. Notably, PDO-based drug screening has been used to improve the accuracy and effectiveness of precision medicine, paving the way for PDO-based personalized therapy[237]. CRC PDOs can be also used to identify patients that benefit from a specific targeted therapy.

CONCLUSION

Given the high molecular heterogeneity associated with CRC, different mechanisms of resistance may develop. A multi-targeted approach to therapy and the use of combination targeted therapy as a first-line treatment, rather than after the patients demonstrate drug-resistance and progress on treatment, have been an active area of research based on the efficacy of these strategies in preclinical models. Several clinical trials have investigated the efficacy of combination therapies targeted at two or three pathways; however, the high toxicity levels associated with these therapies is a limitation to bear in mind as it represents a critical challenge to the development of effective therapies for the treatment of drug-resistant and mCRC. Nevertheless, data from clinical studies are showing promising signs of efficacy. This has been made possible through targeting adaptive feedback pathways and the discovery and implementation of predictive biomarkers for targeted therapy, which are critical in identifying patients that could benefit from combination targeted therapy. Biomarker detection computational algorithms and tools are being designed for this purpose and should be followed by clinical validation and approval. Importantly, personalized treatment could be developed to promote survival and prognosis of CRC patients without causing adverse events. With the advancement of NGS and genome profiling, it has been possible to decipher predictive responses to anti-cancer treatments and to select the appropriate treatment for each individual, depending on the genetic characteristics and clinical tumor features. Strategic planning of treatment regimens is essential to enhance the effectiveness of targeted agents and to decrease the possibility of side effects. Conjugation of inhibitory molecules using Nanoparticle technology is an attractive approach in this case. Nanoparticles are being used for the targeted delivery of drugs to the affected tissues and optimization methods can be applied to increase their uptake efficiency.

Other tools that could help improve personalized medicine include the triphasic enhanced computed tomography radiomics signature that was recently tested by Cao *et al*[238] and has been shown to be effective in predicting CRC MSI status with 0.837 and 0.821 accuracy and sensitivity, respectively. Moreover, whole genome sequencing, multi-region whole exome sequencing, simultaneous single-cell RNA-sequencing, and single-cell targeted cDNA Sanger sequencing are being used to obtain single-cell genomic and transcriptomic landscapes of adjacent normal tissues, primary tumors, and metastatic tumors[239], which could also improve individualized treatment.

Given the importance of the gut microbiota in the progression of CRC, microbiome profiles can be integrated with other genomic and epigenomic profiles to enhance personalized targeted therapies against CRC, resulting in better clinical outcomes. Nonetheless, this adds another level of complexity to the application of this approach. Interestingly, modification of the gut microbiota through targeted inhibition of pathogenic bacteria can be used to prepare patients for CRC treatment by augmenting the host immune system.

Changes in mutations or transcription should be monitored during administration of treatment, in addition to changes in immune responses and inflammatory molecules that can influence the choice of

treatment. These immune signatures may be indispensable for improving clinical outcome. Interestingly, it has been reported that the peripheral blood repertoire of T cell receptor changes during the course of chemotherapy in patients with mCRC, and thus could have a prognostic value[12].

In summary, the application of personalized medicine requires the integration of tumor mutations and epigenetic modifications, TME gene expression, host immune proficiency, and their changes during disease progression and treatment. The constant search for novel targets involved in drug-resistance and metastasis will lead to the identification of interesting molecular traits that can be modulated using biomarker-driven treatments to overcome resistance to therapy.

FOOTNOTES

Author contributions: Al Bitar S designed and wrote the first draft of the paper and collected and analyzed the data; El-Sabban M, Doughan S, and Abou-Kheir W are co-senior authors and contributed to conception and reviewed and edited the paper; Al Bitar S, El-Sabban M, Doughan S, and Abou-Kheir W provided the final approval of the version to be published.

Conflict-of-interest statement: All authors declare no conflicts of interest for this article.

Country/Territory of origin: Lebanon

ORCID number: Samar Al Bitar 0000-0002-0016-1029; Marwan El-Sabban 0000-0001-5084-7654; Samer Doughan 0000-0002-6584-6977; Wassim Abou-Kheir 0000-0001-9719-9324.

S-Editor: Liu GL
L-Editor: Webster JR
P-Editor: Liu GL

REFERENCES

1 **Siegel RL**, Miller KD, Jemal A. Cancer statistics, 2020. *CA Cancer J Clin* 2020; **70**: 7-30 [PMID: 31912902 DOI: 10.3322/caac.21590]
2 **Ferlay J**, Colombet M, Soerjomataram I, Dyba T, Randi G, Bettio M, Gavin A, Visser O, Bray F. Cancer incidence and mortality patterns in Europe: Estimates for 40 countries and 25 major cancers in 2018. *Eur J Cancer* 2018; **103**: 356-387 [PMID: 30100160 DOI: 10.1016/j.ejca.2018.07.005]
3 **Siegel R**, Ma J, Zou Z, Jemal A. Cancer statistics, 2014. *CA Cancer J Clin* 2014; **64**: 9-29 [PMID: 24399786 DOI: 10.3322/caac.21208]
4 **Advani S**, Kopetz S. Ongoing and future directions in the management of metastatic colorectal cancer: Update on clinical trials. *J Surg Oncol* 2019; **119**: 642-652 [PMID: 30852840 DOI: 10.1002/jso.25441]
5 **Shaukat A**, Levin TR. Current and future colorectal cancer screening strategies. *Nat Rev Gastroenterol Hepatol* 2022; **19**: 521-531 [PMID: 35505243 DOI: 10.1038/s41575-022-00612-y]
6 **Longley DB**, Johnston PG. Molecular mechanisms of drug resistance. *J Pathol* 2005; **205**: 275-292 [PMID: 15641020 DOI: 10.1002/path.1706]
7 **Gottesman MM**, Fojo T, Bates SE. Multidrug resistance in cancer: role of ATP-dependent transporters. *Nat Rev Cancer* 2002; **2**: 48-58 [PMID: 11902585 DOI: 10.1038/nrc706]
8 **Dasari S**, Tchounwou PB. Cisplatin in cancer therapy: molecular mechanisms of action. *Eur J Pharmacol* 2014; **740**: 364-378 [PMID: 25058905 DOI: 10.1016/j.ejphar.2014.07.025]
9 **Xie YH**, Chen YX, Fang JY. Comprehensive review of targeted therapy for colorectal cancer. *Signal Transduct Target Ther* 2020; **5**: 22 [PMID: 32296018 DOI: 10.1038/s41392-020-0116-z]
10 **Mardis ER**. The Impact of Next-Generation Sequencing on Cancer Genomics: From Discovery to Clinic. *Cold Spring Harb Perspect Med* 2019; **9** [PMID: 30397020 DOI: 10.1101/cshperspect.a036269]
11 **Messersmith WA**. NCCN Guidelines Updates: Management of Metastatic Colorectal Cancer. *J Natl Compr Canc Netw* 2019; **17**: 599-601 [PMID: 31117039 DOI: 10.6004/jnccn.2019.5014]
12 **Chen K**, Zhang C, Ling S, Wei R, Wang J, Xu X. The metabolic flexibility of quiescent CSC: implications for chemotherapy resistance. *Cell Death Dis* 2021; **12**: 835 [PMID: 34482364 DOI: 10.1038/s41419-021-04116-6]
13 **Mittal V**. Epithelial Mesenchymal Transition in Tumor Metastasis. *Annu Rev Pathol* 2018; **13**: 395-412 [PMID: 29414248 DOI: 10.1146/annurev-pathol-020117-043854]
14 **Begicevic RR**, Falasca M. ABC Transporters in Cancer Stem Cells: Beyond Chemoresistance. *Int J Mol Sci* 2017; **18** [PMID: 29117122 DOI: 10.3390/ijms18112362]

15 **Steinbichler TB**, Dudás J, Skvortsov S, Ganswindt U, Riechelmann H, Skvortsova II. Therapy resistance mediated by cancer stem cells. *Semin Cancer Biol* 2018; **53**: 156-167 [PMID: 30471331 DOI: 10.1016/j.semcancer.2018.11.006]

16 **Gottesman MM**, Ling V. The molecular basis of multidrug resistance in cancer: the early years of P-glycoprotein research. *FEBS Lett* 2006; **580**: 998-1009 [PMID: 16405967 DOI: 10.1016/j.febslet.2005.12.060]

17 **Du J**, He Y, Li P, Wu W, Chen Y, Ruan H. IL-8 regulates the doxorubicin resistance of colorectal cancer cells *via* modulation of multidrug resistance 1 (MDR1). *Cancer Chemother Pharmacol* 2018; **81**: 1111-1119 [PMID: 29693201 DOI: 10.1007/s00280-018-3584-x]

18 **Wu CP**, Ohnuma S, Ambudkar SV. Discovering natural product modulators to overcome multidrug resistance in cancer chemotherapy. *Curr Pharm Biotechnol* 2011; **12**: 609-620 [PMID: 21118092 DOI: 10.2174/138920111795163887]

19 **Hlavata I**, Mohelnikova-Duchonova B, Vaclavikova R, Liska V, Pitule P, Novak P, Bruha J, Vycital O, Holubec L, Treska V, Vodicka P, Soucek P. The role of ABC transporters in progression and clinical outcome of colorectal cancer. *Mutagenesis* 2012; **27**: 187-196 [PMID: 22294766 DOI: 10.1093/mutage/ger075]

20 **Kosuri KV**, Wu X, Wang L, Villalona-Calero MA, Otterson GA. An epigenetic mechanism for capecitabine resistance in mesothelioma. *Biochem Biophys Res Commun* 2010; **391**: 1465-1470 [PMID: 20035722 DOI: 10.1016/j.bbrc.2009.12.095]

21 **Longley DB**, Harkin DP, Johnston PG. 5-fluorouracil: mechanisms of action and clinical strategies. *Nat Rev Cancer* 2003; **3**: 330-338 [PMID: 12724731 DOI: 10.1038/nrc1074]

22 **Blondy S**, David V, Verdier M, Mathonnet M, Perraud A, Christou N. 5-Fluorouracil resistance mechanisms in colorectal cancer: From classical pathways to promising processes. *Cancer Sci* 2020; **111**: 3142-3154 [PMID: 32536012 DOI: 10.1111/cas.14532]

23 **Griffith M**, Mwenifumbo JC, Cheung PY, Paul JE, Pugh TJ, Tang MJ, Chittaranjan S, Morin RD, Asano JK, Ally AA, Miao L, Lee A, Chan SY, Taylor G, Severson T, Hou YC, Griffith OL, Cheng GS, Novik K, Moore R, Luk M, Owen D, Brown CJ, Morin GB, Gill S, Tai IT, Marra MA. Novel mRNA isoforms and mutations of uridine monophosphate synthetase and 5-fluorouracil resistance in colorectal cancer. *Pharmacogenomics J* 2013; **13**: 148-158 [PMID: 22249354 DOI: 10.1038/tpj.2011.65]

24 **Lindskog EB**, Derwinger K, Gustavsson B, Falk P, Wettergren Y. Thymidine phosphorylase expression is associated with time to progression in patients with metastatic colorectal cancer. *BMC Clin Pathol* 2014; **14**: 25 [PMID: 24936150 DOI: 10.1186/1472-6890-14-25]

25 **Uchino J**, Takayama K, Harada A, Sone T, Harada T, Curiel DT, Kuroki M, Nakanishi Y. Tumor targeting carboxylesterase fused with anti-CEA scFv improve the anticancer effect with a less toxic dose of irinotecan. *Cancer Gene Ther* 2008; **15**: 94-100 [PMID: 18157147 DOI: 10.1038/sj.cgt.7701100]

26 **de Man FM**, Goey AKL, van Schaik RHN, Mathijssen RHJ, Bins S. Individualization of Irinotecan Treatment: A Review of Pharmacokinetics, Pharmacodynamics, and Pharmacogenetics. *Clin Pharmacokinet* 2018; **57**: 1229-1254 [PMID: 29520731 DOI: 10.1007/s40262-018-0644-7]

27 **Innocenti F**, Undevia SD, Ramírez J, Mani S, Schilsky RL, Vogelzang NJ, Prado M, Ratain MJ. A phase I trial of pharmacologic modulation of irinotecan with cyclosporine and phenobarbital. *Clin Pharmacol Ther* 2004; **76**: 490-502 [PMID: 15536463 DOI: 10.1016/j.clpt.2004.07.016]

28 **Salonga D**, Danenberg KD, Johnson M, Metzger R, Groshen S, Tsao-Wei DD, Lenz HJ, Leichman CG, Leichman L, Diasio RB, Danenberg PV. Colorectal tumors responding to 5-fluorouracil have low gene expression levels of dihydropyrimidine dehydrogenase, thymidylate synthase, and thymidine phosphorylase. *Clin Cancer Res* 2000; **6**: 1322-1327 [PMID: 10778957]

29 **Soong R**, Shah N, Salto-Tellez M, Tai BC, Soo RA, Han HC, Ng SS, Tan WL, Zeps N, Joseph D, Diasio RB, Iacopetta B. Prognostic significance of thymidylate synthase, dihydropyrimidine dehydrogenase and thymidine phosphorylase protein expression in colorectal cancer patients treated with or without 5-fluorouracil-based chemotherapy. *Ann Oncol* 2008; **19**: 915-919 [PMID: 18245778 DOI: 10.1093/annonc/mdm599]

30 **Maréchal A**, Zou L. DNA damage sensing by the ATM and ATR kinases. *Cold Spring Harb Perspect Biol* 2013; **5** [PMID: 24003211 DOI: 10.1101/cshperspect.a012716]

31 **Reinhardt HC**, Aslanian AS, Lees JA, Yaffe MB. p53-deficient cells rely on ATM- and ATR-mediated checkpoint signaling through the p38MAPK/MK2 pathway for survival after DNA damage. *Cancer Cell* 2007; **11**: 175-189 [PMID: 17292828 DOI: 10.1016/j.ccr.2006.11.024]

32 **Peitzsch C**, Kurth I, Kunz-Schughart L, Baumann M, Dubrovska A. Discovery of the cancer stem cell related determinants of radioresistance. *Radiother Oncol* 2013; **108**: 378-387 [PMID: 23830195 DOI: 10.1016/j.radonc.2013.06.003]

33 **Mirza-Aghazadeh-Attari M**, Darband SG, Kaviani M, Mihanfar A, Aghazadeh Attari J, Yousefi B, Majidinia M. DNA damage response and repair in colorectal cancer: Defects, regulation and therapeutic implications. *DNA Repair (Amst)* 2018; **69**: 34-52 [PMID: 30055507 DOI: 10.1016/j.dnarep.2018.07.005]

34 **Marin JJ**, Sanchez de Medina F, Castaño B, Bujanda L, Romero MR, Martinez-Augustin O, Moral-Avila RD, Briz O. Chemoprevention, chemotherapy, and chemoresistance in colorectal cancer. *Drug Metab Rev* 2012; **44**: 148-172 [PMID: 22497631 DOI: 10.3109/03602532.2011.638303]

35 **Shirota Y**, Stoehlmacher J, Brabender J, Xiong YP, Uetake H, Danenberg KD, Groshen S, Tsao-Wei DD, Danenberg PV, Lenz HJ. ERCC1 and thymidylate synthase mRNA levels predict survival for colorectal cancer patients receiving combination oxaliplatin and fluorouracil chemotherapy. *J Clin Oncol* 2001; **19**: 4298-4304 [PMID: 11731512 DOI: 10.1200/JCO.2001.19.23.4298]

36 **Zhao J**. Cancer stem cells and chemoresistance: The smartest survives the raid. *Pharmacol Ther* 2016; **160**: 145-158 [PMID: 26899500 DOI: 10.1016/j.pharmthera.2016.02.008]

37 **Ayob AZ**, Ramasamy TS. Cancer stem cells as key drivers of tumour progression. *J Biomed Sci* 2018; **25**: 20 [PMID: 29506506 DOI: 10.1186/s12929-018-0426-4]

38 **Hu T**, Li Z, Gao CY, Cho CH. Mechanisms of drug resistance in colon cancer and its therapeutic strategies. *World J Gastroenterol* 2016; **22**: 6876-6889 [PMID: 27570424 DOI: 10.3748/wjg.v22.i30.6876]

39 **Campbell KJ**, Tait SWG. Targeting BCL-2 regulated apoptosis in cancer. *Open Biol* 2018; **8** [PMID: 29769323 DOI: 10.1098/rsob.180002]

40 **Holohan C**, Van Schaeybroeck S, Longley DB, Johnston PG. Cancer drug resistance: an evolving paradigm. *Nat Rev Cancer* 2013; **13**: 714-726 [PMID: 24060863 DOI: 10.1038/nrc3599]

41 **MacDonald BT**, Tamai K, He X. Wnt/beta-catenin signaling: components, mechanisms, and diseases. *Dev Cell* 2009; **17**: 9-26 [PMID: 19619488 DOI: 10.1016/j.devcel.2009.06.016]

42 **Das PK**, Islam F, Lam AK. The Roles of Cancer Stem Cells and Therapy Resistance in Colorectal Carcinoma. *Cells* 2020; **9** [PMID: 32503256 DOI: 10.3390/cells9061392]

43 **Gout S**, Huot J. Role of cancer microenvironment in metastasis: focus on colon cancer. *Cancer Microenviron* 2008; **1**: 69-83 [PMID: 19308686 DOI: 10.1007/s12307-008-0007-2]

44 **Labani-Motlagh A**, Ashja-Mahdavi M, Loskog A. The Tumor Microenvironment: A Milieu Hindering and Obstructing Antitumor Immune Responses. *Front Immunol* 2020; **11**: 940 [PMID: 32499786 DOI: 10.3389/fimmu.2020.00940]

45 **Peddareddigari VG**, Wang D, Dubois RN. The tumor microenvironment in colorectal carcinogenesis. *Cancer Microenviron* 2010; **3**: 149-166 [PMID: 21209781 DOI: 10.1007/s12307-010-0038-3]

46 **Prieto-Vila M**, Takahashi RU, Usuba W, Kohama I, Ochiya T. Drug Resistance Driven by Cancer Stem Cells and Their Niche. *Int J Mol Sci* 2017; **18** [PMID: 29194401 DOI: 10.3390/ijms18122574]

47 **Kim J**, Lee HK. Potential Role of the Gut Microbiome In Colorectal Cancer Progression. *Front Immunol* 2021; **12**: 807648 [PMID: 35069592 DOI: 10.3389/fimmu.2021.807648]

48 **Yu T**, Guo F, Yu Y, Sun T, Ma D, Han J, Qian Y, Kryczek I, Sun D, Nagarsheth N, Chen Y, Chen H, Hong J, Zou W, Fang JY. Fusobacterium nucleatum Promotes Chemoresistance to Colorectal Cancer by Modulating Autophagy. *Cell* 2017; **170**: 548-563.e16 [PMID: 28753429 DOI: 10.1016/j.cell.2017.07.008]

49 **Iida N**, Dzutsev A, Stewart CA, Smith L, Bouladoux N, Weingarten RA, Molina DA, Salcedo R, Back T, Cramer S, Dai RM, Kiu H, Cardone M, Naik S, Patri AK, Wang E, Marincola FM, Frank KM, Belkaid Y, Trinchieri G, Goldszmid RS. Commensal bacteria control cancer response to therapy by modulating the tumor microenvironment. *Science* 2013; **342**: 967-970 [PMID: 24264989 DOI: 10.1126/science.1240527]

50 **Gopalakrishnan V**, Spencer CN, Nezi L, Reuben A, Andrews MC, Karpinets TV, Prieto PA, Vicente D, Hoffman K, Wei SC, Cogdill AP, Zhao L, Hudgens CW, Hutchinson DS, Manzo T, Petaccia de Macedo M, Cotechini T, Kumar T, Chen WS, Reddy SM, Szczepaniak Sloane R, Galloway-Pena J, Jiang H, Chen PL, Shpall EJ, Rezvani K, Alousi AM, Chemaly RF, Shelburne S, Vence LM, Okhuysen PC, Jensen VB, Swennes AG, McAllister F, Marcelo Riquelme Sanchez E, Zhang Y, Le Chatelier E, Zitvogel L, Pons N, Austin-Breneman JL, Haydu LE, Burton EM, Gardner JM, Sirmans E, Hu J, Lazar AJ, Tsujikawa T, Diab A, Tawbi H, Glitza IC, Hwu WJ, Patel SP, Woodman SE, Amaria RN, Davies MA, Gershenwald JE, Hwu P, Lee JE, Zhang J, Coussens LM, Cooper ZA, Futreal PA, Daniel CR, Ajami NJ, Petrosino JF, Tetzlaff MT, Sharma P, Allison JP, Jenq RR, Wargo JA. Gut microbiome modulates response to anti-PD-1 immunotherapy in melanoma patients. *Science* 2018; **359**: 97-103 [PMID: 29097493 DOI: 10.1126/science.aan4236]

51 **Routy B**, Le Chatelier E, Derosa L, Duong CPM, Alou MT, Daillère R, Fluckiger A, Messaoudene M, Rauber C, Roberti MP, Fidelle M, Flament C, Poirier-Colame V, Opolon P, Klein C, Iribarren K, Mondragón L, Jacquelot N, Qu B, Ferrere G, Clémenson C, Mezquita L, Masip JR, Naltet C, Brosseau S, Kaderbhai C, Richard C, Rizvi H, Levenez F, Galleron N, Quinquis B, Pons N, Ryffel B, Minard-Colin V, Gonin P, Soria JC, Deutsch E, Loriot Y, Ghiringhelli F, Zalcman G, Goldwasser F, Escudier B, Hellmann MD, Eggermont A, Raoult D, Albiges L, Kroemer G, Zitvogel L. Gut microbiome influences efficacy of PD-1-based immunotherapy against epithelial tumors. *Science* 2018; **359**: 91-97 [PMID: 29097494 DOI: 10.1126/science.aan3706]

52 **Vétizou M**, Pitt JM, Daillère R, Lepage P, Waldschmitt N, Flament C, Rusakiewicz S, Routy B, Roberti MP, Duong CP, Poirier-Colame V, Roux A, Becharef S, Formenti S, Golden E, Cording S, Eberl G, Schlitzer A, Ginhoux F, Mani S, Yamazaki T, Jacquelot N, Enot DP, Bérard M, Nigou J, Opolon P, Eggermont A, Woerther PL, Chachaty E, Chaput N, Robert C, Mateus C, Kroemer G, Raoult D, Boneca IG, Carbonnel F, Chamaillard M, Zitvogel L. Anticancer immunotherapy by CTLA-4 blockade relies on the gut microbiota. *Science* 2015; **350**: 1079-1084 [PMID: 26541610 DOI: 10.1126/science.aad1329]

53 **Hayase E**, Jenq RR. Role of the intestinal microbiome and microbial-derived metabolites in immune checkpoint blockade immunotherapy of cancer. *Genome Med* 2021; **13**: 107 [PMID: 34162429 DOI: 10.1186/s13073-021-00923-w]

54 **Oh DY**, Bang YJ. HER2-targeted therapies - a role beyond breast cancer. *Nat Rev Clin Oncol* 2020; **17**: 33-48 [PMID: 31548601 DOI: 10.1038/s41571-019-0268-3]

55 **Chan DLH**, Segelov E, Wong RS, Smith A, Herbertson RA, Li BT, Tebbutt N, Price T, Pavlakis N. Epidermal growth factor receptor (EGFR) inhibitors for metastatic colorectal cancer. *Cochrane Database Syst Rev* 2017; **6**: CD007047 [PMID: 28654140 DOI: 10.1002/14651858.CD007047.pub2]

56 **Seshacharyulu P**, Ponnusamy MP, Haridas D, Jain M, Ganti AK, Batra SK. Targeting the EGFR signaling pathway in cancer therapy. *Expert Opin Ther Targets* 2012; **16**: 15-31 [PMID: 22239438 DOI: 10.1517/14728222.2011.648617]

57 **Messa C**, Russo F, Caruso MG, Di Leo A. EGF, TGF-alpha, and EGF-R in human colorectal adenocarcinoma. *Acta Oncol* 1998; **37**: 285-289 [PMID: 9677101 DOI: 10.1080/028418698429595]

58 **Salomon DS**, Brandt R, Ciardiello F, Normanno N. Epidermal growth factor-related peptides and their receptors in human malignancies. *Crit Rev Oncol Hematol* 1995; **19**: 183-232 [PMID: 7612182 DOI: 10.1016/1040-8428(94)00144-i]

59 **Mayer A**, Takimoto M, Fritz E, Schellander G, Kofler K, Ludwig H. The prognostic significance of proliferating cell nuclear antigen, epidermal growth factor receptor, and mdr gene expression in colorectal cancer. *Cancer* 1993; **71**: 2454-2460 [PMID: 8095852 DOI: 10.1002/1097-0142(19930415)71:8<2454::aid-cncr2820710805>3.0.co;2-2]

60 **Douillard JY**, Siena S, Cassidy J, Tabernero J, Burkes R, Barugel M, Humblet Y, Bodoky G, Cunningham D, Jassem J, Rivera F, Kocákova I, Ruff P, Błasińska-Morawiec M, Šmakal M, Canon JL, Rother M, Oliner KS, Wolf M, Gansert J. Randomized, phase III trial of panitumumab with infusional fluorouracil, leucovorin, and oxaliplatin (FOLFOX4) *vs* FOLFOX4 alone as first-line treatment in patients with previously untreated metastatic colorectal cancer: the PRIME study. *J Clin Oncol* 2010; **28**: 4697-4705 [PMID: 20921465 DOI: 10.1200/JCO.2009.27.4860]

61 **Wee P**, Wang Z. Epidermal Growth Factor Receptor Cell Proliferation Signaling Pathways. *Cancers (Basel)* 2017; **9**

[PMID: 28513565 DOI: 10.3390/cancers9050052]

62 **Yarom N**, Jonker DJ. The role of the epidermal growth factor receptor in the mechanism and treatment of colorectal cancer. *Discov Med* 2011; **11**: 95-105 [PMID: 21356164]

63 **Loft M**, Shapiro J, Lee M, Wong R, Tie J, Kosmider S, Wong V, Jalali A, Lee B, Ananda SS, Gibbs P. Compliance with Therapeutic Goods Association prescribing information: weekly or second weekly cetuximab for the treatment of metastatic colorectal cancer. *Intern Med J* 2022 [PMID: 35668542 DOI: 10.1111/imj.15835]

64 **Cunningham D**, Humblet Y, Siena S, Khayat D, Bleiberg H, Santoro A, Bets D, Mueser M, Harstrick A, Verslype C, Chau I, Van Cutsem E. Cetuximab monotherapy and cetuximab plus irinotecan in irinotecan-refractory metastatic colorectal cancer. *N Engl J Med* 2004; **351**: 337-345 [PMID: 15269313 DOI: 10.1056/NEJMoa033025]

65 **Van Cutsem E**, Köhne CH, Hitre E, Zaluski J, Chang Chien CR, Makhson A, D'Haens G, Pintér T, Lim R, Bodoky G, Roh JK, Folprecht G, Ruff P, Stroh C, Tejpar S, Schlichting M, Nippgen J, Rougier P. Cetuximab and chemotherapy as initial treatment for metastatic colorectal cancer. *N Engl J Med* 2009; **360**: 1408-1417 [PMID: 19339720 DOI: 10.1056/NEJMoa0805019]

66 **Bokemeyer C**, Bondarenko I, Makhson A, Hartmann JT, Aparicio J, de Braud F, Donea S, Ludwig H, Schuch G, Stroh C, Loos AH, Zubel A, Koralewski P. Fluorouracil, leucovorin, and oxaliplatin with and without cetuximab in the first-line treatment of metastatic colorectal cancer. *J Clin Oncol* 2009; **27**: 663-671 [PMID: 19114683 DOI: 10.1200/JCO.2008.20.8397]

67 **Maughan TS**, Adams RA, Smith CG, Meade AM, Seymour MT, Wilson RH, Idziaszczyk S, Harris R, Fisher D, Kenny SL, Kay E, Mitchell JK, Madi A, Jasani B, James MD, Bridgewater J, Kennedy MJ, Claes B, Lambrechts D, Kaplan R, Cheadle JP; MRC COIN Trial Investigators. Addition of cetuximab to oxaliplatin-based first-line combination chemotherapy for treatment of advanced colorectal cancer: results of the randomised phase 3 MRC COIN trial. *Lancet* 2011; **377**: 2103-2114 [PMID: 21641636 DOI: 10.1016/S0140-6736(11)60613-2]

68 **Douillard JY**, Siena S, Cassidy J, Tabernero J, Burkes R, Barugel M, Humblet Y, Bodoky G, Cunningham D, Jassem J, Rivera F, Kocákova I, Ruff P, Błasińska-Morawiec M, Šmakal M, Canon JL, Rother M, Oliner KS, Tian Y, Xu F, Sidhu R. Final results from PRIME: randomized phase III study of panitumumab with FOLFOX4 for first-line treatment of metastatic colorectal cancer. *Ann Oncol* 2014; **25**: 1346-1355 [PMID: 24718886 DOI: 10.1093/annonc/mdu141]

69 **Amado RG**, Wolf M, Peeters M, Van Cutsem E, Siena S, Freeman DJ, Juan T, Sikorski R, Suggs S, Radinsky R, Patterson SD, Chang DD. Wild-type KRAS is required for panitumumab efficacy in patients with metastatic colorectal cancer. *J Clin Oncol* 2008; **26**: 1626-1634 [PMID: 18316791 DOI: 10.1200/JCO.2007.14.7116]

70 **Van Cutsem E**, Peeters M, Siena S, Humblet Y, Hendlisz A, Neyns B, Canon JL, Van Laethem JL, Maurel J, Richardson G, Wolf M, Amado RG. Open-label phase III trial of panitumumab plus best supportive care compared with best supportive care alone in patients with chemotherapy-refractory metastatic colorectal cancer. *J Clin Oncol* 2007; **25**: 1658-1664 [PMID: 17470858 DOI: 10.1200/JCO.2006.08.1620]

71 **Modest DP**, Karthaus M, Kasper S, Moosmann N, Keitel V, Kiani A, Uhlig J, Jacobasch L, Fischer V Weikersthal L, Fuchs M, Kaiser F, Lerchenmüller C, Sent D, Junghanß C, Held S, Lorenzen S, Kaczirek K, Jung A, Stintzing S, Heinemann V. FOLFOX plus panitumumab or FOLFOX alone as additive therapy following R0/1 resection of RAS wild-type colorectal cancer liver metastases - The PARLIM trial (AIO KRK 0314). *Eur J Cancer* 2022; **173**: 297-306 [PMID: 35970102 DOI: 10.1016/j.ejca.2022.07.012]

72 **Janani B**, Vijayakumar M, Priya K, Kim JH, Prabakaran DS, Shahid M, Al-Ghamdi S, Alsaidan M, Othman Bahakim N, Hassan Abdelzaher M, Ramesh T. EGFR-Based Targeted Therapy for Colorectal Cancer-Promises and Challenges. *Vaccines (Basel)* 2022; **10** [PMID: 35455247 DOI: 10.3390/vaccines10040499]

73 **Favoni RE**, Pattarozzi A, Lo Casto M, Barbieri F, Gatti M, Paleari L, Bajetto A, Porcile C, Gaudino G, Mutti L, Corte G, Florio T. Gefitinib targets EGFR dimerization and ERK1/2 phosphorylation to inhibit pleural mesothelioma cell proliferation. *Curr Cancer Drug Targets* 2010; **10**: 176-191 [PMID: 20088784 DOI: 10.2174/156800910791054130]

74 **Yonesaka K**, Zejnullahu K, Okamoto I, Satoh T, Cappuzzo F, Souglakos J, Ercan D, Rogers A, Roncalli M, Takeda M, Fujisaka Y, Philips J, Shimizu T, Maenishi O, Cho Y, Sun J, Destro A, Taira K, Takeda K, Okabe T, Swanson J, Itoh H, Takada M, Lifshits E, Okuno K, Engelman JA, Shivdasani RA, Nishio K, Fukuoka M, Varella-Garcia M, Nakagawa K, Jänne PA. Activation of ERBB2 signaling causes resistance to the EGFR-directed therapeutic antibody cetuximab. *Sci Transl Med* 2011; **3**: 99ra86 [PMID: 21900593 DOI: 10.1126/scitranslmed.3002442]

75 **Mohan S**, Heitzer E, Ulz P, Lafer I, Lax S, Auer M, Pichler M, Gerger A, Eisner F, Hoefler G, Bauernhofer T, Geigl JB, Speicher MR. Changes in colorectal carcinoma genomes under anti-EGFR therapy identified by whole-genome plasma DNA sequencing. *PLoS Genet* 2014; **10**: e1004271 [PMID: 24676216 DOI: 10.1371/journal.pgen.1004271]

76 **Popescu NC**, King CR, Kraus MH. Localization of the human erbB-2 gene on normal and rearranged chromosomes 17 to bands q12-21.32. *Genomics* 1989; **4**: 362-366 [PMID: 2565881 DOI: 10.1016/0888-7543(89)90343-1]

77 **Martin V**, Cappuzzo F, Mazzucchelli L, Frattini M. HER2 in solid tumors: more than 10 years under the microscope; where are we now? *Future Oncol* 2014; **10**: 1469-1486 [PMID: 25052756 DOI: 10.2217/fon.14.19]

78 **Graus-Porta D**, Beerli RR, Daly JM, Hynes NE. ErbB-2, the preferred heterodimerization partner of all ErbB receptors, is a mediator of lateral signaling. *EMBO J* 1997; **16**: 1647-1655 [PMID: 9130710 DOI: 10.1093/emboj/16.7.1647]

79 **Holbro T**, Beerli RR, Maurer F, Koziczak M, Barbas CF 3rd, Hynes NE. The ErbB2/ErbB3 heterodimer functions as an oncogenic unit: ErbB2 requires ErbB3 to drive breast tumor cell proliferation. *Proc Natl Acad Sci U S A* 2003; **100**: 8933-8938 [PMID: 12853564 DOI: 10.1073/pnas.1537685100]

80 **Richman SD**, Southward K, Chambers P, Cross D, Barrett J, Hemmings G, Taylor M, Wood H, Hutchins G, Foster JM, Oumie A, Spink KG, Brown SR, Jones M, Kerr D, Handley K, Gray R, Seymour M, Quirke P. HER2 overexpression and amplification as a potential therapeutic target in colorectal cancer: analysis of 3256 patients enrolled in the QUASAR, FOCUS and PICCOLO colorectal cancer trials. *J Pathol* 2016; **238**: 562-570 [PMID: 26690310 DOI: 10.1002/path.4679]

81 **Valtorta E**, Martino C, Sartore-Bianchi A, Penaullt-Llorca F, Viale G, Risio M, Rugge M, Grigioni W, Bencardino K, Lonardi S, Zagonel V, Leone F, Noe J, Ciardiello F, Pinto C, Labianca R, Mosconi S, Graiff C, Aprile G, Frau B, Garufi C, Loupakis F, Racca P, Tonini G, Lauricella C, Veronese S, Truini M, Siena S, Marsoni S, Gambacorta M. Assessment of a HER2 scoring system for colorectal cancer: results from a validation study. *Mod Pathol* 2015; **28**: 1481-1491 [PMID:

26449765 DOI: 10.1038/modpathol.2015.98]
82 **Schuell B**, Gruenberger T, Scheithauer W, Zielinski Ch, Wrba F. HER 2/neu protein expression in colorectal cancer. *BMC Cancer* 2006; **6**: 123 [PMID: 16681853 DOI: 10.1186/1471-2407-6-123]
83 **Kavanagh DO**, Chambers G, O'Grady L, Barry KM, Waldron RP, Bennani F, Eustace PW, Tobbia I. Is overexpression of HER-2 a predictor of prognosis in colorectal cancer? *BMC Cancer* 2009; **9**: 1 [PMID: 19118499 DOI: 10.1186/1471-2407-9-1]
84 **Marx AH**, Burandt EC, Choschzick M, Simon R, Yekebas E, Kaifi JT, Mirlacher M, Atanackovic D, Bokemeyer C, Fiedler W, Terracciano L, Sauter G, Izbicki JR. Heterogenous high-level HER-2 amplification in a small subset of colorectal cancers. *Hum Pathol* 2010; **41**: 1577-1585 [PMID: 20656317 DOI: 10.1016/j.humpath.2010.02.018]
85 **Osako T**, Miyahara M, Uchino S, Inomata M, Kitano S, Kobayashi M. Immunohistochemical study of c-erbB-2 protein in colorectal cancer and the correlation with patient survival. *Oncology* 1998; **55**: 548-555 [PMID: 9778622 DOI: 10.1159/000011911]
86 **Caruso ML**, Valentini AM. Immunohistochemical p53 overexpression correlated to c-erbB-2 and cathepsin D proteins in colorectal cancer. *Anticancer Res* 1996; **16**: 3813-3818 [PMID: 9042263]
87 **Siena S**, Sartore-Bianchi A, Marsoni S, Hurwitz HI, McCall SJ, Penault-Llorca F, Srock S, Bardelli A, Trusolino L. Targeting the human epidermal growth factor receptor 2 (HER2) oncogene in colorectal cancer. *Ann Oncol* 2018; **29**: 1108-1119 [PMID: 29659677 DOI: 10.1093/annonc/mdy100]
88 **Ramanathan RK**, Hwang JJ, Zamboni WC, Sinicrope FA, Safran H, Wong MK, Earle M, Brufsky A, Evans T, Troetschel M, Walko C, Day R, Chen HX, Finkelstein S. Low overexpression of HER-2/neu in advanced colorectal cancer limits the usefulness of trastuzumab (Herceptin) and irinotecan as therapy. A phase II trial. *Cancer Invest* 2004; **22**: 858-865 [PMID: 15641483 DOI: 10.1081/cnv-200039645]
89 **Bertotti A**, Migliardi G, Galimi F, Sassi F, Torti D, Isella C, Corà D, Di Nicolantonio F, Buscarino M, Petti C, Ribero D, Russolillo N, Muratore A, Massucco P, Pisacane A, Molinaro L, Valtorta E, Sartore-Bianchi A, Risio M, Capussotti L, Gambacorta M, Siena S, Medico E, Sapino A, Marsoni S, Comoglio PM, Bardelli A, Trusolino L. A molecularly annotated platform of patient-derived xenografts ("xenopatients") identifies HER2 as an effective therapeutic target in cetuximab-resistant colorectal cancer. *Cancer Discov* 2011; **1**: 508-523 [PMID: 22586653 DOI: 10.1158/2159-8290.CD-11-0109]
90 **Luca T**, Barresi V, Privitera G, Musso N, Caruso M, Condorelli DF, Castorina S. In vitro combined treatment with cetuximab and trastuzumab inhibits growth of colon cancer cells. *Cell Prolif* 2014; **47**: 435-447 [PMID: 25131935 DOI: 10.1111/cpr.12125]
91 **Kavuri SM**, Jain N, Galimi F, Cottino F, Leto SM, Migliardi G, Searleman AC, Shen W, Monsey J, Trusolino L, Jacobs SA, Bertotti A, Bose R. HER2 activating mutations are targets for colorectal cancer treatment. *Cancer Discov* 2015; **5**: 832-841 [PMID: 26243863 DOI: 10.1158/2159-8290.CD-14-1211]
92 **Rubinson DA**, Hochster HS, Ryan DP, Wolpin BM, McCleary NJ, Abrams TA, Chan JA, Iqbal S, Lenz HJ, Lim D, Rose J, Bekaii-Saab T, Chen HX, Fuchs CS, Ng K. Multi-drug inhibition of the HER pathway in metastatic colorectal cancer: results of a phase I study of pertuzumab plus cetuximab in cetuximab-refractory patients. *Invest New Drugs* 2014; **32**: 113-122 [PMID: 23568716 DOI: 10.1007/s10637-013-9956-5]
93 **Chang AY**, Lopes G, Hsin KW, Lim R, Fong FK, Wong J. Phase II trial of 5-fluorouracil/Leucovorin/gemcitabine/cisplatin as second-line treatment in patients with metastatic or recurrent colorectal carcinoma: a cancer therapeutics research group study. *Clin Colorectal Cancer* 2007; **6**: 646-651 [PMID: 17945037 DOI: 10.3816/CCC.2007.n.033]
94 **Bekaii-Saab TS**, Roda JM, Guenterberg KD, Ramaswamy B, Young DC, Ferketich AK, Lamb TA, Grever MR, Shapiro CL, Carson WE 3rd. A phase I trial of paclitaxel and trastuzumab in combination with interleukin-12 in patients with HER2/neu-expressing malignancies. *Mol Cancer Ther* 2009; **8**: 2983-2991 [PMID: 19887543 DOI: 10.1158/1535-7163.MCT-09-0820]
95 **Sartore-Bianchi A**, Trusolino L, Martino C, Bencardino K, Lonardi S, Bergamo F, Zagonel V, Leone F, Depetris I, Martinelli E, Troiani T, Ciardiello F, Racca P, Bertotti A, Siravegna G, Torri V, Amatu A, Ghezzi S, Marrapese G, Palmeri L, Valtorta E, Cassingena A, Lauricella C, Vanzulli A, Regge D, Veronese S, Comoglio PM, Bardelli A, Marsoni S, Siena S. Dual-targeted therapy with trastuzumab and lapatinib in treatment-refractory, KRAS codon 12/13 wild-type, HER2-positive metastatic colorectal cancer (HERACLES): a proof-of-concept, multicentre, open-label, phase 2 trial. *Lancet Oncol* 2016; **17**: 738-746 [PMID: 27108243 DOI: 10.1016/S1470-2045(16)00150-9]
96 **Sartore-Bianchi A**, Lonardi S, Martino C, Fenocchio E, Tosi F, Ghezzi S, Leone F, Bergamo F, Zagonel V, Ciardiello F, Ardizzoni A, Amatu A, Bencardino K, Valtorta E, Grassi E, Torri V, Bonoldi E, Sapino A, Vanzulli A, Regge D, Cappello G, Bardelli A, Trusolino L, Marsoni S, Siena S. Pertuzumab and trastuzumab emtansine in patients with HER2-amplified metastatic colorectal cancer: the phase II HERACLES-B trial. *ESMO Open* 2020; **5**: e000911 [PMID: 32988996 DOI: 10.1136/esmoopen-2020-000911]
97 **Meric-Bernstam F**, Hurwitz H, Raghav KPS, McWilliams RR, Fakih M, VanderWalde A, Swanton C, Kurzrock R, Burris H, Sweeney C, Bose R, Spigel DR, Beattie MS, Blotner S, Stone A, Schulze K, Cuchelkar V, Hainsworth J. Pertuzumab plus trastuzumab for HER2-amplified metastatic colorectal cancer (MyPathway): an updated report from a multicentre, open-label, phase 2a, multiple basket study. *Lancet Oncol* 2019; **20**: 518-530 [PMID: 30857956 DOI: 10.1016/S1470-2045(18)30904-5]
98 **Hainsworth JD**, Meric-Bernstam F, Swanton C, Hurwitz H, Spigel DR, Sweeney C, Burris H, Bose R, Yoo B, Stein A, Beattie M, Kurzrock R. Targeted Therapy for Advanced Solid Tumors on the Basis of Molecular Profiles: Results From MyPathway, an Open-Label, Phase IIa Multiple Basket Study. *J Clin Oncol* 2018; **36**: 536-542 [PMID: 29320312 DOI: 10.1200/JCO.2017.75.3780]
99 **Carmeliet P**. Angiogenesis in health and disease. *Nat Med* 2003; **9**: 653-660 [PMID: 12778163 DOI: 10.1038/nm0603-653]
100 **Dvorak HF**. Vascular permeability factor/vascular endothelial growth factor: a critical cytokine in tumor angiogenesis and a potential target for diagnosis and therapy. *J Clin Oncol* 2002; **20**: 4368-4380 [PMID: 12409337 DOI: 10.1200/JCO.2002.10.088]

101 **Shibuya M**. VEGFR and type-V RTK activation and signaling. *Cold Spring Harb Perspect Biol* 2013; **5**: a009092 [PMID: 24086040 DOI: 10.1101/cshperspect.a009092]

102 **Prabhakar NR**, Semenza GL. Adaptive and maladaptive cardiorespiratory responses to continuous and intermittent hypoxia mediated by hypoxia-inducible factors 1 and 2. *Physiol Rev* 2012; **92**: 967-1003 [PMID: 22811423 DOI: 10.1152/physrev.00030.2011]

103 **Lopez A**, Harada K, Vasilakopoulou M, Shanbhag N, Ajani JA. Targeting Angiogenesis in Colorectal Carcinoma. *Drugs* 2019; **79**: 63-74 [PMID: 30617958 DOI: 10.1007/s40265-018-1037-9]

104 **Javle M**, Smyth EC, Chau I. Ramucirumab: successfully targeting angiogenesis in gastric cancer. *Clin Cancer Res* 2014; **20**: 5875-5881 [PMID: 25281695 DOI: 10.1158/1078-0432.CCR-14-1071]

105 **Rosen LS**, Jacobs IA, Burkes RL. Bevacizumab in Colorectal Cancer: Current Role in Treatment and the Potential of Biosimilars. *Target Oncol* 2017; **12**: 599-610 [PMID: 28801849 DOI: 10.1007/s11523-017-0518-1]

106 **Hurwitz H**, Fehrenbacher L, Novotny W, Cartwright T, Hainsworth J, Heim W, Berlin J, Baron A, Griffing S, Holmgren E, Ferrara N, Fyfe G, Rogers B, Ross R, Kabbinavar F. Bevacizumab plus irinotecan, fluorouracil, and leucovorin for metastatic colorectal cancer. *N Engl J Med* 2004; **350**: 2335-2342 [PMID: 15175435 DOI: 10.1056/NEJMoa032691]

107 **Pfeiffer P**, Yilmaz M, Möller S, Zitnjak D, Krogh M, Petersen LN, Poulsen LØ, Winther SB, Thomsen KG, Qvortrup C. TAS-102 with or without bevacizumab in patients with chemorefractory metastatic colorectal cancer: an investigator-initiated, open-label, randomised, phase 2 trial. *Lancet Oncol* 2020; **21**: 412-420 [PMID: 31999946 DOI: 10.1016/S1470-2045(19)30827-7]

108 **Oki E**, Makiyama A, Miyamoto Y, Kotaka M, Kawanaka H, Miwa K, Kabashima A, Noguchi T, Yuge K, Kashiwada T, Ando K, Shimokawa M, Saeki H, Akagi Y, Baba H, Maehara Y, Mori M. Trifluridine/tipiracil plus bevacizumab as a first-line treatment for elderly patients with metastatic colorectal cancer (KSCC1602): A multicenter phase II trial. *Cancer Med* 2021; **10**: 454-461 [PMID: 33249761 DOI: 10.1002/cam4.3618]

109 **Sommerhäuser G**, Kurreck A, Stintzing S, Heinemann V, von Weikersthal LF, Dechow T, Kaiser F, Karthaus M, Schwaner I, Fuchs M, König A, Roderburg C, Hoyer I, Quante M, Kiani A, Fruehauf S, Müller L, Reinacher-Schick A, Ettrich TJ, Stahler A, Modest DP. Study protocol of the FIRE-8 (AIO-KRK/YMO-0519) trial: a prospective, randomized, open-label, multicenter phase II trial investigating the efficacy of trifluridine/tipiracil plus panitumumab *vs* trifluridine/tipiracil plus bevacizumab as first-line treatment in patients with metastatic colorectal cancer. *BMC Cancer* 2022; **22**: 820 [PMID: 35897060 DOI: 10.1186/s12885-022-09892-8]

110 **Van Cutsem E**, Danielewicz I, Saunders MP, Pfeiffer P, Argilés G, Borg C, Glynne-Jones R, Punt CJA, Van de Wouw AJ, Fedyanin M, Stroyakovskiy D, Kroening H, Garcia-Alfonso P, Wasan H, Falcone A, Kanehisa A, Egorov A, Aubel P, Amellal N, Moiseenko V. Trifluridine/tipiracil plus bevacizumab in patients with untreated metastatic colorectal cancer ineligible for intensive therapy: the randomized TASCO1 study. *Ann Oncol* 2020; **31**: 1160-1168 [PMID: 32497736 DOI: 10.1016/j.annonc.2020.05.024]

111 **Chen YX**, Yang Q, Kuang JJ, Chen SY, Wei Y, Jiang ZM, Xie DR. Efficacy of adding bevacizumab in the first-line chemotherapy of metastatic colorectal cancer: evidence from seven randomized clinical trials. *Gastroenterol Res Pract* 2014; **2014**: 594930 [PMID: 24971091 DOI: 10.1155/2014/594930]

112 **Saltz LB**, Clarke S, Díaz-Rubio E, Scheithauer W, Figer A, Wong R, Koski S, Lichinitser M, Yang TS, Rivera F, Couture F, Sirzén F, Cassidy J. Bevacizumab in combination with oxaliplatin-based chemotherapy as first-line therapy in metastatic colorectal cancer: a randomized phase III study. *J Clin Oncol* 2008; **26**: 2013-2019 [PMID: 18421054 DOI: 10.1200/JCO.2007.14.9930]

113 **Passardi A**, Nanni O, Tassinari D, Turci D, Cavanna L, Fontana A, Ruscelli S, Mucciarini C, Lorusso V, Ragazzini A, Frassineti GL, Amadori D. Effectiveness of bevacizumab added to standard chemotherapy in metastatic colorectal cancer: final results for first-line treatment from the ITACa randomized clinical trial. *Ann Oncol* 2015; **26**: 1201-1207 [PMID: 25735317 DOI: 10.1093/annonc/mdv130]

114 **Heinemann V**, von Weikersthal LF, Decker T, Kiani A, Vehling-Kaiser U, Al-Batran SE, Heintges T, Lerchenmüller C, Kahl C, Seipelt G, Kullmann F, Stauch M, Scheithauer W, Hielscher J, Scholz M, Müller S, Link H, Niederle N, Rost A, Höffkes HG, Moehler M, Lindig RU, Modest DP, Rossius L, Kirchner T, Jung A, Stintzing S. FOLFIRI plus cetuximab *vs* FOLFIRI plus bevacizumab as first-line treatment for patients with metastatic colorectal cancer (FIRE-3): a randomised, open-label, phase 3 trial. *Lancet Oncol* 2014; **15**: 1065-1075 [PMID: 25088940 DOI: 10.1016/S1470-2045(14)70330-4]

115 **Venook AP**, Niedzwiecki D, Lenz HJ, Innocenti F, Fruth B, Meyerhardt JA, Schrag D, Greene C, O'Neil BH, Atkins JN, Berry S, Polite BN, O'Reilly EM, Goldberg RM, Hochster HS, Schilsky RL, Bertagnolli MM, El-Khoueiry AB, Watson P, Benson AB 3rd, Mulkerin DL, Mayer RJ, Blanke C. Effect of First-Line Chemotherapy Combined With Cetuximab or Bevacizumab on Overall Survival in Patients With KRAS Wild-Type Advanced or Metastatic Colorectal Cancer: A Randomized Clinical Trial. *JAMA* 2017; **317**: 2392-2401 [PMID: 28632865 DOI: 10.1001/jama.2017.7105]

116 **Giantonio BJ**, Catalano PJ, Meropol NJ, O'Dwyer PJ, Mitchell EP, Alberts SR, Schwartz MA, Benson AB 3rd; Eastern Cooperative Oncology Group Study E3200. Bevacizumab in combination with oxaliplatin, fluorouracil, and leucovorin (FOLFOX4) for previously treated metastatic colorectal cancer: results from the Eastern Cooperative Oncology Group Study E3200. *J Clin Oncol* 2007; **25**: 1539-1544 [PMID: 17442997 DOI: 10.1200/JCO.2006.09.6305]

117 **Bennouna J**, Sastre J, Arnold D, Österlund P, Greil R, Van Cutsem E, von Moos R, Viéitez JM, Bouché O, Borg C, Steffens CC, Alonso-Orduña V, Schlichting C, Reyes-Rivera I, Bendahmane B, André T, Kubicka S; ML18147 Study Investigators. Continuation of bevacizumab after first progression in metastatic colorectal cancer (ML18147): a randomised phase 3 trial. *Lancet Oncol* 2013; **14**: 29-37 [PMID: 23168366 DOI: 10.1016/S1470-2045(12)70477-1]

118 **Van Cutsem E**, Tabernero J, Lakomy R, Prenen H, Prausová J, Macarulla T, Ruff P, van Hazel GA, Moiseyenko V, Ferry D, McKendrick J, Polikoff J, Tellier A, Castan R, Allegra C. Addition of aflibercept to fluorouracil, leucovorin, and irinotecan improves survival in a phase III randomized trial in patients with metastatic colorectal cancer previously treated with an oxaliplatin-based regimen. *J Clin Oncol* 2012; **30**: 3499-3506 [PMID: 22949147 DOI: 10.1200/JCO.2012.42.8201]

119 **Tabernero J**, Yoshino T, Cohn AL, Obermannova R, Bodoky G, Garcia-Carbonero R, Ciuleanu TE, Portnoy DC, Van Cutsem E, Grothey A, Prausová J, Garcia-Alfonso P, Yamazaki K, Clingan PR, Lonardi S, Kim TW, Simms L, Chang SC,

Nasroulah F; RAISE Study Investigators. Ramucirumab *vs* placebo in combination with second-line FOLFIRI in patients with metastatic colorectal carcinoma that progressed during or after first-line therapy with bevacizumab, oxaliplatin, and a fluoropyrimidine (RAISE): a randomised, double-blind, multicentre, phase 3 study. *Lancet Oncol* 2015; **16**: 499-508 [PMID: 25877855 DOI: 10.1016/S1470-2045(15)70127-0]

120 **Argilés G**, Saunders MP, Rivera F, Sobrero A, Benson A 3rd, Guillén Ponce C, Cascinu S, Van Cutsem E, Macpherson IR, Strumberg D, Köhne CH, Zalcberg J, Wagner A, Luigi Garosi V, Grunert J, Tabernero J, Ciardiello F. Regorafenib plus modified FOLFOX6 as first-line treatment of metastatic colorectal cancer: A phase II trial. *Eur J Cancer* 2015; **51**: 942-949 [PMID: 25818084 DOI: 10.1016/j.ejca.2015.02.013]

121 **Rousseau B**, Boukerma AK, Henriques J, Cohen R, Lucidarme O, Borg C, Tournigand C, Kim S, Bachet JB, Mazard T, Louvet C, Chibaudel B, Vernerey D, Andre T, Hulin A. Impact of trough concentrations of regorafenib and its major metabolites M-2 and M-5 on overall survival of chemorefractory metastatic colorectal cancer patients: Results from a multicentre GERCOR TEXCAN phase II study. *Eur J Cancer* 2022; **168**: 99-107 [PMID: 35489233 DOI: 10.1016/j.ejca.2022.03.009]

122 **Grothey A**, Van Cutsem E, Sobrero A, Siena S, Falcone A, Ychou M, Humblet Y, Bouché O, Mineur L, Barone C, Adenis A, Tabernero J, Yoshino T, Lenz HJ, Goldberg RM, Sargent DJ, Cihon F, Cupit L, Wagner A, Laurent D; CORRECT Study Group. Regorafenib monotherapy for previously treated metastatic colorectal cancer (CORRECT): an international, multicentre, randomised, placebo-controlled, phase 3 trial. *Lancet* 2013; **381**: 303-312 [PMID: 23177514 DOI: 10.1016/S0140-6736(12)61900-X]

123 **Li J**, Qin S, Xu R, Yau TC, Ma B, Pan H, Xu J, Bai Y, Chi Y, Wang L, Yeh KH, Bi F, Cheng Y, Le AT, Lin JK, Liu T, Ma D, Kappeler C, Kalmus J, Kim TW; CONCUR Investigators. Regorafenib plus best supportive care versus placebo plus best supportive care in Asian patients with previously treated metastatic colorectal cancer (CONCUR): a randomised, double-blind, placebo-controlled, phase 3 trial. *Lancet Oncol* 2015; **16**: 619-629 [PMID: 25981818 DOI: 10.1016/S1470-2045(15)70156-7]

124 **Liu Y**, Xiao Q, He J, Hu H, Du J, Zhu Y, Chen J, Liu Z, Wang J, Sun L, Xu D, Li J, Liao X, Cai Y, Cai C, Jin Z, Wang L, Yuan Y, Ding K. Phase II study of anlotinib in combination with oxaliplatin and capecitabine for patients with RAS/BRAF wild-type metastatic colorectal adenocarcinoma as the first-line therapy. *BMC Med* 2022; **20**: 155 [PMID: 35513832 DOI: 10.1186/s12916-022-02357-6]

125 **Li J**, Qin S, Xu RH, Shen L, Xu J, Bai Y, Yang L, Deng Y, Chen ZD, Zhong H, Pan H, Guo W, Shu Y, Yuan Y, Zhou J, Xu N, Liu T, Ma D, Wu C, Cheng Y, Chen D, Li W, Sun S, Yu Z, Cao P, Chen H, Wang J, Wang S, Wang H, Fan S, Hua Y, Su W. Effect of Fruquintinib *vs* Placebo on Overall Survival in Patients With Previously Treated Metastatic Colorectal Cancer: The FRESCO Randomized Clinical Trial. *JAMA* 2018; **319**: 2486-2496 [PMID: 29946728 DOI: 10.1001/jama.2018.7855]

126 **Xu RH**, Shen L, Wang KM, Wu G, Shi CM, Ding KF, Lin LZ, Wang JW, Xiong JP, Wu CP, Li J, Liu YP, Wang D, Ba Y, Feng JP, Bai YX, Bi JW, Ma LW, Lei J, Yang Q, Yu H. Famitinib *vs* placebo in the treatment of refractory metastatic colorectal cancer: a multicenter, randomized, double-blinded, placebo-controlled, phase II clinical trial. *Chin J Cancer* 2017; **36**: 97 [PMID: 29273089 DOI: 10.1186/s40880-017-0263-y]

127 **De Roock W**, De Vriendt V, Normanno N, Ciardiello F, Tejpar S. KRAS, BRAF, PIK3CA, and PTEN mutations: implications for targeted therapies in metastatic colorectal cancer. *Lancet Oncol* 2011; **12**: 594-603 [PMID: 21163703 DOI: 10.1016/S1470-2045(10)70209-6]

128 **Sanz-Garcia E**, Argiles G, Elez E, Tabernero J. BRAF mutant colorectal cancer: prognosis, treatment, and new perspectives. *Ann Oncol* 2017; **28**: 2648-2657 [PMID: 29045527 DOI: 10.1093/annonc/mdx401]

129 **Pentheroudakis G**, Kotoula V, De Roock W, Kouvatseas G, Papakostas P, Makatsoris T, Papamichael D, Xanthakis I, Sgouros J, Televantou D, Kafiri G, Tsamandas AC, Razis E, Galani E, Bafaloukos D, Efstratiou I, Bompolaki I, Pectasides D, Pavlidis N, Tejpar S, Fountzilas G. Biomarkers of benefit from cetuximab-based therapy in metastatic colorectal cancer: interaction of EGFR ligand expression with RAS/RAF, PIK3CA genotypes. *BMC Cancer* 2013; **13**: 49 [PMID: 23374602 DOI: 10.1186/1471-2407-13-49]

130 **Zhao B**, Wang L, Qiu H, Zhang M, Sun L, Peng P, Yu Q, Yuan X. Mechanisms of resistance to anti-EGFR therapy in colorectal cancer. *Oncotarget* 2017; **8**: 3980-4000 [PMID: 28002810 DOI: 10.18632/oncotarget.14012]

131 **Yaeger R**, Saltz L. BRAF mutations in colorectal cancer: clinical relevance and role in targeted therapy. *J Natl Compr Canc Netw* 2012; **10**: 1456-1458 [PMID: 23138171 DOI: 10.6004/jnccn.2012.0148]

132 **Capalbo C**, Marchetti P, Coppa A, Calogero A, Anastasi E, Buffone A, Belardinilli F, Gulino M, Frati P, Catalano C, Cortesi E, Giannini G, Gulino A. Vemurafenib and panitumumab combination tailored therapy in BRAF-mutated metastatic colorectal cancer: a case report. *Cancer Biol Ther* 2014; **15**: 826-831 [PMID: 24755613 DOI: 10.4161/cbt.28878]

133 **Chen J**, Ye Y, Sun H, Shi G. Association between KRAS codon 13 mutations and clinical response to anti-EGFR treatment in patients with metastatic colorectal cancer: results from a meta-analysis. *Cancer Chemother Pharmacol* 2013; **71**: 265-272 [PMID: 23090619 DOI: 10.1007/s00280-012-2005-9]

134 **Roth AD**, Tejpar S, Delorenzi M, Yan P, Fiocca R, Klingbiel D, Dietrich D, Biesmans B, Bodoky G, Barone C, Aranda E, Nordlinger B, Cisar L, Labianca R, Cunningham D, Van Cutsem E, Bosman F. Prognostic role of KRAS and BRAF in stage II and III resected colon cancer: results of the translational study on the PETACC-3, EORTC 40993, SAKK 60-00 trial. *J Clin Oncol* 2010; **28**: 466-474 [PMID: 20008640 DOI: 10.1200/JCO.2009.23.3452]

135 **Wan PT**, Garnett MJ, Roe SM, Lee S, Niculescu-Duvaz D, Good VM, Jones CM, Marshall CJ, Springer CJ, Barford D, Marais R; Cancer Genome Project. Mechanism of activation of the RAF-ERK signaling pathway by oncogenic mutations of B-RAF. *Cell* 2004; **116**: 855-867 [PMID: 15035987 DOI: 10.1016/s0092-8674(04)00215-6]

136 **Kopetz S**, Guthrie KA, Morris VK, Lenz HJ, Magliocco AM, Maru D, Yan Y, Lanman R, Manyam G, Hong DS, Sorokin A, Atreya CE, Diaz LA, Allegra C, Raghav KP, Wang SE, Lieu CH, McDonough SL, Philip PA, Hochster HS. Randomized Trial of Irinotecan and Cetuximab With or Without Vemurafenib in BRAF-Mutant Metastatic Colorectal Cancer (SWOG S1406). *J Clin Oncol* 2021; **39**: 285-294 [PMID: 33356422 DOI: 10.1200/JCO.20.01994]

137 **Van Cutsem E**, Huijberts S, Grothey A, Yaeger R, Cuyle PJ, Elez E, Fakih M, Montagut C, Peeters M, Yoshino T,

Wasan H, Desai J, Ciardiello F, Gollerkeri A, Christy-Bittel J, Maharry K, Sandor V, Schellens JHM, Kopetz S, Tabernero J. Binimetinib, Encorafenib, and Cetuximab Triplet Therapy for Patients With *BRAF* V600E-Mutant Metastatic Colorectal Cancer: Safety Lead-In Results From the Phase III BEACON Colorectal Cancer Study. *J Clin Oncol* 2019; **37**: 1460-1469 [PMID: 30892987 DOI: 10.1200/JCO.18.02459]

138 **Holderfield M**, Deuker MM, McCormick F, McMahon M. Targeting RAF kinases for cancer therapy: BRAF-mutated melanoma and beyond. *Nat Rev Cancer* 2014; **14**: 455-467 [PMID: 24957944 DOI: 10.1038/nrc3760]

139 **Mizukami T**, Izawa N, Nakajima TE, Sunakawa Y. Targeting EGFR and RAS/RAF Signaling in the Treatment of Metastatic Colorectal Cancer: From Current Treatment Strategies to Future Perspectives. *Drugs* 2019; **79**: 633-645 [PMID: 30968289 DOI: 10.1007/s40265-019-01113-0]

140 **Corcoran RB**, André T, Atreya CE, Schellens JHM, Yoshino T, Bendell JC, Hollebecque A, McRee AJ, Siena S, Middleton G, Muro K, Gordon MS, Tabernero J, Yaeger R, O'Dwyer PJ, Humblet Y, De Vos F, Jung AS, Brase JC, Jaeger S, Bettinger S, Mookerjee B, Rangwala F, Van Cutsem E. Combined BRAF, EGFR, and MEK Inhibition in Patients with *BRAF*^{V600E}-Mutant Colorectal Cancer. *Cancer Discov* 2018; **8**: 428-443 [PMID: 29431699 DOI: 10.1158/2159-8290.CD-17-1226]

141 **Corcoran RB**, Atreya CE, Falchook GS, Kwak EL, Ryan DP, Bendell JC, Hamid O, Messersmith WA, Daud A, Kurzrock R, Pierobon M, Sun P, Cunningham E, Little S, Orford K, Motwani M, Bai Y, Patel K, Venook AP, Kopetz S. Combined BRAF and MEK Inhibition With Dabrafenib and Trametinib in BRAF V600-Mutant Colorectal Cancer. *J Clin Oncol* 2015; **33**: 4023-4031 [PMID: 26392102 DOI: 10.1200/JCO.2015.63.2471]

142 **Kopetz S**, Grothey A, Yaeger R, Van Cutsem E, Desai J, Yoshino T, Wasan H, Ciardiello F, Loupakis F, Hong YS, Steeghs N, Guren TK, Arkenau HT, Garcia-Alfonso P, Pfeiffer P, Orlov S, Lonardi S, Elez E, Kim TW, Schellens JHM, Guo C, Krishnan A, Dekervel J, Morris V, Calvo Ferrandiz A, Tarpgaard LS, Braun M, Gollerkeri A, Keir C, Maharry K, Pickard M, Christy-Bittel J, Anderson L, Sandor V, Tabernero J. Encorafenib, Binimetinib, and Cetuximab in *BRAF* V600E-Mutated Colorectal Cancer. *N Engl J Med* 2019; **381**: 1632-1643 [PMID: 31566309 DOI: 10.1056/NEJMoa1908075]

143 **Welsh SJ**, Corrie PG. Management of BRAF and MEK inhibitor toxicities in patients with metastatic melanoma. *Ther Adv Med Oncol* 2015; **7**: 122-136 [PMID: 25755684 DOI: 10.1177/1758834014566428]

144 **Gherardi E**, Birchmeier W, Birchmeier C, Vande Woude G. Targeting MET in cancer: rationale and progress. *Nat Rev Cancer* 2012; **12**: 89-103 [PMID: 22270953 DOI: 10.1038/nrc3205]

145 **Takeuchi H**, Bilchik A, Saha S, Turner R, Wiese D, Tanaka M, Kuo C, Wang HJ, Hoon DS. c-MET expression level in primary colon cancer: a predictor of tumor invasion and lymph node metastases. *Clin Cancer Res* 2003; **9**: 1480-1488 [PMID: 12684423]

146 **Song EK**, Tai WM, Messersmith WA, Bagby S, Purkey A, Quackenbush KS, Pitts TM, Wang G, Blatchford P, Yahn R, Kaplan J, Tan AC, Atreya CE, Eckhardt G, Kelley RK, Venook A, Kwak EL, Ryan D, Arcaroli JJ. Potent antitumor activity of cabozantinib, a c-MET and VEGFR2 inhibitor, in a colorectal cancer patient-derived tumor explant model. *Int J Cancer* 2015; **136**: 1967-1975 [PMID: 25242168 DOI: 10.1002/ijc.29225]

147 **García-Aranda M**, Redondo M. Targeting Receptor Kinases in Colorectal Cancer. *Cancers (Basel)* 2019; **11** [PMID: 30934752 DOI: 10.3390/cancers11040433]

148 **Bardelli A**, Corso S, Bertotti A, Hobor S, Valtorta E, Siravegna G, Sartore-Bianchi A, Scala E, Cassingena A, Zecchin D, Apicella M, Migliardi G, Galimi F, Lauricella C, Zanon C, Perera T, Veronese S, Corti G, Amatu A, Gambacorta M, Diaz LA Jr, Sausen M, Velculescu VE, Comoglio P, Trusolino L, Di Nicolantonio F, Giordano S, Siena S. Amplification of the MET receptor drives resistance to anti-EGFR therapies in colorectal cancer. *Cancer Discov* 2013; **3**: 658-673 [PMID: 23729478 DOI: 10.1158/2159-8290.CD-12-0558]

149 **Van Cutsem E**, Eng C, Nowara E, Swieboda-Sadlej A, Tebbutt NC, Mitchell E, Davidenko I, Stephenson J, Elez E, Prenen H, Deng H, Tang R, McCaffery I, Oliner KS, Chen L, Gansert J, Loh E, Smethurst D, Tabernero J. Randomized phase Ib/II trial of rilotumumab or ganitumab with panitumumab *vs* panitumumab alone in patients with wild-type KRAS metastatic colorectal cancer. *Clin Cancer Res* 2014; **20**: 4240-4250 [PMID: 24919569 DOI: 10.1158/1078-0432.CCR-13-2752]

150 **Bendell JC**, Hochster H, Hart LL, Firdaus I, Mace JR, McFarlane JJ, Kozloff M, Catenacci D, Hsu JJ, Hack SP, Shames DS, Phan SC, Koeppen H, Cohn AL. A Phase II Randomized Trial (GO27827) of First-Line FOLFOX Plus Bevacizumab with or Without the MET Inhibitor Onartuzumab in Patients with Metastatic Colorectal Cancer. *Oncologist* 2017; **22**: 264-271 [PMID: 28209746 DOI: 10.1634/theoncologist.2016-0223]

151 **Zhao S**, Wu W, Jiang H, Ma L, Pan C, Jin C, Mo J, Wang L, Wang K. Selective Inhibitor of the c-Met Receptor Tyrosine Kinase in Advanced Hepatocellular Carcinoma: No Beneficial Effect With the Use of Tivantinib? *Front Immunol* 2021; **12**: 731527 [PMID: 34804015 DOI: 10.3389/fimmu.2021.731527]

152 **Eng C**, Bessudo A, Hart LL, Severtsev A, Gladkov O, Müller L, Kopp MV, Vladimirov V, Langdon R, Kotiv B, Barni S, Hsu C, Bolotin E, von Roemeling R, Schwartz B, Bendell JC. A randomized, placebo-controlled, phase 1/2 study of tivantinib (ARQ 197) in combination with irinotecan and cetuximab in patients with metastatic colorectal cancer with wild-type KRAS who have received first-line systemic therapy. *Int J Cancer* 2016; **139**: 177-186 [PMID: 26891420 DOI: 10.1002/ijc.30049]

153 **Rimassa L**, Bozzarelli S, Pietrantonio F, Cordio S, Lonardi S, Toppo L, Zaniboni A, Bordonaro R, Di Bartolomeo M, Tomasello G, Dadduzio V, Tronconi MC, Piombo C, Giordano L, Gloghini A, Di Tommaso L, Santoro A. Phase II Study of Tivantinib and Cetuximab in Patients With KRAS Wild-type Metastatic Colorectal Cancer With Acquired Resistance to EGFR Inhibitors and Emergence of MET Overexpression: Lesson Learned for Future Trials With EGFR/MET Dual Inhibition. *Clin Colorectal Cancer* 2019; **18**: 125-132.e2 [PMID: 30846365 DOI: 10.1016/j.clcc.2019.02.004]

154 **He AR**, Cohen RB, Denlinger CS, Sama A, Birnbaum A, Hwang J, Sato T, Lewis N, Mynderse M, Niland M, Giles J, Wallin J, Moser B, Zhang W, Walgren R, Plimack ER. First-in-Human Phase I Study of Merestinib, an Oral Multikinase Inhibitor, in Patients with Advanced Cancer. *Oncologist* 2019; **24**: e930-e942 [PMID: 30833489 DOI: 10.1634/theoncologist.2018-0411]

155 **Safaie Qamsari E**, Safaei Ghaderi S, Zarei B, Dorostkar R, Bagheri S, Jadidi-Niaragh F, Somi MH, Yousefi M. The c-

Met receptor: Implication for targeted therapies in colorectal cancer. *Tumour Biol* 2017; **39**: 1010428317699118 [PMID: 28459362 DOI: 10.1177/1010428317699118]

156 **Otte JM**, Schmitz F, Kiehne K, Stechele HU, Banasiewicz T, Krokowicz P, Nakamura T, Fölsch UR, Herzig K. Functional expression of HGF and its receptor in human colorectal cancer. *Digestion* 2000; **61**: 237-246 [PMID: 10878450 DOI: 10.1159/000007764]

157 **Chen RL**, Zhao J, Zhang XC, Lou NN, Chen HJ, Yang X, Su J, Xie Z, Zhou Q, Tu HY, Zhong WZ, Yan HH, Guo WB, Wu YL, Yang JJ. Crizotinib in advanced non-small-cell lung cancer with concomitant ALK rearrangement and c-Met overexpression. *BMC Cancer* 2018; **18**: 1171 [PMID: 30477470 DOI: 10.1186/s12885-018-5078-y]

158 **He X**, Jiao XD, Liu K, Qin BD, Wu Y, Ling Y, Liu J, Xu AQ, Song K, Zang YS. Clinical Responses to Crizotinib, Alectinib, and Lorlatinib in a Metastatic Colorectal Carcinoma Patient With ALK Gene Rearrangement: A Case Report. *JCO Precis Oncol* 2021; **5** [PMID: 34036227 DOI: 10.1200/PO.20.00534]

159 **Cuneo KC**, Mehta RK, Kurapati H, Thomas DG, Lawrence TS, Nyati MK. Enhancing the Radiation Response in KRAS Mutant Colorectal Cancers Using the c-Met Inhibitor Crizotinib. *Transl Oncol* 2019; **12**: 209-216 [PMID: 30412912 DOI: 10.1016/j.tranon.2018.10.005]

160 **Markman JL**, Shiao SL. Impact of the immune system and immunotherapy in colorectal cancer. *J Gastrointest Oncol* 2015; **6**: 208-223 [PMID: 25830040 DOI: 10.3978/j.issn.2078-6891.2014.077]

161 **Kalyan A**, Kircher S, Shah H, Mulcahy M, Benson A. Updates on immunotherapy for colorectal cancer. *J Gastrointest Oncol* 2018; **9**: 160-169 [PMID: 29564182 DOI: 10.21037/jgo.2018.01.17]

162 **Havel JJ**, Chowell D, Chan TA. The evolving landscape of biomarkers for checkpoint inhibitor immunotherapy. *Nat Rev Cancer* 2019; **19**: 133-150 [PMID: 30755690 DOI: 10.1038/s41568-019-0116-x]

163 **Pauken KE**, Wherry EJ. Overcoming T cell exhaustion in infection and cancer. *Trends Immunol* 2015; **36**: 265-276 [PMID: 25797516 DOI: 10.1016/j.it.2015.02.008]

164 **Boukouris AE**, Theochari M, Stefanou D, Papalambros A, Felekouras E, Gogas H, Ziogas DC. Latest evidence on immune checkpoint inhibitors in metastatic colorectal cancer: A 2022 update. *Crit Rev Oncol Hematol* 2022; **173**: 103663 [PMID: 35351582 DOI: 10.1016/j.critrevonc.2022.103663]

165 **Han Y**, Liu D, Li L. PD-1/PD-L1 pathway: current researches in cancer. *Am J Cancer Res* 2020; **10**: 727-742 [PMID: 32266087]

166 **Wang HB**, Yao H, Li CS, Liang LX, Zhang Y, Chen YX, Fang JY, Xu J. Rise of PD-L1 expression during metastasis of colorectal cancer: Implications for immunotherapy. *J Dig Dis* 2017; **18**: 574-581 [PMID: 28851046 DOI: 10.1111/1751-2980.12538]

167 **Lee HT**, Lee SH, Heo YS. Molecular Interactions of Antibody Drugs Targeting PD-1, PD-L1, and CTLA-4 in Immuno-Oncology. *Molecules* 2019; **24** [PMID: 30917623 DOI: 10.3390/molecules24061190]

168 **Le DT**, Uram JN, Wang H, Bartlett BR, Kemberling H, Eyring AD, Skora AD, Luber BS, Azad NS, Laheru D, Biedrzycki B, Donehower RC, Zaheer A, Fisher GA, Crocenzi TS, Lee JJ, Duffy SM, Goldberg RM, de la Chapelle A, Koshiji M, Bhaijee F, Huebner T, Hruban RH, Wood LD, Cuka N, Pardoll DM, Papadopoulos N, Kinzler KW, Zhou S, Cornish TC, Taube JM, Anders RA, Eshleman JR, Vogelstein B, Diaz LA Jr. PD-1 Blockade in Tumors with Mismatch-Repair Deficiency. *N Engl J Med* 2015; **372**: 2509-2520 [PMID: 26028255 DOI: 10.1056/NEJMoa1500596]

169 **Venderbosch S**, Nagtegaal ID, Maughan TS, Smith CG, Cheadle JP, Fisher D, Kaplan R, Quirke P, Seymour MT, Richman SD, Meijer GA, Ylstra B, Heideman DA, de Haan AF, Punt CJ, Koopman M. Mismatch repair status and BRAF mutation status in metastatic colorectal cancer patients: a pooled analysis of the CAIRO, CAIRO2, COIN, and FOCUS studies. *Clin Cancer Res* 2014; **20**: 5322-5330 [PMID: 25139339 DOI: 10.1158/1078-0432.CCR-14-0332]

170 **Tran B**, Kopetz S, Tie J, Gibbs P, Jiang ZQ, Lieu CH, Agarwal A, Maru DM, Sieber O, Desai J. Impact of BRAF mutation and microsatellite instability on the pattern of metastatic spread and prognosis in metastatic colorectal cancer. *Cancer* 2011; **117**: 4623-4632 [PMID: 21456008 DOI: 10.1002/cncr.26086]

171 **Giannakis M**, Mu XJ, Shukla SA, Qian ZR, Cohen O, Nishihara R, Bahl S, Cao Y, Amin-Mansour A, Yamauchi M, Sukawa Y, Stewart C, Rosenberg M, Mima K, Inamura K, Nosho K, Nowak JA, Lawrence MS, Giovannucci EL, Chan AT, Ng K, Meyerhardt JA, Van Allen EM, Getz G, Gabriel SB, Lander ES, Wu CJ, Fuchs CS, Ogino S, Garraway LA. Genomic Correlates of Immune-Cell Infiltrates in Colorectal Carcinoma. *Cell Rep* 2016; **15**: 857-865 [PMID: 27149842 DOI: 10.1016/j.celrep.2016.03.075]

172 **Llosa NJ**, Cruise M, Tam A, Wicks EC, Hechenbleikner EM, Taube JM, Blosser RL, Fan H, Wang H, Luber BS, Zhang M, Papadopoulos N, Kinzler KW, Vogelstein B, Sears CL, Anders RA, Pardoll DM, Housseau F. The vigorous immune microenvironment of microsatellite instable colon cancer is balanced by multiple counter-inhibitory checkpoints. *Cancer Discov* 2015; **5**: 43-51 [PMID: 25358689 DOI: 10.1158/2159-8290.CD-14-0863]

173 **Schrock AB**, Ouyang C, Sandhu J, Sokol E, Jin D, Ross JS, Miller VA, Lim D, Amanam I, Chao J, Catenacci D, Cho M, Braiteh F, Klempner SJ, Ali SM, Fakih M. Tumor mutational burden is predictive of response to immune checkpoint inhibitors in MSI-high metastatic colorectal cancer. *Ann Oncol* 2019; **30**: 1096-1103 [PMID: 31038663 DOI: 10.1093/annonc/mdz134]

174 **McGranahan N**, Furness AJ, Rosenthal R, Ramskov S, Lyngaa R, Saini SK, Jamal-Hanjani M, Wilson GA, Birkbak NJ, Hiley CT, Watkins TB, Shafi S, Murugaesu N, Mitter R, Akarca AU, Linares J, Marafioti T, Henry JY, Van Allen EM, Miao D, Schilling B, Schadendorf D, Garraway LA, Makarov V, Rizvi NA, Snyder A, Hellmann MD, Merghoub T, Wolchok JD, Shukla SA, Wu CJ, Peggs KS, Chan TA, Hadrup SR, Quezada SA, Swanton C. Clonal neoantigens elicit T cell immunoreactivity and sensitivity to immune checkpoint blockade. *Science* 2016; **351**: 1463-1469 [PMID: 26940869 DOI: 10.1126/science.aaf1490]

175 **O'Neil BH**, Wallmark JM, Lorente D, Elez E, Raimbourg J, Gomez-Roca C, Ejadi S, Piha-Paul SA, Stein MN, Abdul Razak AR, Dotti K, Santoro A, Cohen RB, Gould M, Saraf S, Stein K, Han SW. Safety and antitumor activity of the anti-PD-1 antibody pembrolizumab in patients with advanced colorectal carcinoma. *PLoS One* 2017; **12**: e0189848 [PMID: 29284010 DOI: 10.1371/journal.pone.0189848]

176 **Le DT**, Kim TW, Van Cutsem E, Geva R, Jäger D, Hara H, Burge M, O'Neil B, Kavan P, Yoshino T, Guimbaud R, Taniguchi H, Elez E, Al-Batran SE, Boland PM, Crocenzi T, Atreya CE, Cui Y, Dai T, Marinello P, Diaz LA Jr, André T.

Phase II Open-Label Study of Pembrolizumab in Treatment-Refractory, Microsatellite Instability-High/Mismatch Repair-Deficient Metastatic Colorectal Cancer: KEYNOTE-164. *J Clin Oncol* 2020; **38**: 11-19 [PMID: 31725351 DOI: 10.1200/JCO.19.02107]

177 **Brahmer JR**, Drake CG, Wollner I, Powderly JD, Picus J, Sharfman WH, Stankevich E, Pons A, Salay TM, McMiller TL, Gilson MM, Wang C, Selby M, Taube JM, Anders R, Chen L, Korman AJ, Pardoll DM, Lowy I, Topalian SL. Phase I study of single-agent anti-programmed death-1 (MDX-1106) in refractory solid tumors: safety, clinical activity, pharmacodynamics, and immunologic correlates. *J Clin Oncol* 2010; **28**: 3167-3175 [PMID: 20516446 DOI: 10.1200/JCO.2009.26.7609]

178 **Overman MJ**, Lonardi S, Wong KYM, Lenz HJ, Gelsomino F, Aglietta M, Morse MA, Van Cutsem E, McDermott R, Hill A, Sawyer MB, Hendlisz A, Neyns B, Svrcek M, Moss RA, Ledeine JM, Cao ZA, Kamble S, Kopetz S, André T. Durable Clinical Benefit With Nivolumab Plus Ipilimumab in DNA Mismatch Repair-Deficient/Microsatellite Instability-High Metastatic Colorectal Cancer. *J Clin Oncol* 2018; **36**: 773-779 [PMID: 29355075 DOI: 10.1200/JCO.2017.76.9901]

179 **Morse MA**, Overman MJ, Hartman L, Khoukaz T, Brutcher E, Lenz HJ, Atasoy A, Shangguan T, Zhao H, El-Rayes B. Safety of Nivolumab plus Low-Dose Ipilimumab in Previously Treated Microsatellite Instability-High/Mismatch Repair-Deficient Metastatic Colorectal Cancer. *Oncologist* 2019; **24**: 1453-1461 [PMID: 31147488 DOI: 10.1634/theoncologist.2019-0129]

180 **Cercek A**, Lumish M, Sinopoli J, Weiss J, Shia J, Lamendola-Essel M, El Dika IH, Segal N, Shcherba M, Sugarman R, Stadler Z, Yaeger R, Smith JJ, Rousseau B, Argiles G, Patel M, Desai A, Saltz LB, Widmar M, Iyer K, Zhang J, Gianino N, Crane C, Romesser PB, Pappou EP, Paty P, Garcia-Aguilar J, Gonen M, Gollub M, Weiser MR, Schalper KA, Diaz LA Jr. PD-1 Blockade in Mismatch Repair-Deficient, Locally Advanced Rectal Cancer. *N Engl J Med* 2022; **386**: 2363-2376 [PMID: 35660797 DOI: 10.1056/NEJMoa2201445]

181 **Yu X**, Huang X, Chen X, Liu J, Wu C, Pu Q, Wang Y, Kang X, Zhou L. Characterization of a novel anti-human lymphocyte activation gene 3 (LAG-3) antibody for cancer immunotherapy. *MAbs* 2019; **11**: 1139-1148 [PMID: 31242068 DOI: 10.1080/19420862.2019.1629239]

182 **Strosberg JR**, Yeatman T, Weber J, Coppola D, Schell MJ, Han G, Almhanna K, Kim R, Valone T, Jump H, Sullivan D. A phase II study of RO4929097 in metastatic colorectal cancer. *Eur J Cancer* 2012; **48**: 997-1003 [PMID: 22445247 DOI: 10.1016/j.ejca.2012.02.056]

183 **Berlin J**, Bendell JC, Hart LL, Firdaus I, Gore I, Hermann RC, Mulcahy MF, Zalupski MM, Mackey HM, Yauch RL, Graham RA, Bray GL, Low JA. A randomized phase II trial of vismodegib *vs* placebo with FOLFOX or FOLFIRI and bevacizumab in patients with previously untreated metastatic colorectal cancer. *Clin Cancer Res* 2013; **19**: 258-267 [PMID: 23082002 DOI: 10.1158/1078-0432.CCR-12-1800]

184 **Yokoyama Y**, Watanabe T, Tamura Y, Hashizume Y, Miyazono K, Ehata S. Autocrine BMP-4 Signaling Is a Therapeutic Target in Colorectal Cancer. *Cancer Res* 2017; **77**: 4026-4038 [PMID: 28611046 DOI: 10.1158/0008-5472.CAN-17-0112]

185 **Villalba M**, Evans SR, Vidal-Vanaclocha F, Calvo A. Role of TGF-β in metastatic colon cancer: it is finally time for targeted therapy. *Cell Tissue Res* 2017; **370**: 29-39 [PMID: 28560691 DOI: 10.1007/s00441-017-2633-9]

186 **Ghosh N**, Hossain U, Mandal A, Sil PC. The Wnt signaling pathway: a potential therapeutic target against cancer. *Ann N Y Acad Sci* 2019; **1443**: 54-74 [PMID: 31017675 DOI: 10.1111/nyas.14027]

187 **Guo Q**, Grimmig T, Gonzalez G, Giobbie-Hurder A, Berg G, Carr N, Wilson BJ, Banerjee P, Ma J, Gold JS, Nandi B, Huang Q, Waaga-Gasser AM, Lian CG, Murphy GF, Frank MH, Gasser M, Frank NY. ATP-binding cassette member B5 (ABCB5) promotes tumor cell invasiveness in human colorectal cancer. *J Biol Chem* 2018; **293**: 11166-11178 [PMID: 29789423 DOI: 10.1074/jbc.RA118.003187]

188 **Tan AC**, Bagley SJ, Wen PY, Lim M, Platten M, Colman H, Ashley DM, Wick W, Chang SM, Galanis E, Mansouri A, Khagi S, Mehta MP, Heimberger AB, Puduvalli VK, Reardon DA, Sahebjam S, Simes J, Antonia SJ, Berry D, Khasraw M. Systematic review of combinations of targeted or immunotherapy in advanced solid tumors. *J Immunother Cancer* 2021; **9** [PMID: 34215688 DOI: 10.1136/jitc-2021-002459]

189 **Russo M**, Siravegna G, Blaszkowsky LS, Corti G, Crisafulli G, Ahronian LG, Mussolin B, Kwak EL, Buscarino M, Lazzari L, Valtorta E, Truini M, Jessop NA, Robinson HE, Hong TS, Mino-Kenudson M, Di Nicolantonio F, Thabet A, Sartore-Bianchi A, Siena S, Iafrate AJ, Bardelli A, Corcoran RB. Tumor Heterogeneity and Lesion-Specific Response to Targeted Therapy in Colorectal Cancer. *Cancer Discov* 2016; **6**: 147-153 [PMID: 26644315 DOI: 10.1158/2159-8290.CD-15-1283]

190 **Siravegna G**, Mussolin B, Buscarino M, Corti G, Cassingena A, Crisafulli G, Ponzetti A, Cremolini C, Amatu A, Lauricella C, Lamba S, Hobor S, Avallone A, Valtorta E, Rospo G, Medico E, Motta V, Antoniotti C, Tatangelo F, Bellosillo B, Veronese S, Budillon A, Montagut C, Racca P, Marsoni S, Falcone A, Corcoran RB, Di Nicolantonio F, Loupakis F, Siena S, Sartore-Bianchi A, Bardelli A. Clonal evolution and resistance to EGFR blockade in the blood of colorectal cancer patients. *Nat Med* 2015; **21**: 795-801 [PMID: 26030179 DOI: 10.1038/nm.3870]

191 **Benavides M**, Alcaide-Garcia J, Torres E, Gil-Calle S, Sevilla I, Wolman R, Durán G, Álvarez M, Reyna-Fortes C, Ales I, Pereda T, Robles M, Kushnir M, Odegaard J, Faull I, Alba E. Clinical utility of comprehensive circulating tumor DNA genotyping compared with standard of care tissue testing in patients with newly diagnosed metastatic colorectal cancer. *ESMO Open* 2022; **7**: 100481 [PMID: 35525184 DOI: 10.1016/j.esmoop.2022.100481]

192 **Güttlein L**, Luca MR, Esteso F, Fresno C, Mariani J, Otero Pizarro M, Brest E, Starapoli S, Kreimberg K, Teves P, Mendoza Bertelli A, R Girotti M, Salanova R, O'Connor JM. Liquid biopsy for *KRAS, NRAS* and *BRAF* mutation testing in advanced colorectal cancer patients: the Argentinean experience. *Future Oncol* 2022; **18**: 3277-3287 [PMID: 36004810 DOI: 10.2217/fon-2022-0329]

193 **Kumbrink J**, Bohlmann L, Mamlouk S, Redmer T, Peilstöcker D, Li P, Lorenzen S, Algül H, Kasper S, Hempel D, Kaiser F, Michl M, Bartsch H, Neumann J, Klauschen F, von Bergwelt-Baildon M, Modest DP, Stahler A, Stintzing S, Jung A, Kirchner T, Schäfer R, Heinemann V, Holch JW. Serial Analysis of Gene Mutations and Gene Expression during First-Line Chemotherapy against Metastatic Colorectal Cancer: Identification of Potentially Actionable Targets within the Multicenter Prospective Biomarker Study REVEAL. *Cancers (Basel)* 2022; **14** [PMID: 35892888 DOI:

10.3390/cancers14153631]

194 **Sartore-Bianchi A**, Pietrantonio F, Lonardi S, Mussolin B, Rua F, Crisafulli G, Bartolini A, Fenocchio E, Amatu A, Manca P, Bergamo F, Tosi F, Mauri G, Ambrosini M, Daniel F, Torri V, Vanzulli A, Regge D, Cappello G, Marchiò C, Berrino E, Sapino A, Marsoni S, Siena S, Bardelli A. Circulating tumor DNA to guide rechallenge with panitumumab in metastatic colorectal cancer: the phase 2 CHRONOS trial. *Nat Med* 2022; **28**: 1612-1618 [PMID: 35915157 DOI: 10.1038/s41591-022-01886-0]

195 **Chennamadhavuni A**, Kasi PM. Circulating Tumor DNA in Identifying Resistant Sub-Clones Post EGFR Blockade: Implications for EGFR Rechallenge. *Front Oncol* 2022; **12**: 847299 [PMID: 35837097 DOI: 10.3389/fonc.2022.847299]

196 **Santos C**, Azuara D, Viéitez JM, Páez D, Falcó E, Élez E, López-López C, Valladares M, Robles-Díaz L, García-Alfonso P, Bugés C, Durán G, Salud A, Navarro V, Capellá G, Aranda E, Salazar R. Phase II study of high-sensitivity genotyping of KRAS, NRAS, BRAF and PIK3CA to ultra-select metastatic colorectal cancer patients for panitumumab plus FOLFIRI: the ULTRA trial. *Ann Oncol* 2019; **30**: 796-803 [PMID: 30840064 DOI: 10.1093/annonc/mdz082]

197 **Grasselli J**, Elez E, Caratù G, Matito J, Santos C, Macarulla T, Vidal J, Garcia M, Viéitez JM, Paéz D, Falcó E, Lopez Lopez C, Aranda E, Jones F, Sikri V, Nuciforo P, Fasani R, Tabernero J, Montagut C, Azuara D, Dienstmann R, Salazar R, Vivancos A. Concordance of blood- and tumor-based detection of RAS mutations to guide anti-EGFR therapy in metastatic colorectal cancer. *Ann Oncol* 2017; **28**: 1294-1301 [PMID: 28368441 DOI: 10.1093/annonc/mdx112]

198 **Holch JW**, Ricard I, Stintzing S, Modest DP, Heinemann V. The relevance of primary tumour location in patients with metastatic colorectal cancer: A meta-analysis of first-line clinical trials. *Eur J Cancer* 2017; **70**: 87-98 [PMID: 27907852 DOI: 10.1016/j.ejca.2016.10.007]

199 **Arnold D**, Lueza B, Douillard JY, Peeters M, Lenz HJ, Venook A, Heinemann V, Van Cutsem E, Pignon JP, Tabernero J, Cervantes A, Ciardiello F. Prognostic and predictive value of primary tumour side in patients with RAS wild-type metastatic colorectal cancer treated with chemotherapy and EGFR directed antibodies in six randomized trials. *Ann Oncol* 2017; **28**: 1713-1729 [PMID: 28407110 DOI: 10.1093/annonc/mdx175]

200 **Moretto R**, Cremolini C, Rossini D, Pietrantonio F, Battaglin F, Mennitto A, Bergamo F, Loupakis F, Marmorino F, Berenato R, Marsico VA, Caporale M, Antoniotti C, Masi G, Salvatore L, Borelli B, Fontanini G, Lonardi S, De Braud F, Falcone A. Location of Primary Tumor and Benefit From Anti-Epidermal Growth Factor Receptor Monoclonal Antibodies in Patients With RAS and BRAF Wild-Type Metastatic Colorectal Cancer. *Oncologist* 2016; **21**: 988-994 [PMID: 27382031 DOI: 10.1634/theoncologist.2016-0084]

201 **Zhou J**, Ji Q, Li Q. Resistance to anti-EGFR therapies in metastatic colorectal cancer: underlying mechanisms and reversal strategies. *J Exp Clin Cancer Res* 2021; **40**: 328 [PMID: 34663410 DOI: 10.1186/s13046-021-02130-2]

202 **Arena S**, Siravegna G, Mussolin B, Kearns JD, Wolf BB, Misale S, Lazzari L, Bertotti A, Trusolino L, Adjei AA, Montagut C, Di Nicolantonio F, Nering R, Bardelli A. MM-151 overcomes acquired resistance to cetuximab and panitumumab in colorectal cancers harboring EGFR extracellular domain mutations. *Sci Transl Med* 2016; **8**: 324ra14 [PMID: 26843189 DOI: 10.1126/scitranslmed.aad5640]

203 **Bagchi A**, Haidar JN, Eastman SW, Vieth M, Topper M, Iacolina MD, Walker JM, Forest A, Shen Y, Novosiadly RD, Ferguson KM. Molecular Basis for Necitumumab Inhibition of EGFR Variants Associated with Acquired Cetuximab Resistance. *Mol Cancer Ther* 2018; **17**: 521-531 [PMID: 29158469 DOI: 10.1158/1535-7163.MCT-17-0575]

204 **Sánchez-Martín FJ**, Bellosillo B, Gelabert-Baldrich M, Dalmases A, Cañadas I, Vidal J, Martinez A, Argilés G, Siravegna G, Arena S, Koefoed K, Visa L, Arpí O, Horak ID, Iglesias M, Stroh C, Kragh M, Rovira A, Albanell J, Tabernero J, Bardelli A, Montagut C. The First-in-class Anti-EGFR Antibody Mixture Sym004 Overcomes Cetuximab Resistance Mediated by EGFR Extracellular Domain Mutations in Colorectal Cancer. *Clin Cancer Res* 2016; **22**: 3260-3267 [PMID: 26888827 DOI: 10.1158/1078-0432.CCR-15-2400]

205 **Yang L**, Bhattacharya A, Li Y, Sexton S, Ling X, Li F, Zhang Y. Depleting receptor tyrosine kinases EGFR and HER2 overcomes resistance to EGFR inhibitors in colorectal cancer. *J Exp Clin Cancer Res* 2022; **41**: 184 [PMID: 35650607 DOI: 10.1186/s13046-022-02389-z]

206 **Lee HW**, Son E, Lee K, Lee Y, Kim Y, Lee JC, Lim Y, Hur M, Kim D, Nam DH. Promising Therapeutic Efficacy of GC1118, an Anti-EGFR Antibody, against KRAS Mutation-Driven Colorectal Cancer Patient-Derived Xenografts. *Int J Mol Sci* 2019; **20** [PMID: 31771279 DOI: 10.3390/ijms20235894]

207 **Sidaway P**. Microenvironment plasticity confers cetuximab resistance. *Nat Rev Clin Oncol* 2019; **16**: 527 [PMID: 31324873 DOI: 10.1038/s41571-019-0259-4]

208 **Parseghian CM**, Napolitano S, Loree JM, Kopetz S. Mechanisms of Innate and Acquired Resistance to Anti-EGFR Therapy: A Review of Current Knowledge with a Focus on Rechallenge Therapies. *Clin Cancer Res* 2019; **25**: 6899-6908 [PMID: 31263029 DOI: 10.1158/1078-0432.CCR-19-0823]

209 **Martinelli E**, Ciardiello D, Martini G, Troiani T, Cardone C, Vitiello PP, Normanno N, Rachiglio AM, Maiello E, Latiano T, De Vita F, Ciardiello F. Implementing anti-epidermal growth factor receptor (EGFR) therapy in metastatic colorectal cancer: challenges and future perspectives. *Ann Oncol* 2020; **31**: 30-40 [PMID: 31912793 DOI: 10.1016/j.annonc.2019.10.007]

210 **Schulz MS**, Wolf S, Struck V, Thomas N, Husman G, Zeuzem S, Koch C, Trojan J, Schnitzbauer AA, Bechstein WO, Waidmann O. Anti-EGFR Reintroduction and Rechallenge in Metastatic Colorectal Cancer (mCRC): A Real-World Analysis. *Cancers (Basel)* 2022; **14** [PMID: 35406413 DOI: 10.3390/cancers14071641]

211 **Chen C**, Di Bartolomeo M, Corallo S, Strickler JH, Goyal L. Overcoming Resistance to Targeted Therapies in Gastrointestinal Cancers: Progress to Date and Progress to Come. *Am Soc Clin Oncol Educ Book* 2020; **40**: 161-173 [PMID: 32421451 DOI: 10.1200/EDBK_280871]

212 **de Angelo RM**, Almeida MO, de Paula H, Honorio KM. Studies on the Dual Activity of EGFR and HER-2 Inhibitors Using Structure-Based Drug Design Techniques. *Int J Mol Sci* 2018; **19** [PMID: 30477154 DOI: 10.3390/ijms19123728]

213 **Reid A**, Vidal L, Shaw H, de Bono J. Dual inhibition of ErbB1 (EGFR/HER1) and ErbB2 (HER2/neu). *Eur J Cancer* 2007; **43**: 481-489 [PMID: 17208435 DOI: 10.1016/j.ejca.2006.11.007]

214 **Ahcene Djaballah S**, Daniel F, Milani A, Ricagno G, Lonardi S. HER2 in Colorectal Cancer: The Long and Winding Road From Negative Predictive Factor to Positive Actionable Target. *Am Soc Clin Oncol Educ Book* 2022; **42**: 1-14

[PMID: 35580290 DOI: 10.1200/EDBK_351354]

215 **Burris HA 3rd**, Rugo HS, Vukelja SJ, Vogel CL, Borson RA, Limentani S, Tan-Chiu E, Krop IE, Michaelson RA, Girish S, Amler L, Zheng M, Chu YW, Klencke B, O'Shaughnessy JA. Phase II study of the antibody drug conjugate trastuzumab-DM1 for the treatment of human epidermal growth factor receptor 2 (HER2)-positive breast cancer after prior HER2-directed therapy. *J Clin Oncol* 2011; **29**: 398-405 [PMID: 21172893 DOI: 10.1200/JCO.2010.29.5865]

216 **Lopes-Coelho F**, Martins F, Pereira SA, Serpa J. Anti-Angiogenic Therapy: Current Challenges and Future Perspectives. *Int J Mol Sci* 2021; **22** [PMID: 33916438 DOI: 10.3390/ijms22073765]

217 **Lieu CH**, Tran H, Jiang ZQ, Mao M, Overman MJ, Lin E, Eng C, Morris J, Ellis L, Heymach JV, Kopetz S. The association of alternate VEGF ligands with resistance to anti-VEGF therapy in metastatic colorectal cancer. *PLoS One* 2013; **8**: e77117 [PMID: 24143206 DOI: 10.1371/journal.pone.0077117]

218 **Heil F**, Babitzki G, Julien-Laferriere A, Ooi CH, Hidalgo M, Massard C, Martinez-Garcia M, Le Tourneau C, Kockx M, Gerber P, Rossomanno S, Krieter O, Lahr A, Wild N, Harring SV, Lechner K. Vanucizumab mode of action: Serial biomarkers in plasma, tumor, and skin-wound-healing biopsies. *Transl Oncol* 2021; **14**: 100984 [PMID: 33338877 DOI: 10.1016/j.tranon.2020.100984]

219 **Trusolino L**, Bertotti A, Comoglio PM. MET signalling: principles and functions in development, organ regeneration and cancer. *Nat Rev Mol Cell Biol* 2010; **11**: 834-848 [PMID: 21102609 DOI: 10.1038/nrm3012]

220 **Escudier B**, Powles T, Motzer RJ, Olencki T, Arén Frontera O, Oudard S, Rolland F, Tomczak P, Castellano D, Appleman LJ, Drabkin H, Vaena D, Milwee S, Youkstetter J, Lougheed JC, Bracarda S, Choueiri TK. Cabozantinib, a New Standard of Care for Patients With Advanced Renal Cell Carcinoma and Bone Metastases? *J Clin Oncol* 2018; **36**: 765-772 [PMID: 29309249 DOI: 10.1200/JCO.2017.74.7352]

221 **Vinay DS**, Ryan EP, Pawelec G, Talib WH, Stagg J, Elkord E, Lichtor T, Decker WK, Whelan RL, Kumara HMCS, Signori E, Honoki K, Georgakilas AG, Amin A, Helferich WG, Boosani CS, Guha G, Ciriolo MR, Chen S, Mohammed SI, Azmi AS, Keith WN, Bilsland A, Bhakta D, Halicka D, Fujii H, Aquilano K, Ashraf SS, Nowsheen S, Yang X, Choi BK, Kwon BS. Immune evasion in cancer: Mechanistic basis and therapeutic strategies. *Semin Cancer Biol* 2015; **35** Suppl: S185-S198 [PMID: 25818339 DOI: 10.1016/j.semcancer.2015.03.004]

222 **Bai R**, Chen N, Li L, Du N, Bai L, Lv Z, Tian H, Cui J. Mechanisms of Cancer Resistance to Immunotherapy. *Front Oncol* 2020; **10**: 1290 [PMID: 32850400 DOI: 10.3389/fonc.2020.01290]

223 **Murciano-Goroff YR**, Warner AB, Wolchok JD. The future of cancer immunotherapy: microenvironment-targeting combinations. *Cell Res* 2020; **30**: 507-519 [PMID: 32467593 DOI: 10.1038/s41422-020-0337-2]

224 **Fiegle E**, Doleschel D, Koletnik S, Rix A, Weiskirchen R, Borkham-Kamphorst E, Kiessling F, Lederle W. Dual CTLA-4 and PD-L1 Blockade Inhibits Tumor Growth and Liver Metastasis in a Highly Aggressive Orthotopic Mouse Model of Colon Cancer. *Neoplasia* 2019; **21**: 932-944 [PMID: 31412307 DOI: 10.1016/j.neo.2019.07.006]

225 **Rupp T**, Genest L, Babin D, Legrand C, Hunault M, Froget G, Castagné V. Anti-CTLA-4 and anti-PD-1 immunotherapies repress tumor progression in preclinical breast and colon model with independent regulatory T cells response. *Transl Oncol* 2022; **20**: 101405 [PMID: 35339889 DOI: 10.1016/j.tranon.2022.101405]

226 **Monjazeb AM**, Giobbie-Hurder A, Lako A, Thrash EM, Brennick RC, Kao KZ, Manuszak C, Gentzler RD, Tesfaye A, Jabbour SK, Alese OB, Rahma OE, Cleary JM, Sharon E, Mamon HJ, Cho M, Streicher H, Chen HX, Ahmed MM, Mariño-Enríquez A, Kim-Schulze S, Gnjatic S, Maverakis E, Marusina AI, Merleev AA, Severgnini M, Pfaff KL, Lindsay J, Weirather JL, Ranasinghe S, Spektor A, Rodig SJ, Hodi SF, Schoenfeld JD. A Randomized Trial of Combined PD-L1 and CTLA-4 Inhibition with Targeted Low-Dose or Hypofractionated Radiation for Patients with Metastatic Colorectal Cancer. *Clin Cancer Res* 2021; **27**: 2470-2480 [PMID: 33568343 DOI: 10.1158/1078-0432.CCR-20-4632]

227 **Byrne AT**, Alférez DG, Amant F, Annibali D, Arribas J, Biankin AV, Bruna A, Budinská E, Caldas C, Chang DK, Clarke RB, Clevers H, Coukos G, Dangles-Marie V, Eckhardt SG, Gonzalez-Suarez E, Hermans E, Hidalgo M, Jarzabek MA, de Jong S, Jonkers J, Kemper K, Lanfrancone L, Mælandsmo GM, Marangoni E, Marine JC, Medico E, Norum JH, Palmer HG, Peeper DS, Pelicci PG, Piris-Gimenez A, Roman-Roman S, Rueda OM, Seoane J, Serra V, Soucek L, Vanhecke D, Villanueva A, Vinolo E, Bertotti A, Trusolino L. Interrogating open issues in cancer precision medicine with patient-derived xenografts. *Nat Rev Cancer* 2017; **17**: 254-268 [PMID: 28104906 DOI: 10.1038/nrc.2016.140]

228 **Azar J**, Bahmad HF, Daher D, Moubarak MM, Hadadeh O, Monzer A, Al Bitar S, Jamal M, Al-Sayegh M, Abou-Kheir W. The Use of Stem Cell-Derived Organoids in Disease Modeling: An Update. *Int J Mol Sci* 2021; **22** [PMID: 34299287 DOI: 10.3390/ijms22147667]

229 **Al Bitar S**, Ballout F, Monzer A, Kanso M, Saheb N, Mukherji D, Faraj W, Tawil A, Doughan S, Hussein M, Abou-Kheir W, Gali-Muhtasib H. Thymoquinone Radiosensitizes Human Colorectal Cancer Cells in 2D and 3D Culture Models. *Cancers (Basel)* 2022; **14** [PMID: 35326517 DOI: 10.3390/cancers14061363]

230 **Monzer A**, Wakimian K, Ballout F, Al Bitar S, Yehya A, Kanso M, Saheb N, Tawil A, Doughan S, Hussein M, Mukherji D, Faraj D, Gali-Muhtasib H, Abou-Kheir W. Novel therapeutic diiminoquinone exhibits anticancer effects on human colorectal cancer cells in two-dimensional and three-dimensional *in vitro* models. *World J Gastroenterol* 2022; **28**: 4787-4811 [PMID: 36156922 DOI: 10.3748/wjg.v28.i33.4787]

231 **Karapetis CS**, Khambata-Ford S, Jonker DJ, O'Callaghan CJ, Tu D, Tebbutt NC, Simes RJ, Chalchal H, Shapiro JD, Robitaille S, Price TJ, Shepherd L, Au HJ, Langer C, Moore MJ, Zalcberg JR. K-ras mutations and benefit from cetuximab in advanced colorectal cancer. *N Engl J Med* 2008; **359**: 1757-1765 [PMID: 18946061 DOI: 10.1056/NEJMoa0804385]

232 **Yoshida GJ**. Applications of patient-derived tumor xenograft models and tumor organoids. *J Hematol Oncol* 2020; **13**: 4 [PMID: 31910904 DOI: 10.1186/s13045-019-0829-z]

233 **Takeda H**, Kataoka S, Nakayama M, Ali MAE, Oshima H, Yamamoto D, Park JW, Takegami Y, An T, Jenkins NA, Copeland NG, Oshima M. CRISPR-Cas9-mediated gene knockout in intestinal tumor organoids provides functional validation for colorectal cancer driver genes. *Proc Natl Acad Sci U S A* 2019; **116**: 15635-15644 [PMID: 31300537 DOI: 10.1073/pnas.1904714116]

234 **Matano M**, Date S, Shimokawa M, Takano A, Fujii M, Ohta Y, Watanabe T, Kanai T, Sato T. Modeling colorectal cancer using CRISPR-Cas9-mediated engineering of human intestinal organoids. *Nat Med* 2015; **21**: 256-262 [PMID: 25706875

DOI: 10.1038/nm.3802]

235 **van de Wetering M**, Francies HE, Francis JM, Bounova G, Iorio F, Pronk A, van Houdt W, van Gorp J, Taylor-Weiner A, Kester L, McLaren-Douglas A, Blokker J, Jaksani S, Bartfeld S, Volckman R, van Sluis P, Li VS, Seepo S, Sekhar Pedamallu C, Cibulskis K, Carter SL, McKenna A, Lawrence MS, Lichtenstein L, Stewart C, Koster J, Versteeg R, van Oudenaarden A, Saez-Rodriguez J, Vries RG, Getz G, Wessels L, Stratton MR, McDermott U, Meyerson M, Garnett MJ, Clevers H. Prospective derivation of a living organoid biobank of colorectal cancer patients. *Cell* 2015; **161**: 933-945 [PMID: 25957691 DOI: 10.1016/j.cell.2015.03.053]

236 **Vlachogiannis G**, Hedayat S, Vatsiou A, Jamin Y, Fernández-Mateos J, Khan K, Lampis A, Eason K, Huntingford I, Burke R, Rata M, Koh DM, Tunariu N, Collins D, Hulkki-Wilson S, Ragulan C, Spiteri I, Moorcraft SY, Chau I, Rao S, Watkins D, Fotiadis N, Bali M, Darvish-Damavandi M, Lote H, Eltahir Z, Smyth EC, Begum R, Clarke PA, Hahne JC, Dowsett M, de Bono J, Workman P, Sadanandam A, Fassan M, Sansom OJ, Eccles S, Starling N, Braconi C, Sottoriva A, Robinson SP, Cunningham D, Valeri N. Patient-derived organoids model treatment response of metastatic gastrointestinal cancers. *Science* 2018; **359**: 920-926 [PMID: 29472484 DOI: 10.1126/science.aao2774]

237 **Cho YW**, Min DW, Kim HP, An Y, Kim S, Youk J, Chun J, Im JP, Song SH, Ju YS, Han SW, Park KJ, Kim TY. Patient-derived organoids as a preclinical platform for precision medicine in colorectal cancer. *Mol Oncol* 2022; **16**: 2396-2412 [PMID: 34850547 DOI: 10.1002/1878-0261.13144]

238 **Cao Y**, Zhang G, Zhang J, Yang Y, Ren J, Yan X, Wang Z, Zhao Z, Huang X, Bao H, Zhou J. Predicting Microsatellite Instability Status in Colorectal Cancer Based on Triphasic Enhanced Computed Tomography Radiomics Signatures: A Multicenter Study. *Front Oncol* 2021; **11**: 687771 [PMID: 34178682 DOI: 10.3389/fonc.2021.687771]

239 **Wang R**, Li J, Zhou X, Mao Y, Wang W, Gao S, Gao Y, Chen K, Yu S, Wu X, Wen L, Ge H, Fu W, Tang F. Single-cell genomic and transcriptomic landscapes of primary and metastatic colorectal cancer tumors. *Genome Med* 2022; **14**: 93 [PMID: 35974387 DOI: 10.1186/s13073-022-01093-z]

World Journal of Gastroenterology

Submit a Manuscript: https://www.f6publishing.com

World J Gastroenterol 2023 March 7; 29(9): 1427-1445

DOI: 10.3748/wjg.v29.i9.1427

ISSN 1007-9327 (print) ISSN 2219-2840 (online)

REVIEW

Clinical impact of artificial intelligence-based solutions on imaging of the pancreas and liver

M Alvaro Berbís, Felix Paulano Godino, Javier Royuela del Val, Lidia Alcalá Mata, Antonio Luna

Specialty type: Gastroenterology and hepatology

Provenance and peer review: Invited article; Externally peer reviewed.

Peer-review model: Single blind

Peer-review report's scientific quality classification

Grade A (Excellent): 0
Grade B (Very good): B, B
Grade C (Good): C
Grade D (Fair): 0
Grade E (Poor): 0

P-Reviewer: Alves N, Portugal; Ma C, China; Xiao B, China

Received: September 28, 2022
Peer-review started: September 28, 2022
First decision: January 3, 2023
Revised: January 13, 2023
Accepted: February 27, 2023
Article in press: February 27, 2023
Published online: March 7, 2023

M Alvaro Berbís, Javier Royuela del Val, Department of Radiology, HT Médica, San Juan de Dios Hospital, Córdoba 14960, Spain

M Alvaro Berbís, Faculty of Medicine, Autonomous University of Madrid, Madrid 28049, Spain

Felix Paulano Godino, Lidia Alcalá Mata, Antonio Luna, Department of Radiology, HT Médica, Clínica las Nieves, Jaén 23007, Spain

Corresponding author: Antonio Luna, MD, PhD, Director, Department of Radiology, HT Médica, Clínica las Nieves, MRI Unit, 2 Carmelo Torres, Jaén 23007, Spain.
aluna70@htmedica.com

Abstract

Artificial intelligence (AI) has experienced substantial progress over the last ten years in many fields of application, including healthcare. In hepatology and pancreatology, major attention to date has been paid to its application to the assisted or even automated interpretation of radiological images, where AI can generate accurate and reproducible imaging diagnosis, reducing the physicians' workload. AI can provide automatic or semi-automatic segmentation and registration of the liver and pancreatic glands and lesions. Furthermore, using radiomics, AI can introduce new quantitative information which is not visible to the human eye to radiological reports. AI has been applied in the detection and characterization of focal lesions and diffuse diseases of the liver and pancreas, such as neoplasms, chronic hepatic disease, or acute or chronic pancreatitis, among others. These solutions have been applied to different imaging techniques commonly used to diagnose liver and pancreatic diseases, such as ultrasound, endoscopic ultrasonography, computerized tomography (CT), magnetic resonance imaging, and positron emission tomography/CT. However, AI is also applied in this context to many other relevant steps involved in a comprehensive clinical scenario to manage a gastroenterological patient. AI can also be applied to choose the most convenient test prescription, to improve image quality or accelerate its acquisition, and to predict patient prognosis and treatment response. In this review, we summarize the current evidence on the application of AI to hepatic and pancreatic radiology, not only in regard to the interpretation of images, but also to all the steps involved in the radiological workflow in a broader sense. Lastly, we discuss the challenges and future directions of the clinical application of AI methods.

Key Words: Artificial intelligence; Machine learning; Deep learning; Imaging; Liver; Pancreas

Core Tip: The gastroenterology field is changing with the application of artificial intelligence (AI) solutions capable of assisting and even automating the interpretation of radiological images (ultrasound, endoscopic ultrasound, computerized tomography, magnetic resonance imaging, and positron emission tomography), generating accurate and reproducible diagnoses. AI can further be applied to other steps of the radiological workflow beyond image interpretation, including test selection, image quality improvement, acceleration of image acquisition, and prediction of patient prognosis and outcome. We herein discuss the current evidence, challenges, and future directions on the application of AI to hepatic and pancreatic radiology.

Citation: Berbís MA, Paulano Godino F, Royuela del Val J, Alcalá Mata L, Luna A. Clinical impact of artificial intelligence-based solutions on imaging of the pancreas and liver. *World J Gastroenterol* 2023; 29(9): 1427-1445
URL: https://www.wjgnet.com/1007-9327/full/v29/i9/1427.htm
DOI: https://dx.doi.org/10.3748/wjg.v29.i9.1427

INTRODUCTION

Malignant tumors of the liver and pancreas are among the most common and lethal types of cancer. According to the recent GLOBOCAN 2020 data[1], liver and pancreas are the 6th and 12th most common sites for primary cancer, with 905677 and 495773 new cases in 2020, respectively. However, they also represent the 3rd and 7th neoplasia with the highest mortality, causing 830180 and 466003 deaths worldwide in 2020, respectively. If taken combined, cancer at the liver or pancreas thus represents the 5th most incident and the second most lethal one.

Cancer at these locations account for almost as many deaths as cases. Five-year survival rates are 20% for liver cancer[2] and as low as 11% for pancreatic cancer[3], making them two of the cancer sites with the poorest prognosis. Other non-oncologic diseases affecting these organs are also highly prevalent, such as diffuse liver disease, including chronic liver disease, which affects tens of millions of people globally and represents a substantial socioeconomic burden[4].

Clinical outcomes of patients with these types of disease depend on a variety of factors, including stage and disease extension as assessed by imaging, and correct election of treatment. Thus, there is an unmet need for new tools capable of assisting specialists in early detection, characterization, and management of these diseases.

In recent years, artificial intelligence (AI) has shown promise in different areas of healthcare. The evaluation of medical images by machine learning (ML) approaches is a leading research field which, in gastroenterology, has applications in automatic analysis of different types of images, such as radiology, pathology, and endoscopy studies[5].

The first applications of AI to radiology have been dominated by anatomic locations such as the brain or the breast. Image analysis of abdominal organs, such as the liver and pancreas, are more challenging. Magnetic resonance imaging (MRI) in these locations, especially at 3 T, is prone to motion and field inhomogeneity artifacts, which are aggravated by larger fields of view[6]. As a result, advances in automatic analyses of abdominal images have gathered comparatively less attention. Nonetheless, the application of AI in liver and pancreas imaging is also gaining increasing interest (Figure 1). The goal of this review is to summarize the current experience on the use of AI to assist radiologists in their workflow, acquisition, and interpretation of medical images of the liver and pancreas.

AI IN RADIOLOGY: BASIC PRINCIPLES

Artificial intelligence is expected to revolutionize the medical field, deeply impacting the hospital and clinical settings by potentially improving diagnostic accuracy, treatment delivery, and allowing a more personalized medical care[7]. Radiology will arguably be one the most changed areas of medicine because of AI implementation in its workflows, as the information-rich images generated in this field are an excellent source of data for the development of AI algorithms. Broadly, the term AI refers to a wide range of technologies and computing processes capable of imitating human intelligence to extract information from input data to solve a problem. This rapidly evolving area has a vocabulary of its own (Figure 2) that can be daunting to those not familiar with the field, including terms that are oftentimes

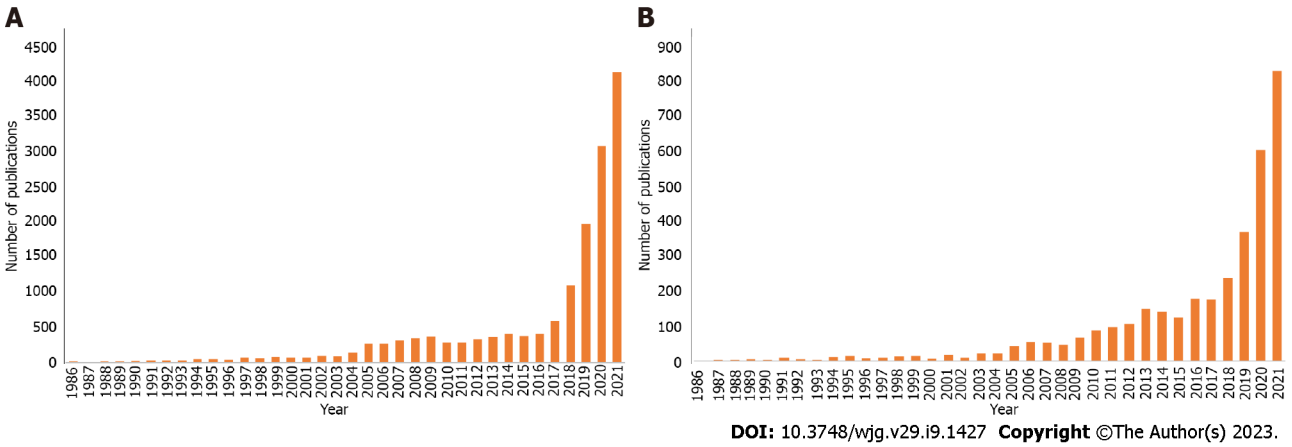

DOI: 10.3748/wjg.v29.i9.1427

Figure 1 PubMed results by year using the search terms. A and B: Artificial intelligence radiology (top) and artificial intelligence AND (liver OR pancreas) (bottom).

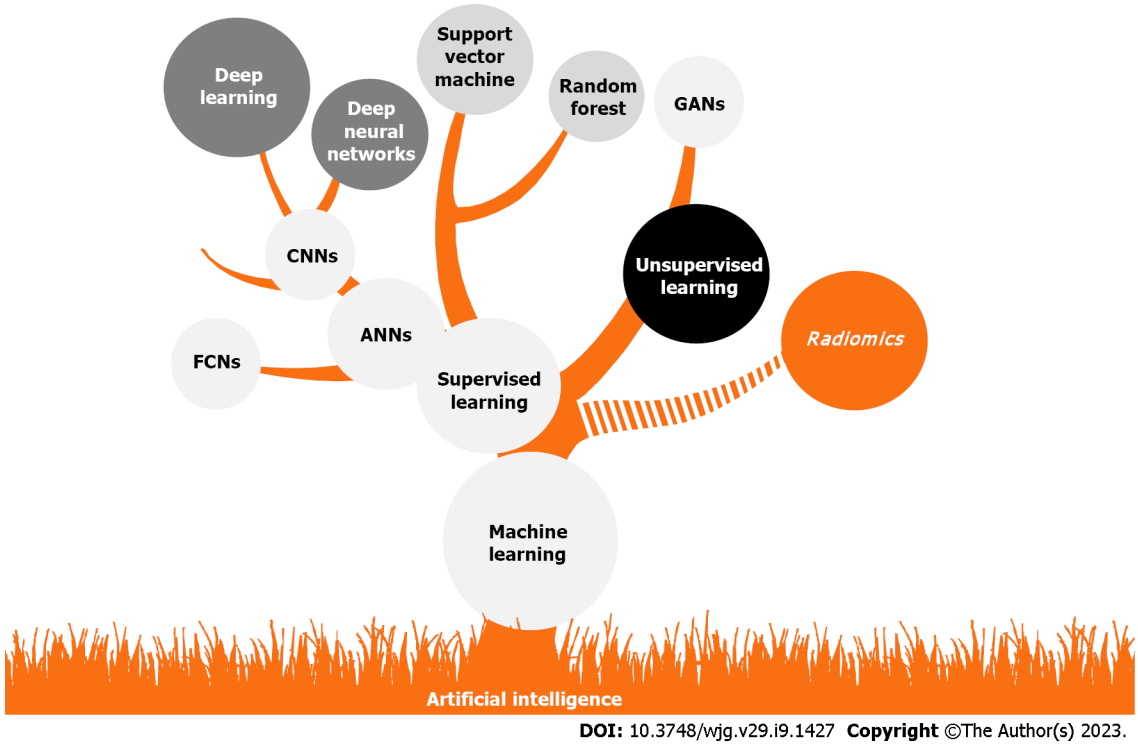

DOI: 10.3748/wjg.v29.i9.1427

Figure 2 Relation between artificial intelligence and related subdisciplines, neural network architectures, and/or techniques. ANN: Artificial neural network; FCN: Fully convolutional network; CNN: Convolutional neural network; GAN: Generation adversarial network.

used as synonyms to AI, such as ML.

ML is actually a subset of AI consisting of those methods capable of training a computer system to perform a given task based on provided information or experience without explicit programming, thus conferring machines the ability to learn[8]. The aim of ML is to predict an output based on a given input (a training dataset). Common ML applications in radiology include classification, image segmentation, regression, and clustering[9]. ML can be sub-divided into supervised and unsupervised learning[10]. In supervised learning, the most common type used in medical research, the algorithm is trained with labeled examples (*i.e.*, the correct output for these training data, known as ground truth, is already known). Among the methods employed in supervised learning, random forest (RF), and specially, support vector machine (SVM), are powerful algorithms frequently used for the classification of images [7], including image segmentation. Conversely, in unsupervised learning, the ground truth is not known, as the algorithm is trained with unlabeled data that must be classified by the algorithm itself.

Artificial neural networks (ANNs), named after their brain-inspired structure and functioning process, can be trained *via* both supervised and unsupervised ML. In these ANNs, input information flows through a variable number of layers composed of artificial neurons, joined by weighted

connectors, that process the data to obtain an output that matches the ground truth as closely as possible. Generative adversarial networks (GANs) are an example of ANN trained *via* unsupervised learning. GANs include two networks: One which creates new data based on input examples (*i.e.*, generator), and one which distinguishes between different types of data (*i.e.*, discriminator)[11]. These networks can be used to produce realistic, synthetic images as a strategy for data augmentation[12]. Similarly, the structure of convolutional neural networks (CNNs), a type of ANN specially designed for computer vision tasks, is based on that of the animal visual cortex. Typically used in image recognition and classification, in CNNs the input information is filtered and analyzed through a convolutional layer, and the size of the resulting image is subsequently reduced by a pooling layer. This two-step process will be repeated as many times as layers integrate the CNN, with a final step in which an ANN will classify the image (Figure 3). Fully convolutional networks (FCNs, a type of ANN that only performs the convolution step) are the basis for U-net, a modified architecture that consists of a contracting path including several convolutional and pooling layers to capture context, followed by a symmetric expanding path including a number of up-sampling and convolutional layers to enable accurate localization. U-net is a popular network for the development of automatic segmentation algorithms, as it requires relatively small datasets for algorithm training[13].

Deep learning (DL) is a section of ML that utilizes multi-layered ANNs, referred to as deep neural networks (DNN), allowing the exploration of more complex data[14]. DL algorithms are gaining attention and raising considerable enthusiasm thanks to their scalability, easy accessibility, and ability to extract relevant information from the data without further indications other than input data. The recently developed nnU-Net, a publicly available DL-based segmentation tool capable of automatically configuring itself, has set a new state-of-the-art standard thanks to the systematization of the configuration process, which used to be a manual, complicated, and oftentimes limited task in previous approaches[15]. Improvement of the computational resources and the development of cloud technologies are also contributing to the application of DL architectures in a wide variety of research fields beyond medicine[14].

Closely related to the development of AI, the term radiomics refers to the computational extraction (*via* ML and DL algorithms) of quantitative data from radiological image features[16]. A particularly useful and valuable application of radiomics is the analysis of radiologic textures, defined as the differences in the grayscale intensities in the area of interest, which have been associated with intratumor heterogeneity[17] and that can potentially provide clinically relevant information that otherwise would remain unknown.

IMAGE ACQUISITION

The ultimate aim of computerized tomography (CT) and MRI is to unveil clinically relevant information; thus, the importance of this information relies heavily on the quality of the image. For CT, radiation dose is a parameter as important as image quality, and both are closely related to acquisition and reconstruction times. Iterative reconstruction (IR) algorithms[18] are the current technique of choice to transform the raw data into a 3D volume presented as an anatomical image. These algorithms generate an image estimate that is projected forward into a synthetic sinogram; subsequently, this image estimate is iteratively rectified by comparison with the real raw data sinogram until the algorithm's predefined endpoint condition is met, resulting in enhanced image quality and thus allowing an important dose reduction[19]. DL reconstruction algorithms (DLR) are currently being developed with the aim to further improve image quality, therefore further reducing radiation doses. Compared to IR algorithms, DLR algorithms trained with low-dose data offer an improved signal-to-noise (SNR) ratio, as demonstrated by the U-net-based CNN developed by Jin *et al*[20], thus facilitating the detection of lesions of any kind and the increased use of low-dose imaging. Currently, there are two commercially available DLRs: TrueFidelity (GE Healthcare, Chicago, IL, United States) and AiCE (Canon Medical Systems, Otawara, Japan). Akagi *et al*[21] employed AiCE in their study and reported improved contrast-to-noise ratio and image quality in CT images, compared to images created with a hybrid IR algorithm. Although the preliminary results are exciting, further validation for these DLR algorithms is required, and real dose reduction in the clinical setting has yet to be demonstrated.

An important setback of MRI is the long acquisition time, forcing the patient to lay still for a relatively long period and with any movement affecting the quality of the image. One way to reduce acquisition time is compressed sensing, based on the idea that if signal information is only present in a small portion of pixels, that sparsity can be used to reconstruct a high-definition image from considerably less collected data (undersampling). Kaga *et al*[22] evaluated the usefulness of the Compressed SENSE algorithm (Philips, Amsterdam, The Netherlands) in MRI of the abdomen using diffusion weighted images (DWIs) and reported a significantly improved image noise and contour of the liver and pancreas and higher apparent diffusion coefficient values, thus offering superior image quality compared to parallel imaging (PI)-DWI[22].

AI applications have also been designed to automate MRI and CT protocol selection with the aim to standardize workflows and increase effectiveness in the radiology setting. The selection of an

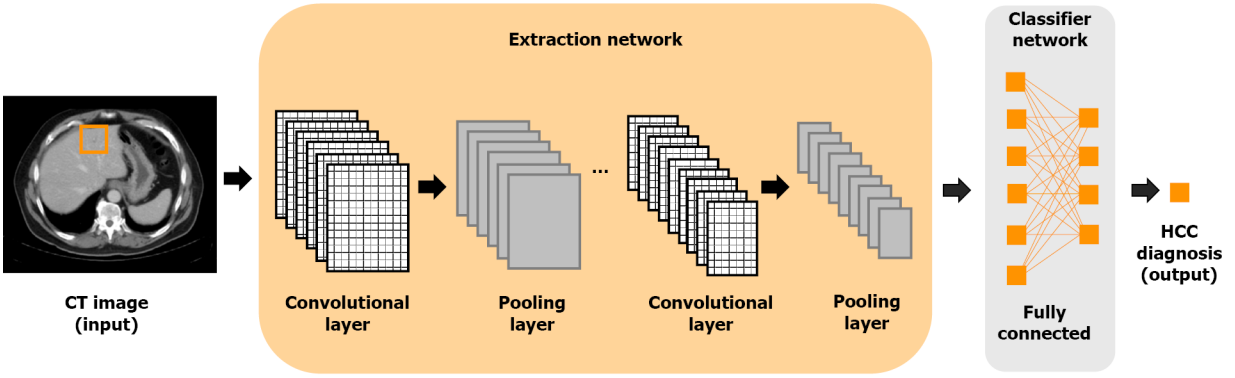

DOI: 10.3748/wjg.v29.i9.1427

Figure 3 Diagram of a convolutional neural network used for the classification of a focal liver lesion in a computerized tomography image. HCC: Hepatocellular carcinoma; CT: Computed tomography.

appropriate imaging protocol requires taking into account factors including the type of procedure, clinical indication, and the patient's medical history. The increasing incorporation of electronic medical records and other digital content has opened opportunities for the application of natural language processing (NLP) methods to extract structured data from unstructured radiology reports. López-Úbeda *et al*[23] developed an NLP-based classification system for automated protocol assignment that offered an overall accuracy of 92.25% for the CT and 86.91% for the MRI datasets. This system has already been successfully implemented and is currently in use at the HT Médica centers.

Information about the respiration of the patient can be used for functional studies, overall monitoring, or motion compensation during the performance of an MRI. Typically, breathing is measured *via* belts or nasal sensors that can potentially alter the raw MRI data. Using adaptive intelligence, the laser-based VitalEye system (Philips) registers a contactless continuous respiratory signal, with up to 50 body locations analyzed simultaneously and in real time, thus producing a more robust respiratory trace compared to traditional respiratory belts[24]. Moreover, as soon as the patient is lying on the table, the BioMatrix Respiratory Sensors (Siemens AG, Munich, Germany) embedded in the spinal coil produce a local magnetic field that changes with the variation of lung volume during breathing. These changes are registered, and the breathing pattern is integrated to optimize image quality[25]. By standardizing and accelerating the workflow, these advances allow technicians and radiologists to concentrate on the patient.

IMAGE ANALYSIS

Segmentation of liver and pancreas

Image analysis has experimented a huge progression with the advent of AI, and especially with DL, reaching state-of-art performances in many biomedical image analysis tasks[26-28] (Table 1). Among them, segmentation is one of the most important in radiology. For instance, accurate pancreas segmentation has applications in surgical planning, assessment of diabetes, and detection and analysis of pancreatic tumors[29]. Another key application of organ and lesion contouring is treatment volume calculation for radiotherapy planning. However, boundary delimitation of anatomical structures in medical images remains a challenge due to their complexity, particularly in the upper abdominal cavity, where there are constant changes in the position of the different organs with the respiratory cycle, as well as the occurrence of anatomical variants and pathological changes of organs[30].

The intersubject variability and complexity of the pancreas make segmentation of this organ a demanding task. Segmentation of pancreatic cancer lesions is particularly challenging because of their limited contrast and blurred boundaries against the background pancreatic parenchyma in CT and MR images[31]. In addition, other factors such as body mass index, visceral abdominal fat, volume of the pancreas, standard deviation of CT attenuation within pancreas, and median and average CT attenuation in the immediate neighborhood of the pancreas may affect segmentation accuracy[29,32].

These problems lead to high segmentation uncertainty and inaccurate results. To tackle these problems, Zheng *et al*[33] proposed a 2D, DL-based method that describes the uncertain regions of pancreatic MR images based on shadowed sets theory. It demonstrated high accuracy, with a dice similarity coefficient (DSC) of 73.88% on a cancer MRI dataset and 84.37% on the National Institutes of Health (NIH) Pancreas dataset (which contains 82 CT scans of healthy pancreas), respectively. The same authors reported[34] a more sophisticated 2.5D network that benefits from multi-level slice interaction. They surpassed state-of-art performances in the NIH dataset, with a DSC of 86.21% ± 4.37%, sensitivity of 87.49% ± 6.38%, and a specificity of 85.11% ± 6.49%.

Table 1 Works proposed for automated image analysis

Image analysis	Anatomical area	Modality	AI model	Ref.
Segmentation	Pancreas	MRI	CNN	[33,34,110]
			UDCGAN	[111]
			3D-Unet	[112]
	Liver	CT	SSC (no AI)	[36]
			PA (Atlas-no AI)	[39]
		MRI	CNN	[37,38,42,113]
			GAN	[43]
Registration	Liver	CT, MRI	CNN	[47]
			SG-DIR (no AI)	[48]
			Cycle-GAN + UR-Net	[46]
		4D-MRI	Non-rigid	[49]

MRI: Magnetic resonance imaging; CT: Computerized tomography; 4D-MRI: Four-dimensional magnetic resonance imaging; CNN: Convolutional neural network; UDCGAN: U-Type densely connected generation adversarial network; SCC: Sparse shape composition; AI: Artificial intelligence; PA: Probabilistic atlas; GAN: Generation adversarial network; SG-DIR: Structure-guided deformable image registration; UR-Net: Unsupervised registration network.

The liver is also a popular target for automated segmentation algorithms. Automatic segmentation of this organ is regarded as somewhat less challenging than that of the pancreas, with reported DSC scores typically in the > 0.90 range[35].

Li *et al*[36] presented a liver segmentation method from abdominal CT volumes for both healthy and pathological tissues, based on the level set and sparse shape composition (SSC) method. The experiments, performed using public databases SILVER07 and 3Dicardb, showed good results, with mean ASD, RMSD, MSD, VOE, and RVD of 0.9 mm, 1.8 mm, 19.4 mm, 5.1%, and 0.1%, respectively. Moreover, Winther *et al*[37] used a 3D DNN for automatic liver segmentation along with a Gd-EOB-DTPA-enhanced liver MR images dataset. Results show an intraclass correlation coefficient (ICC) of 0.987, DSC of 96.7% ± 1.9%, and a Hausdorff distance of 24.9 mm ± 14.7 mm compared with two expert readers who corresponded to an ICC of 0.973 and a DSC of 95.2% ± 2.8%. Finally, Mohagheghi *et al*[38] used a CNN but further incorporated prior knowledge. The model learnt the global shape information as prior knowledge by using a convolutional denoising auto-encoder; then, this knowledge was used to define a loss function and combine it with the Dice loss in the main segmentation model. This model with prior knowledge improved the performance of the 3D U-Net model and reached a DSC of 97.62% segmenting CT images of the Silver07-liver dataset.

Organ segmentation is even more challenging in pediatric patients studied with CT, as it is acquired at a low dose to minimize harmful radiation to children, thus having a lower SNR. Nakayama *et al*[39] proposed a liver segmentation algorithm for pediatric CT scans using a patient-specific level set distribution model to generate a probabilistic atlas, obtaining a DSC index of 88.21% in the segmentation. This approach may be useful for low dose studies in general, *i.e.*, also in the adult population.

Algorithms for automatic segmentation of the liver using MR images have proven equally efficient. For instance, Bobo *et al*[40] used a 2D FCN architecture to segment livers on T2-weighted MR images with a DSC score of 0.913. In a recent paper, Saunders *et al*[41] systematically analyzed the performance of different types of MR images in the training of CNN for liver segmentation, using a 3D U-net architecture. Water and fat images outperformed other modalities, such as T2* images, with a DSC of 0.94.

Conversely, high-quality automatic segmentation of liver lesions is not an easy task, since the low contrast between tumors and healthy liver parenchyma in CT images, their inhomogeneity, and its complexity pose a challenge for liver tumor segmentation. In addition, motion-induced phase errors due to peristaltic and respiratory movements negatively affect image quality and assessment of liver lesions in MR images. A 3D CNN was used by Meng *et al*[42] where a special three-dimensional dual path multiscale convolutional neural network (TDP-CNN) was designed for liver tumor segmentation. Results achieved in the LiTS public dataset were a DSC of 68.9%, Hausdorff distance of 7.96 mm, and average distance of 1.07 mm for liver tumor segmentation and a DSC of 96.5%, Hausdorff distance of 29.162 mm, and average distance of 0.197 mm for liver segmentation. A different approach for liver tumor segmentation was proposed by Chen *et al*[43]. In this work, an adversarial densely connected network algorithm was trained and evaluated using the Liver Tumor Segmentation challenge dataset. Results revealed an average Dice score of 68.4% and ASD, MSD, VOE, and RVD of 21 mm, 124 mm,

0.46%, and 0.73%, respectively.

Automatic contouring of hepatic tumor volumes has also been reported using CT scans, a modified SegNet CNN[44], and dynamic contrast enhanced (DCE)-MRI images in a U-net-like architecture[45], for example.

Some medical imaging vendors incorporate solutions for liver segmentation and hepatic lesion characterization integrated in the proprietary radiologist's workflow. For instance, the Liver Analysis research application from Siemens Healthcare (Erlangen, Germany) aims to provide AI support for liver MRI and CT reading. The tool includes DL-based algorithms for automatic segmentation of the whole liver, functional liver segments, and other abdominal organs like the spleen and kidneys (Figure 4A). It also features an AI method to automatically detect and segment focal liver lesions, providing lesion diameter, volume, and 3D contours (Figure 4B).

Registration

Medical image registration seeks to find an optimal spatial transformation that best aligns the underlying anatomical structures. Medical image registration is used in many clinical applications such as image guidance systems (IGS), motion tracking, segmentation, dose accumulation, image reconstruction, *etc*[28]. In clinical practice, image registration is a major problem in image-guided liver interventions, especially for the soft-tissues, where organ shape changes occurring between pre-procedural and intra-procedural imaging pose significant challenges[46]. Schneider *et al*[47] showed how semi-automatic registration in IGS may improve patient safety by enabling 3D visualization of critical intra- and extra-hepatic structures. A novel IGS (SmartLiver) offering augmented reality visualization was developed to provide intuitive visualization by using DL algorithms for semi-automatic image registration. Results showed a mean registration accuracy of 10.9 mm ± 4.2 mm (manual) *vs* 13.9 mm ± 4.4 mm (semi-automatic), hence significantly improving the manual registration. Kuznetsova *et al*[48] assessed the performance of structure-guided deformable image registration (SG-DIR) relative to rigid registration and DIR using TG-132 recommendations for 14 patients with liver tumors to whom stereotactic body radiation therapy (SBRT) was applied. The median DSC for rigid registration was 88% and 89% for DIR, and 90% for both SG-DIR using liver contours only and using liver structures along with anatomical landmarks. However, most of the existing volumetric registration algorithms are not suitable for the intra-procedural stage, as they involve time-consuming optimization. In the report by Wei *et al*[46], a fast MR-CT image registration method was proposed for overlaying pre-procedural MR (pMR) and pre-procedural CT (pCT) images onto an intra-procedural CT (iCT) image to guide thermal ablation of liver tumors. This method, consisting of four DL-based modules and one conventional ANTs registration module, showed higher Dice ratios (around 7% improvement) over tumors and compatible Dice ratios over livers. However, its main advantage was the computational time cost of around 7 s in the intra-procedural stage, which is only 0.1% runtime in the conventional way (*i.e.*, ANTs).

Treatment planning concepts using the mid-ventilation and internal-target volume concept are based on the extent of tumor motion between expiration and inspiration. Therefore, four-dimensional (4D) imaging is required to provide the necessary information about the individual respiration-associated motion pattern. Weick *et al*[49] proposed a method to increase the image quality of the end-expiratory and end-inspiratory phases of retrospective respiratory self-gated 4D MRI data sets using two different non-rigid image registration schemes for improved target delineation of moving liver tumors. In the first scheme, all phases were registered directly (dir-Reg), while in the second next neighbors were successively registered until the target was reached (nn-Reg). Results showed that the Median dir-Reg coefficient of variation of all regions of interest (ROIs) was 5.6% lower for expiration and 7.0% lower for inspiration compared with nn-Reg. Statistically significant differences were found in all comparisons.

DIAGNOSIS

Two decades ago, the methods proposed for ML-based diagnosis required manually extracting the features from the images. This tedious step has been partially relieved with the irruption of CNNs. However, techniques such as radiomics are still in use to try to improve the performance of novel AI methods for medical diagnosis. Radiomics concerns the high throughput extracting of comprehensible features from radiological images that can be further analyzed by ML algorithms for classification or regression tasks. In this section, different methods proposed for liver and pancreas imaging diagnosis are reviewed (Table 2).

Liver-CT

Starting with chronic liver disease, Choi *et al*[50] presented a CNN model for staging liver fibrosis from contrast-enhanced CT images. Before using the CT image as input for the CNN, the liver is segmented. The testing dataset included 891 patients and the CNN achieved a staging accuracy of 79.4% and an AUC of 96%, 97%, and 95% for diagnosing significant fibrosis, advanced fibrosis, and cirrhosis, respectively. A different approach was proposed by Nayak *et al*[51], where SVM was used instead of CNN for aiding in the diagnosis of cirrhosis and hepatocellular carcinoma (HCC) from multi-phase

Table 2 Summary of works based on artificial intelligence for automated diagnosis of pancreas and hepatobiliary system diseases

Anatomical area	Modality	AI model	What is diagnosed?	Ref.
Liver	Scintiscan	ANN	Chronic hepatitis and cirrhosis	[114]
	CT	ANN	HCC, intra-hepatic peripheral cholangiocarcinoma, hemangioma, metastases	[52]
		CNN	HCC, malignant liver tumors, indeterminate mases, hemangiomas, cysts	[53]
			Liver fibrosis	[50,115]
		SVM	Cirrhosis and HCC	[51]
			Malignant liver tumors	[54]
		KNN, SVM, RF	HCC	[116]
	MRI	CNN	HCC	[55]
			Simple cyst, cavernous hemangioma, FNH, HCC, ICC	[56,57]
		Extremely randomized trees	Adenomas, cysts, hemangiomas, HCC, metastases	[58]
	US	PNN	Benign and malignant focal liver lesions	[65]
		SVM	Fatty liver	[68]
			HCC	[66]
		CNN	Focal liver lesions: Angioma, metastasis, HCC, cyst, FNH	[67]
			Liver fibrosis stages	[69]
Biliary system	MRI	ANN	Cholangiocarcinoma	[59,60]
			Lymph node status in ICC	[117]
Pancreas	CT	Hybrid SVM-RF	Pancreas cancer	[76]
		SVM	Serous cystic neoplasms	[72]
		CNN	IPMN, mucinous cystic neoplasm, serous cystic neoplasm, solid pseudopapillary tumor	[73]
	MRI	SVM	IPMN	[78]
	US	ANN	Chronic pancreatitis, pancreatic adenocarcinoma	[81]
		CNN	Malignancy in IPMN	[82]
			Autoimmune pancreatitis, pancreatic ductal adenocarcinoma, chronic pancreatitis	[83]

CT: Computerized tomography; MRI: Magnetic resonance imaging; US: Ultrasound; ANN: Artificial neural network; CNN: Convolutional neural network; SVM: Support vector machine; KNN: K-nearest neighbors; RF: Random forest; PNN: Probabilistic neural network; HCC: Hepatocellular carcinoma; FNH: Focal nodular hyperplasia; ICC: Intrahepatic cholangiocarcinoma; IPMN: Intra-ductal papillary mucinous neoplasm.

abdomen CT. Features were extracted from the segmented liver in all the phases, which were previously registered. Using 5-fold cross validation, they reported an accuracy of 86.9% and 81% for the detection of cirrhosis and HCC, respectively.

There are also several reports exploring the role of DL in the characterization of focal liver lesions (Figure 5). In this sense, Matake *et al*[52] applied an ANN to assist in the diagnosis of hepatic mases using clinical and radiological parameters extracted from CT images. The authors used 120 cases of liver diseases and implemented a leave-one-out cross-validation method for training and testing the ANN, reporting an AUC of 96.1%. Also using CT images, Yasaka *et al*[53] used a CNN for the differentiation of five different types of liver masses from contrast-enhanced CT. For testing, they used 100 liver mass images, reporting an accuracy of 84%. Similarly, Khan and Narejo[54] proposed Fuzzy Linguistic Constant (FLC) to enhance low contrast CT images of the liver before training a SVM to distinguish between cancerous or non-cancerous lesions. The reported classification accuracy was 98.3%. The proposed method also showed the ability to automatically segment the tumor with an improved detection rate of 78% and a precision value of 60%.

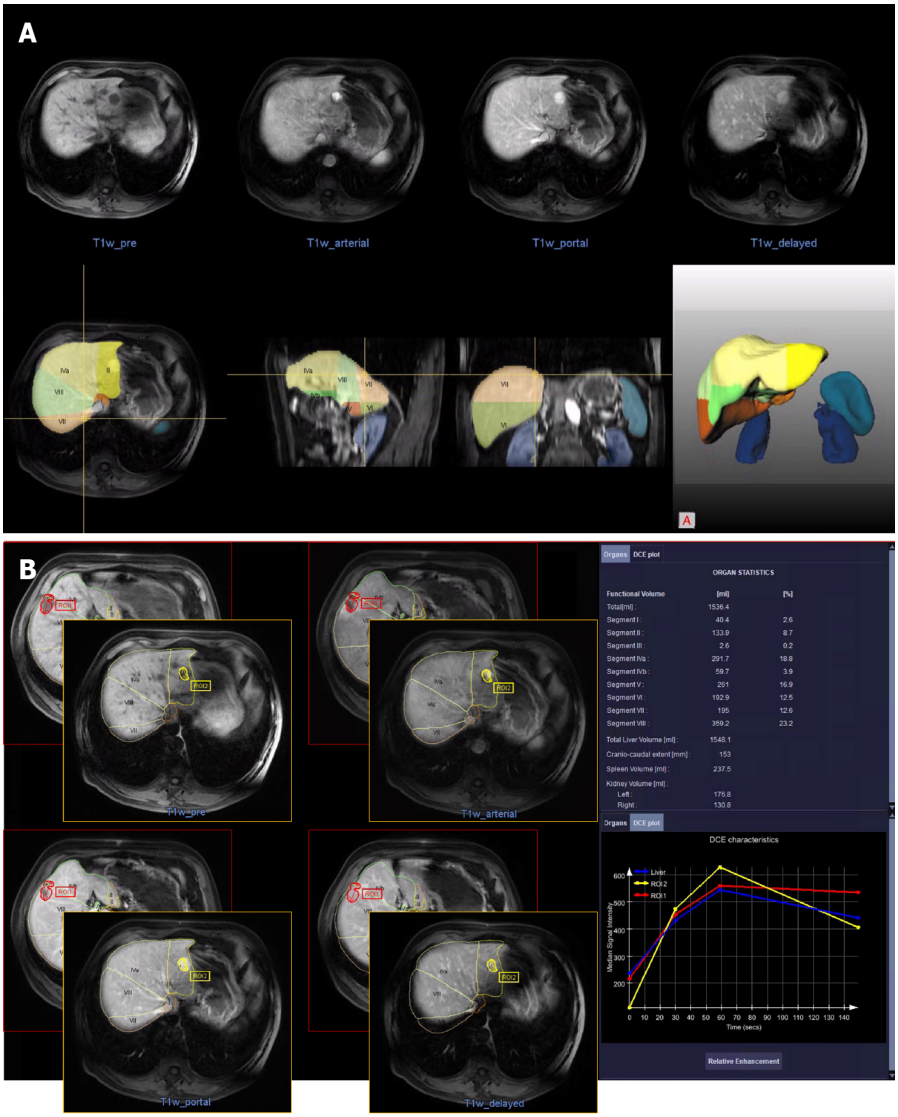

DOI: 10.3748/wjg.v29.i9.1427

Figure 4 In-house experience on liver assessment with artificial intelligence. Magnetic resonance studies of a patient with liver focal lesions (liver hemangiomas), processed with the Liver Analysis research application from Siemens Healthcare. A: Automatic segmentation of the whole liver, liver segments, and other abdominal organs; B: Automatic detection, segmentation, and measurement of the two liver hemangiomas.

Liver and biliary system MRI

Techniques concerning MR images have also been developed for the diagnosis and classification of focal liver lesions (Figure 6). Zhou *et al*[55] proposed a method using a novel CNN to grade HCC from DWIs. They applied a 2D CNN to log maps generated from different b-value images. In their work, they reported a validation AUC of 83% using 40 cases. A CNN was also trained by Hamm *et al*[56] and Wang *et al*[57] to classify six different focal hepatic lesions from T1-weighted MR images in the postcontrast phase. They used 60 cases for testing and reported a sensitivity and specificity of 90% and 98%, respectively. In the second part of their study, they transformed it into an "interpretable" DL system by analyzing the relative contributions of specific imaging features to its predictions in order to shed light on the factors involved in the network's decision-making process. Finally, DCE-MRI and T2-weighted MRI, together with risk factor features, were applied to build an extremely randomized trees classifier for focal liver lesions[58], achieving an overall accuracy of 77%.

Some advancements have also been reached in the automatic diagnosis of lesions in the biliary system from MR cholangiopancreatography (MRCP) sequences. Logeswaran[59,60] trained an ANN classifier for assisting in the diagnosis of cholangiocarcinoma. He utilized 55 MRCP studies for testing and reported an accuracy of 94% when differentiating healthy and tumor images and of 88% in multi-disease tests.

MRI is a superior technique in the evaluation of chronic liver disease in comparison with CT, but making the most of it requires considerable skills and optimization at the acquisition, post-processing, and interpretation phases[61]. AI has proved useful to assist radiologists in the MR-guided diagnosis and grading of these diseases, including liver fibrosis and non-alcoholic fatty liver disease[62].

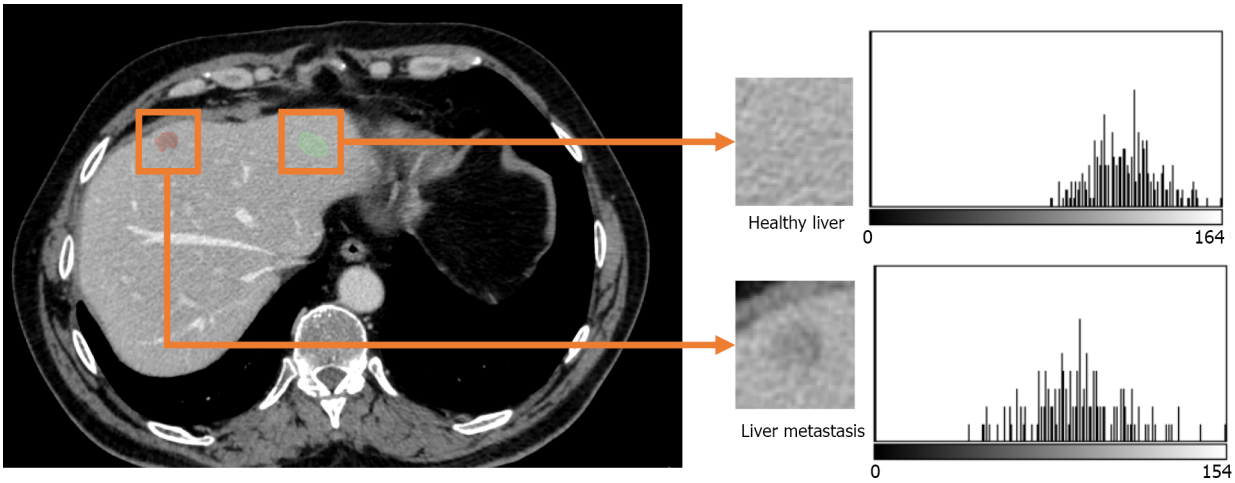

DOI: 10.3748/wjg.v29.i9.1427

Figure 5 Computerized tomography scan of a 61-year-old male patient with colon carcinoma and liver metastases. The intensity histograms of regions with and without metastases are different; hence, the first order radiomics features[109], which are based on the intensity histogram will potentially be different.

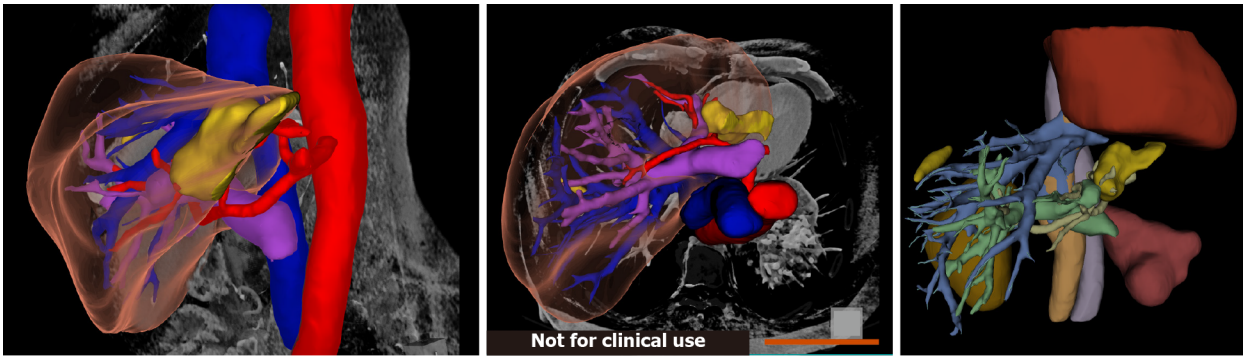

DOI: 10.3748/wjg.v29.i9.1427

Figure 6 Sixty-seven-year-old patient with pancreatic carcinoma and liver metastases treated with chemotherapy. The Digital Oncology Companion (Siemens Healthineers, Germany) artificial intelligence-based prototype automatically segments liver, portal and hepatic vessels, lesions, and surrounding anatomical structures. From left to right: screenshots of the segmented liver, vessels, and lesions; and generated 3D models.

Radiomics studies have been proposed to aid in the diagnosis of liver fibrosis. Kato *et al*[63] performed texture analysis of the liver parenchyma processed by an ANN to detect and grade hepatic fibrosis, with varying success depending on the type of MR sequence used (AUC of 0.801, 0.597, and 0.525 for gadolinium-enhanced equilibrium phase, T1-weighted, and T2-weighted images, respectively).

Later, Hectors *et al*[64] developed a DL algorithm for liver fibrosis staging using gadolinium enhancement sequences acquired in the hepatobiliary phase, which showed good to excellent diagnostic performance, comparable to that of MR elastography.

Liver-US

Ultrasound (US) and endoscopic ultrasonography (EUS) are commonly used in the diagnostic work-up of several pancreatic and liver lesions. AI-based solutions have also been applied to US images in the assessment of focal and diffuse liver diseases in order to enhance their diagnostic capabilities. Acharya *et al*[65] suggested a method for aiding in the diagnosis of focal liver lesions from liver US images. The authors extracted features from US images and trained several classifiers, obtaining the highest AUC (94.1%) using a probabilistic neural network (PNN) classifier. Another approach is shown in Yao *et al* [66], where a radiomics analysis was established for the diagnosis and clinical behavior prediction of HCC, showing an AUC of 94% for benign and malignant classification. Rightly, CNN architectures have also been developed for US images as in the report by Schmauch *et al*[67], where a CNN was employed to help in the diagnosis of focal liver lesions from US images. The authors used a dataset composed by 367 2D US images for training and another dataset from 177 patients for testing, reporting a mean score of 89.1%.

There is limited experience in the use of AI with US images with regards to diffuse liver disease. Li *et al*[68] used a SVM classifier to help in the diagnosis of fatty liver from US images. Input features were computed from ROIs selected by examiners. A total of 93 images were used for training and testing using leave-one-out cross-validation. The authors reported an 84% accuracy for normal livers and 97.1% for fatty livers. Moreover, a mix of radiomics features and DL techniques were used with two-dimensional shear waver elastography (2D-SWE) for assessing liver fibrosis stages in Wang *et al*[69]. Results reached AUCs of 97% for cirrhosis, 98% for advanced fibrosis, and 85% for significant fibrosis.

Pancreas CT and PET/CT

The role of AI in the detection of pancreatic lesions from CT has been extensively investigated. Pancreatic cancer detection is a challenging task for radiologists and its improvement is a hot research topic. Chen *et al*[70] developed a DL-based tool including a segmentation CNN and a 5-CNN classifier for the detection of pancreatic cancer lesions, with a special focus on lesions smaller than 2 cm, in abdominal CT scans. Their model was able to distinguish between cancer and control scans with an AUC of 0.95, 89.7% sensitivity, and 92.8% specificity. Sensitivity for the detection of lesions smaller than 2 cm was 74.7%[70]. Still focused on the identification of lesions smaller than 2 cm, Alves *et al*[71] proposed an automatic framework for pancreatic ductal adenocarcinoma (PDAC) detection based on state-of-the-art DL models. They trained an nnUnet (nnUnet_T) on a dataset including contrast-enhanced CT scans from 119 PDAC patients and 123 healthy individuals for automatic lesion detection and segmentation. Additionally, two other nnUnets were trained to investigate the impact of anatomy integration, with nnUnet_TP segmenting both the pancreas and the tumor and nnUnet_MS segmenting the pancreas, tumor, and adjacent anatomical structures. All three networks were compared on an open access external dataset, with nnUnet_MS offering the best results with an AUC of 0.91 for the entire dataset and of 0.88 for lesions smaller than 2 cm[71]. Several studies have focused on the role of AI-based solutions in the detection of pancreatic cystic lesions. Wei *et al*[72] presented a ML-based computer-aided diagnosis system to help in the diagnosis of pancreas serous cystic neoplasms from CT images. They extracted radiomic features from manual ROIs outlining the peripheral margin of each neoplasm. After selecting the most important features by using least absolute shrinkage selection operator regression, they trained a SVM classifier by a 5-fold cross validation with 200 patients. The authors used a validation cohort of 60 patients and reported and AUC of 83.7%, a sensitivity of 66.7%, and a specificity of 81.8%. Along the same lines, Li *et al*[73] also proposed a computer-aided framework for early differential diagnosis of pancreatic cysts without pre-segmenting the lesions by using densely connected convolutional networks (Dense-Net). In this approach, saliency maps were integrated in the framework to assist physicians to understand the decisions of the DL methods. Accuracy reported on a cohort of 206 patients with four pathologically confirmed subtypes of pancreatic cysts was 72.8%, significantly higher than the baseline of 48.1% according to the authors. Park *et al*[74] developed a 3D nnU-Net-based model for the automatic diagnosis of solid and cystic pancreatic neoplasms on abdominal CT scans. The model was trained on CT scans (852 patients) from both patients who underwent resection for pancreatic lesions and subjects without any pancreatic abnormalities, and performance was evaluated using receiver operating characteristic analysis in a temporally independent cohort (test set 1, including 603 patients) and a temporally and spatially independent cohort (test set 2, including 589 patients). This approach showed a remarkable capacity to identify solid and cystic pancreatic lesions on CT, with an AUC of 0.91 for the test set 1 and 0.87 for the test set 2. Furthermore, it offered a high sensitivity in the identification of solid lesions of any size (98%-100%) and cystic lesions of at least 1 cm (92%-93%)[74].

In the pursuit of more accurate models, some authors have combined CT images with other biomarkers, such as molecular markers or multimodal images. For example, Qiao *et al*[75] used CT scans and serum tumor markers (including serum carbohydrate antigens 50, 199, and 242) to train different types of networks (CNN, FCN, and U-Net) to diagnose pancreatic cancer with high sensitivity and specificity. Li *et al*[76] also used a hybrid SVM-RF model to classify normal and pancreas cancer from PET/CT images. First, they segmented the pancreas from CT images and registered the CT and PET series, then they extracted features from the segmented ROI in both types of studies. The authors tested the model using 10-fold cross validation with 80 cases and achieved 96.47% accuracy, 95.23% sensitivity, and 97.51% specificity.

Pancreas-MRI

MR is the technique of election for the assessment of complex pancreatic conditions. Thus, its association with AI is regarded as promising to help radiologists in diagnostic dilemmas regarding this organ. For instance, radiomics has been proposed as a way to predict the malignant potential of pancreatic cystic lesions, differentiating benign cysts from those likely to transform into pancreatic cancer[77].

There is limited experience with the use of AI in the detection of focal lesions with pancreatic MR studies. Corral *et al*[78] proposed the use of SVM to classify intraductal papillary mucinous neoplasms (IPMN). First, features were extracted using a CNN from T2-weighted and post-contrast T1-weighted MR images. For validation, authors used 10-fold cross-validation using 139 cases. They achieved an AUC of 78%. Kaissis *et al*[79] also developed a supervised ML algorithm which predicted the above-

versus-below median overall survival of patients with pancreatic ductal adenocarcinoma, with 87% sensitivity and 80% specificity, using preoperative DWIs.

Lastly, the generation of synthetic MR images of pancreatic neuroendocrine tumors (PNET) has been explored using GANs. This data augmentation technique can alleviate the relative low abundance of these type of pancreatic tumors in order to train AI models. Gao and Wang then used the synthetic images to evaluate the performance of a CNN in the prediction of PNET grading on contrast-enhanced images[80].

Pancreas-EUS

Application of AI to EUS has focused on the differentiation of focal pancreatic lesions. In this sense, Săftoiu *et al*[81] developed an ANN to help in the difficult differentiation between PDAC and focal chronic pancreatitis (CP) with EUS-elastography. They included 258 patients in the study and reported 84.27% testing accuracy using 10-fold cross-validation. In addition, Kuwahara *et al*[82] used a CNN to assist in the distinction between benign and malignant IPMNs of the pancreas from EUS images. For testing, the authors used images from 50 patients, obtaining an AUC of 98% and sensitivity, specificity, and accuracy values of 95.7%, 92.6%, and 94%, respectively. Finally, in the report by Marya *et al*[83] an EUS-based CNN model was trained to differentiate autoimmune pancreatitis (AIP) from PDAC, CP, and normal pancreas (NP). Results obtained from 583 patients (146 AIP, 292 PDAC, 72 CP, and 73 NP) demonstrated a sensitivity of 99% and a specificity of 98% to distinguish between AIP and NP, 94% and 71% for AIP and CP, and 90% and 93% for AIP and PDAC. Furthermore, the sensitivity and specificity to distinguish AIP from all study conditions (*i.e.*, PDAC, CP, and NP) were 90% and 85%, respectively. In view of these results, the application of AI to EUS in the assessment of focal pancreatic lesions is promising, although limited due to the short number of available databases for algorithm training and validation[84].

TREATMENT PREDICTION

Prediction of treatment response and patient outcome based on AI is a very appealing idea which has been explored in a number of liver and pancreatic diseases, particularly in patients with HCC (Table 3).

The idea of using ML to predict the prognosis of patients with HCC emerged decades ago. Already in 1995 the progression of hepatectomized patients with HCC was analyzed using ANN[85]. Liver volume, which was measured in CT studies, was used, among others, as an input parameter. Fifty-four example cases were used to train an ANN composed of three layers, and the model was successfully used to predict the prognosis of 11 patients. Nevertheless, the model was not tested with enough cases to determine its usefulness in actual clinical activity. However, the rise of AI has prompted many more works to be developed in the last few years. The response to intra-arterial treatment of HCC prior to intervention has been predicted using ML[86,87]. Specifically, logistic regression (LR) and RF models were trained with 35 patients using features extracted from clinical data and the segmentations of liver and liver lesions in a contrast-enhanced 3D fat-suppressed spoiled gradient-echo T1-weighted sequence in the arterial phase. Both trained models predicted treatment response with an overall accuracy of 78% (62.5% sensitivity, 82.1% specificity). Other authors tried to predict the early recurrence of HCC employing a CNN model based on the combination of CT images and clinical data[88]. They used 10-fold cross-validation with data from 167 patients and reported an AUC of 0.825. A RestNet CNN model was also trained for preoperative response prediction of patients with intermediate-stage HCC undergoing transarterial chemoembolization[89]. The model used the segmented ROI of the tumor area in a CT study as input. The training cohort included 162 patients and the two validation cohorts included 89 and 138 patients, respectively. The authors reported an accuracy of 85.1% and 82.8% in the two evaluation datasets.

Radiomics has also been applied to predict treatment response of HCC to different therapies based on studies of several imaging modalities. The early recurrence of HCC after curative treatment was evaluated using an LR model based on radiomics features[90], which were extracted from manually delineated peritumoral areas in CT images. They used 109 patients for training and 47 patients for validation, reporting an AUC of 0.79 with the validation dataset. Guo *et al*[91] also predicted the recurrence of HCC after liver transplantation. For that purpose, authors extracted radiomic features from ROIs delineated around the lesion in arterial-phase CT images. Then, they combined clinical risk factors and radiomic features to build a multivariable Cox regression model. The authors used a training dataset of 93 patients and a validation dataset of 40 patients and they reported a C-index of 0.789 in the validation dataset.

ML models have also been used to predict hepatobiliary toxicity after liver SBRT[92]. The authors built a CNN model which was previously pretrained using CT images of human organs. Then, using transfer learning, the model was trained with liver SBRT cases. They used 125 patients for training and validation using a 20-fold cross-validation approach, reporting an AUC of 0.79.

Regarding the pancreas, postoperative pancreatic fistulas were predicted using ML-based texture analysis[93] performed to extract features from ROIs segmented in non-contrast CT images. Then, after

Table 3 Summary of the works proposed to predict patient prognosis using artificial intelligence

Anatomical area	Pathology	Modality	AI model	What is prognosed?	Ref.
Liver	HCC	CT	ANN	Progression of hepatectomized patients with HCC	[85]
			CNN	Early recurrence of HCC	[88]
				Response to transarterial chemoembolization for patients with intermediate-stage HCC	[89]
			LASSO Cox regression	Early recurrence of HCC	[90]
				Recurrence of HCC after liver transplantation	[91]
				Recurrence of HCC after resection	[118]
		MRI	LR, RF	Response to intra-arterial treatment of HCC	[86,87]
		US	CNN, SVM	Response to transarterial chemoembolization for patients with HCC	[119]
Biliary system	Liver metastases, HCC, cholangiocarcinoma	CT	CNN	Prediction of hepatobiliary toxicity after liver SBRT	[92]
Pancreas	Postoperative pancreatic fistula	CT	RepTree	Prediction of postoperative pancreas fistulas after pancreatoduodenectomy	[93]

HCC: Hepatocellular carcinoma; CT: Computerized tomography; MRI: Magnetic resonance imaging; US: Ultrasound; ANN: Artificial neural network; CNN: Convolutional neural network; LR: Logistic regression; RF: Random forest; SVM: Support vector machine; SBRT: Stereotactic body radiotherapy.

dimension reduction, several ML classifiers were built using Auto-WEKA 2.0, obtaining the best results using a REPTree classifier. The authors used 10-fold cross-validation using data from 110 patients, and reported an AUC of 0.95, sensitivity of 96%, and specificity of 98%.

DISCUSSION

In recent years, a large number of AI-based solutions have been developed with the aim of easing and streamlining the radiologist's workflow. Many of these tools are focused on imaging of the liver, biliary system, and pancreas. The developed tools range from improving image quality to the prediction of the patient's prognosis after treatment. The literature shows that many AI-based solutions targeting liver and pancreas imaging allow for improved disease detection and characterization, lower inter-reader variability, and increased diagnostic efficiency. A key factor for their success in the clinical setting is to attain a seamless integration in the radiologist's workflow, requiring minimal additional work by the radiologist and adding significant value to the radiologist's work. In this sense, it is crucial that there is a fluid collaboration between the radiologists, technicians, and bioengineers in charge of the tools.

Image analysis and processing are transversal parts of most AI methods described in this review. Improving their performance is thus a key task. Unfortunately, some image processing techniques such as registration are still time-consuming, hence making the incorporation of some of these procedures in clinical practice unfeasible. Some new methods are arising to minimize this impact[94], especially in critical applications like image IGS. Semi-automatic or even automatic segmentation is another important step that some of the AI tools may incorporate for diagnosis or prognosis purposes[95]. Therefore, it is of paramount importance for these algorithms to achieve a high level of performance.

The literature reports many applications of AI to aid in the detection and characterization of pancreatic and liver focal lesions using a variety of imaging modalities as input, either single (*e.g.*, T1-weighted MRI) or in combination with other techniques and data (*e.g.*, T2-weighted and DCE-MRI plus risk factors). In chronic liver disease, radiomics-based tools have been developed to assist in the diagnosis and grading of hepatic fibrosis, among others. These models have been built using different imaging modalities, such as MRI or US.

With regard to the prognosis of liver, biliary or pancreatic diseases, tools based on radiological information have hardly been developed. Many of these tools are focused on the prognosis of HCC based on information extracted from CT[96]. In this field of research, literature shows a clear trend toward integrating genetic information[97-101]. There are also studies that try to include variables extracted from clinical data and laboratory values[102,103]. In a scenario that advances towards integrated diagnosis, increasing volumes of data of different nature are available. This should allow for the generation of more accurate predictive models of clinical prognosis using information from many sources.

For the AI-based tools developed to be used in daily clinical practice, they must obtain regulatory clearance, such as Food and Drug Administration (FDA) approval in the United States or CE marking in Europe. Despite the explosive production of such tools in the last years, to date only a small group of them have obtained this approval. One of the main problems is the lack of appropriately annotated data. Without large datasets of properly labeled studies, the performance of data-hungry algorithms like CNNs will not be sufficient to be massively deployed in clinical environments. Furthermore, algorithms demand diverse data, such as multi-centric and multi-vendor, to avoid selection biases that would challenge their implementation in a real-world environment[104]. Another limitation of most AI-based tools found today is that they are aimed at a very concrete application (narrow AI applications), within a specific imaging modality, rather than being valid for a wide range of tasks at the radiologist's work practice.

Yet, the general attitude of radiology staff toward AI is positive. In a recent survey, European radiographers declared excitement about AI (83%), although only 8% had been taught on this matter in their qualification studies[105].

In another survey, European radiologists regarded the outcomes of AI algorithms for diagnostic purposes as generally reliable (75.7%), and algorithms for workload prioritization as very helpful (23.4%) or moderately helpful (62.2%) to reduce the workload of the medical staff[106].

The sentiment of gastroenterologists toward AI is also generally favorable, with a wide majority of United Kingdom[107] and European[108] specialists perceiving it as beneficial to key aspects of their clinical practice. Their main concerns according to these studies are related to algorithm bias, lack of guidelines, and potential increase in procedural times and operator dependence.

CONCLUSION

The rapid advance of AI is already transforming the gastrointestinal field with the development of applications aimed to assist and streamline image diagnosis. Traditional diagnostic imaging techniques such as US, EUS, CT, MRI, and PET/CT are already benefitting from a variety of AI algorithms that can perform automatic or semi-automatic segmentation and registration of the liver and pancreas and their lesions, aid the diagnosis and characterization of pancreatic and liver focal lesions and diffuse illnesses, improve image quality, accelerate image acquisition, and anticipate treatment response and patient prognosis. Moreover, with the use of radiomics, AI can add quantitative information previously undetected by radiologists to radiological reports. The massive adoption of AI in radiology of pancreatic and liver diseases is still incipient, but irreversible, and the sector is clearly moving in this direction. Advances in the field, such as the availability of regulatory cleared, robust algorithms trained and validated multicentrically, increased awareness on AI by the medical staff, and access to products that seamlessly integrate with their workflow should pave the way for a rapid adoption of AI in the clinical practice, impacting the outcomes of hepatic and pancreatic patients for the better.

FOOTNOTES

Author contributions: Berbís MA, Paulano Godino F, Royuela del Val J, and Alcalá Mata L performed information compilation and manuscript writing; Luna A performed information compilation and critical reading of the manuscript.

Conflict-of-interest statement: Berbís MA is a board member of Cells IA Technologies; Luna A received institutional royalties and institutional payments for lectures, presentations, speaker bureaus, manuscript writing or educational events from Canon, Bracco, Siemens Healthineers, and Philips Healthcare and is a board member of Cells IA Technologies; the remaining authors declare no competing interests.

Country/Territory of origin: Spain

ORCID number: M Alvaro Berbís 0000-0002-0331-7762; Felix Paulano Godino 0000-0001-9712-3952; Javier Royuela del Val 0000-0002-4347-2783; Lidia Alcalá Mata 0000-0001-6461-3891; Antonio Luna 0000-0001-9358-3396.

S-Editor: Chen YL
L-Editor: A
P-Editor: Chen YL

REFERENCES

1 **Sung H**, Ferlay J, Siegel RL, Laversanne M, Soerjomataram I, Jemal A, Bray F. Global Cancer Statistics 2020: GLOBOCAN Estimates of Incidence and Mortality Worldwide for 36 Cancers in 185 Countries. *CA Cancer J Clin* 2021; **71**: 209-249 [PMID: 33538338 DOI: 10.3322/caac.21660]

2 **American Cancer Society**. Liver Cancer Early Detection, Diagnosis, and Staging. [cited 3 January 2023]. Available from: https://www.cancer.org/cancer/Liver-cancer/detection-diagnosis-staging/survival-rates.html

3 **American Cancer Society**. Survival Rates for Pancreatic Cancer. [cited 3 January 2023]. Available from: https://www.cancer.org/cancer/pancreatic-cancer/detection-diagnosis-staging/survival-rates.html

4 **Hirode G**, Saab S, Wong RJ. Trends in the Burden of Chronic Liver Disease Among Hospitalized US Adults. *JAMA Netw Open* 2020; **3**: e201997 [PMID: 32239220 DOI: 10.1001/jamanetworkopen.2020.1997]

5 **Berbís MA**, Aneiros-Fernández J, Mendoza Olivares FJ, Nava E, Luna A. Role of artificial intelligence in multidisciplinary imaging diagnosis of gastrointestinal diseases. *World J Gastroenterol* 2021; **27**: 4395-4412 [PMID: 34366612 DOI: 10.3748/wjg.v27.i27.4395]

6 **Chang KJ**, Kamel IR, Macura KJ, Bluemke DA. 3.0-T MR imaging of the abdomen: comparison with 1.5 T. *Radiographics* 2008; **28**: 1983-1998 [PMID: 19001653 DOI: 10.1148/rg.287075154]

7 **Jiang F**, Jiang Y, Zhi H, Dong Y, Li H, Ma S, Wang Y, Dong Q, Shen H. Artificial intelligence in healthcare: past, present and future. *Stroke Vasc Neurol* 2017; **2**: 230-243 [PMID: 29507784 DOI: 10.1136/svn-2017-000101]

8 **Samuel AL**. Some Studies in Machine Learning Using the Game of Checkers. *IBM J Res Dev* 1959; **3**: 210-229 [DOI: 10.1147/rd.33.0210]

9 **Galbusera F**, Casaroli G, Bassani T. Artificial intelligence and machine learning in spine research. *JOR Spine* 2019; **2**: e1044 [PMID: 31463458 DOI: 10.1002/jsp2.1044]

10 **Alloghani M**, Al-Jumeily D, Mustafina J, Hussain A, Aljaaf AJ. A Systematic Review on Supervised and Unsupervised Machine Learning Algorithms for Data Science. In: Berry M, Mohamed A, Yap B. Supervised and Unsupervised Learning for Data Science. Unsupervised and Semi-Supervised Learning. Cham: Springer, 2019: 3-21 [DOI: 10.1007/978-3-030-22475-2_1]

11 **Goodfellow I**, Pouget-Abadie J, Mirza M, Xu B, Warde-Farley D, Ozair S, Courville A, Bengio Y. Generative adversarial networks. *Commun ACM* 2014; **63**: 139-144

12 **Frid-Adar M**, Diamant I, Klang E, Amitai M, Goldberger J, Greenspan H. GAN-based synthetic medical image augmentation for increased CNN performance in liver lesion classification. *Neurocomputing* 2018; **321**: 321-331 [DOI: 10.1016/j.neucom.2018.09.013]

13 **Ronneberger O**, Fischer P, Brox T. U-Net: Convolutional Networks for Biomedical Image Segmentation. In: Navab N, Hornegger J, Wells W, Frangi A. Medical Image Computing and Computer-Assisted Intervention-MICCAI 2015. MICCAI 2015. Lecture Notes in Computer Science. Cham: Springer, 2015; 1-8 [DOI: 10.1007/978-3-319-24574-4_28]

14 **LeCun Y**, Bengio Y, Hinton G. Deep learning. *Nature* 2015; **521**: 436-444 [PMID: 26017442 DOI: 10.1038/nature14539]

15 **Isensee F**, Jaeger PF, Kohl SAA, Petersen J, Maier-Hein KH. nnU-Net: a self-configuring method for deep learning-based biomedical image segmentation. *Nat Methods* 2021; **18**: 203-211 [PMID: 33288961 DOI: 10.1038/s41592-020-01008-z]

16 **Li Y**, Beck M, Päßler T, Lili C, Hua W, Mai HD, Amthauer H, Biebl M, Thuss-Patience PC, Berger J, Stromberger C, Tinhofer I, Kruppa J, Budach V, Hofheinz F, Lin Q, Zschaeck S. A FDG-PET radiomics signature detects esophageal squamous cell carcinoma patients who do not benefit from chemoradiation. *Sci Rep* 2020; **10**: 17671 [PMID: 33077841 DOI: 10.1038/s41598-020-74701-w]

17 **Varghese BA**, Cen SY, Hwang DH, Duddalwar VA. Texture Analysis of Imaging: What Radiologists Need to Know. *AJR Am J Roentgenol* 2019; **212**: 520-528 [PMID: 30645163 DOI: 10.2214/AJR.18.20624]

18 **Fleischmann D**, Boas FE. Computed tomography--old ideas and new technology. *Eur Radiol* 2011; **21**: 510-517 [PMID: 21249371 DOI: 10.1007/s00330-011-2056-z]

19 **den Harder AM**, Willemink MJ, de Ruiter QM, Schilham AM, Krestin GP, Leiner T, de Jong PA, Budde RP. Achievable dose reduction using iterative reconstruction for chest computed tomography: A systematic review. *Eur J Radiol* 2015; **84**: 2307-2313 [PMID: 26212557 DOI: 10.1016/j.ejrad.2015.07.011]

20 **Kyong Hwan Jin**, McCann MT, Froustey E, Unser M. Deep Convolutional Neural Network for Inverse Problems in Imaging. *IEEE Trans Image Process* 2017; **26**: 4509-4522 [PMID: 28641250 DOI: 10.1109/TIP.2017.2713099]

21 **Akagi M**, Nakamura Y, Higaki T, Narita K, Honda Y, Zhou J, Yu Z, Akino N, Awai K. Deep learning reconstruction improves image quality of abdominal ultra-high-resolution CT. *Eur Radiol* 2019; **29**: 6163-6171 [PMID: 30976831 DOI: 10.1007/s00330-019-06170-3]

22 **Kaga T**, Noda Y, Mori T, Kawai N, Takano H, Kajita K, Yoneyama M, Akamine Y, Kato H, Hyodo F, Matsuo M. Diffusion-weighted imaging of the abdomen using echo planar imaging with compressed SENSE: Feasibility, image quality, and ADC value evaluation. *Eur J Radiol* 2021; **142**: 109889 [PMID: 34388627 DOI: 10.1016/j.ejrad.2021.109889]

23 **López-Úbeda P**, Díaz-Galiano MC, Martín-Noguerol T, Luna A, Ureña-López LA, Martín-Valdivia MT. Automatic medical protocol classification using machine learning approaches. *Comput Methods Programs Biomed* 2021; **200**: 105939 [PMID: 33486337 DOI: 10.1016/j.cmpb.2021.105939]

24 **Professional Foundation**. The Next MR Wave|Philips Healthcare. [cited 1 January 2023]. Available from: https://www.philips-foundation.com/healthcare/resources/Landing/the-next-mr-wave#triggername=close_vitaleye

25 **BioMatrix Technology**. Siemens Healthineers España. [cited 1 January 2023]. Available from: https://www.siemens-healthineers.com/es/magnetic-resonance-imaging/technologies-and-innovations/biomatrix-technology [DOI: 10.1016/j.clinimag.2021.08.025]

26 **Seo H**, Badiei Khuzani M, Vasudevan V, Huang C, Ren H, Xiao R, Jia X, Xing L. Machine learning techniques for biomedical image segmentation: An overview of technical aspects and introduction to state-of-art applications. *Med Phys* 2020; **47**: e148-e167 [PMID: 32418337 DOI: 10.1002/mp.13649]

27 **Song J**, Patel M, Girgensohn A, Kim C. Combining Deep Learning with Geometric Features for Image based Localization in the Gastrointestinal Tract. *Expert syst appl* 2021; **185**: ; 115631 [DOI: 10.1016/j.eswa.2021.115631]

28 **Fu Y**, Lei Y, Wang T, Curran WJ, Liu T, Yang X. Deep learning in medical image registration: a review. *Phys Med Biol* 2020; **65**: 20TR01 [PMID: 32217829 DOI: 10.1088/1361-6560/ab843e]

29 **Bagheri MH**, Roth H, Kovacs W, Yao J, Farhadi F, Li X, Summers RM. Technical and Clinical Factors Affecting Success Rate of a Deep Learning Method for Pancreas Segmentation on CT. *Acad Radiol* 2020; **27**: 689-695 [PMID: 31537506 DOI: 10.1016/j.acra.2019.08.014]

30 **Krasoń A**, Woloshuk A, Spinczyk D. Segmentation of abdominal organs in computed tomography using a generalized statistical shape model. *Comput Med Imaging Graph* 2019; **78**: 101672 [PMID: 31715378 DOI: 10.1016/j.compmedimag.2019.101672]

31 **Antwi K**, Wiesner P, Merkle EM, Zech CJ, Boll DT, Wild D, Christ E, Heye T. Investigating difficult to detect pancreatic lesions: Characterization of benign pancreatic islet cell tumors using multiparametric pancreatic 3-T MRI. *PLoS One* 2021; **16**: e0253078 [PMID: 34115803 DOI: 10.1371/journal.pone.0253078]

32 **Kumar H**, DeSouza SV, Petrov MS. Automated pancreas segmentation from computed tomography and magnetic resonance images: A systematic review. *Comput Methods Programs Biomed* 2019; **178**: 319-328 [PMID: 31416559 DOI: 10.1016/j.cmpb.2019.07.002]

33 **Zheng H**, Chen Y, Yue X, Ma C, Liu X, Yang P, Lu J. Deep pancreas segmentation with uncertain regions of shadowed sets. *Magn Reson Imaging* 2020; **68**: 45-52 [PMID: 31987903 DOI: 10.1016/j.mri.2020.01.008]

34 **Zheng H**, Qian L, Qin Y, Gu Y, Yang J. Improving the slice interaction of 2.5D CNN for automatic pancreas segmentation. *Med Phys* 2020; **47**: 5543-5554 [PMID: 32502278 DOI: 10.1002/mp.14303]

35 **Cardobi N**, Dal Palù A, Pedrini F, Beleù A, Nocini R, De Robertis R, Ruzzenente A, Salvia R, Montemezzi S, D'Onofrio M. An Overview of Artificial Intelligence Applications in Liver and Pancreatic Imaging. *Cancers (Basel)* 2021; **13** [PMID: 33946223 DOI: 10.3390/cancers13092162]

36 **Li Y**, Zhao YQ, Zhang F, Liao M, Yu LL, Chen BF, Wang YJ. Liver segmentation from abdominal CT volumes based on level set and sparse shape composition. *Comput Methods Programs Biomed* 2020; **195**: 105533 [PMID: 32502932 DOI: 10.1016/j.cmpb.2020.105533]

37 **Winther H**, Hundt C, Ringe KI, Wacker FK, Schmidt B, Jürgens J, Haimerl M, Beyer LP, Stroszczynski C, Wiggermann P, Verloh N. A 3D Deep Neural Network for Liver Volumetry in 3T Contrast-Enhanced MRI. *Rofo* 2021; **193**: 305-314 [PMID: 32882724 DOI: 10.1055/a-1238-2887]

38 **Mohagheghi S**, Foruzan AH. Incorporating prior shape knowledge *via* data-driven loss model to improve 3D liver segmentation in deep CNNs. *Int J Comput Assist Radiol Surg* 2020; **15**: 249-257 [PMID: 31686380 DOI: 10.1007/s11548-019-02085-y]

39 **Nakayama K**, Saito A, Biggs E, Linguraru MG, Shimizu A. Liver segmentation from low-radiation-dose pediatric computed tomography using patient-specific, statistical modeling. *Int J Comput Assist Radiol Surg* 2019; **14**: 2057-2068 [PMID: 30875059 DOI: 10.1007/s11548-019-01929-x]

40 **Bobo MF**, Bao S, Huo Y, Yao Y, Virostko J, Plassard AJ, Lyu I, Assad A, Abramson RG, Hilmes MA, Landman BA. Fully Convolutional Neural Networks Improve Abdominal Organ Segmentation. *Proc SPIE Int Soc Opt Eng* 2018; **10574** [PMID: 29887665 DOI: 10.1117/12.2293751]

41 **Saunders SL**, Clark JM, Rudser K, Chauhan A, Ryder JR, Bolan PJ. Comparison of automatic liver volumetry performance using different types of magnetic resonance images. *Magn Reson Imaging* 2022; **91**: 16-23 [PMID: 35537665 DOI: 10.1016/j.mri.2022.05.002]

42 **Meng L**, Tian Y, Bu S. Liver tumor segmentation based on 3D convolutional neural network with dual scale. *J Appl Clin Med Phys* 2020; **21**: 144-157 [PMID: 31793212 DOI: 10.1002/acm2.12784]

43 **Chen L**, Song H, Wang C, Cui Y, Yang J, Hu X, Zhang L. Liver tumor segmentation in CT volumes using an adversarial densely connected network. *BMC Bioinformatics* 2019; **20**: 587 [PMID: 31787071 DOI: 10.1186/s12859-019-3069-x]

44 **Almotairi S**, Kareem G, Aouf M, Almutairi B, Salem MA. Liver Tumor Segmentation in CT Scans Using Modified SegNet. *Sensors (Basel)* 2020; **20** [PMID: 32164153 DOI: 10.3390/s20051516]

45 **Chlebus G**, Meine H, Thoduka S, Abolmaali N, van Ginneken B, Hahn HK, Schenk A. Reducing inter-observer variability and interaction time of MR liver volumetry by combining automatic CNN-based liver segmentation and manual corrections. *PLoS One* 2019; **14**: e0217228 [PMID: 31107915 DOI: 10.1371/journal.pone.0217228]

46 **Wei D**, Ahmad S, Huo J, Huang P, Yap PT, Xue Z, Sun J, Li W, Shen D, Wang Q. SLIR: Synthesis, localization, inpainting, and registration for image-guided thermal ablation of liver tumors. *Med Image Anal* 2020; **65**: 101763 [PMID: 32623279 DOI: 10.1016/j.media.2020.101763]

47 **Schneider C**, Thompson S, Totz J, Song Y, Allam M, Sodergren MH, Desjardins AE, Barratt D, Ourselin S, Gurusamy K, Stoyanov D, Clarkson MJ, Hawkes DJ, Davidson BR. Comparison of manual and semi-automatic registration in augmented reality image-guided liver surgery: a clinical feasibility study. *Surg Endosc* 2020; **34**: 4702-4711 [PMID: 32780240 DOI: 10.1007/s00464-020-07807-x]

48 **Kuznetsova S**, Grendarova P, Roy S, Sinha R, Thind K, Ploquin N. Structure guided deformable image registration for treatment planning CT and post stereotactic body radiation therapy (SBRT) Primovist(®) (Gd-EOB-DTPA) enhanced MRI. *J Appl Clin Med Phys* 2019; **20**: 109-118 [PMID: 31755658 DOI: 10.1002/acm2.12773]

49 **Weick S**, Breuer K, Richter A, Exner F, Ströhle SP, Lutyj P, Tamihardja J, Veldhoen S, Flentje M, Polat B. Non-rigid image registration of 4D-MRI data for improved delineation of moving tumors. *BMC Med Imaging* 2020; **20**: 41 [PMID: 32326879 DOI: 10.1186/s12880-020-00439-6]

50 **Choi KJ**, Jang JK, Lee SS, Sung YS, Shim WH, Kim HS, Yun J, Choi JY, Lee Y, Kang BK, Kim JH, Kim SY, Yu ES. Development and Validation of a Deep Learning System for Staging Liver Fibrosis by Using Contrast Agent-enhanced CT Images in the Liver. *Radiology* 2018; **289**: 688-697 [PMID: 30179104 DOI: 10.1148/radiol.2018180763]

51 **Nayak A**, Baidya Kayal E, Arya M, Culli J, Krishan S, Agarwal S, Mehndiratta A. Computer-aided diagnosis of cirrhosis and hepatocellular carcinoma using multi-phase abdomen CT. *Int J Comput Assist Radiol Surg* 2019; **14**: 1341-1352 [PMID: 31062266 DOI: 10.1007/s11548-019-01991-5]

52 **Matake K**, Yoshimitsu K, Kumazawa S, Higashida Y, Irie H, Asayama Y, Nakayama T, Kakihara D, Katsuragawa S, Doi K, Honda H. Usefulness of artificial neural network for differential diagnosis of hepatic masses on CT images. *Acad Radiol* 2006; **13**: 951-962 [PMID: 16843847 DOI: 10.1016/j.acra.2006.04.009]

53 **Yasaka K**, Akai H, Abe O, Kiryu S. Deep Learning with Convolutional Neural Network for Differentiation of Liver Masses at Dynamic Contrast-enhanced CT: A Preliminary Study. *Radiology* 2018; **286**: 887-896 [PMID: 29059036 DOI: 10.1148/radiol.2017170706]

54 **Khan AA**, Narejo GB. Analysis of Abdominal Computed Tomography Images for Automatic Liver Cancer Diagnosis Using Image Processing Algorithm. *Curr Med Imaging Rev* 2019; **15**: 972-982 [PMID: 32008524 DOI: 10.2174/1573405615666190716122040]

55 **Zhou W**, Wang G, Xie G, Zhang L. Grading of hepatocellular carcinoma based on diffusion weighted images with multiple b-values using convolutional neural networks. *Med Phys* 2019; **46**: 3951-3960 [PMID: 31169907 DOI: 10.1002/mp.13642]

56 **Hamm CA**, Wang CJ, Savic LJ, Ferrante M, Schobert I, Schlachter T, Lin M, Duncan JS, Weinreb JC, Chapiro J, Letzen B. Deep learning for liver tumor diagnosis part I: development of a convolutional neural network classifier for multi-phasic MRI. *Eur Radiol* 2019; **29**: 3338-3347 [PMID: 31016442 DOI: 10.1007/s00330-019-06205-9]

57 **Wang CJ**, Hamm CA, Savic LJ, Ferrante M, Schobert I, Schlachter T, Lin M, Weinreb JC, Duncan JS, Chapiro J, Letzen B. Deep learning for liver tumor diagnosis part II: convolutional neural network interpretation using radiologic imaging features. *Eur Radiol* 2019; **29**: 3348-3357 [PMID: 31093705 DOI: 10.1007/s00330-019-06214-8]

58 **Jansen MJA**, Kuijf HJ, Veldhuis WB, Wessels FJ, Viergever MA, Pluim JPW. Automatic classification of focal liver lesions based on MRI and risk factors. *PLoS One* 2019; **14**: e0217053 [PMID: 31095624 DOI: 10.1371/journal.pone.0217053]

59 **Logeswaran R**. Cholangiocarcinoma--an automated preliminary detection system using MLP. *J Med Syst* 2009; **33**: 413-421 [PMID: 20052894 DOI: 10.1007/s10916-008-9203-3]

60 **Logeswaran R**. Improved biliary detection and diagnosis through intelligent machine analysis. *Comput Methods Programs Biomed* 2012; **107**: 404-412 [PMID: 21194781 DOI: 10.1016/j.cmpb.2010.12.002]

61 **Chundru S**, Kalb B, Arif-Tiwari H, Sharma P, Costello J, Martin DR. MRI of diffuse liver disease: characteristics of acute and chronic diseases. *Diagn Interv Radiol* 2014; **20**: 200-208 [PMID: 24808418 DOI: 10.5152/dir.2014.13170]

62 **Decharatanachart P**, Chaiteerakij R, Tiyarattanachai T, Treeprasertsuk S. Application of artificial intelligence in chronic liver diseases: a systematic review and meta-analysis. *BMC Gastroenterol* 2021; **21**: 10 [PMID: 33407169 DOI: 10.1186/s12876-020-01585-5]

63 **Kato H**, Kanematsu M, Zhang X, Saio M, Kondo H, Goshima S, Fujita H. Computer-aided diagnosis of hepatic fibrosis: preliminary evaluation of MRI texture analysis using the finite difference method and an artificial neural network. *AJR Am J Roentgenol* 2007; **189**: 117-122 [PMID: 17579160 DOI: 10.2214/AJR.07.2070]

64 **Hectors SJ**, Kennedy P, Huang KH, Stocker D, Carbonell G, Greenspan H, Friedman S, Taouli B. Fully automated prediction of liver fibrosis using deep learning analysis of gadoxetic acid-enhanced MRI. *Eur Radiol* 2021; **31**: 3805-3814 [PMID: 33201285 DOI: 10.1007/s00330-020-07475-4]

65 **Acharya UR**, Koh JEW, Hagiwara Y, Tan JH, Gertych A, Vijayananthan A, Yaakup NA, Abdullah BJJ, Bin Mohd Fabell MK, Yeong CH. Automated diagnosis of focal liver lesions using bidirectional empirical mode decomposition features. *Comput Biol Med* 2018; **94**: 11-18 [PMID: 29353161 DOI: 10.1016/j.compbiomed.2017.12.024]

66 **Yao Z**, Dong Y, Wu G, Zhang Q, Yang D, Yu JH, Wang WP. Preoperative diagnosis and prediction of hepatocellular carcinoma: Radiomics analysis based on multi-modal ultrasound images. *BMC Cancer* 2018; **18**: 1089 [PMID: 30419849 DOI: 10.1186/s12885-018-5003-4]

67 **Schmauch B**, Herent P, Jehanno P, Dehaene O, Saillard C, Aubé C, Luciani A, Lassau N, Jégou S. Diagnosis of focal liver lesions from ultrasound using deep learning. *Diagn Interv Imaging* 2019; **100**: 227-233 [PMID: 30926443 DOI: 10.1016/j.diii.2019.02.009]

68 **Li G**, Luo Y, Deng W, Xu X, Liu A, Song E. Computer aided diagnosis of fatty liver ultrasonic images based on support vector machine. *Annu Int Conf IEEE Eng Med Biol Soc* 2008; **2008**: 4768-4771 [PMID: 19163782 DOI: 10.1109/IEMBS.2008.4650279]

69 **Wang K**, Lu X, Zhou H, Gao Y, Zheng J, Tong M, Wu C, Liu C, Huang L, Jiang T, Meng F, Lu Y, Ai H, Xie XY, Yin LP, Liang P, Tian J, Zheng R. Deep learning Radiomics of shear wave elastography significantly improved diagnostic performance for assessing liver fibrosis in chronic hepatitis B: a prospective multicentre study. *Gut* 2019; **68**: 729-741 [PMID: 29730602 DOI: 10.1136/gutjnl-2018-316204]

70 **Chen PT**, Wu T, Wang P, Chang D, Liu KL, Wu MS, Roth HR, Lee PC, Liao WC, Wang W. Pancreatic Cancer Detection on CT Scans with Deep Learning: A Nationwide Population-based Study. *Radiology* 2023; **306**: 172-182 [PMID: 36098642 DOI: 10.1148/radiol.220152]

71 **Alves N**, Schuurmans M, Litjens G, Bosma JS, Hermans J, Huisman H. Fully Automatic Deep Learning Framework for Pancreatic Ductal Adenocarcinoma Detection on Computed Tomography. *Cancers (Basel)* 2022; **14** [PMID: 35053538 DOI: 10.3390/cancers14020376]

72 **Wei R**, Lin K, Yan W, Guo Y, Wang Y, Li J, Zhu J. Computer-Aided Diagnosis of Pancreas Serous Cystic Neoplasms: A Radiomics Method on Preoperative MDCT Images. *Technol Cancer Res Treat* 2019; **18**: 1533033818824339 [PMID: 30803366 DOI: 10.1177/1533033818824339]

73 **Li H**, Shi K, Reichert M, Lin K, Tselousov N, Braren R, Fu D, Schmid R, Li J, Menze B. Differential Diagnosis for Pancreatic Cysts in CT Scans Using Densely-Connected Convolutional Networks. *Annu Int Conf IEEE Eng Med Biol Soc* 2019; **2019**: 2095-2098 [PMID: 31946314 DOI: 10.1109/EMBC.2019.8856745]

74 **Park HJ**, Shin K, You MW, Kyung SG, Kim SY, Park SH, Byun JH, Kim N, Kim HJ. Deep Learning-based Detection of Solid and Cystic Pancreatic Neoplasms at Contrast-enhanced CT. *Radiology* 2023; **306**: 140-149 [PMID: 35997607 DOI: 10.1148/radiol.220171]

75 **Qiao Z**, Ge J, He W, Xu X, He J. Artificial Intelligence Algorithm-Based Computerized Tomography Image Features Combined with Serum Tumor Markers for Diagnosis of Pancreatic Cancer. *Comput Math Methods Med* 2022; **2022**:

8979404 [PMID: 35281945 DOI: 10.1155/2022/8979404]
76 **Li S**, Jiang H, Wang Z, Zhang G, Yao YD. An effective computer aided diagnosis model for pancreas cancer on PET/CT images. *Comput Methods Programs Biomed* 2018; **165**: 205-214 [PMID: 30337075 DOI: 10.1016/j.cmpb.2018.09.001]
77 **Dalal V**, Carmicheal J, Dhaliwal A, Jain M, Kaur S, Batra SK. Radiomics in stratification of pancreatic cystic lesions: Machine learning in action. *Cancer Lett* 2020; **469**: 228-237 [PMID: 31629933 DOI: 10.1016/j.canlet.2019.10.023]
78 **Corral JE**, Hussein S, Kandel P, Bolan CW, Bagci U, Wallace MB. Deep Learning to Classify Intraductal Papillary Mucinous Neoplasms Using Magnetic Resonance Imaging. *Pancreas* 2019; **48**: 805-810 [PMID: 31210661 DOI: 10.1097/MPA.0000000000001327]
79 **Kaissis G**, Ziegelmayer S, Lohöfer F, Algül H, Eiber M, Weichert W, Schmid R, Friess H, Rummeny E, Ankerst D, Siveke J, Braren R. A machine learning model for the prediction of survival and tumor subtype in pancreatic ductal adenocarcinoma from preoperative diffusion-weighted imaging. *Eur Radiol Exp* 2019; **3**: 41 [PMID: 31624935 DOI: 10.1186/s41747-019-0119-0]
80 **Gao X**, Wang X. Deep learning for World Health Organization grades of pancreatic neuroendocrine tumors on contrast-enhanced magnetic resonance images: a preliminary study. *Int J Comput Assist Radiol Surg* 2019; **14**: 1981-1991 [PMID: 31555998 DOI: 10.1007/s11548-019-02070-5]
81 **Săftoiu A**, Vilmann P, Gorunescu F, Janssen J, Hocke M, Larsen M, Iglesias-Garcia J, Arcidiacono P, Will U, Giovannini M, Dietrich CF, Havre R, Gheorghe C, McKay C, Gheonea DI, Ciurea T; European EUS Elastography Multicentric Study Group. Efficacy of an artificial neural network-based approach to endoscopic ultrasound elastography in diagnosis of focal pancreatic masses. *Clin Gastroenterol Hepatol* 2012; **10**: 84-90.e1 [PMID: 21963957 DOI: 10.1016/j.cgh.2011.09.014]
82 **Kuwahara T**, Hara K, Mizuno N, Okuno N, Matsumoto S, Obata M, Kurita Y, Koda H, Toriyama K, Onishi S, Ishihara M, Tanaka T, Tajika M, Niwa Y. Usefulness of Deep Learning Analysis for the Diagnosis of Malignancy in Intraductal Papillary Mucinous Neoplasms of the Pancreas. *Clin Transl Gastroenterol* 2019; **10**: 1-8 [PMID: 31117111 DOI: 10.14309/ctg.0000000000000045]
83 **Marya NB**, Powers PD, Chari ST, Gleeson FC, Leggett CL, Abu Dayyeh BK, Chandrasekhara V, Iyer PG, Majumder S, Pearson RK, Petersen BT, Rajan E, Sawas T, Storm AC, Vege SS, Chen S, Long Z, Hough DM, Mara K, Levy MJ. Utilisation of artificial intelligence for the development of an EUS-convolutional neural network model trained to enhance the diagnosis of autoimmune pancreatitis. *Gut* 2021; **70**: 1335-1344 [PMID: 33028668 DOI: 10.1136/gutjnl-2020-322821]
84 **Tonozuka R**, Mukai S, Itoi T. The Role of Artificial Intelligence in Endoscopic Ultrasound for Pancreatic Disorders. *Diagnostics (Basel)* 2020; **11** [PMID: 33374181 DOI: 10.3390/diagnostics11010018]
85 **Hamamoto I**, Okada S, Hashimoto T, Wakabayashi H, Maeba T, Maeta H. Prediction of the early prognosis of the hepatectomized patient with hepatocellular carcinoma with a neural network. *Comput Biol Med* 1995; **25**: 49-59 [PMID: 7600761 DOI: 10.1016/0010-4825(95)98885-h]
86 **Abajian A**, Murali N, Savic LJ, Laage-Gaupp FM, Nezami N, Duncan JS, Schlachter T, Lin M, Geschwind JF, Chapiro J. Predicting Treatment Response to Image-Guided Therapies Using Machine Learning: An Example for Trans-Arterial Treatment of Hepatocellular Carcinoma. *J Vis Exp* 2018 [PMID: 30371657 DOI: 10.3791/58382]
87 **Abajian A**, Murali N, Savic LJ, Laage-Gaupp FM, Nezami N, Duncan JS, Schlachter T, Lin M, Geschwind JF, Chapiro J. Predicting Treatment Response to Intra-arterial Therapies for Hepatocellular Carcinoma with the Use of Supervised Machine Learning-An Artificial Intelligence Concept. *J Vasc Interv Radiol* 2018; **29**: 850-857.e1 [PMID: 29548875 DOI: 10.1016/j.jvir.2018.01.769]
88 **Wang W**, Chen Q, Iwamoto Y, Han X, Zhang Q, Hu H, Lin L, Chen YW. Deep Learning-Based Radiomics Models for Early Recurrence Prediction of Hepatocellular Carcinoma with Multi-phase CT Images and Clinical Data. *Annu Int Conf IEEE Eng Med Biol Soc* 2019; **2019**: 4881-4884 [PMID: 31946954 DOI: 10.1109/EMBC.2019.8856356]
89 **Peng J**, Kang S, Ning Z, Deng H, Shen J, Xu Y, Zhang J, Zhao W, Li X, Gong W, Huang J, Liu L. Residual convolutional neural network for predicting response of transarterial chemoembolization in hepatocellular carcinoma from CT imaging. *Eur Radiol* 2020; **30**: 413-424 [PMID: 31332558 DOI: 10.1007/s00330-019-06318-1]
90 **Shan QY**, Hu HT, Feng ST, Peng ZP, Chen SL, Zhou Q, Li X, Xie XY, Lu MD, Wang W, Kuang M. CT-based peritumoral radiomics signatures to predict early recurrence in hepatocellular carcinoma after curative tumor resection or ablation. *Cancer Imaging* 2019; **19**: 11 [PMID: 30813956 DOI: 10.1186/s40644-019-0197-5]
91 **Guo D**, Gu D, Wang H, Wei J, Wang Z, Hao X, Ji Q, Cao S, Song Z, Jiang J, Shen Z, Tian J, Zheng H. Radiomics analysis enables recurrence prediction for hepatocellular carcinoma after liver transplantation. *Eur J Radiol* 2019; **117**: 33-40 [PMID: 31307650 DOI: 10.1016/j.ejrad.2019.05.010]
92 **Ibragimov B**, Toesca D, Chang D, Yuan Y, Koong A, Xing L. Development of deep neural network for individualized hepatobiliary toxicity prediction after liver SBRT. *Med Phys* 2018; **45**: 4763-4774 [PMID: 30098025 DOI: 10.1002/mp.13122]
93 **Kambakamba P**, Mannil M, Herrera PE, Müller PC, Kuemmerli C, Linecker M, von Spiczak J, Hüllner MW, Raptis DA, Petrowsky H, Clavien PA, Alkadhi H. The potential of machine learning to predict postoperative pancreatic fistula based on preoperative, non-contrast-enhanced CT: A proof-of-principle study. *Surgery* 2020; **167**: 448-454 [PMID: 31727325 DOI: 10.1016/j.surg.2019.09.019]
94 **Tahmasebi N**, Boulanger P, Yun J, Fallone G, Noga M, Punithakumar K. Real-Time Lung Tumor Tracking Using a CUDA Enabled Nonrigid Registration Algorithm for MRI. *IEEE J Transl Eng Health Med* 2020; **8**: 4300308 [PMID: 32411543 DOI: 10.1109/JTEHM.2020.2989124]
95 **Ahn Y**, Yoon JS, Lee SS, Suk HI, Son JH, Sung YS, Lee Y, Kang BK, Kim HS. Deep Learning Algorithm for Automated Segmentation and Volume Measurement of the Liver and Spleen Using Portal Venous Phase Computed Tomography Images. *Korean J Radiol* 2020; **21**: 987-997 [PMID: 32677383 DOI: 10.3348/kjr.2020.0237]
96 **Hu W**, Yang H, Xu H, Mao Y. Radiomics based on artificial intelligence in liver diseases: where we are? *Gastroenterol Rep (Oxf)* 2020; **8**: 90-97 [PMID: 32280468 DOI: 10.1093/gastro/goaa011]
97 **Shen S**, Kong J, Qiu Y, Yang X, Wang W, Yan L. Identification of core genes and outcomes in hepatocellular carcinoma by bioinformatics analysis. *J Cell Biochem* 2019; **120**: 10069-10081 [PMID: 30525236 DOI: 10.1002/jcb.28290]

98 **Zhang L**, Huang Y, Ling J, Zhuo W, Yu Z, Shao M, Luo Y, Zhu Y. Screening and function analysis of hub genes and pathways in hepatocellular carcinoma *via* bioinformatics approaches. *Cancer Biomark* 2018; **22**: 511-521 [PMID: 29843214 DOI: 10.3233/CBM-171160]

99 **Bai Y**, Long J, Liu Z, Lin J, Huang H, Wang D, Yang X, Miao F, Mao Y, Sang X, Zhao H. Comprehensive analysis of a ceRNA network reveals potential prognostic cytoplasmic lncRNAs involved in HCC progression. *J Cell Physiol* 2019; **234**: 18837-18848 [PMID: 30916406 DOI: 10.1002/jcp.28522]

100 **Chaudhary K**, Poirion OB, Lu L, Garmire LX. Deep Learning-Based Multi-Omics Integration Robustly Predicts Survival in Liver Cancer. *Clin Cancer Res* 2018; **24**: 1248-1259 [PMID: 28982688 DOI: 10.1158/1078-0432.CCR-17-0853]

101 **Zhou Z**, Li Y, Hao H, Wang Y, Zhou Z, Wang Z, Chu X. Screening Hub Genes as Prognostic Biomarkers of Hepatocellular Carcinoma by Bioinformatics Analysis. *Cell Transplant* 2019; **28**: 76S-86S [PMID: 31822116 DOI: 10.1177/0963689719893950]

102 **Cucchetti A**, Vivarelli M, Heaton ND, Phillips S, Piscaglia F, Bolondi L, La Barba G, Foxton MR, Rela M, O'Grady J, Pinna AD. Artificial neural network is superior to MELD in predicting mortality of patients with end-stage liver disease. *Gut* 2007; **56**: 253-258 [PMID: 16809421 DOI: 10.1136/gut.2005.084434]

103 **Cristoferi L**, Nardi A, Ronca V, Invernizzi P, Mells G, Carbone M. Prognostic models in primary biliary cholangitis. *J Autoimmun* 2018; **95**: 171-178 [PMID: 30420264 DOI: 10.1016/j.jaut.2018.10.024]

104 **Sun W**, Nasraoui O, Shafto P. Evolution and impact of bias in human and machine learning algorithm interaction. *PLoS One* 2020; **15**: e0235502 [PMID: 32790666 DOI: 10.1371/journal.pone.0235502]

105 **Coakley S**, Young R, Moore N, England A, O'Mahony A, O'Connor OJ, Maher M, McEntee MF. Radiographers' knowledge, attitudes and expectations of artificial intelligence in medical imaging. *Radiography (Lond)* 2022; **28**: 943-948 [PMID: 35839662 DOI: 10.1016/j.radi.2022.06.020]

106 **European Society of Radiology (ESR)**. Current practical experience with artificial intelligence in clinical radiology: a survey of the European Society of Radiology. *Insights Imaging* 2022; **13**: 107 [PMID: 35727355 DOI: 10.1186/s13244-022-01247-y]

107 **Kader R**, Baggaley RF, Hussein M, Ahmad OF, Patel N, Corbett G, Dolwani S, Stoyanov D, Lovat LB. Survey on the perceptions of UK gastroenterologists and endoscopists to artificial intelligence. *Frontline Gastroenterol* 2022; **13**: 423-429 [PMID: 36046492 DOI: 10.1136/flgastro-2021-101994]

108 **Wadhwa V**, Alagappan M, Gonzalez A, Gupta K, Brown JRG, Cohen J, Sawhney M, Pleskow D, Berzin TM. Physician sentiment toward artificial intelligence (AI) in colonoscopic practice: a survey of US gastroenterologists. *Endosc Int Open* 2020; **8**: E1379-E1384 [PMID: 33015341 DOI: 10.1055/a-1223-1926]

109 **Zwanenburg A**, Vallières M, Abdalah MA, Aerts HJWL, Andrearczyk V, Apte A, Ashrafinia S, Bakas S, Beukinga RJ, Boellaard R, Bogowicz M, Boldrini L, Buvat I, Cook GJR, Davatzikos C, Depeursinge A, Desseroit MC, Dinapoli N, Dinh CV, Echegaray S, El Naqa I, Fedorov AY, Gatta R, Gillies RJ, Goh V, Götz M, Guckenberger M, Ha SM, Hatt M, Isensee F, Lambin P, Leger S, Leijenaar RTH, Lenkowicz J, Lippert F, Losnegård A, Maier-Hein KH, Morin O, Müller H, Napel S, Nioche C, Orlhac F, Pati S, Pfaehler EAG, Rahmim A, Rao AUK, Scherer J, Siddique MM, Sijtsema NM, Socarras Fernandez J, Spezi E, Steenbakkers RJHM, Tanadini-Lang S, Thorwarth D, Troost EGC, Upadhaya T, Valentini V, van Dijk LV, van Griethuysen J, van Velden FHP, Whybra P, Richter C, Löck S. The Image Biomarker Standardization Initiative: Standardized Quantitative Radiomics for High-Throughput Image-based Phenotyping. *Radiology* 2020; **295**: 328-338 [PMID: 32154773 DOI: 10.1148/radiol.2020191145]

110 **Cai J**, Lu L, Zhang Z, Xing F, Yang L, Yin Q. Pancreas Segmentation in MRI using Graph-Based Decision Fusion on Convolutional Neural Networks. *Med Image Comput Comput Assist Interv* 2016; **9901**: 442-450 [PMID: 28083570 DOI: 10.1007/978-3-319-46723-8_51]

111 **Li M**, Lian F, Guo S. Pancreas segmentation based on an adversarial model under two-tier constraints. *Phys Med Biol* 2020; **65**: 225021 [PMID: 32906095 DOI: 10.1088/1361-6560/abb6bf]

112 **Boers TGW**, Hu Y, Gibson E, Barratt DC, Bonmati E, Krdzalic J, van der Heijden F, Hermans JJ, Huisman HJ. Interactive 3D U-net for the segmentation of the pancreas in computed tomography scans. *Phys Med Biol* 2020; **65**: 065002 [PMID: 31978921 DOI: 10.1088/1361-6560/ab6f99]

113 **Tang X**, Jafargholi Rangraz E, Coudyzer W, Bertels J, Robben D, Schramm G, Deckers W, Maleux G, Baete K, Verslype C, Gooding MJ, Deroose CM, Nuyts J. Whole liver segmentation based on deep learning and manual adjustment for clinical use in SIRT. *Eur J Nucl Med Mol Imaging* 2020; **47**: 2742-2752 [PMID: 32314026 DOI: 10.1007/s00259-020-04800-3]

114 **Shiomi S**, Kuroki T, Kuriyama M, Morikawa H, Masaki K, Ikeoka N, Tanaka T, Ikeda H, Ochi H. Diagnosis of chronic liver disease from liver scintiscans by artificial neural networks. *Ann Nucl Med* 1997; **11**: 75-80 [PMID: 9212885 DOI: 10.1007/BF03164813]

115 **Yasaka K**, Akai H, Kunimatsu A, Abe O, Kiryu S. Deep learning for staging liver fibrosis on CT: a pilot study. *Eur Radiol* 2018; **28**: 4578-4585 [PMID: 29761358 DOI: 10.1007/s00330-018-5499-7]

116 **Mokrane FZ**, Lu L, Vavasseur A, Otal P, Peron JM, Luk L, Yang H, Ammari S, Saenger Y, Rousseau H, Zhao B, Schwartz LH, Dercle L. Radiomics machine-learning signature for diagnosis of hepatocellular carcinoma in cirrhotic patients with indeterminate liver nodules. *Eur Radiol* 2020; **30**: 558-570 [PMID: 31444598 DOI: 10.1007/s00330-019-06347-w]

117 **Xu L**, Yang P, Liang W, Liu W, Wang W, Luo C, Wang J, Peng Z, Xing L, Huang M, Zheng S, Niu T. A radiomics approach based on support vector machine using MR images for preoperative lymph node status evaluation in intrahepatic cholangiocarcinoma. *Theranostics* 2019; **9**: 5374-5385 [PMID: 31410221 DOI: 10.7150/thno.34149]

118 **Ji GW**, Zhu FP, Xu Q, Wang K, Wu MY, Tang WW, Li XC, Wang XH. Machine-learning analysis of contrast-enhanced CT radiomics predicts recurrence of hepatocellular carcinoma after resection: A multi-institutional study. *EBioMedicine* 2019; **50**: 156-165 [PMID: 31735556 DOI: 10.1016/j.ebiom.2019.10.057]

119 **Liu D**, Liu F, Xie X, Su L, Liu M, Kuang M, Huang G, Wang Y, Zhou H, Wang K, Lin M, Tian J. Accurate prediction of responses to transarterial chemoembolization for patients with hepatocellular carcinoma by using artificial intelligence in contrast-enhanced ultrasound. *Eur Radiol* 2020; **30**: 2365-2376 [PMID: 31900703 DOI: 10.1007/s00330-019-06553-6]

World Journal of Gastroenterology

Submit a Manuscript: https://www.f6publishing.com

World J Gastroenterol 2023 March 7; 29(9): 1446-1459

DOI: 10.3748/wjg.v29.i9.1446

ISSN 1007-9327 (print) ISSN 2219-2840 (online)

MINIREVIEWS

Role of noncoding RNAs in liver fibrosis

Qing-Yuan Li, Tao Gong, Yi-Ke Huang, Lan Kang, Charlotte A Warner, He Xie, Li-Min Chen, Xiao-Qiong Duan

Specialty type: Gastroenterology and hepatology

Provenance and peer review: Invited article; Externally peer reviewed.

Peer-review model: Single blind

Peer-review report's scientific quality classification

Grade A (Excellent): A
Grade B (Very good): 0
Grade C (Good): C
Grade D (Fair): 0
Grade E (Poor): 0

P-Reviewer: Agrawal P, United States; Liu Z, China

Received: October 4, 2022
Peer-review started: October 4, 2022
First decision: October 17, 2022
Revised: October 27, 2022
Accepted: February 27, 2023
Article in press: February 27, 2023
Published online: March 7, 2023

Qing-Yuan Li, Tao Gong, Department of Clinical Medicine, North Sichuan Medical College, Nanchong 637000, Sichuan Province, China

Yi-Ke Huang, Lan Kang, Li-Min Chen, Xiao-Qiong Duan, Center for Transfusion-transmitted Infectious Diseases, Institute of Blood Transfusion, Chinese Academy of Medical Sciences and Peking Union Medical College, Chengdu 610052, Sichuan Province, China

Charlotte A Warner, Liver Center and Gastrointestinal Division, Department of Medicine, Massachusetts General Hospital, Harvard Medical School, Boston, MA 02114, United States

He Xie, Li-Min Chen, Department of Clinical Laboratory, The Hospital of Xidian Group, Xi'an 710077, Shaanxi Province, China

Corresponding author: Xiao-Qiong Duan, PhD, Associate Professor, Center for Transfusion-transmitted Infectious Diseases, Institute of Blood Transfusion, Chinese Academy of Medical Sciences and Peking Union Medical College, No. 26 Huacai Road, Chengdu 610052, Sichuan Province, China. xiaoqiongduan@163.com

Abstract

Liver fibrosis is a wound-healing response following chronic liver injury caused by hepatitis virus infection, obesity, or excessive alcohol. It is a dynamic and reversible process characterized by the activation of hepatic stellate cells and excess accumulation of extracellular matrix. Advanced fibrosis could lead to cirrhosis and even liver cancer, which has become a significant health burden worldwide. Many studies have revealed that noncoding RNAs (ncRNAs), including microRNAs, long noncoding RNAs and circular RNAs, are involved in the pathogenesis and development of liver fibrosis by regulating signaling pathways including transforming growth factor-β pathway, phosphatidylinositol 3-kinase/protein kinase B pathway, and Wnt/β-catenin pathway. NcRNAs in serum or exosomes have been reported to tentatively applied in the diagnosis and staging of liver fibrosis and combined with elastography to improve the accuracy of diagnosis. NcRNAs mimics, ncRNAs in mesenchymal stem cell-derived exosomes, and lipid nanoparticles-encapsulated ncRNAs have become promising therapeutic approaches for the treatment of liver fibrosis. In this review, we update the latest knowledge on ncRNAs in the pathogenesis and progression of liver fibrosis, and discuss the potentials and challenges to use these ncRNAs for diagnosis, staging and treatment of liver fibrosis. All these will help us to develop a comprehensive understanding of the role of ncRNAs in liver fibrosis.

Key Words: MicroRNAs; Long noncoding RNAs; Circular RNAs; Liver fibrosis;

Diagnosis; Treatment

Core Tip: Liver fibrosis is an inevitable stage in the development of various chronic liver diseases, and manifests as an imbalance between the formation and degradation of extracellular matrix. The key mechanism of liver fibrosis is the activation of hepatic stellate cells, which is coordinately regulated by a variety of cytokines, inflammatory factors and chemokines involved in multiple cells signaling pathways. In this review, we discuss the role of noncoding RNAs (ncRNAs) in regulating the signaling pathways in the formation and regression of liver fibrosis, and the limitations, challenges, and prospects of ncRNAs in the diagnosis and treatment of liver fibrosis.

Citation: Li QY, Gong T, Huang YK, Kang L, Warner CA, Xie H, Chen LM, Duan XQ. Role of noncoding RNAs in liver fibrosis. *World J Gastroenterol* 2023; 29(9): 1446-1459
URL: https://www.wjgnet.com/1007-9327/full/v29/i9/1446.htm
DOI: https://dx.doi.org/10.3748/wjg.v29.i9.1446

INTRODUCTION

Liver fibrosis is the result of excessive accumulation of extracellular matrix (ECM) caused by continuous liver injuries that promote wound healing[1]. Liver injuries can be caused by many factors including persistent hepatitis B virus (HBV)/hepatitis C virus (HCV) infections, excessive alcohol consumption, metabolic diseases, drugs, genetic diseases, cholestasis, and autoimmune diseases. Due to an increase in the prevalence of obesity and type 2 diabetes, liver fibrosis caused by nonalcoholic steatohepatitis (NASH) has been increasing annually in recent years[2]. Liver fibrosis can resolve at an early stage if the injuries subside. Progressive fibrosis is associated with architectural changes to hepatic lobules and may lead to cirrhosis, liver failure, portal hypertension, and even hepatocellular carcinoma (HCC).

Hepatic stellate cells (HSCs) play a central role in liver fibrosis. HSCs, also known as perisinusoidal cells, are located in the Disse space under healthy conditions. When injury occurs, HSCs are activated and transdifferentiate into myofibroblast-like cells which are the main source of ECM[3]. Hepatic fibrosis is a dynamic process coordinated by multiple cells in the liver. Acute injury, such as viral infection, induces an inflammatory response, necrosis, and apoptosis in hepatocytes which leads to liver regeneration and limited ECM deposition. However, if the damage persists, the injured hepatocytes attract an infiltration of inflammatory cells such as T lymphocytes and neutrophils, which will in turn activate HSCs by releasing cytokines, chemokines, and reactive oxygen species (ROS). Activated HSCs can maintain the active state by the mediators produced by the autocrine and paracrine system. In addition, platelet-derived growth factor (PDGF) secreted by liver macrophages (Kupffer cells) stimulates the continuous proliferation of HSCs. Therefore, inhibiting the activation and proliferation of HSCs, promoting the apoptosis of activated HSCs, and reducing the expression of fibrogenic factors are considered to be the key measures for the successful treatment of liver fibrosis.

Noncoding RNAs (ncRNAs) refer to RNAs that are transcribed from the genome but do not normally encode proteins, although some of them have recently been reported to encode small proteins[4]. According to their length, ncRNAs can be divided into short ncRNAs and long ncRNAs (lncRNAs). MicroRNAs (miRNAs) are a class of short ncRNAs of approximately 22 nucleotides in length that act as gene repressors by complementary binding to the 3' untranslated region of target mRNA to degrade or prevent it from being translated to protein[5,6]. LncRNAs are defined as ncRNAs longer than 200 bp with 5′-end m7G caps and 3′-end poly(A) tails. LncRNAs can regulate gene expression in *cis* or *trans*, change the structure and function of chromatin *via* interaction with proteins, or act as competitive endogenous RNAs (ce-RNAs) for post-transcriptional regulation[7]. Circular RNAs (circRNAs) are a novel form of ncRNAs with a covalently closed single-stranded structure, which is formed by back-splicing of the 3' and 5' ends of mRNAs[8]. Depending on their subcellular localization, circRNAs have different biological functions: interfering with signal transduction pathways and regulating the transcription and translation of target genes, sponge proteins and miRNAs[9].

In this review, we summarize the latest findings about miRNAs, lncRNAs, and circRNAs in the pathogenesis and progression of liver fibrosis and discuss the potential of ncRNAs as biomarkers for diagnosis and as therapeutic targets for liver fibrosis.

NCRNAS IN THE PATHOGENESIS AND PROGRESSION OF LIVER FIBROSIS

The activation and proliferation of HSCs are essential steps in the development of liver fibrosis. Numerous studies have shown that ncRNAs exert profibrotic effects by regulating genes in the activation and proliferation signaling pathways of HSCs. Signaling pathways closely related to liver fibrosis mainly include transforming growth factor-β (TGF-β)/Smad, phosphatidylinositol 3-kinase (PI3K)/serine/threonine kinase 1 (AKT), Wnt/β-catenin, and nuclear factor κ light chain enhancer of activated B cells (NF-κB) pathways. Although some miRNAs[10] and lncRNAs[11] involved in liver fibrosis have been reviewed elsewhere, we focus on the most recent data published in the past 3 years as summarized in Figure 1.

ncRNAs regulating TGF-β/Smad signaling pathway in liver fibrosis

Transforming growth factor-β1 (TGF-β1) is a well-recognized fibrogenic cytokine that is widely expressed in damaged hepatocytes, Kupffer cells, HSCs, sinusoidal endothelial cells, and platelets. TGF-β1 promotes HSC activation through a canonical (Smad) or noncanonical pathway[12]. In the TGF-β1/Smad signaling pathway, TGF-β1 binds to the TGF-β type II receptor (TGF-βRII) on the cell membrane and then recruits the TGF-β type I receptor (TGF-βRI) to form a heterotetrameric complex. This complex induces the phosphorylation of intracellular Smad2 and Smad3, which then bind with Smad4 and translocate to the nucleus to regulate expression of target genes[13-15]. In addition, TGF-β1 induces the expression of Smad7, which maintains the balance between profibrotic and antifibrosis by negatively regulating TGF-βRI and Smad2[13].

Many miRNAs are involved in the regulation of the TGF-β/Smad signaling pathway and liver fibrosis. These miRNAs include miR-21, miR-497, miR-16, miR-98-5p, miR-199a-3p, miR-29a, and miR-130a-3p. MiR-21 is expressed abundantly in liver, is present in serum, and is positively associated with liver inflammation, fibrosis, and cancer[16]. TGF-β1 induces transcription, processing and maturation of pri-miR-21 through a Smad3-dependent pathway, while mature miR-21 promotes the development of fibrosis by targeting the inhibitory Smad gene-small mothers against decapentaplegic7[15]. *Clonorchis sinensis* promotes hepatic fibrosis by inducing miR-497 and activating the TGF-β/Smad pathway[17]. Pan *et al*[18] revealed that miR-16 plays an essential role in the phenotypic remodeling of myofibroblasts. Overexpression of miR-16 restored the phenotype of HSCs and led to fibrotic regression by targeting Smad2 and Wnt3a to interfere with TGF-β and Wnt signaling pathways, respectively[18]. In patients with chronic HBV-induced liver fibrosis, expression of miR-98-5p was significantly downregulated. Further studies indicated that overexpression of miR-98-5p significantly inhibited HSC activation through targeting the TGF-β1/Smad3 signaling pathway[19]. Yang *et al*[20] demonstrated that expression of miR-199a-3p was upregulated in carbon tetrachloride (CCl_4)-induced liver fibrotic rats, and miR-199a-3p activated HSCs by targeting caveolin-2 (CAV2) to increase expression of TGF-βRI. Stimulation with TGF-β resulted in the downregulation of miR-29a, which increased follistatin-like 1 expression and accelerated the progression of fibrosis by enhanced phosphorylation of Smad2[21]. MiR-130a-3p was significantly decreased in liver fibrosis caused by *Schistosoma japonicum*[22]. It has been shown that miR-130a-3p attenuates fibrosis by inhibiting the activation and proliferation of HSCs and promoting their apoptosis through regulation of mitogen-activated protein kinase 1 and TGF-βRI/II both *in vitro* and *in vivo*[22].

In addition to miRNAs, lncRNAs and circRNAs are associated with the TGF-β pathway and liver fibrogenesis. LncRNA small Cajal body-specific RNA 10 (lncRNA SCARNA10) was found to inhibit the expression of polycomb repressive complex 2 to induce hepatocytes apoptosis and HSC activation, thereby stimulating the TGF-β pathway and liver fibrogenesis[23]. CircRNA mitochondrial tRNA translation optimization 1 (circMTO1) was reported to inhibit liver fibrosis through interaction with miR-17-5p and Smad7[24].

ncRNAs regulating PI3K/AKT signaling pathway in liver fibrosis

The PI3K/AKT pathway is an essential intracellular signaling pathway in the regulation of the cell cycle. The AKT cascade can be activated by cytokine receptors such as receptors of TGF-β and PDGF. PI3K is activated to induce phosphorylation of Phosphatidylinositol-4,5-biophosphate (PIP2) on the cell surface, leading to production of phosphatidylinositol-3,4,5-trisphosphate (PIP3). AKT (also known as protein kinase B, PKB) binds to PIP3 and they are co-translocated to the nucleus, where they regulate target gene expression to stimulate cell proliferation and inhibit apoptosis. Phosphatase and tensin homology deleted on chromosome ten (PTEN) increases the number of activated HSCs by catalyzing dephosphorylation of PIP3 and downregulating the PI3K/AKT signaling pathway. A variety of miRNAs regulate the PI3K/AKT signaling pathway. MiR-21 is significantly upregulated in liver fibrosis induced by cadmium exposure, which leads to the progression of fibrosis by activating the PI3K/AKT pathway[25]. Lipotoxic hepatocyte-derived exosomal miR-1297 promotes HSC proliferation and activation by inhibiting expression of PTEN[26]. MiR-23a-5p activates the PI3K/AKT/mammalian target of rapamycin (mTOR) signaling pathway by inhibiting PTEN and can be targeted by lncRNA LOC102551149 to reduce liver fibrosis[27]. All these results indicate that ncRNAs, especially miRNAs and lncRNAs, play important roles in liver fibrosis through targeting the PI3K/AKT pathway.

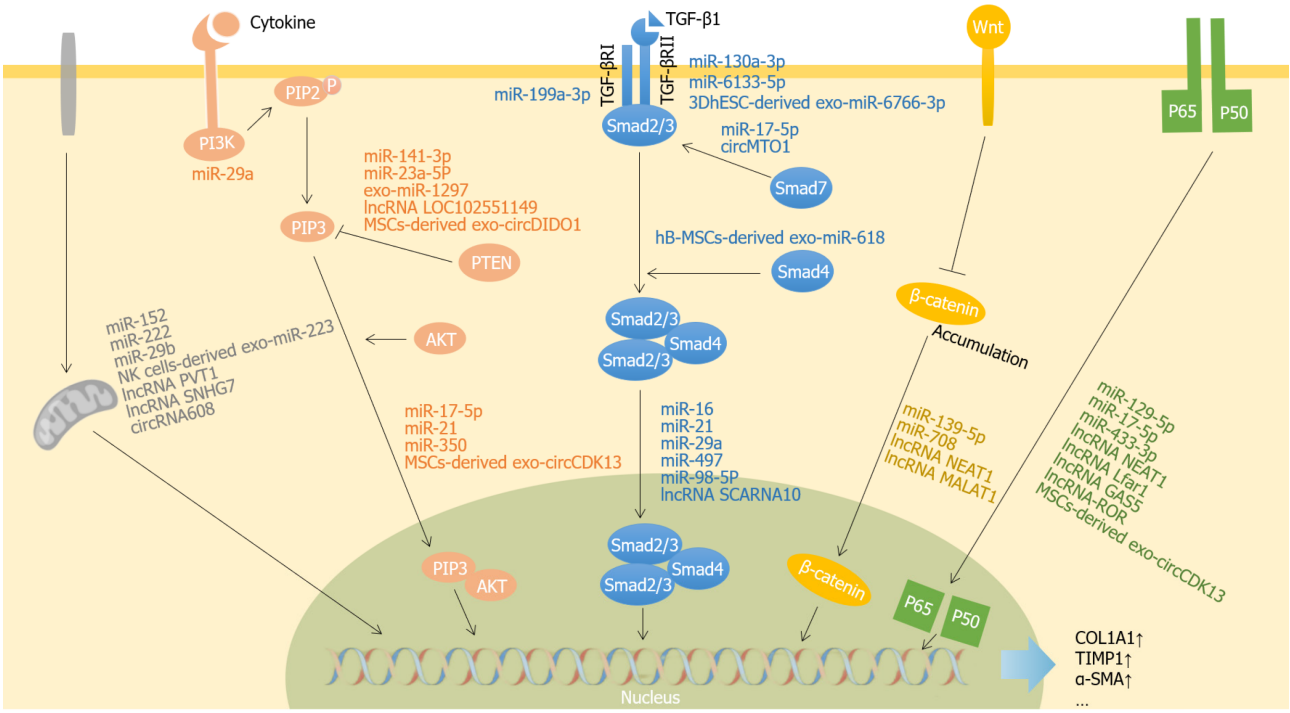

DOI: 10.3748/wjg.v29.i9.1446

Figure 1 Reported pathways and targets of noncoding RNAs involved in liver fibrosis. Noncoding RNAs regulate the target gene transcription in the pathogenesis and progression of liver fibrosis through inhibiting or activating the key genes in different signaling pathways. PI3K: Phosphatidylinositol 3-kinase; AKT: Serine/threonine kinase 1; PIP2: Phosphatidylinositol-4,5-biophosphate; PTEN: Phosphatase and tensin homology deleted on chromosome ten; Col1A1: Collagen 1A1; TIMP1: Targeted tissue inhibitor of metalloproteinase1; α-SMA: α-smooth muscle actin; PIP3: Phosphatidylinositol-3,4,5-trisphosphate; TGF-β: Transforming growth factor-β; TGF-βRII: TGF-β type II receptor; MSC: Mesenchymal stem cell; hB-MSC: Human bone MSC; hT-MSC: Human tonsil-derived MSC; 3DhESC: 3D-cultured human embryonic stem cells;PVT1: Plasmacytoma variant translocation 1; SNHG7: Small nucleolar RNA host gene 7; DIDO1: Death inducer-obliterator 1; CDK13: Cyclin dependent kinase 13; MTO1: Mitochondrial tRNA translation optimization 1; SCARNA10: Small Cajal body-specific RNA 10; MALAT1: Metastasis-associated lung adenocarcinoma transcript1; NEAT1: Nuclear enriched abundant transcript1; Lfar1: Liver fibrosis associated lncRNA1; GAS5: Growth arrest-special transcript 5; ROR: Regulator of reprogramming.

ncRNAs regulating Wnt/β-catenin signaling pathway in liver fibrosis

Wnt/β-catenin is involved in the development of fibrosis of several tissues, including kidney, lung, skin, and liver. Wnt proteins are cysteine-rich glycoproteins generally secreted to the ECM. β-Catenin is a cytoplasmic protein that can be activated by Wnt and is translocated to the nucleus to activate transcription of target genes, thereby regulating occurrence of fibrosis[28]. Yang *et al*[29] demonstrated that expression of miR-708 was downregulated in fibrotic liver tissue. The authors further demonstrated that overexpression of miR-708 inhibited activation of HSCs by targeting zinc finger E-box binding homeobox 1 and regulating the Wnt/β-catenin signaling pathway[29]. Different forms of ncRNAs may work together to have a synergistic effect in the pathogenesis and progression of liver fibrosis. For example, lncRNA nuclear enriched abundant transcript1 (lncRNA NEAT1) and miR-139-5p have a synergistic effect that exacerbates the development of liver fibrosis[30]. Another study has revealed that lncRNA metastasis-associated lung adenocarcinoma transcript1 (lncRNA MALAT1) upregulates expression of β-catenin and promotes liver fibrosis through the Wnt/β-catenin pathway[31].

ncRNAs regulating NF-κB signaling pathway in liver fibrosis

NF-κB is one of the transcription factors that regulates important cellular events, particularly inflammation. NF-κB consists of two subunits p50 and p65, which can be activated by extracellular signals. Activated NF-κB translocate to the nucleus to regulate expression of various cytokines, growth factors, and other target genes. LncRNA NEAT1 plays critical roles in hepatic fibrosis of different etiologies by targeting various miRNAs associated with NF-κB signaling pathways. In NASH-induced liver fibrotic mice, Zhang *et al*[32] found that lncRNA NEAT1 stimulated expression of paternally expressed gene 3 (PEG3) by inhibiting miR-129-5p, which reduced HSC apoptosis through the NF-κB (p65/p50) signaling pathway. The effect of the lncRNA NEAT1/miR-129-5p axis on liver fibrosis had also been confirmed in alcoholic steatohepatitis mice by targeting suppressor of cytokine signaling 2[33]. In addition, lncRNA NEAT1 also promotes fibrosis *via* inhibition of miR-148a-3p and miR-22-3p and regulation of cytohesin 3 expression[34]. LncRNA liver fibrosis associated lncRNA1 (lncRNA Lfar1) was demonstrated to promote hepatic fibrosis through activation of HSCs, probably by way of its regulatory effect on macrophages through the NF-κB signaling pathway[35]. Overexpression of lncRNA growth arrest-

special transcript 5 (lncRNA GAS5) decreased expression of miR-433-3p, which then intercepted the NF-κB signaling pathway through targeting of toll-like receptor 10[36]. In addition, lncRNA maternally expressed gene 3 (lncRNA MEG3) targeted NLR Family CARD Domain Containing 5 (NLRC5) to reverse liver fibrosis[37]. All of these results indicate that ncRNAs regulating liver fibrosis through targeting the NF-κB pathway are mainly lncRNAs, including lncRNAs NEAT1, Lfar1, GAS5, and MEG3.

ncRNAs regulating autophagy pathway in liver fibrosis

Autophagy is a process that regulates self-metabolism and maintains cellular homeostasis by removing cell debris, misfolded proteins and lipid droplets[38]. Activation of autophagy promotes liver fibrosis by increasing the digestion of lipid droplets and activating multiple signaling pathways, which implies that promoting regeneration of lipid droplets and restraining expression of proinflammatory factors inhibits liver fibrosis[38]. In hypoxic conditions, lncRNA plasmacytoma variant translocation 1 (lncRNA PVT1) regulates expression levels of autophagy-related gene (ATG)14 by decreasing miR-152, thereby activating HSCs through the autophagy pathway[39]. LncRNA small nucleolar RNA host gene 7 (lncRNA SNHG7) increased DNA methyltransferase 3 alpha (DNMT3A) expression through binding to miR-29b, which is involved in liver fibrosis and autophagy. Inhibition of lncRNA SNHG7 significantly decreases expression of collagen and autophagy factors, leading to inhibition of liver fibrosis[40]. In addition to lncRNAs, circRNAs are also associated with autophagy and mitophagy. Xu *et al*[41] illustrated that circRNA608/miR-222 regulates PTEN-induced putative kinase 1-mediated mitophagy and liver fibrosis in NASH-induced fibrotic mice.

Other ncRNAs targeting host genes involved in liver fibrosis

Chen *et al*[42] demonstrated that miR-451 and miR-185 were downregulated in activated HSCs, and they exerted antifibrotic effects synergistically by targeting erythropoietin-producing hepatocellular receptor B2. MiR-451 upregulated expression of miR-185. This occurs at the post-transcriptional level by targeting nuclear export receptor exportin 1 (XPO-1). Zhao *et al*[43] demonstrated that lncRNA molecule interacting with CasL2 (lncRNA Mical2) upregulated p66 Src homologous-collagen homologue (p66Shc) through sponging miR-203a-3p, which promoted reactive oxygen species (ROS)-mediated epithelial–mesenchymal transition and liver fibrosis. It has been reported that lncRNA X-inactive-specific transcript (lncRNA XIST) damages mitochondrial function and increases ROS production to promote HSC activation by regulating miR-539-3p and ADAM metallopeptidase with thrombospondin type 1 motif 5 (ADAMTS5)[44]. Studies from cholestatic liver injury caused by biliary atresia have indicated that expression of lncRNA H19 is significantly upregulated in exosomes derived from liver and serum. LncRNA H19 deficiency protects mice from liver fibrosis by inhibiting sphingosine-1-phosphate receptor 2/sphingosine kinase 2 activation and by sponging let-7 to upregulate high-mobility group AT-hook 2 expression[45]. It has also been reported that depletion of macrophages significantly reduced lncRNA H19 and inhibited cholestatic liver injury in bile duct ligation mice[46]. LncRNA actin alpha 2-antisense RNA 1 (lncRNA ACTA2-AS1) accelerated liver fibrosis and epigenetic activation by targeting the p300/ETS transcription factor (ELK1) complex in biliary diseases[47]. CircRNA F-box and WD repeat domain containing 4 (circFBXW4) was downregulated significantly in HSCs of mice with liver fibrosis. Overexpression of circFBXW4 inhibited HSC activation by targeting miR-18b-3p to increase FBXW7 expression[48]. Similarly, CircRNA CREB binding protein (circCREBBP) inhibited liver fibrosis by targeting miR-1291 to regulate the expression of left-right determinant cluster 2 (LEFTY2) [49]. Hsa_circ_0071410 inhibited activation of HSCs by binding to miR-9-5p in irradiation-induce liver fibrosis[50]. All these ncRNAs in the pathogenesis and progression of liver fibrosis are summarized in Table 1[51-60].

POTENTIAL APPLICATION OF NCRNAS IN THE DIAGNOSIS OF LIVER FIBROSIS

Liver-related mortality increases with the progression of fibrosis. Therefore, it is essential for the early diagnosis of liver fibrosis. At present, the gold standard for the diagnosis of liver fibrosis is still liver biopsy, although it has some limitations such as sampling error, inter- and intra-observer variability [61], invasiveness to patients, and many other complications. Several noninvasive examinations have been introduced in clinical settings, including serum markers, combined indices or scores, and imaging techniques. Hepascore and enhanced liver fibrosis score are based on serum liver fibrosis markers such as tissue metalloproteinases and hyaluronic acid [62]. Elastography, including ultrasound elastography and magnetic resonance elastography, is a method to access liver stiffness quantitatively and it is more accurate than serological markers for diagnosis of advanced liver fibrosis. However, elastography has disadvantages such as unreliable results due to high body mass index (BMI) and high cost, making it unsuitable for population screening[62]. As ncRNAs in the blood are easily accessible for detection, they have potential as novel noninvasive biomarkers for diagnosis of liver fibrosis.

Recent research has shown that stimulation of HSCs with TGF-β and PDGF-BB decreased the intracellular miR-29 expression level but significantly increased miR-29 level in the supernatant vesicles [63]. They verified the results in serum from patients with HCV-related liver fibrosis and mice with CCl_4

Table 1 Noncoding RNAs in the pathogenesis and progression of liver fibrosis

ncRNAs	Target genes	Signaling pathways	Ref.
miR-199a-3p	*CAV2*	TGF-β/Smad	[20]
miR-497	*Smad7*	TGF-β/Smad	[17]
miR-21	*Smad2/3/7*	TGF-β/Smad	[15]
	TGF-β	PI3K/AKT	[25]
	-	PPARα	[51]
	-	PDCD4/AP-1	[51,52]
	-	Smad7/Smad2/3/NOX4, Spry1/ERK/NF-κB	[51,53]
	-	HIF-1α/VEGF	[54]
miR-16	*Smad2*, *Wnt3a*	TGF-β/Smad, Wnt	[18]
miR-130a-3p	*TGF-βRI*, *TGF-βRII*; *MAPK1*	TGF-β; MAPK	[22]
miR-98-5p	*TGF-βRI*	TGF-β1/Smad3	[19]
miR-6133-5p	*TGF-βRII*, *FGFRI*	TGF-β/Smad2/3, AKT/ERK/JNK	[55]
miR-708	*ZEB1*	Wnt/β-catenin	[29]
exo-miR-1297	*PTEN*	PI3K/AKT	[26]
miR-350	*SPRY2*	PI3K/AKT and ERK	[56]
miR-34c	*ACSL1*	-	[57]
miR-200c	*HAS2*	-	[58]
miR-451, miR-185	*EphB2*	-	[42]
miR-20b-5p	*STAT3*	STAT3	[97]
lncRNA SNHG7	*miR-29b*, *DNMT3A*	Autophagy pathway	[40]
lncRNA PVT1	*miR-152*, *ATG14*	Autophagy pathway	[39]
lncRNA SCARNA10	*PRC2*	TGF-β	[23]
lncRNA LOC102551149	*miR-23a-5p*, *PTEN*	PI3K/AKT/mTOR/Snail	[27]
lncRNA MALAT1	-	Wnt/β-catenin	[31]
lncRNA NEAT1	*miR-139-5p*, *β-catenin*	β-catenin/SOX9/TGF-β1	[30]
	miR-129-5p, *PEG3*	NF-κB	[32]
	miR-129-5p, *SOCS2*	-	[33]
	miR-148a-3p, *miR-22-3p*, *Cyth3*	-	[34]
lncRNA Lfar1	-	NF-κB	[35]
lncRNA GAS5	*miR-433-3p*, *TLR10*	NF-κB	[36]
lncRNA-ROR	*miR-6499-3p*	NF-κB	[99]
lncRNA Airn	*EZH2*	KLF2-eNOS-sGC	[98]
lncRNA MEG3	*NLRC5*	-	[37]
lncRNA NORAD	*miR-495-3p*, *S1PR3*	-	[60]
lncRNA XIST	*miR-539-3p*, *ADAMTS5*	-	[44]
lncRNA Mical2	*miR-203a-3p*, *p66Shc*	-	[43]
circRNA608	*miR222*, *PINK1*	Autophagy pathway	[41]
circMTO1	*miR-17-5p*, *Smad7*	-	[24]
circFBXW4	*miR-18b-3p*, *FBXW7*	-	[48]
circCREBBP	*miR-1291*, *LEFTY2*	-	[49]
circ_0071410	*miR-9-5p*	-	[50]

circUbe2k	*miR-149-5p*, *TGF-β2*	-	[59]

ncRNAs: Noncoding RNAs; CAV2: Caveolin-2; TGF-β: Transforming growth factor-β; PI3K: Phosphatidylinositol 3-kinase; AKT: Serine/threonine kinase 1; PPAR: Peroxisome proliferator-activated receptor; PDCD4: Programmed cell death protein 4; AP-1: Activation protein-1; NOX4: Nicotinamide adenine dinucleotide phosphate oxidase 4; Spry1: Sprouty 1; ERK: Extracellular regulated kinase; NF-κB: Nuclear factor κ light chain enhancer of activated B cells; HIF-1α: Hypoxia-inducible factor-1α; VEGF: Vascular endothelial growth factor; TGF-βRI: TGF-β type I receptor; MAPK: Mitogen-activated protein kinase; FGFR: Fibroblast growth factor receptor; JNK: c-Jun N-terminal kinase; ZEB1: Zinc finger E-box binding homeobox 1; PTEN: Phosphatase and tensin homology deleted on chromosome ten; ACSL1: Acyl-CoA synthetase long chain family member 1; HAS2: Hyaluronic acid synthase; EphB2: Erythropoietin-producing hepatocellular receptor B2; SNHG7: Small nucleolar RNA host gene 7; DNMT3A: DNA methyltransferase 3 alpha; PVT1: Plasmacytoma variant translocation 1; ATG: Autophagy-related gene; SCARNA10: Small Cajal body-specific RNA 10; PRC2: Polycomb repressive complex 2; mTOR: Mammalian target of rapamycin; MALAT1: Metastasis-associated lung adenocarcinoma transcript1; NEAT1: Nuclear enriched abundant transcript1; SOX9: SRY-related high mobility group-box gene9; PEG3: Paternally expressed gene 3; SOCS2: Suppressor of cytokine signaling 2; Cyth3: Cytohesin 3; Lfar1: Liver fibrosis associated lncRNA1; GAS5: Growth arrest-special transcript 5; TLR: Toll-like receptor; MEG3: Materally expressed gene 3; NLRC5: NLR Family CARD Domain Containing 5; NORAD: Non-coding RNA activated by DNA damage; S1PR3: Sphingosine 1-phosphate receptor 3; XIST: X-inactive-specific transcript; ADAMTS5: ADAM metallopeptidase with thrombospondin type 1 motif 5; Mical2: Molecule interacting with CasL2; Shc: Src homologous-collagen homologue; PINK1: PTEN-induced putative kinase 1; MTO1: Mitochondrial tRNA translation optimization 1; FBXW4: F-box and WD repeat domain containing 4; CREBBP: CREB binding protein; LEFTY2: Left-right determinant cluster 2; Ube2k:Ubiquitin conjugating enzyme E2 K; STAT3: Signal transducer and activator of transcription 3; Airn: Antisense Igf2r RNA; ROR: Regulator of reprogramming; EZH2: Enhancer of zeste homolog 2; KLF2: Krüppel-like transcription factor 2; eNOS: Endothelial nitric oxide synthase; sGC: Soluble guanylate cyclase.

-induced fibrosis[63]. These findings indicate that elevated miR-29 Level in serum may be a promising biomarker for diagnosis of liver fibrosis[63]. Another set of biomarkers (NIS4) consisting of miR-34a-5p, α-2 macroglobulin, YKL-40 and glycated hemoglobin have been developed to successfully identify patients who have a higher risk of disease progression with non-alcoholic fatty liver disease and liver fibrosis. The diagnostic value of the NIS4 algorithm was not affected by age, gender, BMI and transaminase[64]. Similarly, Azar *et al*[65] constructed a miRNA regulatory network using bioinformatics tools and identified five upregulated miRNAs (miR-21-5p, miR-222-3p, miR-221-3p, miR-181b-5p, and miR-17-5p) that targeted tissue inhibitor of metalloproteinase 3 in activated HSCs, and these results have been verified in a mouse model of liver fibrosis. Zhang *et al*[66] performed a logistic regression analysis to show that miR-1225-3p, miR-1238, miR-3162-3p, miR-4721, and miR-H7 could distinguish, with high sensitivity and specificity, nonsignificant fibrosis from significant fibrosis in chronic hepatitis B (CHB) patients. Some researchers screened miRNAs in serum from HCV-related liver fibrosis patients and found that miR-484 was significantly downregulated in advanced liver fibrosis compared to early liver fibrosis and liver cancer[67], which indicates that miR-484 may be used as a biomarker for staging liver fibrosis in patients with HCV. Besheer *et al*[68] performed diffusion-weighted magnetic resonance imaging of livers in patients with liver fibrosis caused by chronic hepatitis C and compared the apparent diffusion coefficient (ADC) with miRNA expression pattern in liver biopsies. They found that ADC was closely associated with expression of miR-200b, miR-21, and miR-29, and the accuracy of ADC combined with miR-200b to distinguish early and late liver fibrosis was 80.2%[68]. In a discovery cohort of 183 patients with non-alcoholic fatty liver disease, scientists identified that plasma miR-193a-5p was consistently maintained at a high level and was closely associated with grade of fibrosis, which was verified in a cohort of 372 additional cases[69]. Results from another study confirmed that miR-103a-3p and miR-425-5p were stably expressed in exosomes of serum derived from mice and humans infected with schistosomiasis[70]. MiR-146a-5p could distinguish mild (grades 0 and I) and severe fibrosis (grades II and III) and could be used for staging liver fibrosis[70].

LncRNAs are useful in the diagnosis of liver fibrosis. A study compared lncRNAs profiles of serum exosomes from patients with liver fibrosis and healthy controls and found that the expression level of lncRNA MALAT1 was significantly increased in the serum of fibrotic patients[31]. Serum lncRNA GAS5 was significantly upregulated in patients with advanced liver fibrosis compared with nonfibrotic patients[71]. Serum lncRNA-p21 had 70% specificity and 100% sensitivity in diagnosing liver fibrosis in patients with CHB[72]. LncRNA SCARNA10 was higher in liver and serum samples in patients with advanced liver fibrosis compared with healthy controls[23].

In addition to miRNAs and lncRNAs, circRNAs have shown differential expression in patients with liver fibrosis. The expression level of circRNA death inducer-obliterator 1 (circDIDO1) was decreased in serous exosomes derived from patients with liver fibrosis[73], while serum circMTO1 was negatively correlated with the degree of liver fibrosis in patients with CHB[24]. All these findings suggest that ncRNAs have potential as novel noninvasive biomarkers for the diagnosis and staging of liver fibrosis with high sensitivity and specificity.

POTENTIAL APPLICATION OF NCRNAS FOR THE TREATMENT OF LIVER FIBROSIS

Early liver fibrosis is deemed to be reversible. When the injury is removed, activated HSCs (myofibroblasts) are reduced through deactivation or apoptosis to slow down the fibrotic process and even lead to

regression. Studies have shown that patients with chronic hepatitis B or chronic hepatitis C have reduced liver fibrosis after receiving antiviral therapy[74]. In addition, therapies such as antioxidants, renin–angiotensin system inhibitors, and traditional Chinese medicine[75] are also considered promising for treatment of liver fibrosis, although more clinical trials are needed to confirm their safety and efficacy. As extensive cytokines and signaling pathways are involved in the pathogenesis and progression of liver fibrosis, ncRNA-based therapies that target various signaling pathways are being developed based on the outstanding gene silencing effect of miRNAs and the sponging effect of lncRNAs and circRNAs.

With strong inhibitory effects on a variety of fibrotic diseases such as myocardial fibrosis[76], pulmonary fibrosis[77], and renal fibrosis[78], miR-29 families are regarded as a potential therapeutic target for fibrosis. Yang *et al*[79] reported that miR-29a reduced liver fibrosis and ECM by directly targeting PI3KP85α in cholestatic liver fibrosis, and this supports the potential of miR-29a for the treatment of liver fibrosis. However, recent studies showed that, even though upregulation of miR-29 inhibited fibrosis, it could also lead to type 2 diabetes and insulin resistance[80]. Researchers have assessed the therapeutic effect of a synthetic miR-223 analog in a murine NASH model and have found that miR-223 treatment inhibited HSC activation through the downregulation of transcription of proinflammatory cytokines and chemokines together with NOD-like receptor 3 (NLRP3) inflammasome [81]. In addition, miR-223 was reported to inhibit the activation and proliferation of HSCs by targeting Gliotactin family zinc finger 2 (GLI2) and PDGFRα/β in CCl_4-induced liver fibrotic mice[82]. These studies clearly demonstrate the potential of miR-223 as a therapeutic strategy for liver fibrosis, although the underlying mechanisms vary.

Exosomes are small vesicles that are stable in body fluids, low in immunogenicity, can be engulfed by cells, and have been used as delivery vectors for easily degradable molecules such as RNA to treat diseases like liver cancer[83]. Exosomes have also been explored in treating liver fibrosis. Gao *et al*[84] found that miR-690 produced by Kupffer cells could be delivered to HSCs by exosomes to inhibit fibrosis by targeting nicotinamide adenine dinucleotide kinase. In a murine NASH model, miR-690 mimics decreased liver fibrosis markers and alleviated NASH phenotypes significantly. Exosomal miR-223 derived from natural killer cells has also been shown to target ATG7 in HSCs by inhibiting autophagy, leading to reduced fibrosis[85]. In addition, mesenchymal stem cell (MSC)-derived exosomes have been well studied as a promising treatment option for liver fibrosis[86]. Human bone MSCs (hB-MSCs)-derived exosomal miR-618[87] and human tonsil-derived MSCs (hT-MSCs)-derived exosomal miR-486[88] have been shown to alleviate liver fibrosis by targeting *Smad4* and smoothened (*Smo*) genes, respectively. MiR-6766-3p derived from 3D-cultured human embryonic stem cells were enriched in exosomes and attenuated TGFβ1/SMADs by targeting TGFβRII to inhibit proliferation of HSCs[89]. In another study, adipose-derived stromal cells were transfected with miR-150, and the culture supernatants were collected to treat HSCs or infuse into mice with liver fibrosis. Expression of several fibrosis markers such as Collagen 1A1 and α-smooth muscle actin (α-SMA), as well as the levels of systemic inflammatory cytokines such as interleukin-6 and tumor necrosis factor-α were significantly decreased in miR-150-treated mice compared with the control group[90]. This indicates that the exosomal miR-150 has antifibrotic activity through targeting of the TGF-β pathway. Zhou *et al*[91] co-cultured HSCs with human umbilical cord MSCs and found that expression of miR-148a-5p in HSCs was significantly upregulated, which decreased liver fibrosis by inhibiting Notch2 *in vivo* and *in vitro*.

Bone marrow MSCs have also been shown to reduce liver fibrosis by altering expression of lncRNAs. One such example comes from lncRNA BIHAA1 derived from bone marrow MSC-treated HSCs. Bone marrow MSCs inhibited liver fibrosis by lncRNA BIHAA1 targeting miR-667-5p[92]. Sun *et al*[93] found that silencing lncRNA SNHG promoted differentiation of bone marrow MSCs into hepatocyte-like cells and reduced cirrhosis through the miR-15a/Smad ubiquitin regulatory factor 1 (SMURF1)/UV radiation resistance associated gene (UVRAG)/ATG5/Wnt5a axis.

CircRNAs have also been investigated to treat liver fibrosis. Ma *et al*[73] reported that circDIDO1 in exosomes derived from MSCs regulated the PTEN/AKT pathway by sponging miR-141-3p, thereby inhibiting activation of HSCs and reducing expression of α-SMA and Collagen I to alleviate liver fibrosis. Similarly, MSC-derived exosomal circRNA cyclin dependent kinase 13 (circCDK13) inhibited activation of PI3K/AKT and NF-κB signaling pathways to reduce liver fibrosis by regulating miR-17-5p and its target gene K (lysine) acetyltransferase 2B (KAT2B)[94].

Delivery systems are one of the key issues to be resolved in order to protect ncRNAs from being degraded. Lipid nanoparticles (NPs) for ncRNAs delivery have been developed. Hu *et al*[95] encapsulated miR-30a-5p and an antifibrotic peptide Relaxin into NPs and injected them into fibrotic mice. NPs increased the exosomal miR-30a-5p level, which in turn reversed the activated HSCs into a quiescent state by targeting liver macrophages[95]. Furthermore, NPs encapsulated with miR-29b and Germacrone, a major component of the traditional Chinese medicine *Rhizoma curcuma*, have been shown to have robust antifibrotic activity *in vitro* and *in vivo*[96]. The ncRNAs showed the potential for the treatment of liver fibrosis are collected in Table 2.

Table 2 Noncoding RNAs for the potential treatment of liver fibrosis

ncRNAs	Target genes	Signaling pathways	Ref.
miR-29a	*PI3KP85α*	PI3K/AKT	[79]
	Fstl	TGF-β/Smad2, JNK	[21]
miR-223	*NLRP3* inflammasome	NOD signaling pathway	[81]
	GLI2, PDGFRα/β	Hedgehog, PDGF	[82]
hB-MSCs-derived exo-miR-618	*Smad4*	TGF-β/Smad2	[87]
3DhESCs-derived exo-miR-6766-3p	*TGFβRII*	TGF-β/Smad	[89]
hT-MSCs-derived exo-miR-486	*Smo*	Hedgehog/GlI2	[88]
NK cells-derived exo-miR-223	*ATG7*	Autophagy pathway	[85]
KCs-derived exo-miR-690	*NADK*	-	[84]
lncRNA SNHG	*miR-15a, MURF1*	UVRAG/ATG5/Wnt5a	[93]
lncRNA BIHAA1	*miR-667-5p*	-	[92]
MSCs-derived exo-circDIDO1	*miR-141-3p*	PTEN/AKT	[73]
MSCs-derived exo-circCDK13	*miR-17-5p, KAT2B*	PI3K/AKT, NF-κB	[94]

ncRNAs: Noncoding RNAs; PI3K: Phosphatidylinositol 3-kinase; AKT: Serine/threonine kinase 1; Fstl: Follistatin-like 1; TGF-β: Transforming growth factor-β; JNK: c-Jun N-terminal kinase; NLRP3: NOD-like receptor family, pyrin domain containing 3; Smo: Smoothened; GLI2: Gliotactin family zinc finger 2; PDGFR: Platelet-derived growth factor receptor; MSC: Mesenchymal stem cell; hB-MSC: Human bone MSC; hT-MSC: Human tonsil-derived MSC; 3DhESC: 3D-cultured human embryonic stem cells; TGF-βRII: TGF-β type II receptor; ATG: Autophagy-related gene; KCs: Kupffer cells; NADK: NAD kinase; SNHG: Small nucleolar RNA host gene; SMURF1: Smad ubiquitin regulatory factor 1; UVRAG: UV radiation resistance associated gene; DIDO1: Death inducer-obliterator 1; PTEN: Phosphatase and tensin homology deleted on chromosome ten; CDK13: Cyclin dependent kinase 13; KAT2B: K (lysine) acetyltransferase 2B.

CONCLUSION

It is well known that persistent liver fibrosis leads to irreversible fibrosis, decompensated cirrhosis, and even HCC, which emphasizes the importance of treatment during early-stage fibrosis to prevent disease progression. Therefore, it is important to diagnose liver fibrosis before clinical symptoms appear. Although liver biopsy is considered the gold standard for the diagnosis of liver fibrosis, its invasive nature limits its clinical use, especially in early disease stages. Although some ncRNAs are closely associated with the pathogenesis and progression of liver fibrosis, there is still insufficient evidence for diagnosing and staging liver fibrosis using ncRNAs alone. Some studies have suggested combining ncRNAs with other indicators (biomarkers) in blood or with imaging techniques to increase the accuracy of liver fibrosis diagnosis. There is no specific anti-hepatic fibrosis drug in clinical use, although several candidates have already been enrolled in clinical trials. The main strategy for antifibrosis therapy is to treat the etiology and alleviate liver inflammation. NcRNAs are able to target various inflammation-related signaling pathways to reduce liver fibrosis. The latest studies have found that miR-20b-5p[97] and lncRNA Antisense Igf2r RNA (lncRNA Airn)[98] can inhibit HSCs activation to alleviate liver fibrosis process. Salvianolic acid B treatment relieved the activation of HSCs through decreasing the expression of lncRNA regulator of reprogramming (lncRNA-ROR)[99], which providing new targets for the treatment of liver fibrosis. Although most of these findings are based on *in vitro* studies, and therefore, need validation *in vivo*. With the rapid progress of techniques such as gene editing, NP-based delivery systems, and synthetic biology, MSC-derived exosomal ncRNAs may become promising treatment options for liver fibrosis in the near future.

FOOTNOTES

Author contributions: Gong T and Xie H collected the references; Li QY drafted the initial manuscript; Huang YK and Kang L drew the figure and tables; Chen LM and Duan XQ reviewed and revised the initial draft; Warner CA polished the language; all authors contributed to the manuscript and approved the submitted version; Chen LM and Duan XQ contributed equally to this manuscript.

Supported by Science and Technology Innovation Talent Project of Sichuan Province, No. 2022JDRC0047; the Central Government-directed Special Funds for Local Science and Technology Development Project, No. 2021ZYD0085; Natural Science Foundation of China, No. 82102383; and Qin Chuangyuan Recruited High-level Innovation and

Entrepreneurship Talents Project of Science and Technology Department of Shaanxi Province, No. QCYRCXM-2022-56.

Conflict-of-interest statement: There is no conflict of interest associated with any of authors contributed their efforts in this manuscript.

Country/Territory of origin: China

ORCID number: Qing-Yuan Li 0000-0001-9523-1597; Tao Gong 0000-0002-2259-3295; Yi-Ke Huang 0000-0002-6850-493X; Lan Kang 0000-0002-3152-3731; Charlotte A Warner 0000-0001-5086-9482; He Xie 0000-0002-4123-7683; Li-Min Chen 0000-0001-5228-3522; Xiao-Qiong Duan 0000-0001-8907-0029.

S-Editor: Gong ZM
L-Editor: A
P-Editor: Gong ZM

REFERENCES

1 **Parola M**, Pinzani M. Liver fibrosis: Pathophysiology, pathogenetic targets and clinical issues. *Mol Aspects Med* 2019; **65**: 37-55 [PMID: 30213667 DOI: 10.1016/j.mam.2018.09.002]
2 **Younossi ZM**. Non-alcoholic fatty liver disease - A global public health perspective. *J Hepatol* 2019; **70**: 531-544 [PMID: 30414863 DOI: 10.1016/j.jhep.2018.10.033]
3 **Cai X**, Wang J, Zhou Q, Yang B, He Q, Weng Q. Intercellular crosstalk of hepatic stellate cells in liver fibrosis: New insights into therapy. *Pharmacol Res* 2020; **155**: 104720 [PMID: 32092405 DOI: 10.1016/j.phrs.2020.104720]
4 **Wang J**, Zhu S, Meng N, He Y, Lu R, Yan GR. ncRNA-Encoded Peptides or Proteins and Cancer. *Mol Ther* 2019; **27**: 1718-1725 [PMID: 31526596 DOI: 10.1016/j.ymthe.2019.09.001]
5 **Ha M**, Kim VN. Regulation of microRNA biogenesis. *Nat Rev Mol Cell Biol* 2014; **15**: 509-524 [PMID: 25027649 DOI: 10.1038/nrm3838]
6 **Gebert LFR**, MacRae IJ. Regulation of microRNA function in animals. *Nat Rev Mol Cell Biol* 2019; **20**: 21-37 [PMID: 30108335 DOI: 10.1038/s41580-018-0045-7]
7 **Statello L**, Guo CJ, Chen LL, Huarte M. Gene regulation by long non-coding RNAs and its biological functions. *Nat Rev Mol Cell Biol* 2021; **22**: 96-118 [PMID: 33353982 DOI: 10.1038/s41580-020-00315-9]
8 **Xie H**, Sun H, Mu R, Li S, Li Y, Yang C, Xu M, Duan X, Chen L. The role of circular RNAs in viral infection and related diseases. *Virus Res* 2021; **291**: 198205 [PMID: 33132144 DOI: 10.1016/j.virusres.2020.198205]
9 **Liu CX**, Chen LL. Circular RNAs: Characterization, cellular roles, and applications. *Cell* 2022; **185**: 2016-2034 [PMID: 35584701 DOI: 10.1016/j.cell.2022.04.021]
10 **Tadokoro T**, Morishita A, Masaki T. Diagnosis and Therapeutic Management of Liver Fibrosis by MicroRNA. *Int J Mol Sci* 2021; **22** [PMID: 34360904 DOI: 10.3390/ijms22158139]
11 **He Z**, Yang D, Fan X, Zhang M, Li Y, Gu X, Yang M. The Roles and Mechanisms of lncRNAs in Liver Fibrosis. *Int J Mol Sci* 2020; **21** [PMID: 32098245 DOI: 10.3390/ijms21041482]
12 **Tsuchida T**, Friedman SL. Mechanisms of hepatic stellate cell activation. *Nat Rev Gastroenterol Hepatol* 2017; **14**: 397-411 [PMID: 28487545 DOI: 10.1038/nrgastro.2017.38]
13 **Xu F**, Liu C, Zhou D, Zhang L. TGF-β/SMAD Pathway and Its Regulation in Hepatic Fibrosis. *J Histochem Cytochem* 2016; **64**: 157-167 [PMID: 26747705 DOI: 10.1369/0022155415627681]
14 **Hu HH**, Chen DQ, Wang YN, Feng YL, Cao G, Vaziri ND, Zhao YY. New insights into TGF-β/Smad signaling in tissue fibrosis. *Chem Biol Interact* 2018; **292**: 76-83 [PMID: 30017632 DOI: 10.1016/j.cbi.2018.07.008]
15 **Noetel A**, Kwiecinski M, Elfimova N, Huang J, Odenthal M. microRNA are Central Players in Anti- and Profibrotic Gene Regulation during Liver Fibrosis. *Front Physiol* 2012; **3**: 49 [PMID: 22457651 DOI: 10.3389/fphys.2012.00049]
16 **Wang X**, He Y, Mackowiak B, Gao B. MicroRNAs as regulators, biomarkers and therapeutic targets in liver diseases. *Gut* 2021; **70**: 784-795 [PMID: 33127832 DOI: 10.1136/gutjnl-2020-322526]
17 **Zhou QY**, Yang HM, Liu JX, Xu N, Li J, Shen LP, Zhang YZ, Koda S, Zhang BB, Yu Q, Chen JX, Zheng KY, Yan C. MicroRNA-497 induced by Clonorchis sinensis enhances the TGF-β/Smad signaling pathway to promote hepatic fibrosis by targeting Smad7. *Parasit Vectors* 2021; **14**: 472 [PMID: 34521449 DOI: 10.1186/s13071-021-04972-3]
18 **Pan Q**, Guo CJ, Xu QY, Wang JZ, Li H, Fang CH. miR-16 integrates signal pathways in myofibroblasts: determinant of cell fate necessary for fibrosis resolution. *Cell Death Dis* 2020; **11**: 639 [PMID: 32801294 DOI: 10.1038/s41419-020-02832-z]
19 **Ma Y**, Yuan X, Han M, Xu Y, Han K, Liang P, Liu S, Chen J, Xing H. miR-98-5p as a novel biomarker suppress liver fibrosis by targeting TGFβ receptor 1. *Hepatol Int* 2022; **16**: 614-626 [PMID: 35188624 DOI: 10.1007/s12072-021-10277-5]

20 **Yang X**, Ma L, Wei R, Ye T, Zhou J, Wen M, Men R, Aqeilan RI, Peng Y, Yang L. Twist1-induced miR-199a-3p promotes liver fibrosis by suppressing caveolin-2 and activating TGF-β pathway. *Signal Transduct Target Ther* 2020; **5**: 75 [PMID: 32499481 DOI: 10.1038/s41392-020-0169-z]

21 **Xu XY**, Du Y, Liu X, Ren Y, Dong Y, Xu HY, Shi JS, Jiang D, Xu X, Li L, Xu ZH, Geng Y. Targeting Follistatin like 1 ameliorates liver fibrosis induced by carbon tetrachloride through TGF-β1-miR29a in mice. *Cell Commun Signal* 2020; **18**: 151 [PMID: 32933544 DOI: 10.1186/s12964-020-00610-0]

22 **Liu L**, Wang P, Wang YS, Zhang YN, Li C, Yang ZY, Liu ZH, Zhan TZ, Xu J, Xia CM. MiR-130a-3p Alleviates Liver Fibrosis by Suppressing HSCs Activation and Skewing Macrophage to Ly6C^{lo} Phenotype. *Front Immunol* 2021; **12**: 696069 [PMID: 34421906 DOI: 10.3389/fimmu.2021.696069]

23 **Zhang K**, Han Y, Hu Z, Zhang Z, Shao S, Yao Q, Zheng L, Wang J, Han X, Zhang Y, Chen T, Yao Z, Han T, Hong W. SCARNA10, a nuclear-retained long non-coding RNA, promotes liver fibrosis and serves as a potential biomarker. *Theranostics* 2019; **9**: 3622-3638 [PMID: 31281502 DOI: 10.7150/thno.32935]

24 **Wang W**, Dong R, Guo Y, He J, Shao C, Yi P, Yu F, Gu D, Zheng J. CircMTO1 inhibits liver fibrosis *via* regulation of miR-17-5p and Smad7. *J Cell Mol Med* 2019; **23**: 5486-5496 [PMID: 31148365 DOI: 10.1111/jcmm.14432]

25 **Cui W**, Zhou S, Wang Y, Shi X, Liu H. Cadmium exposure activates the PI3K/AKT signaling pathway through miRNA-21, induces an increase in M1 polarization of macrophages, and leads to fibrosis of pig liver tissue. *Ecotoxicol Environ Saf* 2021; **228**: 113015 [PMID: 34823215 DOI: 10.1016/j.ecoenv.2021.113015]

26 **Luo X**, Luo SZ, Xu ZX, Zhou C, Li ZH, Zhou XY, Xu MY. Lipotoxic hepatocyte-derived exosomal miR-1297 promotes hepatic stellate cell activation through the PTEN signaling pathway in metabolic-associated fatty liver disease. *World J Gastroenterol* 2021; **27**: 1419-1434 [PMID: 33911465 DOI: 10.3748/wjg.v27.i14.1419]

27 **Dong Z**, Li S, Si L, Ma R, Bao L, Bo A. Identification lncRNA LOC102551149/miR-23a-5p pathway in hepatic fibrosis. *Eur J Clin Invest* 2020; **50**: e13243 [PMID: 32306379 DOI: 10.1111/eci.13243]

28 **Hu HH**, Cao G, Wu XQ, Vaziri ND, Zhao YY. Wnt signaling pathway in aging-related tissue fibrosis and therapies. *Ageing Res Rev* 2020; **60**: 101063 [PMID: 32272170 DOI: 10.1016/j.arr.2020.101063]

29 **Yang J**, Tao Q, Zhou Y, Chen Q, Li L, Hu S, Liu Y, Zhang Y, Shu J, Zhang X, Zhang L. MicroRNA-708 represses hepatic stellate cells activation and proliferation by targeting ZEB1 through Wnt/β-catenin pathway. *Eur J Pharmacol* 2020; **871**: 172927 [PMID: 31962101 DOI: 10.1016/j.ejphar.2020.172927]

30 **Wang Q**, Wei S, Li L, Bu Q, Zhou H, Su W, Liu Z, Wang M, Lu L. miR-139-5p sponged by LncRNA NEAT1 regulates liver fibrosis *via* targeting β-catenin/SOX9/TGF-β1 pathway. *Cell Death Discov* 2021; **7**: 243 [PMID: 34531378 DOI: 10.1038/s41420-021-00632-8]

31 **Wang T**, Zhang C, Meng X, Zhu B, Wang S, Yuan W, Zhang S, Xu J. Long Noncoding RNA Metastasis-Associated Lung Adenocarcinoma Transcript 1 in Extracellular Vesicles Promotes Hepatic Stellate Cell Activation, Liver Fibrosis and β-Catenin Signaling Pathway. *Front Physiol* 2022; **13**: 792182 [PMID: 35237178 DOI: 10.3389/fphys.2022.792182]

32 **Zhang Z**, Wen H, Peng B, Weng J, Zeng F. Downregulated microRNA-129-5p by Long Non-coding RNA NEAT1 Upregulates PEG3 Expression to Aggravate Non-alcoholic Steatohepatitis. *Front Genet* 2020; **11**: 563265 [PMID: 33574830 DOI: 10.3389/fgene.2020.563265]

33 **Ye J**, Lin Y, Yu Y, Sun D. LncRNA NEAT1/microRNA-129-5p/SOCS2 axis regulates liver fibrosis in alcoholic steatohepatitis. *J Transl Med* 2020; **18**: 445 [PMID: 33228663 DOI: 10.1186/s12967-020-02577-5]

34 **Huang W**, Huang F, Zhang R, Luo H. LncRNA Neat1 expedites the progression of liver fibrosis in mice through targeting miR-148a-3p and miR-22-3p to upregulate *Cyth3*. *Cell Cycle* 2021; **20**: 490-507 [PMID: 33550894 DOI: 10.1080/15384101.2021.1875665]

35 **Zhang K**, Shi Z, Zhang M, Dong X, Zheng L, Li G, Han X, Yao Z, Han T, Hong W. Silencing lncRNA Lfar1 alleviates the classical activation and pyoptosis of macrophage in hepatic fibrosis. *Cell Death Dis* 2020; **11**: 132 [PMID: 32071306 DOI: 10.1038/s41419-020-2323-5]

36 **Su SB**, Tao L, Liang XL, Chen W. Long noncoding RNA GAS5 inhibits LX-2 cells activation by suppressing NF-κB signalling through regulation of the miR-433-3p/TLR10 axis. *Dig Liver Dis* 2022; **54**: 1066-1075 [PMID: 34903500 DOI: 10.1016/j.dld.2021.11.002]

37 **Wu YY**, Wu S, Li XF, Luo S, Wang A, Yin SQ, Huang C, Li J. LncRNA MEG3 reverses CCl_4-induced liver fibrosis by targeting NLRC5. *Eur J Pharmacol* 2021; **911**: 174462 [PMID: 34536366 DOI: 10.1016/j.ejphar.2021.174462]

38 **Li Y**, Liu R, Wu J, Li X. Self-eating: friend or foe? *Theranostics* 2020; **10**: 7993-8017 [PMID: 32724454 DOI: 10.7150/thno.47826]

39 **Yu F**, Dong B, Dong P, He Y, Zheng J, Xu P. Hypoxia induces the activation of hepatic stellate cells through the PVT1-miR-152-ATG14 signaling pathway. *Mol Cell Biochem* 2020; **465**: 115-123 [PMID: 31893334 DOI: 10.1007/s11010-019-03672-y]

40 **Xie Z**, Wu Y, Liu S, Lai Y, Tang S. LncRNA-SNHG7/miR-29b/DNMT3A axis affects activation, autophagy and proliferation of hepatic stellate cells in liver fibrosis. *Clin Res Hepatol Gastroenterol* 2021; **45**: 101469 [PMID: 32893175 DOI: 10.1016/j.clinre.2020.05.017]

41 **Xu ZX**, Li JZ, Li Q, Xu MY, Li HY. CircRNA608-microRNA222-PINK1 axis regulates the mitophagy of hepatic stellate cells in NASH related fibrosis. *Biochem Biophys Res Commun* 2022; **610**: 35-42 [PMID: 35436629 DOI: 10.1016/j.bbrc.2022.04.008]

42 **Chen X**, Zhang D, Wang Y, Chen K, Zhao L, Xu Y, Jiang H, Wang S. Synergistic antifibrotic effects of miR-451 with miR-185 partly by co-targeting EphB2 on hepatic stellate cells. *Cell Death Dis* 2020; **11**: 402 [PMID: 32467578 DOI: 10.1038/s41419-020-2613-y]

43 **Zhao Y**, Wang Z, Zhou J, Feng D, Li Y, Hu Y, Zhang F, Chen Z, Wang G, Ma X, Tian X, Yao J. LncRNA Mical2/miR-203a-3p sponge participates in epithelial-mesenchymal transition by targeting p66Shc in liver fibrosis. *Toxicol Appl Pharmacol* 2020; **403**: 115125 [PMID: 32659284 DOI: 10.1016/j.taap.2020.115125]

44 **Wu XJ**, Xie Y, Gu XX, Zhu HY, Huang LX. LncRNA XIST promotes mitochondrial dysfunction of hepatocytes to aggravate hepatic fibrogenesis *via* miR-539-3p/ADAMTS5 axis. *Mol Cell Biochem* 2023; **478**: 291-303 [PMID: 35794289 DOI: 10.1007/s11010-022-04506-0]

45 **Xiao Y**, Liu R, Li X, Gurley EC, Hylemon PB, Lu Y, Zhou H, Cai W. Long Noncoding RNA H19 Contributes to Cholangiocyte Proliferation and Cholestatic Liver Fibrosis in Biliary Atresia. *Hepatology* 2019; **70**: 1658-1673 [PMID: 31063660 DOI: 10.1002/hep.30698]

46 **Tian X**, Wang Y, Lu Y, Wang W, Du J, Chen S, Zhou H, Cai W, Xiao Y. Conditional depletion of macrophages ameliorates cholestatic liver injury and fibrosis *via* lncRNA-H19. *Cell Death Dis* 2021; **12**: 646 [PMID: 34168124 DOI: 10.1038/s41419-021-03931-1]

47 **Navarro-Corcuera A**, Sehrawat TS, Jalan-Sakrikar N, Gibbons HR, Pirius NE, Khanal S, Hamdan FH, Aseem SO, Cao S, Banales JM, Kang N, Faubion WA, LaRusso NF, Shah VH, Huebert RC. Long non-coding RNA ACTA2-AS1 promotes ductular reaction by interacting with the p300/ELK1 complex. *J Hepatol* 2022; **76**: 921-933 [PMID: 34953958 DOI: 10.1016/j.jhep.2021.12.014]

48 **Chen X**, Li HD, Bu FT, Li XF, Chen Y, Zhu S, Wang JN, Chen SY, Sun YY, Pan XY, Yin NN, Xu JJ, Huang C, Li J. Circular RNA circFBXW4 suppresses hepatic fibrosis *via* targeting the miR-18b-3p/FBXW7 axis. *Theranostics* 2020; **10**: 4851-4870 [PMID: 32308754 DOI: 10.7150/thno.42423]

49 **Yang YR**, Hu S, Bu FT, Li H, Huang C, Meng XM, Zhang L, Lv XW, Li J. Circular RNA CREBBP Suppresses Hepatic Fibrosis *Via* Targeting the hsa-miR-1291/LEFTY2 Axis. *Front Pharmacol* 2021; **12**: 741151 [PMID: 34887753 DOI: 10.3389/fphar.2021.741151]

50 **Chen Y**, Yuan B, Wu Z, Dong Y, Zhang L, Zeng Z. Microarray profiling of circular RNAs and the potential regulatory role of hsa_circ_0071410 in the activated human hepatic stellate cell induced by irradiation. *Gene* 2017; **629**: 35-42 [PMID: 28774651 DOI: 10.1016/j.gene.2017.07.078]

51 **Zhang T**, Yang Z, Kusumanchi P, Han S, Liangpunsakul S. Critical Role of microRNA-21 in the Pathogenesis of Liver Diseases. *Front Med (Lausanne)* 2020; **7**: 7 [PMID: 32083086 DOI: 10.3389/fmed.2020.00007]

52 **Zhang Z**, Zha Y, Hu W, Huang Z, Gao Z, Zang Y, Chen J, Dong L, Zhang J. The autoregulatory feedback loop of microRNA-21/programmed cell death protein 4/activation protein-1 (MiR-21/PDCD4/AP-1) as a driving force for hepatic fibrosis development. *J Biol Chem* 2013; **288**: 37082-37093 [PMID: 24196965 DOI: 10.1074/jbc.M113.517953]

53 **Ning ZW**, Luo XY, Wang GZ, Li Y, Pan MX, Yang RQ, Ling XG, Huang S, Ma XX, Jin SY, Wang D, Li X. MicroRNA-21 Mediates Angiotensin II-Induced Liver Fibrosis by Activating NLRP3 Inflammasome/IL-1β Axis *via* Targeting Smad7 and Spry1. *Antioxid Redox Signal* 2017; **27**: 1-20 [PMID: 27502441 DOI: 10.1089/ars.2016.6669]

54 **Sun J**, Shi L, Xiao T, Xue J, Li J, Wang P, Wu L, Dai X, Ni X, Liu Q. microRNA-21, *via* the HIF-1α/VEGF signaling pathway, is involved in arsenite-induced hepatic fibrosis through aberrant cross-talk of hepatocytes and hepatic stellate cells. *Chemosphere* 2021; **266**: 129177 [PMID: 33310519 DOI: 10.1016/j.chemosphere.2020.129177]

55 **Hamada-Tsutsumi S**, Onishi M, Matsuura K, Isogawa M, Kawashima K, Sato Y, Tanaka Y. Inhibitory Effect of a Human MicroRNA, miR-6133-5p, on the Fibrotic Activity of Hepatic Stellate Cells in Culture. *Int J Mol Sci* 2020; **21** [PMID: 33019495 DOI: 10.3390/ijms21197251]

56 **Zhu Y**, Pan X, Du N, Li K, Hu Y, Wang L, Zhang J, Liu Y, Zuo L, Meng X, Hu C, Wu X, Jin J, Wu W, Chen X, Wu F, Huang Y. ASIC1a regulates miR-350/SPRY2 by N^6 -methyladenosine to promote liver fibrosis. *FASEB J* 2020; **34**: 14371-14388 [PMID: 32949431 DOI: 10.1096/fj.202001337R]

57 **Li B**, Liu J, Xin X, Zhang L, Zhou J, Xia C, Zhu W, Yu H. MiR-34c promotes hepatic stellate cell activation and Liver Fibrogenesis by suppressing ACSL1 expression. *Int J Med Sci* 2021; **18**: 615-625 [PMID: 33437196 DOI: 10.7150/ijms.51589]

58 **Kim SM**, Song GY, Shim A, Lee JH, Eom CB, Liu C, Yang YM, Seki E. Hyaluronan synthase 2, a target of miR-200c, promotes carbon tetrachloride-induced acute and chronic liver inflammation *via* regulation of CCL3 and CCL4. *Exp Mol Med* 2022; **54**: 739-752 [PMID: 35662287 DOI: 10.1038/s12276-022-00781-5]

59 **Zhu S**, Chen X, Wang JN, Xu JJ, Wang A, Li JJ, Wu S, Wu YY, Li XF, Huang C, Li J. Circular RNA circUbe2k promotes hepatic fibrosis *via* sponging miR-149-5p/TGF-β2 axis. *FASEB J* 2021; **35**: e21622 [PMID: 33982351 DOI: 10.1096/fj.202002738R]

60 **Zou L**, Shi C, Wang D, Cheng J, Wang Q, Wang L, Yang G. Long non-coding RNA-non-coding RNA activated by DNA damage inhibition suppresses hepatic stellate cell activation *via* microRNA-495-3p/sphingosine 1-phosphate receptor 3 axis. *Bioengineered* 2022; **13**: 6150-6162 [PMID: 35200103 DOI: 10.1080/21655979.2022.2037841]

61 **Sumida Y**, Nakajima A, Itoh Y. Limitations of liver biopsy and non-invasive diagnostic tests for the diagnosis of nonalcoholic fatty liver disease/nonalcoholic steatohepatitis. *World J Gastroenterol* 2014; **20**: 475-485 [PMID: 24574716 DOI: 10.3748/wjg.v20.i2.475]

62 **Loomba R**, Adams LA. Advances in non-invasive assessment of hepatic fibrosis. *Gut* 2020; **69**: 1343-1352 [PMID: 32066623 DOI: 10.1136/gutjnl-2018-317593]

63 **Yu X**, Elfimova N, Müller M, Bachurski D, Koitzsch U, Drebber U, Mahabir E, Hansen HP, Friedman SL, Klein S, Dienes HP, Hösel M, Buettner R, Trebicka J, Kondylis V, Mannaerts I, Odenthal M. Autophagy-Related Activation of Hepatic Stellate Cells Reduces Cellular miR-29a by Promoting Its Vesicular Secretion. *Cell Mol Gastroenterol Hepatol* 2022; **13**: 1701-1716 [PMID: 35219894 DOI: 10.1016/j.jcmgh.2022.02.013]

64 **Harrison SA**, Ratziu V, Boursier J, Francque S, Bedossa P, Majd Z, Cordonnier G, Sudrik FB, Darteil R, Liebe R, Magnanensi J, Hajji Y, Brozek J, Roudot A, Staels B, Hum DW, Megnien SJ, Hosmane S, Dam N, Chaumat P, Hanf R, Anstee QM, Sanyal AJ. A blood-based biomarker panel (NIS4) for non-invasive diagnosis of non-alcoholic steatohepatitis and liver fibrosis: a prospective derivation and global validation study. *Lancet Gastroenterol Hepatol* 2020; **5**: 970-985 [PMID: 32763196 DOI: 10.1016/S2468-1253(20)30252-1]

65 **Azar F**, Courtet K, Dekky B, Bonnier D, Dameron O, Colige A, Legagneux V, Théret N. Integration of miRNA-regulatory networks in hepatic stellate cells identifies TIMP3 as a key factor in chronic liver disease. *Liver Int* 2020; **40**: 2021-2033 [PMID: 32306499 DOI: 10.1111/liv.14476]

66 **Zhang Q**, Zhang Q, Li B, Qu Y, Li Z, Lu L, Li R, Cai X. The Diagnosis Value of a Novel Model with 5 Circulating miRNAs for Liver Fibrosis in Patients with Chronic Hepatitis B. *Mediators Inflamm* 2021; **2021**: 6636947 [PMID: 33727891 DOI: 10.1155/2021/6636947]

67 **El-Maraghy SA**, Adel O, Zayed N, Yosry A, El-Nahaas SM, Gibriel AA. Circulatory miRNA-484, 524, 615 and 628

expression profiling in HCV mediated HCC among Egyptian patients; implications for diagnosis and staging of hepatic cirrhosis and fibrosis. *J Adv Res* 2020; **22**: 57-66 [PMID: 31956442 DOI: 10.1016/j.jare.2019.12.002]

68 **Besheer T**, Elalfy H, Abd El-Maksoud M, Abd El-Razek A, Taman S, Zalata K, Elkashef W, Zaghloul H, Elshahawy H, Raafat D, Elemshaty W, Elsayed E, El-Gilany AH, El-Bendary M. Diffusion-weighted magnetic resonance imaging and micro-RNA in the diagnosis of hepatic fibrosis in chronic hepatitis C virus. *World J Gastroenterol* 2019; **25**: 1366-1377 [PMID: 30918429 DOI: 10.3748/wjg.v25.i11.1366]

69 **Johnson K**, Leary PJ, Govaere O, Barter MJ, Charlton SH, Cockell SJ, Tiniakos D, Zatorska M, Bedossa P, Brosnan MJ, Cobbold JF, Ekstedt M, Aithal GP, Clément K, Schattenberg JM, Boursier J, Ratziu V, Bugianesi E, Anstee QM, Daly AK; LITMUS Consortium Investigators§; LITMUS Consortium Investigators. Increased serum miR-193a-5p during non-alcoholic fatty liver disease progression: Diagnostic and mechanistic relevance. *JHEP Rep* 2022; **4**: 100409 [PMID: 35072021 DOI: 10.1016/j.jhepr.2021.100409]

70 **Cai P**, Mu Y, Olveda RM, Ross AG, Olveda DU, McManus DP. Serum Exosomal miRNAs for Grading Hepatic Fibrosis Due to Schistosomiasis. *Int J Mol Sci* 2020; **21** [PMID: 32443549 DOI: 10.3390/ijms21103560]

71 **Han MH**, Lee JH, Kim G, Lee E, Lee YR, Jang SY, Lee HW, Chun JM, Han YS, Yoon JS, Kang MK, Lee WK, Kweon YO, Tak WY, Park SY, Park JG, Hur K. Expression of the Long Noncoding RNA GAS5 Correlates with Liver Fibrosis in Patients with Nonalcoholic Fatty Liver Disease. *Genes (Basel)* 2020; **11** [PMID: 32413995 DOI: 10.3390/genes11050545]

72 **Yu F**, Zhou G, Huang K, Fan X, Li G, Chen B, Dong P, Zheng J. Serum lincRNA-p21 as a potential biomarker of liver fibrosis in chronic hepatitis B patients. *J Viral Hepat* 2017; **24**: 580-588 [PMID: 28107589 DOI: 10.1111/jvh.12680]

73 **Ma L**, Wei J, Zeng Y, Liu J, Xiao E, Kang Y. Mesenchymal stem cell-originated exosomal circDIDO1 suppresses hepatic stellate cell activation by miR-141-3p/PTEN/AKT pathway in human liver fibrosis. *Drug Deliv* 2022; **29**: 440-453 [PMID: 35099348 DOI: 10.1080/10717544.2022.2030428]

74 **Butt AA**, Yan P, Aslam S, Abou-Samra AB, Sherman KE, Shaikh OS. Liver Fibrosis Progression and Mortality in Hepatitis B- and C-Coinfected Persons Treated With Directly Acting Antiviral Agents: Results From ERCHIVES. *Clin Infect Dis* 2020; **71**: 664-666 [PMID: 31840746 DOI: 10.1093/cid/ciz1097]

75 **Ge C**, Tan J, Lou D, Zhu L, Zhong Z, Dai X, Sun Y, Kuang Q, Zhao J, Wang L, Liu J, Wang B, Xu M. Mulberrin confers protection against hepatic fibrosis by Trim31/Nrf2 signaling. *Redox Biol* 2022; **51**: 102274 [PMID: 35240537 DOI: 10.1016/j.redox.2022.102274]

76 **Liu MN**, Luo G, Gao WJ, Yang SJ, Zhou H. miR-29 family: A potential therapeutic target for cardiovascular disease. *Pharmacol Res* 2021; **166**: 105510 [PMID: 33610720 DOI: 10.1016/j.phrs.2021.105510]

77 **Yu Y**, Liu X, Zhao Z, Xu Z, Qiao Y, Zhou Y, Qiao H, Zhong J, Dai J, Suo G. The Extracellular Matrix Enriched With Exosomes for the Treatment on Pulmonary Fibrosis in Mice. *Front Pharmacol* 2021; **12**: 747223 [PMID: 34938180 DOI: 10.3389/fphar.2021.747223]

78 **Shi S**, Song L, Yu H, Feng S, He J, Liu Y, He Y. Knockdown of LncRNA-H19 Ameliorates Kidney Fibrosis in Diabetic Mice by Suppressing miR-29a-Mediated EndMT. *Front Pharmacol* 2020; **11**: 586895 [PMID: 33324218 DOI: 10.3389/fphar.2020.586895]

79 **Yang YL**, Wang FS, Lin HY, Huang YH. Exogenous Therapeutics of Microrna-29a Attenuates Development of Hepatic Fibrosis in Cholestatic Animal Model through Regulation of Phosphoinositide 3-Kinase p85 Alpha. *Int J Mol Sci* 2020; **21** [PMID: 32455716 DOI: 10.3390/ijms21103636]

80 **Dalgaard LT**, Sørensen AE, Hardikar AA, Joglekar MV. The microRNA-29 family: role in metabolism and metabolic disease. *Am J Physiol Cell Physiol* 2022; **323**: C367-C377 [PMID: 35704699 DOI: 10.1152/ajpcell.00051.2022]

81 **Jimenez Calvente C**, Del Pilar H, Tameda M, Johnson CD, Feldstein AE. MicroRNA 223 3p Negatively Regulates the NLRP3 Inflammasome in Acute and Chronic Liver Injury. *Mol Ther* 2020; **28**: 653-663 [PMID: 31585800 DOI: 10.1016/j.ymthe.2019.09.013]

82 **Wang X**, Seo W, Park SH, Fu Y, Hwang S, Rodrigues RM, Feng D, Gao B, He Y. MicroRNA-223 restricts liver fibrosis by inhibiting the TAZ-IHH-GLI2 and PDGF signaling pathways *via* the crosstalk of multiple liver cell types. *Int J Biol Sci* 2021; **17**: 1153-1167 [PMID: 33867837 DOI: 10.7150/ijbs.58365]

83 **Li S**, Chen L. Exosomes in Pathogenesis, Diagnosis, and Treatment of Hepatocellular Carcinoma. *Front Oncol* 2022; **12**: 793432 [PMID: 35155236 DOI: 10.3389/fonc.2022.793432]

84 **Gao H**, Jin Z, Bandyopadhyay G, Cunha E Rocha K, Liu X, Zhao H, Zhang D, Jouihan H, Pourshahian S, Kisseleva T, Brenner DA, Ying W, Olefsky JM. MiR-690 treatment causes decreased fibrosis and steatosis and restores specific Kupffer cell functions in NASH. *Cell Metab* 2022; **34**: 978-990.e4 [PMID: 35700738 DOI: 10.1016/j.cmet.2022.05.008]

85 **Wang L**, Wang Y, Quan J. Exosomal miR-223 derived from natural killer cells inhibits hepatic stellate cell activation by suppressing autophagy. *Mol Med* 2020; **26**: 81 [PMID: 32873229 DOI: 10.1186/s10020-020-00207-w]

86 **Rong X**, Liu J, Yao X, Jiang T, Wang Y, Xie F. Human bone marrow mesenchymal stem cells-derived exosomes alleviate liver fibrosis through the Wnt/β-catenin pathway. *Stem Cell Res Ther* 2019; **10**: 98 [PMID: 30885249 DOI: 10.1186/s13287-019-1204-2]

87 **Sun C**, Shi C, Duan X, Zhang Y, Wang B. Exosomal microRNA-618 derived from mesenchymal stem cells attenuate the progression of hepatic fibrosis by targeting Smad4. *Bioengineered* 2022; **13**: 5915-5927 [PMID: 35199612 DOI: 10.1080/21655979.2021.2023799]

88 **Kim J**, Lee C, Shin Y, Wang S, Han J, Kim M, Kim JM, Shin SC, Lee BJ, Kim TJ, Jung Y. sEVs from tonsil-derived mesenchymal stromal cells alleviate activation of hepatic stellate cells and liver fibrosis through miR-486-5p. *Mol Ther* 2021; **29**: 1471-1486 [PMID: 33348053 DOI: 10.1016/j.ymthe.2020.12.025]

89 **Wang N**, Li X, Zhong Z, Qiu Y, Liu S, Wu H, Tang X, Chen C, Fu Y, Chen Q, Guo T, Li J, Zhang S, Zern MA, Ma K, Wang B, Ou Y, Gu W, Cao J, Chen H, Duan Y. 3D hESC exosomes enriched with miR-6766-3p ameliorates liver fibrosis by attenuating activated stellate cells through targeting the TGFβRII-SMADS pathway. *J Nanobiotechnology* 2021; **19**: 437 [PMID: 34930304 DOI: 10.1186/s12951-021-01138-2]

90 **Paik KY**, Kim KH, Park JH, Lee JI, Kim OH, Hong HE, Seo H, Choi HJ, Ahn J, Lee TY, Kim SJ. A novel antifibrotic strategy utilizing conditioned media obtained from miR-150-transfected adipose-derived stem cells: validation of an animal model of liver fibrosis. *Exp Mol Med* 2020; **52**: 438-449 [PMID: 32152450 DOI: 10.1038/s12276-020-0393-1]

91 **Zhou Q**, Rong C, Gu T, Li H, Wu L, Zhuansun X, Zhao X, Xiao Z, Kuang Y, Xu S, Wang S. Mesenchymal stem cells improve liver fibrosis and protect hepatocytes by promoting microRNA-148a-5p-mediated inhibition of Notch signaling pathway. *Stem Cell Res Ther* 2022; **13**: 354 [PMID: 35883205 DOI: 10.1186/s13287-022-03030-8]

92 **Feng Y**, Li Y, Xu M, Meng H, Dai C, Yao Z, Lin N. Bone marrow mesenchymal stem cells inhibit hepatic fibrosis *via* the AABR07028795.2/rno-miR-667-5p axis. *Stem Cell Res Ther* 2022; **13**: 375 [PMID: 35902883 DOI: 10.1186/s13287-022-03069-7]

93 **Sun J**, Sun X, Hu S, Wang M, Ma N, Chen J, Duan F. Long noncoding RNA SNHG1 silencing accelerates hepatocyte-like cell differentiation of bone marrow-derived mesenchymal stem cells to alleviate cirrhosis *via* the microRNA-15a/SMURF1/UVRAG axis. *Cell Death Discov* 2022; **8**: 77 [PMID: 35194023 DOI: 10.1038/s41420-022-00850-8]

94 **Ma J**, Li Y, Chen M, Wang W, Zhao Q, He B, Zhang M, Jiang Y. hMSCs-derived exosome circCDK13 inhibits liver fibrosis by regulating the expression of MFGE8 through miR-17-5p/KAT2B. *Cell Biol Toxicol* 2022 [PMID: 35484432 DOI: 10.1007/s10565-022-09714-4]

95 **Hu M**, Wang Y, Liu Z, Yu Z, Guan K, Liu M, Wang M, Tan J, Huang L. Hepatic macrophages act as a central hub for relaxin-mediated alleviation of liver fibrosis. *Nat Nanotechnol* 2021; **16**: 466-477 [PMID: 33495618 DOI: 10.1038/s41565-020-00836-6]

96 **Ji**, Wang Q, Zhao Q, Tong H, Yu M, Wang M, Lu T, Jiang C. Co-delivery of miR-29b and germacrone based on cyclic RGD-modified nanoparticles for liver fibrosis therapy. *J Nanobiotechnology* 2020; **18**: 86 [PMID: 32513194 DOI: 10.1186/s12951-020-00645-y]

97 **Lv L**, Wang D, Yin J, Yang T, Huang B, Cao Y, Lu J. Downregulation of miR-20b-5p Contributes to the Progression of Liver Fibrosis *via* the STAT3 Signaling Pathway In Vivo and In Vitro. *Dig Dis Sci* 2023; **68**: 487-496 [PMID: 35947307 DOI: 10.1007/s10620-022-07660-z]

98 **Chen T**, Shi Z, Zhao Y, Meng X, Zhao S, Zheng L, Han X, Hu Z, Yao Q, Lin H, Du X, Zhang K, Han T, Hong W. LncRNA Airn maintains LSEC differentiation to alleviate liver fibrosis *via* the KLF2-eNOS-sGC pathway. *BMC Med* 2022; **20**: 335 [PMID: 36171606 DOI: 10.1186/s12916-022-02523-w]

99 **Wang R**, Li S, Chen P, Yue X, Wang S, Gu Y, Yuan Y. Salvianolic acid B suppresses hepatic stellate cell activation and liver fibrosis by inhibiting the NF-κB signaling pathway *via* miR-6499-3p/LncRNA-ROR. *Phytomedicine* 2022; **107**: 154435 [PMID: 36155216 DOI: 10.1016/j.phymed.2022.154435]

World Journal of Gastroenterology

Submit a Manuscript: https://www.f6publishing.com

World J Gastroenterol 2023 March 7; 29(9): 1460-1474

DOI: 10.3748/wjg.v29.i9.1460

ISSN 1007-9327 (print) ISSN 2219-2840 (online)

MINIREVIEWS

Approach to thromboelastography-based transfusion in cirrhosis: An alternative perspective on coagulation disorders

Sahil Kataria, Deven Juneja, Omender Singh

Specialty type: Gastroenterology and hepatology

Provenance and peer review: Invited article; Externally peer reviewed.

Peer-review model: Single blind

Peer-review report's scientific quality classification

Grade A (Excellent): 0
Grade B (Very good): B, B
Grade C (Good): 0
Grade D (Fair): 0
Grade E (Poor): 0

P-Reviewer: Ding X, China; Saito H, Japan

Received: October 15, 2022
Peer-review started: October 15, 2022
First decision: January 3, 2023
Revised: January 12, 2023
Accepted: February 27, 2023
Article in press: February 27, 2023
Published online: March 7, 2023

Sahil Kataria, Deven Juneja, Omender Singh, Institute of Critical Care Medicine, Max Super Speciality Hospital, New Delhi 110017, India

Corresponding author: Deven Juneja, DNB, FCCP, MBBS, Director, Institute of Critical Care Medicine, Max Super Speciality Hospital, Saket, 1, Press Enclave Road, New Delhi 110017, India. devenjuneja@gmail.com

Abstract

Viscoelastic tests, specifically thromboelastography and rotational thromboelastometry, are increasingly being used in the management of postoperative bleeding in surgical intensive care units (ICUs). However, life-threatening bleeds may complicate the clinical course of many patients admitted to medical ICUs, especially those with underlying liver dysfunction. Patients with cirrhosis have multiple coagulation abnormalities that can lead to bleeding or thrombotic complications. Compared to conventional coagulation tests, a comprehensive depiction of the coagulation process and point-of-care availability are advantages favoring these devices, which may aid physicians in making a rapid diagnosis and instituting early interventions. These tests may help predict bleeding and rationalize the use of blood products in these patients.

Key Words: Bleeding; Chronic liver disease; Cirrhosis; Thromboelastography; Viscoelastic tests

Core Tip: Viscoelastic hemostatic assays are increasingly used as "point-of-care" tests, providing real-time, dynamic insight into the complex coagulation aberrations seen in cirrhotic patients. In cirrhosis, all patients undergoing a high-risk invasive procedure or who are actively bleeding should undergo thromboelastography (TEG) on initial evaluation, if this testing is available. Any reasonable TEG-based strategy will likely represent an improvement over strategies using traditional coagulation tests. The best approach will be to use TEG supplemented by standard platelet count and fibrinogen testing. TEG is a promising diagnostic modality and may help in predicting bleeding and aid in the rationalization of the use of blood products in these patients.

Citation: Kataria S, Juneja D, Singh O. Approach to thromboelastography-based transfusion in cirrhosis: An alternative perspective on coagulation disorders. *World J Gastroenterol* 2023; 29(9): 1460-1474
URL: https://www.wjgnet.com/1007-9327/full/v29/i9/1460.htm
DOI: https://dx.doi.org/10.3748/wjg.v29.i9.1460

INTRODUCTION

The liver is essential in maintaining hemostasis[1]. Patients with cirrhosis may demonstrate altered coagulation and are often considered "auto-anticoagulated"[2]. However, the current understanding of coagulopathy is that patients with cirrhosis have a rebalanced coagulation status[3]. This balance is precarious due to alterations in the hepatic synthesis of pro- and anticoagulant factors. The resilience of the hemostatic system can be further decreased in cirrhotic patients by acute clinical conditions like systemic infection, altered volume status, and impaired renal function.

Given our current understanding of coagulation status in cirrhosis patients, there is considerable interest in tests of coagulation that could provide a truly global view of the coagulation system. Conventional coagulation tests (CCTs), like prothrombin time (PT) and activated partial thromboplastin time (aPTT), are indicators of general liver dysfunction. However, these tests fail to depict the totality of *in vivo* coagulation dysfunction, and lack insight into factors such as blood flow dynamics, endothelial tissue factor (TF), platelet function. They are also limited in their ability to aid in the decision of whether to administer plasma or whole blood[4,5]. Despite such concerns, these CCTs are commonly used to drive clinical decisions.

Thromboelastography (TEG) provides a more physiologically accurate assessment of the coagulation system. TEG has been used effectively as a rapid point-of-care test to assess hypercoagulable, hypocoagulable, and rebalanced coagulation states to evaluate blood transfusion requirements, suggest whether anticoagulation is required, and, if so, aid in the selection of anticoagulant therapy[6].

However, the ideal strategy for using TEG to guide the determination of blood product transfusion is unclear. Although the literature is replete with prospective data demonstrating the superiority of TEG over CCTs for non-surgical patients in terms of the requirement of blood transfusion, a mortality benefit has not been established[7-9]. The present article aims to review the current evidence supporting the use of TEG and the clinical significance of this testing modality in the guidance of blood transfusion in cirrhosis patients.

HEMOSTATIC SYSTEM IN LIVER DISEASE

Per the cell-based model of hemostasis, coagulation occurs not as a "cascade" but in 3 overlapping stages: (1) The initiation phase ensues on tissue factor (TF)-carrying cells. If the procoagulant stimulus is sufficiently strong, factors Xa, IXa, and thrombin are formed in adequate levels to initiate the coagulation process; (2) The amplification phase occurs as the activity moves from the TF-carrying cell to the platelet surface. The procoagulant stimulus is intensified causing platelets to attach, activate, and hoard activated cofactors on their surfaces; and (3) The propagation phase in which the "tenase" and "prothrombinase" complexes gather on the platelet surface and generate the large amounts of thrombin necessary to form a hemostatic fibrin clot[10].

In cirrhosis, all three phases are limited by hepatic synthetic dysfunction and portal hypertension, resulting in a delicate state of "new equilibrium" (Figure 1)[11]. However, this balance can be altered by concomitant conditions such as sepsis or acute kidney injury (AKI) as a result of the interaction between platelets and released inflammatory mediators (Figure 2). Thus, the coagulation profile in cirrhotic patients is dynamic, with possible resolution of global coagulation deficiencies once the acute critical illness resolves. The cell-based model of coagulation also explains why regional hemostatic changes at an injury site do not override the systemic hemostatic equilibrium. Accordingly, CCTs may remain unchanged in patients with liver dysfunction, even with clinically evident bleeding.

According to Hoffman's concept of the cell-based coagulation model, bleeding can arise from disorders of primary hemostasis (abnormal platelet plug formation) or secondary hemostasis (reduced thrombin generation and subsequent fibrin clot formation). The liver plays a critical role in maintaining both primary and secondary hemostasis[11]. In fact, the liver is the site of synthesis of most coagulation factors, with the exception of von Willebrand factor (vWF), factor VIII (only partly synthesized in the liver), and calcium[12].

Bleeding complications in cirrhotic patients may occur due to hemostatic failure or non-hemostatic causes. The term "spontaneous hemostasis-related bleeding" has recently been introduced to distinguish bleeding due to hemostatic anomalies from that related to portal hypertension, trauma, or peptic ulcers. It is defined as an unprovoked hemorrhage of unexplained cause. However, it should be emphasized that spontaneous bleeding is uncommon in patients with cirrhosis, and bleeding is typically

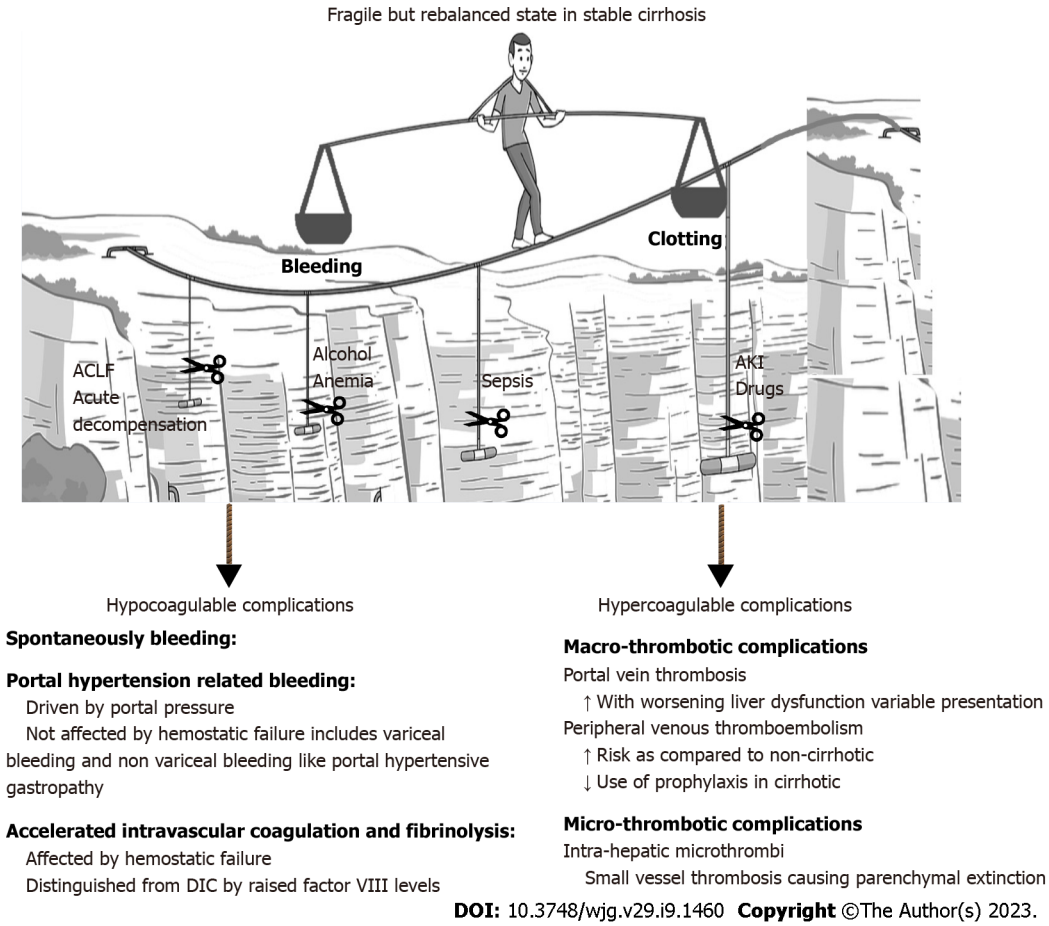

Figure 1 Rebalanced hemostasis in cirrhosis. ACLF: Acute-on-chronic liver failure; AKI: Acute kidney injury; DIC: Disseminated intravascular coagulation.

related to portal hypertension caused by increased portal pressure rather than hemostatic failure. This was conclusively demonstrated by the inability of recombinant factor VII to achieve better control of variceal rebleeding[13,14]. Notably, a bleed not primarily caused by hemostatic failure can evolve into a hemostatic bleed due to severe blood loss and consumptive coagulopathy. Bleeding (tertiary hemostasis disorder) can also be due to premature platelet or fibrin clot dissolution or excessive fibrinolysis, which in cirrhotic patients has been termed "accelerated intravascular coagulation and fibrinolysis" (AICF). AICF manifests as mucosal or puncture wound bleeding, and the pathophysiology of this disorder is not entirely understood. Hyperfibrinolysis parallels the severity of liver disease: mild systemic fibrinolysis is encountered in 30%-45% of cirrhotic patients, with clinically detectable fibrinolysis in only 5%-10%. AICF can be distinguished from disseminated intravascular coagulation by increased factor VIII levels (Figure 1)[15,16]. The 3 phases of coagulation in liver disease resulting in a "rebalancing" of hemostasis are summarized in Table 1[17,18].

For the past several decades, bleeding has been a major concern in the management of cirrhotic patients. However, thrombotic complications are being increasingly acknowledged and are attributed to shifts in hemostatic balance. In one case-control study, the relative risk of venous thromboembolism (VTE) in patients with cirrhosis was 1.74 (95%CI: 1.54-1.95)[19]. These conclusions were mirrored in a study by Wu *et al*[20], which showed an increased likelihood of VTE in cirrhosis [odds ratio (OR) 1.23 in compensated cirrhotic patients; OR 1.39 in decompensated cirrhotic patients]. Dysfibrinogenemia (*i.e.* altered fibrinogen) may result in decreased permeability of the formed clot, as well as other factors that contribute to coagulopathy. It may even confer hypercoagulable features, manifesting as macro- and micro-thrombotic complications. A hypercoagulable state also frequently occurs in cirrhosis patients due to concomitant primary biliary cholangitis, non-alcoholic fatty liver disease, or primary sclerosing cholangitis[21].

The most common macro-thrombotic presentation in liver disease is portal vein thrombosis (PVT), occurring in 8% to 18% of cirrhosis patients[18]. The incidence of PVT increases with deteriorating liver function and decreased portal flow. Deep venous thrombosis and pulmonary embolism (PE) are other macro-thrombotic complications, which have been reported in 5% of hospitalized patients with chronic liver disease (CLD)[17,22]. Micro-thrombotic complications include intrahepatic microthrombi ("parenchymal extinction"), resulting in nodules, porto-pulmonary hypertension, and cirrhosis arising as an ischemic/reinjury process. These complications often merit exigent consideration of anticoagulant

Table 1 Three phases of coagulation in liver disease

Hemostasis stage	Hypocoagulable state	Hypercoagulable state
Primary hemostasis: Platelet activation and interaction with injured endothelium	Thrombocytopenia: (1) Decreased amount: Splenic sequestration, decreased thrombopoietin levels, bone marrow suppression, autoantibody destruction; and (2) Poor function: Uremia, changes to the vessel wall phospholipid composition, anemia (Hgb < 7 g/dL), decreased margination	Low levels of ADAMTS-13; Increased levels of vWF; Increased number of activated platelets
Secondary hemostasis: Fibrin clot formation	Low levels of factors II, V, VII, IX, X, and XI; Low levels of fibrinogen; Vitamin K deficiency (malabsorption in cholestatic disorders)	Elevated levels of factor VIII; Decreased levels of proteins C and S; Decreased levels of antithrombin, and heparin cofactor II
Fibrinolysis	Accelerated intravascular coagulation and fibrinolysis: (1) Low levels of factor XIII and thrombin-activated fibrinolysis inhibitor; (2) Elevated levels of tPA; (3) Decreased level of α2-antiplasmin; and (4) Dysfibrinogenemia	Low plasminogen levels; Dysfibrinogenemia; High plasminogen activator inhibitor

Hgb: Hemoglobin; tPA: Tissue plasminogen activator; vWF: von Willebrand factor.

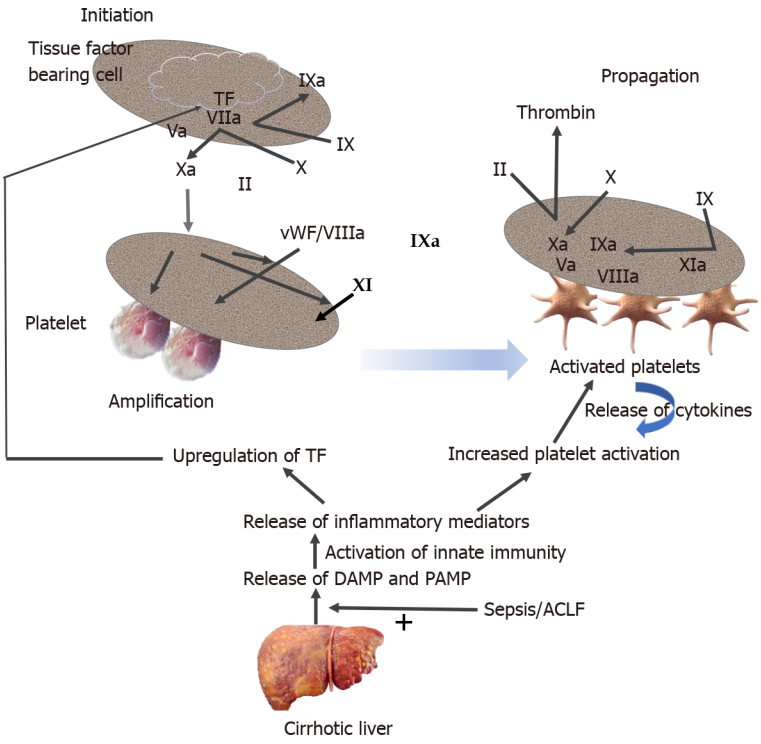

DOI: 10.3748/wjg.v29.i9.1460

Figure 2 Dynamic coagulation profile in cirrhosis. ACLF: Acute-on-chronic liver failure; DAMP: Damage-associated molecular patterns; PAMP: Pathogen-associated molecular patterns; TF: Tissue factor.

usage.

TESTS OF COAGULATION IN CIRRHOSIS

As of this article, all available laboratory hemostasis measures have significant limitations when applied to patients with liver disease. The paradigm of this phenomenon is the cirrhotic patient, for which PT and international normalized ratio (INR) were developed to monitor warfarin-treated patients by measuring the activity of an added commercially available thromboplastin reagent. PT and aPTT indicate the onset of thrombin generation; however, they do not reflect enzymatic coagulation. PT/INR has been validated as a prognostic marker for mortality in liver disease, but has never been validated to predict bleeding risk or guide transfusion of blood products, especially for pre-procedure risk mitigation[14]. Nonetheless, this measure has been used for decades as a surrogate for bleeding risk in cirrhosis despite the fact that the arbitrary cut-off points used as clinical targets for the prevention of bleeding are not supported by scientific evidence. Furthermore, using fresh frozen plasma (FFP) to

normalize a raised INR in cirrhosis does not alter thrombin (factor II) production, but exacerbates portal hypertension[23-25].

Thrombocytopenia is the most common hematological abnormality in patients with liver disease. Platelet count thresholds are often specified for invasive procedures in patients with severe cirrhosis-related thrombocytopenia. In vitro data suggest that a threshold of 50-55 × 10^9/L is necessary for adequate platelet activity, and levels below this range fail to promote thrombin generation[26]. However, the platelet function associated with primary hemostasis (*i.e.* adhesiveness and aggregation) has not been evaluated. Current guidelines and expert opinion recommend considering platelet-raising treatments before high-risk procedures, or in patients with active bleeding with platelet counts < 50 × 10^9/L. However, there is no firm evidence that prophylactic platelet transfusion to achieve this target enhances hemostasis[15,23].

As mentioned previously, platelet count alone does not account for other factors affecting platelet function in cirrhosis[27]. For example, uremic platelet dysfunction (*e.g.*, hepatorenal syndrome) can result in impaired platelet activity with decreased serotonin in alpha granules and dysregulated metabolism of thromboxane A2. Anemia can also affect platelet function. In patients with hematocrit < 25%, erythrocyte concentration is inadequate to facilitate platelet margination, impairing the clotting process. Sepsis and endotoxemia due to bacterial translocation also can affect platelet function.

Recently, fibrinogen levels have replaced INR to couple with platelet count in the evaluation of bleeding risk. The Clauss method for detecting fibrinogen is turbidimetric and relies on thrombin-induced fibrin formation. Nevertheless, fibrinogen levels do not account for the synthesis of abnormal fibrinogen in cirrhotic patients caused by hypersialylation of the fibrinogen, leading to impaired fibrinogen-to-fibrin conversion[28]. In trauma surgery patients without underlying liver disorder, administration of fibrinogen factor to accomplish levels of fibrinogen > 200 mg/dL is associated with improved hemostasis. However, in routine clinical practice, the most agreed-upon cut-off for fibrinogen in cirrhotic patients with active bleeding is > 120 mg/dL[29]. In cirrhotic patients, spontaneous or procedure-related bleeding is relatively common when plasma fibrinogen levels are less than 100 mg/dL. Whether this relationship is causal or reflects disease severity is unclear. As such, the available evidence suggests that tests measuring clot formation and strength (*i.e.* fibrinogen) may have better predictive value for bleeding events than coagulation initiation tests[29,30].

Primary hyperfibrinolysis is an increasingly vital pathophysiological process in CLD, resulting in an increased risk of variceal bleeding. D-dimer is a nonspecific marker of fibrin degradation. While evidence suggests that elevated D-dimer indicates hyperfibrinolysis and can predict gastrointestinal bleeding in this population, elevated D-dimer alone provides limited information regarding an individual's fibrinolytic state[31,32].

Thrombin generation assays (TGAs) evaluate the time of thrombin generation and its decline when plasma is triggered by TF and phospholipids. Thus, TGA can reflect the activity of both pro- and anticoagulant factors[33,34]. Nevertheless, clinical trials are needed to test this conjecture. Similar to PT and aPTT, TGA is performed on plasma rather than whole blood. However, because of their method, TGAs approximate the *in vivo* coagulation balance better than CCTs.

TEG quantitatively assesses the capability of whole blood to form a clot, providing a comprehensive picture of coagulation status compared to standard laboratory tests, which are confined to developing the first fibrin strands. However, TEG is insensitive to the platelet adhesion and aggregation activity of vWF and the anticoagulant actions of protein C and protein S; therefore, it may lead to an underestimation of hemostatic capacity[17] (Table 2).

PRINCIPLES OF TEG

The principle of the *in vitro* TEG test is to detect and quantify dynamic changes in the viscoelastic properties of whole blood during clotting under low shear stress (Figure 3A). TEG results are depicted as 2-dimensional graphs, with time on the x-axis and amplitude (in millimeters) on the y-axis (Figure 3B). A normal TEG trace appears similar to a cognac glass lying on its side (Figure 4)[17]. An evident prolongation of R is associated with clotting factor levels of 30% or less[35]. Different activators can be added to the blood to better assess various aspects of the clotting cascade (Table 3). Conventional TEG involves clot initiation by adding kaolin, simulating the intrinsic coagulation pathway. In contrast, rapid TEG involves the addition of kaolin and TF, causing massive thrombin burst and providing initial results (K time) within 6 min and alpha angle/MA within 15 min[36,37]. Thus, the results of rapid TEG can be achieved approximately 10 min earlier than the kaolin TEG and about 30 min earlier than CCTs [37]. This could guide critical resuscitations more competently, enabling real-time monitoring and goal-directed therapy. Though the activators reduce the test turnaround time (*e.g.*, kaolin), the sensitivity of viscoelastic tests (VETs) could be blunted, and subtle changes in coagulation and clot lysis might not be detected[17] (Table 4).

Correlation of CCTs and VETs

A strong correlation between TEG measures of clot formation and clot strength and conventional

Table 2 Thromboelastography components and their clinical implications

Nomenclature	Definition	Function	Significance	Most closely related CCT
Reaction time or R-time	Time (min) to reach an amplitude of 2 mm	Clot initiation	Informs about enzymatic reaction leading to thrombin and fibrin generation. Increased R-time, factor deficiency or reduced function, resulting in hypocoagulability; Shortened R-time, factor hypercoagulability	PT and aPTT
K-time	Time (min) from 2-20 mm amplitude	Clot kinetics	Depicts rate of clot development–fibrin polymerization, cross-linking, and platelet interaction. Long K-time, hypocoagulability; Short K-time, hypercoagulability	Fibrinogen level and platelet count
Angle or α	Slope between R and K	Clot kinetics	Also depicts the kinetics of clot development. Low-angle, hypocoagulability; High-angle, hypercoagulability	
MA	Highest level of amplitude achieved by the clot	Clot strength	Provides assessment of overall clot strength	Platelet count and fibrinogen levels
Coagulation index	Composite indicator of coagulation profile		A linear combination of the above parameters serving as a global view of the patient's hemostatic profile. Increased in hypercoagulable states; Decreased in hypocoagulable states	
LY30	Degree of lysis (%) 30 min after MA is reached	Clot stability	Measure of fibrinolysis. Above normal LY30 suggests hyperfibrinolysis	No equivalent test

aPTT: Activated partial thromboplastin time; CCT: Conventional coagulation test; MA: Maximum amplitude; PT: Prothrombin time.

Table 3 Procedural bleeding risk in patients with cirrhosis

High-risk procedures	Intermediate-risk procedures	Lower-risk procedures
Intrabdominal/orthopedic/cardiac surgery	Percutaneous endoscopic gastrostomy	Paracentesis
Brain or spinal surgery	Percutaneous or transjugular liver biopsy	Thoracentesis
Intracranial catheter insertion	Transjugular intrahepatic portosystemic shunt	Central line placement
Endoscopic mucosal resection or endoscopic submucosal dissection	Endoscopy (*e.g.*, percutaneous gastrostomy placement, cystogastrostomy, biliary sphincterotomy)	Endoscopy (*e.g.*, diagnostic, variceal ligation, uncomplicated polypectomy)
Complicated polypectomy	Percutaneous biopsy of extra-hepatic organ or lesions	Cardiac catheterization
Natural orifice transluminal endoscopic surgery	Trans-arterial or percutaneous hepatocellular carcinoma therapies	Hepatic venous pressure gradient measurement
	Lumbar puncture	

Table 4 Various types of thromboelastography assays

TEG channel	Activator	Function
Native TEG	None	Theoretically most sensitive to subtle coagulopathic changes and hyperfibrinolysis
Conventional TEG	Kaolin	Activates clotting cascade to expedite results
Rapid TEG	Tissue factor + kaolin	Activates clotting cascade to expedite results
Functional fibrinogen TEG	Glycoprotein IIb/IIIa inhibitor	Inhibits platelets to isolate the contribution of fibrinogen
Heparinase TEG	Heparinase	Inhibits heparin; the presence of heparin (endogenous or exogenous) is suggested when this channel shows improved clotting compared to other channels

TEG: Thromboelastography.

fibrinogen level has been observed in CLD patients who are critically ill. Nevertheless, weak or unpredictable correlations exist between TEG and CCTs in measuring coagulation initiation (*i.e.* TEG R-time and PT/INR/aPTT), TEG and conventional platelet count, and measures of fibrinolysis (TEG LY30 and traditional D-dimer)[38-40]. The absence of a correlation between PT/INR and R may be explained by several elements, such as the use of different activators, the use of whole blood *vs* plasma, and the

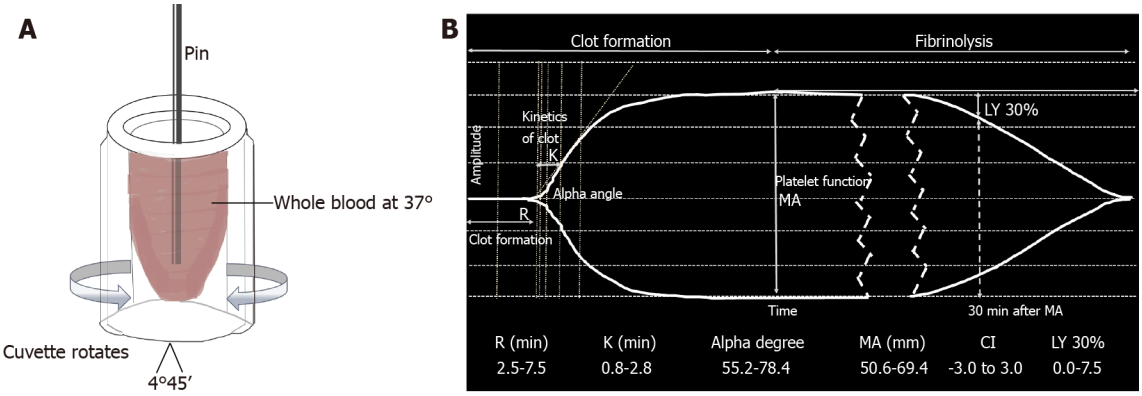

DOI: 10.3748/wjg.v29.i9.1460

Figure 3 Basis and results of the thromboelastography. A: Basis of the thromboelastography (TEG) test; B: TEG tracing and relevant parameters (kaolin-activated). MA: Maximum amplitude.

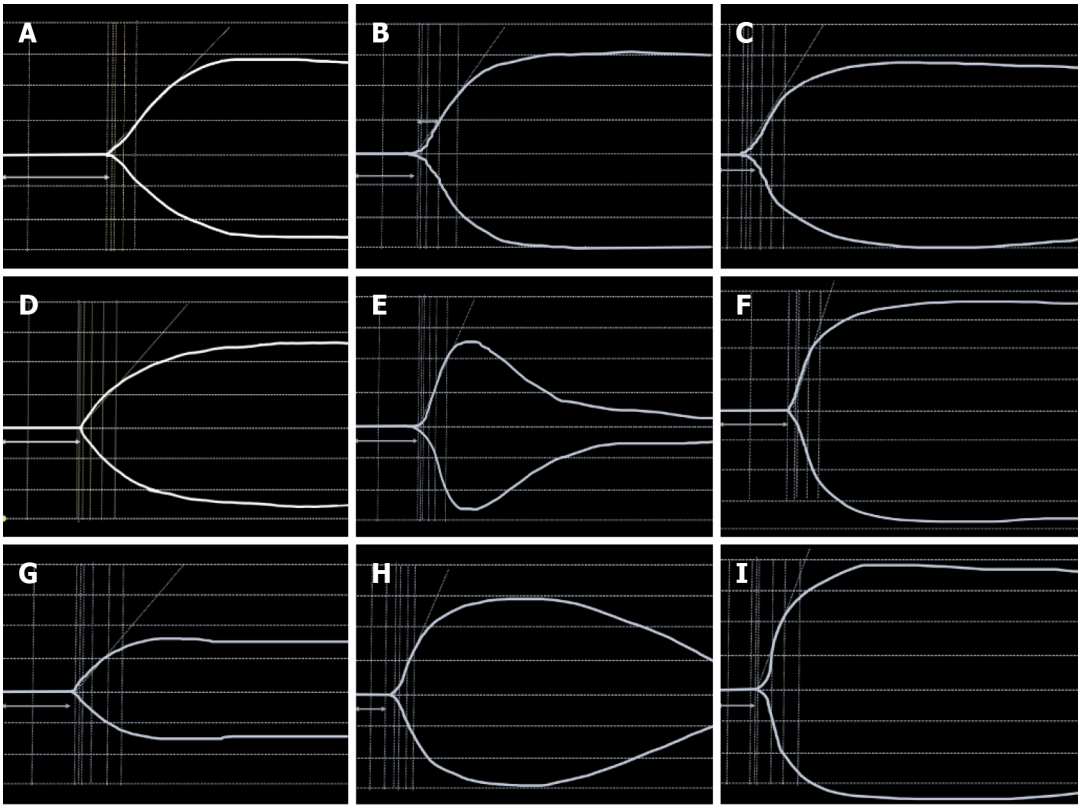

DOI: 10.3748/wjg.v29.i9.1460

Figure 4 Tracing of thromboelastography in various clinical conditions. A: Low clotting factors; B: Normal trace; C: Enzymatic hypercoagulability; D: Low fibrinogen levels; E: Primary fibrinolysis; F: Platelet hypercoagulability; G: Low platelet function; H: Secondary fibrinolysis; I: Enzymatic and platelet hypercoagulability.

fact that R-time, unlike INR, reflects the balance of both pro- and anticoagulant factors. This supports the evidence that clotting initiation and speed measures are challenging to interpret in this cohort, while TEG maximum amplitude (MA) and conventional fibrinogen may be more reliable. Nonetheless, the results of these tests should always be correlated with the clinical situation.

CLINICAL APPLICATIONS OF TEG IN LIVER DISEASE

TEG and invasive procedures in patients with cirrhosis

Bleeding complications after invasive procedures are always a concern in cirrhotic patients, though the incidence varies widely[41]. Although the risk of bleeding after the procedure is related to alterations in

clotting factors, the risk is also inherent to a given procedure (Table 3) and the given clinical situation [41]. In cirrhotic patients with acute illness or acute-on-chronic liver failure, the association between clotting tests and bleeding may not be as apparent or evident as in stable patients. Moreover, managing complications, such as sepsis or AKI, instead of correcting hemostatic abnormality, may result in improved outcomes. A retrospective study revealed that AKI was the only independent risk factor for post-paracentesis hemoperitoneum. In contrast, no significant difference was observed in CCTs (platelet count and INR levels) between patients with or without this complication[42].

Three recent randomized trials conducted in cirrhotic patients undergoing invasive procedures demonstrated a decreased requirement for prophylactic blood product transfusions using TEG-guided transfusions compared to standard test-based protocols[7-9]. However, they could not demonstrate any relationship between abnormal TEG tracing and bleeding, primarily due to the scarcity of documented bleeding events. Similarly, TEG did not help to predict the inability to control bleeding or prevent rebleeding. Also, no impact on other clinically relevant outcomes was observed. Moreover, each study used a different transfusion protocol, making it difficult to know whether the lower cutoff for transfusion would have been more beneficial. In another study of cirrhotic patients undergoing various invasive procedures without prophylactic administration of blood products, even with abnormal CCT and TEG R-time and MA, 1 patient experienced bleeding (0.7%)[43]. Also, a recent study in 90 patients with cirrhosis undergoing central venous cannulation demonstrated that a prolonged TEG K-time (≥ 3.05 min) could not predict bleeding complications (accuracy 69.4%, P = 0.047)[44]. These studies indicate that post-procedural bleeding events are rare, implying that uncorrected coagulopathy does not modify the post-procedural outcome. Nevertheless, coagulation tests can be utilized to evaluate the severity of liver disease or the patient's baseline hemostatic function and to provide a baseline to guide management in the case of post-procedural bleeding.

Most of the latest guidelines recommend against using CCTs and correction of coagulopathy before undergoing common gastrointestinal procedures in patients with stable cirrhosis. Also, there are no recommendations for or against using TEG in such patient populations (Table 5)[15,23,45,46]. However, in patients with severely abnormal coagulation parameters or thrombocytopenia undergoing a moderate- to high-risk procedure, clinical judgment regarding prophylactic blood transfusion should consider the possible benefits and risks (Figure 5)[7,15].

Use of TEG in cirrhosis with active bleeding

Bleeding related to portal hypertension, variceal and non-variceal, is primarily managed with local measures such as endoscopic band ligation, laser or injection therapy, and by lowering portal pressure using vasoactive drugs than pro-hemostatic therapy. The observation that variceal bleeding in patients on anticoagulants was not severe or associated with worse outcomes compared to patients who are not on anticoagulants confirms that the role of the hemostatic system in variceal bleeding, if present, is minor[47]. Randomized controlled studies have shown that in cirrhotic patients with variceal and non-variceal bleeding, using VETs to guide blood product transfusion did not result in superior control of bleeding nor any morbidity or mortality benefit compared to CCTs[48-50]. However, the transfusion requirement was significantly lower in the VET group. Although the study by Kumar *et al*[51] demonstrated significantly shorter ICU stays using TEG-guided resuscitation, there was no difference in other outcomes. Nevertheless, it is questionable whether in active variceal bleeding, VETs-guided pro-hemostatic therapy is beneficial or contributes to the control of bleeding when the standard treatment with vasoactive drugs and endoscopic therapy is provided.

If local measures and portal pressure-lowering drugs cannot contain bleeding, the decision to correct coagulopathy by transfusing blood products should be considered on a case-by-case basis[13]. Since VETs are quicker and more accurate than CCTs and provide a more practical understanding of fibrinolysis, which may indicate the need to start antifibrinolytic therapy, they have a theoretical advantage over CCTs in guiding the management of active bleeding.

Unlike pressure-driven bleeding, AICF arises due to disturbed hemostatic mechanisms[15]. Antifibrinolytic therapy, such as epsilon aminocaproic acid or tranexamic acid, is potentially effective, inhibiting the fibrin clot's dissolution. Neither agent is thought to have inherent hypercoagulable risk, except in the case of a preexisting pathological thrombus such as PVT. The "native TEG" can detect this condition in liver disease patients by the presence of an increase in LY30[17].

TEG-based algorithms may allow targeted and specific blood product transfusions in patients with severe bleeding (*e.g.*, FFP or cryoprecipitates)[17]. However, the threshold values of various VETs to trigger transfusion are yet to be validated in appropriate clinical studies.

Heparin-like effect in cirrhosis

A stressful condition such as surgery or sepsis can trigger the release of endogenous glycosaminoglycans (GAGs) (*e.g.*, heparin sulfate and dermatan sulfate) from the endothelium glycocalyx layer or mast cell, which, when shed, retain their anticoagulant activity[52,53]. This is thought to be an adaptive reaction to maintain the patency of progressively procoagulant microvasculature through endogenous heparinization, thus preventing spontaneous thrombosis.

Table 5 Thresholds for coagulation parameters prior to high-risk procedures in patients with cirrhosis

Parameters	EASL 2022	ISTH 2021	AASLD 2021	AGA 2021
PT/INR	Against routine evaluation and correction	Against correction	Against correction	Against routine evaluation and correction[a]
Platelet count	Against correction[b]	Against correction[b]	Against correction	Against routine evaluation and correction[a]
Fibrinogen	Against routine correction	Against routine evaluation	Against correction	No specific recommendation
TEG	Against routine evaluation[c]	Do not use routinely	Do not use routinely	No specific recommendation

[a]In case of severe coagulopathy, prophylactic blood transfusions should be considered on case-to-case basis by evaluating potential benefits and risks in consultation with a hematologist.
[b]If the bleeding cannot be controlled by the local hemostasis method, administration of platelet concentrate or thrombopoietin receptor agonist can be considered if the platelet count is < 50000 × 10^6/L.
[c]May provide a baseline coagulation status and guide in the case of bleeding events.
AASLD: American Association for the Study of Liver Diseases; AGA: American Gastroenterological Association; EASL: European Association for the Study of the Liver; INR: International normalized ratio; ISTH: International Society on Thrombosis and Hemostasis; PT: Prothrombin time; TEG: Thromboelastography.

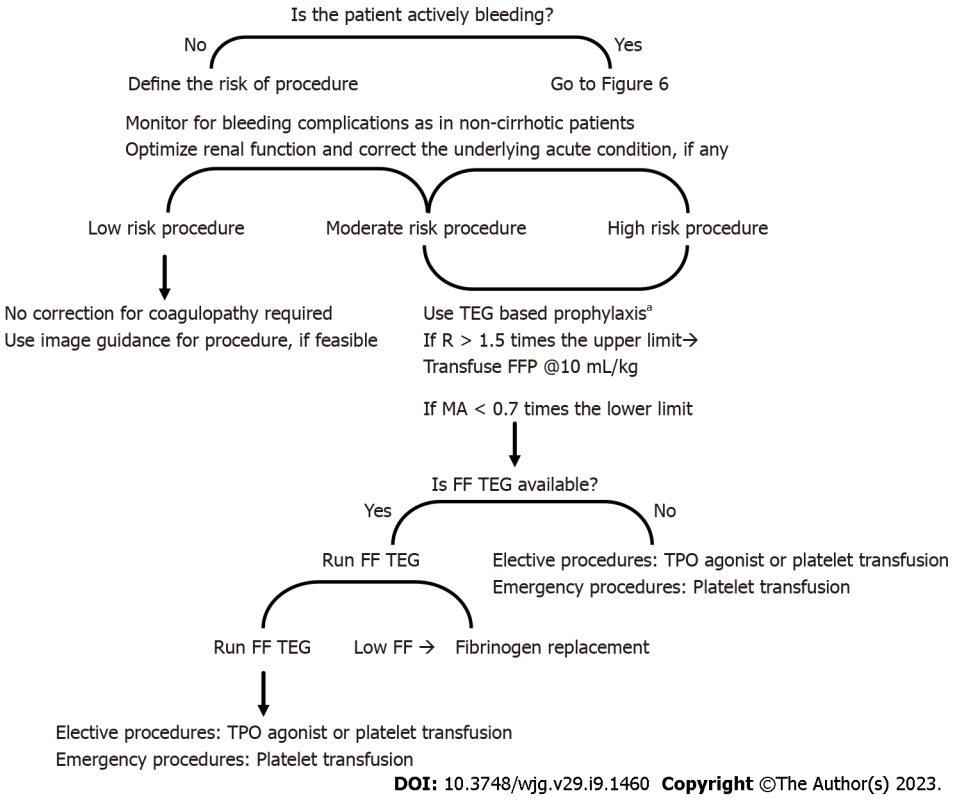

DOI: 10.3748/wjg.v29.i9.1460

Figure 5 Algorithm for coagulation factor administration in the cirrhotic patient with coagulopathy undergoing an invasive procedure. FF: Functional fibrinogen; FFP: Fresh frozen plasma; MA: Maximum amplitude; TEG: Thromboelastography; TPO: Thrombopoietin.

Endogenous GAGs may increase the bleeding risk in some patients. This was illustrated by Senzolo *et al*[54], where GAGs affected hemostasis in cirrhotic patients with sepsis. Another prospective analysis further confirmed the presence of an endogenous heparinoid in patients with cirrhosis and acute variceal bleeding and was found to be associated with bleeding-related mortality[55]. After appropriate therapy, endogenous heparinoids are cleared with normalization of the coagulation profile, emphasizing the association between the coagulation cascade and inflammatory pathways.

Although CCTs are insensitive to this effect, the native TEG is extremely sensitive to the presence of heparin and heparin-like substances, which is detectable by an increased R-time on TEG analysis[56]. Adding heparinase I, which cleaves heparin-like compounds, can demonstrate a heparin-like effect due to elevated GAGs, correlating with an anti-Xa activity[57]. Therefore, heparinase TEG will normalize the prolongation of the R-value observed with native TEG. Thus, TEG helps differentiate between a coagulation factor deficiency and heparin-produced coagulopathy by using heparinase-modified TEG

and the native TEG (Table 4).

TEG in orthotopic liver transplant

Kang *et al*[58] at the University of Pittsburgh introduced TEG-based algorithms to guide blood product transfusion for correcting coagulopathy in orthotopic liver transplantation in the early 1980s (Figure 6). It was shown that TEG reduced transfusion requirements by 33% compared with a historical cohort. Secondary endpoints like re-intervention for bleeding, AKI, or hemodynamic instability were significantly lower in the VET group. Although numerous studies have described the usefulness of VET in lowering transfusion requirements in liver transplant (LT), most of these studies commonly compared the results with historical cohorts having a relatively high baseline transfusion rate[59,60]. A recent study of 60 LT patients showed no significant differences with and without VET monitoring though overall transfusion was low, with many patients receiving no transfusion[61]. As bleeding and transfusion management continues to evolve, the results of these earlier studies cannot be easily employed in the present era. Also, the thresholds described for VET for initiating transfusion are still to be established, and values may be substantially above the normal ranges before an intervention is advised.

A significant proportion of patients undergoing LT will inevitably have enormous blood loss, and VET can be helpful in such occasions to enable goal-targeted treatment and assess the effectiveness of any therapeutic intervention. The short turnaround times of VET (10-20 min) are vital for directing therapy and averting inappropriate transfusion during surgery and in the ICU. Monitoring coagulation with functional fibrinogen TEG (Table 4) for goal-directed fibrinogen substitution seems more appropriate and avoids unnecessary platelet transfusions. This is particularly important in LT, as platelet administration is associated with a substantial decline in 1-year survival[62].

Fibrinolysis and orthotopic liver transplant

It is well known that increased fibrinolytic activity can occur at any juncture during LT. However, it is significantly enhanced during the anhepatic period due to a lack of tissue plasminogen activator (tPA) clearance[63]. Also, it may become most pronounced in the post-reperfusion stage by an erratic upsurge in tPA, leading to diffuse uncontrolled bleeding due to primary hyperfibrinolysis[64]. If the graft function is good, hyperfibrinolysis after reperfusion is usually self-limiting and does not require treatment. However, in the presence of an inadequately functioning graft, it may persist[65]. During LT, prophylactic antifibrinolytic agents were often used in earlier years because of the high mortality associated with tremendous blood loss, and the potential peril associated with antifibrinolytics was minor. As massive bleeding is currently less frequent, there is a preference towards the selective use of antifibrinolytics only in high-risk patients. Systemic fibrinolysis can be efficiently detected using VETs (demonstrated by increased or worsening LY30 and LY60), which may not be possible with CCTs. Thus, the transfusion requirement may be decreased with VET use in liver transplantation, where hyperfibrinolysis commonly occurs.

TEG and hypercoagulability

The risk of developing VTE is similar in cirrhotic and non-cirrhotic patients[15,23]. Hypercoagulability detected on TEG can either be due to shortened R or K, enhanced clot strength (MA), or a combination of both. Huang *et al*[66] observed a significantly shorter R in cirrhosis with non-malignancy PVT. Zanetto *et al*[67] found that elevated MA was associated with PVT in cirrhotic patients with hepatocellular carcinoma. Given that malignancy itself could also cause hypercoagulation, the clinical use of TEG in this setting may be questionable. In another study, hypercoagulability was defined as the presence of at least 2 of the following criteria: reduced R, reduced K, raised α, or increased MA. Hypercoagulability was not associated with PVT in cirrhosis[68].

In cirrhotic patients with elevated CCTs, we tend to avoid prophylactic anticoagulation in hospitalized patients. Presently, the European Association for the Study of the Liver Clinical Practice Guidelines in cirrhosis does not recommend using VETs to identify the risk of VTE[23]. Further prospective studies may explore the utility of TEG in predicting the risk of VTE during hospitalization.

Acute intracardiac thrombi and PEs are rare, although a well-recognized, potentially fatal complication of LT, associated with high mortality. Krzanicki *et al*[69] demonstrated that a hypercoagulable state is quite common during liver transplantation. A review of 27 case reports of TE in orthotopic LT showed that TEG indicated hypercoagulability in greater than 70% of cases[70]. Also, hypercoagulable TEG patterns correlated well with the formation of intracardiac thrombi. Indeed, a quick inspection of the rapid TEG after 5 or 10 min of clotting time might predict thrombosis, demonstrated by the increase in the MA. The clinical importance of hypercoagulability on TEG during LT is yet to be recognized. However, it would appear unreasonable to transfuse blood products or avoid anticoagulants based on raised CCTs when a hypercoagulable state is seen on TEG.

Patients with cirrhosis and VTE should be treated with anticoagulation, similar to other non-cirrhotic patients. In patients at increased risk of bleeding, unfractionated heparin (UFH) is the preferred anticoagulant, owing to its shorter half-life (45 min) and the availability of an effective antidote (protamine sulfate). aPTT is the most commonly used test to monitor UFH therapy. Although the anti-Xa activity

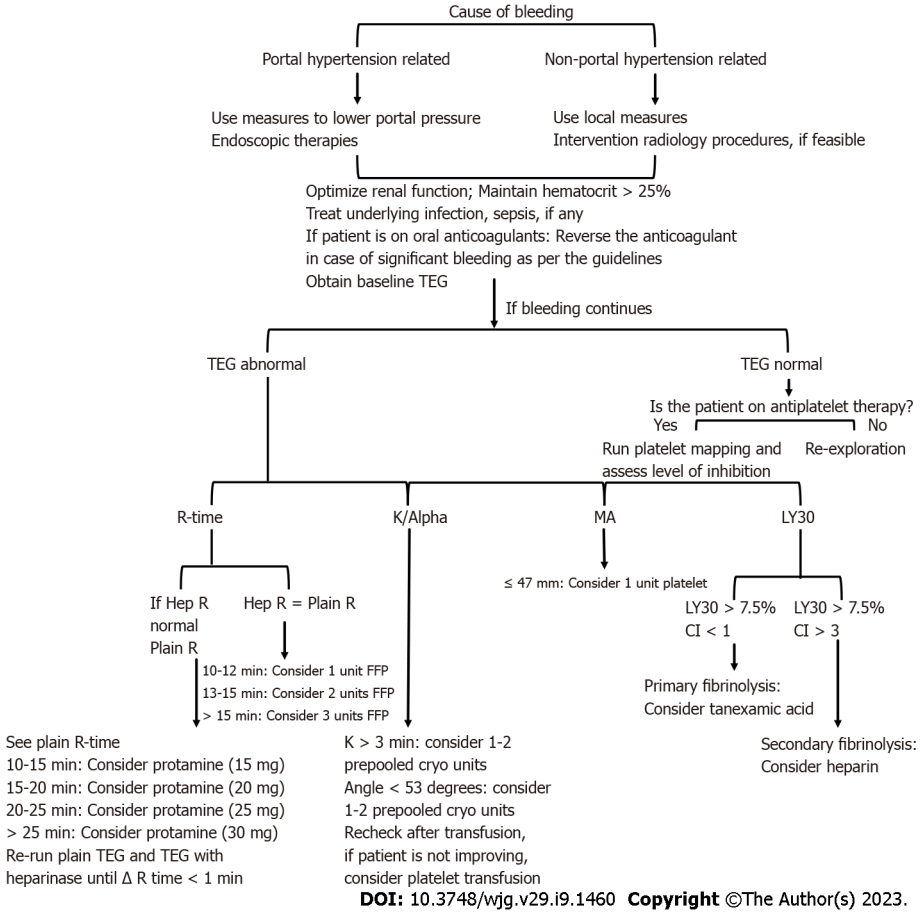

DOI: 10.3748/wjg.v29.i9.1460

Figure 6 Algorithm for guiding blood product transfusion by thromboelastography. Cryo: Cryoprecipitate; FFP: Fresh frozen plasma; Hep R: Heparinase R-Time; MA: Maximum amplitude; TEG: Thromboelastography.

assay is used explicitly for monitoring low molecular weight heparins, as they primarily inhibit factor Xa, it may also be superior to aPTT for titrating UFH[71].

Given that heparin activity mainly depends on the liver-derived activity of the heparin cofactor antithrombin III, monitoring heparin therapy with CCT in patients with cirrhosis is challenging. TEG may provide a better representation of the *in vivo* heparin effect than aPTT[72,73]. A higher concentration of heparin tends to be associated with larger R-values with dose-dependence. Levels of anti-factor Xa activity correlate with the R-value of TEG. In addition, TEG can help diagnose and treat heparin-induced coagulopathy. Thus, platelet and enzymatic hypercoagulability demonstrated with TEG mandates aggressive treatment with a direct thrombin inhibitor.

LIMITATIONS OF TEG

Like any other test, TEG is associated with certain limitations. It measures blood coagulation *in vitro* instead of during flow within the vasculature, and as such does not reflect the endothelium's function in coagulation. Inherently, the test is less sensitive to platelet adhesion and interactions between vWF and protein C and S system. TEG results do not correlate with the effects of hypothermia, as TEG is performed at 37 °C. Kaolin cannot effectively detect alterations in the extrinsic coagulation pathway, as it only activates the intrinsic coagulation pathway. Thus, INR is still the gold standard for monitoring warfarin therapy, and TEG may overlook a clinically significant coagulopathy. TEG detects fibrinolysis only when tPA levels are 5 times normal. Studies have shown that using plasmin-α2-antiplasmin as a biomarker for fibrinolysis can detect fibrinolytic activation in over 80% of severely injured patients, whereas TEG detected hyperfibrinolysis in only 5%-18%. Each TEG run generally takes 30 min to an hour, and only a few tests can run simultaneously, unlike CCT. The optimization of TEG is essential in providing appropriate patient laboratory testing. Additionally, testing should be performed by trained personnel and is susceptible to technical variations.

CONCLUSION

VETs are increasingly used as "point-of-care" tests, providing a real-time, dynamic picture of complex coagulation aberrations (*e.g.*, hypocoagulability, hypercoagulability and hyperfibrinolysis) in cirrhotic patients. In cirrhosis, all patients undergoing a high-risk invasive procedure or who are actively bleeding should undergo TEG at initial evaluation, if this testing is available. Any reasonable TEG-based strategy will likely represent an improvement over strategies using traditional coagulation tests. The best approach will be to use TEG supplemented by platelet count and fibrinogen measures. TEG is a promising diagnostic modality, but given the limited clinical trials, there are no consensus guidelines for its use. Further prospective studies are required to validate TEG algorithms for use in the context of patients with cirrhosis.

FOOTNOTES

Author contributions: Kataria S and Juneja D wrote the manuscript, researched the project, prepared the figures and tables, and performed data acquisition; Singh O reviewed draft and final versions of the manuscript.

Conflict-of-interest statement: No conflict-of-interest to declare.

Country/Territory of origin: India

ORCID number: Sahil Kataria 0000-0002-0756-4154; Deven Juneja 0000-0002-8841-5678; Omender Singh 0000-0002-3847-4645.

S-Editor: Zhang H
L-Editor: Filipodia
P-Editor: Zhang H

REFERENCES

1 **Lisman T**, Leebeek FW, de Groot PG. Haemostatic abnormalities in patients with liver disease. *J Hepatol* 2002; **37**: 280-287 [PMID: 12127437 DOI: 10.1016/s0168-8278(02)00199-x]
2 **Tripodi A**, Mannucci PM. The coagulopathy of chronic liver disease. *N Engl J Med* 2011; **365**: 147-156 [PMID: 21751907 DOI: 10.1056/NEJMra1011170]
3 **Tripodi A**, Primignani M, Mannucci PM, Caldwell SH. Changing Concepts of Cirrhotic Coagulopathy. *Am J Gastroenterol* 2017; **112**: 274-281 [PMID: 27801884 DOI: 10.1038/ajg.2016.498]
4 **Mannucci PM**, Tripodi A. Liver disease, coagulopathies and transfusion therapy. *Blood Transfus* 2013; **11**: 32-36 [PMID: 23058863 DOI: 10.2450/2012.0151-12]
5 **Peck-Radosavljevic M**. Review article: coagulation disorders in chronic liver disease. *Aliment Pharmacol Ther* 2007; **26** Suppl 1: 21-28 [PMID: 17958516 DOI: 10.1111/j.1365-2036.2007.03509.x]
6 **Mallett SV**. Clinical Utility of Viscoelastic Tests of Coagulation (TEG/ROTEM) in Patients with Liver Disease and during Liver Transplantation. *Semin Thromb Hemost* 2015; **41**: 527-537 [PMID: 26049072 DOI: 10.1055/s-0035-1550434]
7 **De Pietri L**, Bianchini M, Montalti R, De Maria N, Di Maira T, Begliomini B, Gerunda GE, di Benedetto F, Garcia-Tsao G, Villa E. Thrombelastography-guided blood product use before invasive procedures in cirrhosis with severe coagulopathy: A randomized, controlled trial. *Hepatology* 2016; **63**: 566-573 [PMID: 26340411 DOI: 10.1002/hep.28148]
8 **Kovalic AJ**, Khan MA, Malaver D, Whitson MJ, Teperman LW, Bernstein DE, Singal A, Satapathy SK. Thromboelastography versus standard coagulation testing in the assessment and reversal of coagulopathy among cirrhotics: a systematic review and meta-analysis. *Eur J Gastroenterol Hepatol* 2020; **32**: 291-302 [PMID: 32012141 DOI: 10.1097/MEG.0000000000001588]
9 **Vuyyuru SK**, Singh AD, Gamanagatti SR, Rout G, Gunjan D, Shalimar. A Randomized Control Trial of Thromboelastography-Guided Transfusion in Cirrhosis for High-Risk Invasive Liver-Related Procedures. *Dig Dis Sci* 2020; **65**: 2104-2111 [PMID: 31720889 DOI: 10.1007/s10620-019-05939-2]
10 **Hoffman M**, Monroe DM 3rd. A cell-based model of hemostasis. *Thromb Haemost* 2001; **85**: 958-965 [PMID: 11434702]
11 **Northup PG**, Caldwell SH. Coagulation in liver disease: a guide for the clinician. *Clin Gastroenterol Hepatol* 2013; **11**: 1064-1074 [PMID: 23506859 DOI: 10.1016/j.cgh.2013.02.026]
12 **Rodriguez-Castro KI**, Simioni P, Burra P, Senzolo M. Anticoagulation for the treatment of thrombotic complications in patients with cirrhosis. *Liver Int* 2012; **32**: 1465-1476 [PMID: 22734713 DOI: 10.1111/j.1478-3231.2012.02839.x]
13 **Bosch J**, Thabut D, Albillos A, Carbonell N, Spicak J, Massard J, D'Amico G, Lebrec D, de Franchis R, Fabricius S, Cai Y,

Bendtsen F; International Study Group on rFVIIa in UGI Hemorrhage. Recombinant factor VIIa for variceal bleeding in patients with advanced cirrhosis: A randomized, controlled trial. *Hepatology* 2008; **47**: 1604-1614 [PMID: 18393319 DOI: 10.1002/hep.22216]

14 **Bosch J**, Thabut D, Bendtsen F, D'Amico G, Albillos A, González Abraldes J, Fabricius S, Erhardtsen E, de Franchis R; European Study Group on rFVIIa in UGI Haemorrhage. Recombinant factor VIIa for upper gastrointestinal bleeding in patients with cirrhosis: a randomized, double-blind trial. *Gastroenterology* 2004; **127**: 1123-1130 [PMID: 15480990 DOI: 10.1053/j.gastro.2004.07.015]

15 **O'Shea RS**, Davitkov P, Ko CW, Rajasekhar A, Su GL, Sultan S, Allen AM, Falck-Ytter Y. AGA Clinical Practice Guideline on the Management of Coagulation Disorders in Patients With Cirrhosis. *Gastroenterology* 2021; **161**: 1615-1627.e1 [PMID: 34579936 DOI: 10.1053/j.gastro.2021.08.015]

16 **Rijken DC**, Kock EL, Guimarães AH, Talens S, Darwish Murad S, Janssen HL, Leebeek FW. Evidence for an enhanced fibrinolytic capacity in cirrhosis as measured with two different global fibrinolysis tests. *J Thromb Haemost* 2012; **10**: 2116-2122 [PMID: 22906184 DOI: 10.1111/j.1538-7836.2012.04901.x]

17 **Gish RG**, Stravitz RT. Correction of Coagulopathy of Liver Disease Prior to Procedures. *Gastroenterol Hepatol (N Y)* 2021; **17**: 16-23 [PMID: 34135700]

18 **Drolz A**, Ferlitsch A, Fuhrmann V. Management of Coagulopathy during Bleeding and Invasive Procedures in Patients with Liver Failure. *Visc Med* 2018; **34**: 254-258 [PMID: 30345282 DOI: 10.1159/000491106]

19 **Søgaard KK**, Horváth-Puhó E, Grønbaek H, Jepsen P, Vilstrup H, Sørensen HT. Risk of venous thromboembolism in patients with liver disease: a nationwide population-based case-control study. *Am J Gastroenterol* 2009; **104**: 96-101 [PMID: 19098856 DOI: 10.1038/ajg.2008.34]

20 **Wu H**, Nguyen GC. Liver cirrhosis is associated with venous thromboembolism among hospitalized patients in a nationwide US study. *Clin Gastroenterol Hepatol* 2010; **8**: 800-805 [PMID: 20566312 DOI: 10.1016/j.cgh.2010.05.014]

21 **Buliarca A**, Horhat A, Mocan T, Craciun R, Procopet B, Sparchez Z. Viscoelastic tests in liver disease: where do we stand now? *World J Gastroenterol* 2021; **27**: 3290-3302 [PMID: 34163112 DOI: 10.3748/wjg.v27.i23.3290]

22 **Abdel-Razik A**, Mousa N, Elhelaly R, Tawfik A. De-novo portal vein thrombosis in liver cirrhosis: risk factors and correlation with the Model for End-stage Liver Disease scoring system. *Eur J Gastroenterol Hepatol* 2015; **27**: 585-592 [PMID: 25769098 DOI: 10.1097/MEG.0000000000000325]

23 **European Association for the Study of the Liver**. EASL Clinical Practice Guidelines on prevention and management of bleeding and thrombosis in patients with cirrhosis. *J Hepatol* 2022; **76**: 1151-1184 [PMID: 35300861 DOI: 10.1016/j.jhep.2021.09.003]

24 **Tripodi A**, Chantarangkul V, Primignani M, Clerici M, Dell'era A, Aghemo A, Mannucci PM. Thrombin generation in plasma from patients with cirrhosis supplemented with normal plasma: considerations on the efficacy of treatment with fresh-frozen plasma. *Intern Emerg Med* 2012; **7**: 139-144 [PMID: 21298360 DOI: 10.1007/s11739-011-0528-4]

25 **Giannini EG**, Stravitz RT, Caldwell SH. Correction of hemostatic abnormalities and portal pressure variations in patients with cirrhosis. *Hepatology* 2014; **60**: 1442 [PMID: 24452495 DOI: 10.1002/hep.27029]

26 **Giannini EG**, Greco A, Marenco S, Andorno E, Valente U, Savarino V. Incidence of bleeding following invasive procedures in patients with thrombocytopenia and advanced liver disease. *Clin Gastroenterol Hepatol* 2010; **8**: 899-902; quiz e109 [PMID: 20601131 DOI: 10.1016/j.cgh.2010.06.018]

27 **Mitchell O**, Feldman DM, Diakow M, Sigal SH. The pathophysiology of thrombocytopenia in chronic liver disease. *Hepat Med* 2016; **8**: 39-50 [PMID: 27186144 DOI: 10.2147/HMER.S74612]

28 **Arif S**, Khan AS, Khan AR. Changes in fibrinogen level in liver cirrhosis. *J Ayub Med Coll Abbottabad* 2002; **14**: 19-21 [PMID: 12238339]

29 **Drolz A**, Horvatits T, Roedl K, Rutter K, Staufer K, Kneidinger N, Holzinger U, Zauner C, Schellongowski P, Heinz G, Perkmann T, Kluge S, Trauner M, Fuhrmann V. Coagulation parameters and major bleeding in critically ill patients with cirrhosis. *Hepatology* 2016; **64**: 556-568 [PMID: 27124745 DOI: 10.1002/hep.28628]

30 **Bolliger D**, Szlam F, Molinaro RJ, Rahe-Meyer N, Levy JH, Tanaka KA. Finding the optimal concentration range for fibrinogen replacement after severe haemodilution: an in vitro model. *Br J Anaesth* 2009; **102**: 793-799 [PMID: 19420005 DOI: 10.1093/bja/aep098]

31 **Schöchl H**, Frietsch T, Pavelka M, Jámbor C. Hyperfibrinolysis after major trauma: differential diagnosis of lysis patterns and prognostic value of thrombelastometry. *J Trauma* 2009; **67**: 125-131 [PMID: 19590321 DOI: 10.1097/TA.0b013e31818b2483]

32 **Violl F**, Basili S, Ferro D, Quintarelli C, Alessandril C, Cordova C. Association between high values of D-dimer and tissue-plasminogen activator activity and first gastrointestinal bleeding in cirrhotic patients. CALC Group. *Thromb Haemost* 1996; **76**: 177-183 [PMID: 8865526]

33 **Tripodi A**, Salerno F, Chantarangkul V, Clerici M, Cazzaniga M, Primignani M, Mannuccio Mannucci P. Evidence of normal thrombin generation in cirrhosis despite abnormal conventional coagulation tests. *Hepatology* 2005; **41**: 553-558 [PMID: 15726661 DOI: 10.1002/hep.20569]

34 **Groeneveld D**, Porte RJ, Lisman T. Thrombomodulin-modified thrombin generation testing detects a hypercoagulable state in patients with cirrhosis regardless of the exact experimental conditions. *Thromb Res* 2014; **134**: 753-756 [PMID: 25065556 DOI: 10.1016/j.thromres.2014.07.010]

35 **Coleman JR**, Moore EE, Chapman MP, Banerjee A, Silliman CC, Ghasabyan A, Chandler J, Samuels JM, Sauaia A. Rapid TEG efficiently guides hemostatic resuscitation in trauma patients. *Surgery* 2018; **164**: 489-493 [PMID: 29903508 DOI: 10.1016/j.surg.2018.04.029]

36 **Jeger V**, Zimmermann H, Exadaktylos AK. Can RapidTEG accelerate the search for coagulopathies in the patient with multiple injuries? *J Trauma* 2009; **66**: 1253-1257 [PMID: 19359945 DOI: 10.1097/TA.0b013e31819d3caf]

37 **Cotton BA**, Faz G, Hatch QM, Radwan ZA, Podbielski J, Wade C, Kozar RA, Holcomb JB. Rapid thrombelastography delivers real-time results that predict transfusion within 1 hour of admission. *J Trauma* 2011; **71**: 407-14; discussion 414 [PMID: 21825945 DOI: 10.1097/TA.0b013e31821e1bf0]

38 **Wang Z**, Li J, Cao Q, Wang L, Shan F, Zhang H. Comparison Between Thromboelastography and Conventional

Coagulation Tests in Surgical Patients With Localized Prostate Cancer. *Clin Appl Thromb Hemost* 2018; **24**: 755-763 [PMID: 28870084 DOI: 10.1177/1076029617724229]

39 **Pekelharing J**, Furck A, Banya W, Macrae D, Davidson SJ. Comparison between thromboelastography and conventional coagulation tests after cardiopulmonary bypass surgery in the paediatric intensive care unit. *Int J Lab Hematol* 2014; **36**: 465-471 [PMID: 24325756 DOI: 10.1111/ijlh.12171]

40 **Park MS**, Martini WZ, Dubick MA, Salinas J, Butenas S, Kheirabadi BS, Pusateri AE, Vos JA, Guymon CH, Wolf SE, Mann KG, Holcomb JB. Thromboelastography as a better indicator of hypercoagulable state after injury than prothrombin time or activated partial thromboplastin time. *J Trauma* 2009; **67**: 266-75; discussion 275 [PMID: 19667878 DOI: 10.1097/TA.0b013e3181ae6f1c]

41 **Intagliata NM**, Argo CK, Stine JG, Lisman T, Caldwell SH, Violi F; faculty of the 7th International Coagulation in Liver Disease. Concepts and Controversies in Haemostasis and Thrombosis Associated with Liver Disease: Proceedings of the 7th International Coagulation in Liver Disease Conference. *Thromb Haemost* 2018; **118**: 1491-1506 [PMID: 30060258 DOI: 10.1055/s-0038-1666861]

42 **Hung A**, Garcia-Tsao G. Acute kidney injury, but not sepsis, is associated with higher procedure-related bleeding in patients with decompensated cirrhosis. *Liver Int* 2018; **38**: 1437-1441 [PMID: 29393567 DOI: 10.1111/liv.13712]

43 **Somani V**, Amarapurkar D, Shah A. Thromboelastography for Assessing the Risk of Bleeding in Patients With Cirrhosis-Moving Closer. *J Clin Exp Hepatol* 2017; **7**: 284-289 [PMID: 29234191 DOI: 10.1016/j.jceh.2017.03.001]

44 **Pandey CK**, Saluja V, Gaurav K, Tandon M, Pandey VK, Bhadoria AS. K time & maximum amplitude of thromboelastogram predict post-central venous cannulation bleeding in patients with cirrhosis: A pilot study. *Indian J Med Res* 2017; **145**: 84-89 [PMID: 28574019 DOI: 10.4103/ijmr.IJMR_749_14]

45 **Roberts LN**, Lisman T, Stanworth S, Hernandez-Gea V, Magnusson M, Tripodi A, Thachil J. Periprocedural management of abnormal coagulation parameters and thrombocytopenia in patients with cirrhosis: Guidance from the SSC of the ISTH. *J Thromb Haemost* 2022; **20**: 39-47 [PMID: 34661370 DOI: 10.1111/jth.15562]

46 **Northup PG**, Garcia-Pagan JC, Garcia-Tsao G, Intagliata NM, Superina RA, Roberts LN, Lisman T, Valla DC. Vascular Liver Disorders, Portal Vein Thrombosis, and Procedural Bleeding in Patients With Liver Disease: 2020 Practice Guidance by the American Association for the Study of Liver Diseases. *Hepatology* 2021; **73**: 366-413 [PMID: 33219529 DOI: 10.1002/hep.31646]

47 **Cerini F**, Gonzalez JM, Torres F, Puente Á, Casas M, Vinaixa C, Berenguer M, Ardevol A, Augustin S, Llop E, Senosiaín M, Villanueva C, de la Peña J, Bañares R, Genescá J, Sopeña J, Albillos A, Bosch J, Hernández-Gea V, Garcia-Pagán JC. Impact of anticoagulation on upper-gastrointestinal bleeding in cirrhosis. A retrospective multicenter study. *Hepatology* 2015; **62**: 575-583 [PMID: 25773591 DOI: 10.1002/hep.27783]

48 **Rout G**, Shalimar, Gunjan D, Mahapatra SJ, Kedia S, Garg PK, Nayak B. Thromboelastography-guided Blood Product Transfusion in Cirrhosis Patients With Variceal Bleeding: A Randomized Controlled Trial. *J Clin Gastroenterol* 2020; **54**: 255-262 [PMID: 31008867 DOI: 10.1097/MCG.0000000000001214]

49 **Maria A**, Lal BB, Khanna R, Sood V, Mukund A, Bajpai M, Alam S. Rotational thromboelastometry-guided blood component use in cirrhotic children undergoing invasive procedures: Randomized controlled trial. *Liver Int* 2022; **42**: 2492-2500 [PMID: 35977053 DOI: 10.1111/liv.15398]

50 **Wei H**, Child LJ. Clinical utility of viscoelastic testing in chronic liver disease: A systematic review. *World J Hepatol* 2020; **12**: 1115-1127 [PMID: 33312434 DOI: 10.4254/wjh.v12.i11.1115]

51 **Kumar M**, Ahmad J, Maiwall R, Choudhury A, Bajpai M, Mitra LG, Saluja V, Mohan Agarwal P, Bihari C, Shasthry SM, Jindal A, Bhardwaj A, Kumar G, Sarin SK. Thromboelastography-Guided Blood Component Use in Patients With Cirrhosis With Nonvariceal Bleeding: A Randomized Controlled Trial. *Hepatology* 2020; **71**: 235-246 [PMID: 31148204 DOI: 10.1002/hep.30794]

52 **McKee RF**, Hodson S, Dawes J, Garden OJ, Carter DC. Plasma concentrations of endogenous heparinoids in portal hypertension. *Gut* 1992; **33**: 1549-1552 [PMID: 1452082 DOI: 10.1136/gut.33.11.1549]

53 **Montalto P**, Vlachogiannakos J, Cox DJ, Pastacaldi S, Patch D, Burroughs AK. Bacterial infection in cirrhosis impairs coagulation by a heparin effect: a prospective study. *J Hepatol* 2002; **37**: 463-470 [PMID: 12217599 DOI: 10.1016/s0168-8278(02)00208-8]

54 **Senzolo M**, Agarwal S, Zappoli P, Vibhakorn S, Mallett S, Burroughs AK. Heparin-like effect contributes to the coagulopathy in patients with acute liver failure undergoing liver transplantation. *Liver Int* 2009; **29**: 754-759 [PMID: 19220741 DOI: 10.1111/j.1478-3231.2009.01977.x]

55 **Thalheimer U**, Triantos C, Samonakis D, Patch D, Burroughs AK, Riddell A, Perry D. Endogenous heparinoids in acute variceal bleeding. *Gut* 2005; **54**: 310-311 [PMID: 15647203 DOI: 10.1136/gut.2004.051474]

56 **Chau TN**, Chan YW, Patch D, Tokunaga S, Greenslade L, Burroughs AK. Thrombelastographic changes and early rebleeding in cirrhotic patients with variceal bleeding. *Gut* 1998; **43**: 267-271 [PMID: 10189856 DOI: 10.1136/gut.43.2.267]

57 **Triantos C**, Louvros E, Kalafateli M, Riddell A, Thalheimer U, Michailidou M, Thomopoulos K, Lampropoulou-Karatza C, Gogos C, Nikolopoulou V, Burroughs AK. Endogenous heparinoids detected by anti-Xa activity are present in blood during acute variceal bleeding in cirrhosis. A prospective study. *J Gastrointestin Liver Dis* 2014; **23**: 187-194 [PMID: 24949611 DOI: 10.15403/jgld.2014.1121.232.cht1]

58 **Kang YG**, Martin DJ, Marquez J, Lewis JH, Bontempo FA, Shaw BW Jr, Starzl TE, Winter PM. Intraoperative changes in blood coagulation and thrombelastographic monitoring in liver transplantation. *Anesth Analg* 1985; **64**: 888-896 [PMID: 3896028]

59 **Trzebicki J**, Flakiewicz E, Kosieradzki M, Blaszczyk B, Kołacz M, Jureczko L, Pacholczyk M, Chmura A, Lagiewska B, Lisik W, Wasiak D, Kosson D, Kwiatkowski A, Lazowski T. The use of thromboelastometry in the assessment of hemostasis during orthotopic liver transplantation reduces the demand for blood products. *Ann Transplant* 2010; **15**: 19-24 [PMID: 20877262]

60 **Wang SC**, Shieh JF, Chang KY, Chu YC, Liu CS, Loong CC, Chan KH, Mandell S, Tsou MY. Thromboelastography-guided transfusion decreases intraoperative blood transfusion during orthotopic liver transplantation: randomized clinical

trial. *Transplant Proc* 2010; **42**: 2590-2593 [PMID: 20832550 DOI: 10.1016/j.transproceed.2010.05.144]

61 **Roullet S**, Freyburger G, Cruc M, Quinart A, Stecken L, Audy M, Chiche L, Sztark F. Management of bleeding and transfusion during liver transplantation before and after the introduction of a rotational thromboelastometry-based algorithm. *Liver Transpl* 2015; **21**: 169-179 [PMID: 25331016 DOI: 10.1002/lt.24030]

62 **Pereboom IT**, de Boer MT, Haagsma EB, Hendriks HG, Lisman T, Porte RJ. Platelet transfusion during liver transplantation is associated with increased postoperative mortality due to acute lung injury. *Anesth Analg* 2009; **108**: 1083-1091 [PMID: 19299765 DOI: 10.1213/ane.0b013e3181948a59]

63 **Ferro D**, Celestini A, Violi F. Hyperfibrinolysis in liver disease. *Clin Liver Dis* 2009; **13**: 21-31 [PMID: 19150306 DOI: 10.1016/j.cld.2008.09.008]

64 **Porte RJ**, Bontempo FA, Knot EA, Lewis JH, Kang YG, Starzl TE. Systemic effects of tissue plasminogen activator-associated fibrinolysis and its relation to thrombin generation in orthotopic liver transplantation. *Transplantation* 1989; **47**: 978-984 [PMID: 2499962 DOI: 10.1097/00007890-198906000-00012]

65 **Homatas J**, Wasantapruek S, Von Kaulla E, Von Kaulla KN, Eiseman B. Clotting abnormalities following orthotopic and heterotopic transplantation of marginally preserved pig livers. *Acta Hepatosplenol* 1971; **18**: 14-26 [PMID: 4927688]

66 **Huang X**, Fan X, Zhang R, Jiang S, Yang K, Chen S. Systemic inflammation and portal vein thrombosis in cirrhotic patients with gastroesophageal varices. *Eur J Gastroenterol Hepatol* 2020; **32**: 401-405 [PMID: 31356372 DOI: 10.1097/MEG.0000000000001526]

67 **Zanetto A**, Senzolo M, Vitale A, Cillo U, Radu C, Sartorello F, Spiezia L, Campello E, Rodriguez-Castro K, Ferrarese A, Farinati F, Burra P, Simioni P. Thromboelastometry hypercoagulable profiles and portal vein thrombosis in cirrhotic patients with hepatocellular carcinoma. *Dig Liver Dis* 2017; **49**: 440-445 [PMID: 28109767 DOI: 10.1016/j.dld.2016.12.019]

68 **He Y**, Yuan S, Guo X, Yi F, Xu X, An Y, Xu S, Ageno W, Qi X. Association of thromboelastography profile with severity of liver cirrhosis and portal venous system thrombosis. *BMC Gastroenterol* 2021; **21**: 253 [PMID: 34098892 DOI: 10.1186/s12876-021-01832-3]

69 **Krzanicki D**, Sugavanam A, Mallett S. Intraoperative hypercoagulability during liver transplantation as demonstrated by thromboelastography. *Liver Transpl* 2013; **19**: 852-861 [PMID: 23696318 DOI: 10.1002/lt.23668]

70 **Lerner AB**, Sundar E, Mahmood F, Sarge T, Hanto DW, Panzica PJ. Four cases of cardiopulmonary thromboembolism during liver transplantation without the use of antifibrinolytic drugs. *Anesth Analg* 2005; **101**: 1608-1612 [PMID: 16301227 DOI: 10.1213/01.ANE.0000184256.28981.2B]

71 **Ha NB**, Regal RE. Anticoagulation in Patients With Cirrhosis: Caught Between a Rock-Liver and a Hard Place. *Ann Pharmacother* 2016; **50**: 402-409 [PMID: 26861989 DOI: 10.1177/1060028016631760]

72 **Artang R**, Frandsen NJ, Nielsen JD. Application of basic and composite thrombelastography parameters in monitoring of the antithrombotic effect of the low molecular weight heparin dalteparin: an in vivo study. *Thromb J* 2009; **7**: 14 [PMID: 19903343 DOI: 10.1186/1477-9560-7-14]

73 **Dias JD**, Lopez-Espina CG, Panigada M, Dalton HJ, Hartmann J, Achneck HE. Cartridge-Based Thromboelastography Can Be Used to Monitor and Quantify the Activity of Unfractionated and Low-Molecular-Weight Heparins. *TH Open* 2019; **3**: e295-e305 [PMID: 31523746 DOI: 10.1055/s-0039-1696658]

World Journal of Gastroenterology

Submit a Manuscript: https://www.f6publishing.com

World J Gastroenterol 2023 March 7; 29(9): 1475-1491

DOI: 10.3748/wjg.v29.i9.1475

ISSN 1007-9327 (print) ISSN 2219-2840 (online)

ORIGINAL ARTICLE

Basic Study

Adenosine 2A receptor contributes to the facilitation of post-infectious irritable bowel syndrome by γδ T cells *via* the PKA/CREB/NF-κB signaling pathway

Li-Wei Dong, Yi-Yao Chen, Chao-Chao Chen, Zhi-Chao Ma, Jiao Fu, Bai-Li Huang, Fu-Jin Liu, Dong-Chun Liang, De-Ming Sun, Cheng Lan

Specialty type: Gastroenterology and hepatology

Provenance and peer review: Unsolicited article; Externally peer reviewed.

Peer-review model: Single blind

Peer-review report's scientific quality classification

Grade A (Excellent): A
Grade B (Very good): B
Grade C (Good): C
Grade D (Fair): 0
Grade E (Poor): 0

P-Reviewer: Lee EW, South Korea; Shin CM, South Korea; Yashiro M, Japan

Received: December 5, 2022
Peer-review started: December 5, 2022
First decision: January 2, 2023
Revised: January 11, 2023
Accepted: February 22, 2023
Article in press: February 22, 2023
Published online: March 7, 2023

Li-Wei Dong, Yi-Yao Chen, Chao-Chao Chen, Zhi-Chao Ma, Jiao Fu, Bai-Li Huang, Fu-Jin Liu, Cheng Lan, Department of Gastroenterology, Hainan General Hospital, Affiliated Hainan Hospital, Hainan Medical University, Haikou 570311, Hainan Province, China

Dong-Chun Liang, De-Ming Sun, Doheny Eye Institute, Department of Ophthalmology, David Geffen School of Medicine, University of California Los Angeles, Los Angeles, CA 90033, United States

Corresponding author: Cheng Lan, MD, PhD, Chief Doctor, Professor, Department of Gastroenterology, Hainan General Hospital, Affiliated Hainan Hospital, Hainan Medical University, No. 19 Xiuhua Road, Xiuying District, Haikou 570311, Hainan Province, China. lancheng71@163.com

Abstract

BACKGROUND

Immunological dysfunction-induced low-grade inflammation is regarded as one of the predominant pathogenetic mechanisms in post-infectious irritable bowel syndrome (PI-IBS). γδ T cells play a crucial role in innate and adaptive immunity. Adenosine receptors expressed on the surface of γδ T cells participate in intestinal inflammation and immunity regulation.

AIM

To investigate the role of γδ T cell regulated by adenosine 2A receptor (A2AR) in PI-IBS.

METHODS

The PI-IBS mouse model has been established with *Trichinella spiralis (T. spiralis)* infection. The intestinal A2AR and A2AR in γδ T cells were detected by immunohistochemistry, and the inflammatory cytokines were measured by western blot. The role of A2AR on the isolated γδ T cells, including proliferation, apoptosis, and cytokine production, were evaluated *in vitro*. Their A2AR expression was measured by western blot and reverse transcription polymerase chain reaction (RT-PCR). The animals were administered with A2AR agonist, or A2AR antagonist. Besides, γδ T cells were also injected back into the animals, and the

parameters described above were examined, as well as the clinical features. Furthermore, the A2AR-associated signaling pathway molecules were assessed by western blot and RT-PCR.

RESULTS

PI-IBS mice exhibited elevated ATP content and A2AR expression ($P < 0.05$), and suppression of A2AR enhanced PI-IBS clinical characteristics, indicated by the abdominal withdrawal reflex and colon transportation test. PI-IBS was associated with an increase in intestinal T cells, and cytokine levels of interleukin-1 (IL-1), IL-6, IL-17A, and interferon-α (IFN-α). Also, γδ T cells expressed A2AR *in vitro* and generated IL-1, IL-6, IL-17A, and IFN-α, which can be controlled by A2AR agonist and antagonist. Mechanistic studies demonstrated that the A2AR antagonist improved the function of γδ T cells through the PKA/CREB/NF-κB signaling pathway.

CONCLUSION

Our results revealed that A2AR contributes to the facilitation of PI-IBS by regulating the function of γδ T cells *via* the PKA/CREB/NF-κB signaling pathway.

Key Words: Irritable bowel syndrome; Adenosine 2A receptor; γδ T cells; Post-infectious irritable bowel syndrome; Signaling pathway; Regulation

Core Tip: Immunological dysfunction-induced low-grade inflammation is regarded as one of the most important pathogenetic mechanisms in post-infectious irritable bowel syndrome. γδ T cells play a crucial role in innate and adaptive immunity. The adenosine molecule and receptors regulate intestinal inflammation and immunity. Through the PKA/CREB/NF-κB signaling pathway, we showed that adenosine 2A receptor contributes to the facilitation of post-infectious irritable bowel syndrome by T cells.

Citation: Dong LW, Chen YY, Chen CC, Ma ZC, Fu J, Huang BL, Liu FJ, Liang DC, Sun DM, Lan C. Adenosine 2A receptor contributes to the facilitation of post-infectious irritable bowel syndrome by γδ T cells *via* the PKA/CREB/NF-κB signaling pathway. *World J Gastroenterol* 2023; 29(9): 1475-1491
URL: https://www.wjgnet.com/1007-9327/full/v29/i9/1475.htm
DOI: https://dx.doi.org/10.3748/wjg.v29.i9.1475

INTRODUCTION

Irritable bowel syndrome (IBS), a functional gastrointestinal disorder with abnormal bowel habits and/or faecal traits, has been increasing in prevalence in developing countries since 1990[1]. The concept of post-infectious IBS (PI-IBS) was derived from clinical observations of patients with previous acute gastrointestinal infections[2]. Patients often suffer from refractory discomfort, low quality of life, and high healthcare economic burden, but current treatments reap unsatisfactory therapeutic results due to the lack of specific targets[3]. Numerous studies in the literature have shown that 1/3 of IBS patients have a history of gastrointestinal infection, suggesting that a persistent inflammatory response may explain the inconsistency between the intestinal response of PI-IBS patients and the normal gut[4]. Therefore, researchers generally agree that PI-IBS is also essentially a post-inflammatory immune dysfunction[5] and that reducing the intestinal inflammatory response is expected to improve clinical symptoms and life quality. For the potential therapeutic target of PI-IBS, upregulation of EphA2 expression and activation of the NF-κB signaling pathway have been reported to alleviate PI-IBS-related symptoms[6], while miRNA-510 has also been proved to regulate the intestinal inflammatory response in PI-IBS by targeting PRDX1[7].

γδ T cells are a subpopulation of T lymphocytes with a distinct phenotype and function, although they represent only a small proportion of the total T cells. γδ T cells bridge the gap between innate and adaptive immunity, determining the type of immune response and maintaining homeostasis in mucosal tissues. In inflammatory and immune responses, γδ T cells play a complex dual role depending on the context. On the one hand, γδ T cells present antigens to immune cells and trigger the recognition of these antigens by immune cells, leading to an adaptive immune response, promoting the secretion of chemokines and cytokines, and recruiting inflammatory cells[8,9]. On the other hand, γδ T cells inhibit the inflammatory process by conducting regulatory cytokines such as interferon-α (IFN-α), interleukin-10 (IL-10), tumor necrosis factor-α (TNF-α), and IL-17 and eliminating over-activated inflammatory effector cells such as macrophages and polymorphonuclear leukocytes through cytotoxic effects[10]. In animal models of experimental autoimmune encephalomyelitis, rheumatoid arthritis and non-fatty

diabetes, γδ T cells are proved to be the causative factor whereas rats with colitis and sepsis and mice with EAU were found to benefit from their presence[11]. According to our previous research, we have demonstrated that γδ T cells could alleviate PI-IBS through promoting Th17 polarization *via* their HSP70 receptor[12].

One of the many receptors expressed on the surface of γδ T cells is adenosine 2A receptor (A2AR), a classical G protein-coupled receptor with a high affinity for adenosine (ADO)[13]. A2AR is expressed in many immune cells, such as regulatory T cells, cytotoxic T cells, macrophages, *etc*. Its homologous family members include four isoforms, namely A1R, A2aR, A2bR, and A3R. These ARs are distributed in different tissues. For example, A1R is in the small intestine, A2aR and A2bR are in the cecum and colon, and A3R is in the ileum and colon[14]. A2AR forms the CD39-CD73-A2AR adenosine metabolic pathway with CD39 and CD73: first, CD39 cleaves extracellular ATP into AMP, which then binds to CD73 and is converted to ADO by CD73. ADO then binds to A2AR, which in turn interacts with Gs family proteins to increase intracellular cAMP levels and activate the downstream PKA/CREB-related pathway. Thus, the adenosine-A2AR pathway plays an important role in protecting normal organs and tissues from the autoimmune response of immune cells[15-17]. There are fewer reports on A2AR and intestinal inflammatory injury. Researchers have found that ADO can inhibit intestinal inflammatory injury in chronically septic mice *via* interacting with A1AR and A2AR[18]. And according to the research from Hou *et al*[19], electroacupuncture reduced visceral pain in rats with inflammatory bowel disease by interfering with adenosine receptors. However, there are no studies correlating A2AR with the pathogenesis of IBS, especially PI-IBS. Recently, Sun *et al*[20] reported that A2AR is able to bind to mGluR5 and exhibits a unique role in maintaining the function of the intestinal barrier in enteric glial cells against hypoxia-induced cellular damage. The above findings suggest that ARs, especially the A2AR isoform, may play a key role in the pathogenesis of PI-IBS and could potentially be a novel target for intervention in PI-IBS progression.

Hence, considering that the correlation between A2AR and PI-IBS remains unclear, the function of A2AR on the surface of γδ T cells has not been fully elucidated, and the precise A2AR-related signaling pathway mediating PI-IBS progression in γδ T cells awaits to be explored. It is an urgent issue to evaluate the role of A2AR in regulating γδ T cells on PI-IBS pathogenesis.

MATERIALS AND METHODS

Animals and experimental design

Ninety-six female 57BL/6 mice were provided by the Medical Animal Center of the Hainan Medical College. All animals were housed in a sterile, suitable environment and fed *ad libitum* with food and water that met cleanliness standards. The animals used in the experiments were cared for and handled by the Chinese Guide for Laboratory Animals. The experimental procedures were examined and approved by the Animal Care and Utilization Committee of Hainan.

Animals were randomly divided into 4 groups (n = 24 per group): The control group, the PI-IBS group, the IBS + SCH58261 group, and the IBS + CGS21680 group. A quarter of mice were killed in each group, then intestinal A2AR protein and mRNA levels, cytokine expression and secretion plus signaling pathway activation were investigated, respectively. Another six mice were used for γδ T cell isolation. The remaining mice were used for A2AR lentivirus infection and cell reinfusion assay.

PI-IBS Model

The Trichinella spiralis (*T. spiralis*) infected the mice as described earlier in Lanzhou Animal Medical Institute[21,22]. Briefly, parasite larvae were isolated from cysts of SD rats, which have been infected with *T. spiralis* for 60 d and digested with 1.5% pepsin. Mice were then fed with larvae, which were resuspended in 0.2 mL of saline (300 larvae per mouse). At the same time, the control group was only fed with 0.9% saline.

Histopathological analysis

After 8 wk of infection, animals were euthanized, meanwhile, their ileal tissues were fixed with 10% formalin at 4 °C for 10 d, then dried in ethanol, and embedded in paraffin. The 5 micrometers sections were made. After dewaxing and hydration, they were stained with hematoxylin-eosin (HE). In addition, HE staining was used to assess inflammation scores according to a previous scoring system[23].

Abdominal withdrawal reflex

The abdominal withdrawal reflex (AWR) was administered to assess visceral hypersensitivity[24]. A catheter and air chamber were introduced *via* the anus of sedated animals. The air chamber was inflated to a capacity of 0.25/0.35/0.5/0.66 mL in 15 min on a number of occasions. The animals were allowed 30 s of rest between each distending period. The AWR criterion for scoring: When stimulated, the animals' mood is stable, 0 points; if they are unstable, occasionally bending their necks, 1 point; slightly contracting their abdomen and back muscles, 2 points; intensively contracting their abdomen muscles

and lifting the abdomen from the ground, 3 points; intensively contracting abdomen muscles, bowing abdomen, and lifting abdomen and perineum, 4 points.

Colon transportation test and stool scale

The colon transit test (CTT) was used to assess intestinal motility. After ingesting 0.4 mL of active carbon, the timing was documented. The entire feces collected during 8 h were graded using the Bristol stool scale: 1 point for normal-shaped stools; 2 points for stools that are soft or malformed; 3 points for stools that are watery[25].

Immunohistochemistry

Immunohistochemistry was performed on the cells as previously described[26]. Briefly, cells were fixed in suspension with 4% PFA for uniform distribution on the slides. After rinsing in phosphate-buffered saline (PBS), slides were incubated with anti-mouse A2AR monoclonal antibody (1:150; Abcam, Cambridge, United Kingdom) overnight at 4 °C and then with HRP secondary antibody (SP-9001, Beijing Sequoia Jinqiao, Beijing, China) for 1 h at room temperature. Reactivity was detected using the DAB reagent (Beijing Sequoia Jinqiao, Beijing, China). The primary antibody was substituted with PBS as a negative control. As the cell membrane was the main localization site of A2AR, the expression of A2AR was evaluated by a semi-quantitative integration technique. A2AR protein expression staining intensity was rated as 0 (no staining), 1 (weak staining), 2 (moderate staining), and 3 (strong staining). The percentage of positively stained cells in the visual field was categorized as 0 (5%), 1 (5%-25%), 2 (26%-50%), 3 (51%-75%), or 4 (> 75%). The evaluation was represented as the product of the positive rate score and staining intensity score, with a score of greater than or equal to 6 indicating a favorable evaluation. The above staining was examined using Nikon DR-Si2 cell counting software and digital image analysis was employed. Moreover, the scoring was done in a double-blind way, which was confirmed by two pathologists who were not involved in this study and unaware of the clinical-pathological data.

Western blotting

Western blot was used to detect altered protein expression. Ileal tissue samples were lysed with RIPA coupled with brief ultrasonic pulverization. After lysis was completed, the homogenate was centrifuged at 4 °C for 30 min, the precipitate was discarded and the supernatant was retained. The protein content of the supernatant was determined by the Bradford method. 40 μg of protein was taken for SDS-PAGE gel electrophoresis, and the protein blot was transferred to the PVDF membrane. Transfer conditions: β-actin, A2AR (200 mA, 90 min); PKA, p-PKA (200 mA, 120 min followed by 300 mA, 30 min); CREB, p-CREB (200 mA, 20 min followed by 300 mA, 15 min); NF-κB (200 mA, 120 min); claudin-1 (200 mA, 70 min), occludin (200 mA, 120 min); ZO-1 (200 mA, 120 min followed by 300 mA, 60 min); IL-1β (200 mA, 50 min); IL-6 (200 mA, 70 min); IL-17A (200 mA, 50 min); IFN-α (200 mA, 60 min). The primary antibodies presented in Table 1 were rabbit anti-mouse multi-clonal.

The diluted primary antibodies were incubated with the PVDF membrane at 4 °C for over 12 h. On the following day, the membrane was rinsed with TBST for three times, and ECL chemiluminescent test was performed. In a dark setting, the grayscale value was identified by improved chemiluminescence. The protein/actin grayscale value represented the relative protein expression level.

Real-time quantitative polymerase chain reaction

mRNA alteration was determined through Real-time quantitative polymerase chain reaction (PCR). Briefly, RNA was extracted from the tissue of the terminal ileum by using Trizol and DNase I. Primers were constructed based on the gene sequences of mice (Table 2). β-Actin served as an internal reference. The RNA was then reverse transcribed to cDNA according to the steps of the TAKARA PrimeScript kit (TAKARA-RR047A), and real-time quantitative PCR was performed according to the following procedure: pre-denaturation at 94 °C for 5 min; denaturation at 94 °C for 1 min; 30 cycles of amplification and qualification at 57 °C and 60 °C; the ultimate step was prolongation at 72 °C for 7 min. Results are expressed as the ratio of target genes to control genes.

Measurement of ATP concentration

The tissue samples were sonicated and centrifuged at 4 °C for 15 min followed by the addition of double distilled water (1:9). The 10% homogenate was continued to be centrifuged at 3000 rpm for another 10 min. The supernatant was collected for subsequent analysis.

The ATP concentration was determined by the colorimetric method. Specifically, the OD value of the liquid in the colorimetric tube was measured at 636 nm. ATP concentration was calculated as: ATP concentration (mol/g prot) = (measured OD - control OD)/(standard OD - blank OD) × standard concentration (1000 mol/L)/sample concentration (g prot/L).

Isolation and purification of γδ T cells

γδ T cells were extracted from the spleen of animals[27]. Spleens were collected aseptically from 8 to 10-week female mice and stored in 1 × PBS on ice. Splenocytes were then isolated and red blood cells were

Table 1 The dilution ratio for primary antibodies

Primary antibodies	Dilution ratio
β-actin	1:1000
A2AR	1:500
NF-κB	1:2000
PKA	1:1000
p-PKA	1:2000
CREB	1:1000
p-CREB	1:1000
ZO-1	1:1000
Occludin	1:1000
Claudin-1	1:1000
IL-1β	1:1000
IL-6	1:1000
IL-17A	1:500
IFN-α	1:1000

A2AR: Adenosine 2A receptor; IL: Interleukin; IFN-α: Interferon-α.

Table 2 Primers used in this study

Name	Primer	Sequence	Size
β-actin	Forward	5′-CACGATGGAGGGGCCGGACTCATC-3′	240 bp
	Reverse	5′-TAAAGACCTCTATGCCAACACAGT-3′	
NF-κB	Forward	5′-CACCGGATTGAAGAGAAGCG-3′	194 bp
	Reverse	5′-AAGTTGATGGTGCTGAGGGA-3′	
CREB	Forward	5′-GCTGGCTAACAATGGTACGG-3′	230 bp
	Reverse	5′-CCATAACAACTCCAGGGGCA-3′	
PKA	Forward	5′-GGGCGTGCTGATCTATGAGA -3′	169 bp
	Reverse	5′-TCGCTTTGTCAGATCCACCT-3′	
A2AR	Forward	5′-GCCTCTTCTTCGCCTGCTTTGTCC-3′	140 bp
	Reverse	5′-GCCCTTCGCCCTCATACCCGTCAC-3′	

lysed with a hypotonic solution. γδ TCR cells were selected by depletion of CD11b, B220, CD4 and CD8 cells, negative selection using biotinylated antibodies and EasySep Biotin Positive Selection Kit (StemCell) according to the manufacturer's protocol.

The magnetic separation process was carried out as follows: Biotin Anti-CD11b, Biotin Anti-B220, Biotin Anti-CD4, and Biotin Anti-CD8 (1/100 × dilution, 10 μL/mL) were added respectively, then the whole system was mixed thoroughly and incubated at room temperature for 15 min. After that, 10 mL 1 × PBS + 0.526 mmol/L EDTA + 2% FBS was added and rotated at 1.4 k for 5 min at 4 °C. Discarding the supernatant and then the cells were resuspended at 1 × 10^8 cells/mL in the mentioned buffer. Then, Biotin Select Cocktail (100 μL/mL) was added and mixed thoroughly, following the incubation at room temperature for 15 min. Next, the beads from the EasySep kit were vortexed for 15 to 30 min and added (50 μL/mL), the new system was mixed thoroughly and incubated at room temperature for 10 min. At room temperature, tubes were placed into silver EasySep magnets, incubated for 5 min, and the supernatant fraction was poured into a new 15 mL tube. Then the cells were counted for further cell sorting.

The antibodies for sorting were as follows: γδTCR Alexa 488 (1/100 × dilution), CD8 PE (1/100 × dilution), CD4 PerCP Cy5.5 (1/100 × dilution), CD11b APC (1/100 × dilution) and B220 PEcy7 (1/100 × dilution). Before sorting, cells were stained at 4 °C for 30 min on ice with the mentioned antibodies.

Then, we washed the cells with 1 × PBS and resuspended to 5 × 10^6 cells/mL for sorting[28].

Cell proliferation assays

The proliferation of isolated γδ T cells was detected by CCK8 assay. Cells were resuspended in 100 μL of the medium at the density of 5 × 10^4 cells per well, then added to 96-well plates and waited for the cells to stick. After that, 100 nmol/L CGS-21680 or 1 μnmol/L SCH58261 was added to different wells of the 96-well plate, and the cells were continued to be cultured at 37 °C with 5% CO_2 for more than half an hour. Finally, 20 μL CCK8 was added to each well and the incubation was continued at 37 °C, 5% CO_2 for another 2 h, and the OD value at 450 nm was measured by Multiscan Spectrum.

Cell apoptosis assays

The extracted γδ T cells were uniformly distributed in six-well plates (5 × 10^5 cells/well). Subsequently, 100 nnmol/L CGS-21680 or 1 μnmol/L SCH58261 were added, respectively, and incubated at 37 °C with 5% CO_2 for 0.5 h. After that, the apoptosis rate was detected by fluorescence-activated cell sorting (FACS).

Cytokines production

ELISA was performed to determine the levels of IL-1β, IL-6, IL-17A, and IFN-α in cultivated γδ T cells and colonic tissue supernatants. Specifically, the original supernatant was removed and replaced with a new medium (RPMI-1640), and typical culture conditions were re-established for another 24 h. The content of cytokine proteins in the supernatant was quantitatively analyzed by using IL-1, IL-6, IL-17A, and IFN-α high sensitivity (0.25-16 pg/mL sensitivity range) ELISA kits (R&D Systems, Minneapolis, Minnesota, United States) according to the manufacturer's instructions.

Cell reinfusion

Isolated γδ T cells were treated with SCH58261 or CGS21680 at 37 °C, 5% CO_2 for 48 h. The cell concentration was then adjusted to 2 × 10^6 cells/mL with RMPI-1640. Mice were injected separately with γδ T cells at an inoculum of 2 × 10^6 cells per mouse. Clinical characteristics were observed as described previously.

Transient transfection

LV-mA2AR-shRNA was synthesized by Fubio (Suzhou) Biopharmaceutical Technology Co., Ltd. and Suzhou Genepharma Co., Ltd. The sequence is as follows: the sense is 5'-GGAGACAGCUGA-AGCAGAUTT-3'; the antisense sequence is 5'- AUCUGCUUCAGCUCUCUCCTT-3'. The HEK293T A2AR knock-down cell line was obtained by transfecting LV-mA2AR-shRNA with γδ T cells and incubating at 37 °C for 48 h after transfection. Similarly, the HEK293T cell line infected with a negative control sequence (sh-NC) was constructed.

Statistical analysis

Data are represented as mean ± SD. All data were analyzed using Grubb's test, followed by one-way analysis of variance (ANOVA) and Levene's test to assess the homogeneity of variance, and finally Ducan's multiple comparison test for multiple comparisons (SPSS 22.0 software). $P < 0.05$ were considered statistically significant.

RESULTS

The establishment of PI-IBS mouse model and the impact of A2AR on PI-IBS

First, we chose the *T. spiralis* infection to construct the PI-IBS mouse model. On day 56 after the *T. spiralis* infection, the model was evaluated, which demonstrated that there was no obvious inflammation in the animal colon (Figure 1), but the AWR rating was significantly higher than that of the control group, and the results of CTT experiment were significantly abnormal, as shown by the shortened first black stool time and a higher Bristol stool level (Tables 3 and 4). This indicated that a successful PI-IBS mouse model has been established.

After that, we applied the A2AR agonist or antagonist to PI-IBS mice in order to find potential interventions for curing PI-IBS. A further novel finding was that only the injection of A2AR antagonist SCH58261 significantly relieved the severe clinical manifestations of the model animal whereas A2AR agonist CGS21680 could not. At this stage of understanding, these findings suggest that A2AR may have a crucial impact on the development of PI-IBS.

The intestinal levels of ATP and A2AR expression are upregulated in PI-IBS mice

To further assess the relationship between A2AR and PI-IBS, we compared the altered expression of A2AR and ATP content in mice with PI-IBS or in normal mice, as A2AR plays a vital role in the conversion of ATP. From the results, it is clear that compared with the control group, intestinal ATP

Table 3 The effect of adenosine 2A receptor on the abdominal withdrawal reflex score in post-infectious irritable bowel syndrome mouse

Distending air volume (mL)	AWR			
	0.25	0.35	0.5	0.65
Control (n = 6)	0.00 ± 0.00	1.67 ± 0.05	2.52 ± 0.18	3.65 ± 0.08
PI-IBS (n = 6)	0.00 ± 0.00	2.13 ± 0.12[a]	3.15 ± 0.14	3.90 ± 0.15
IBS + SCH58261 (n = 6)	0.00 ± 0.00	1.79 ± 0.12[c]	2.90 ± 0.25	3.57 ± 0.05
IBS + CGS21680 (n = 6)	0.00 ± 0.00	2.01 ± 0.42	3.09 ± 0.53	3.62 ± 0.11

[a]P < 0.05 *vs* the control group.
[c]P < 0.05 *vs* the PI-IBS group.
AWR: Abdominal withdrawal reflex; PI-IBS: Post-infectious irritable bowel syndrome.

Table 4 The effect of adenosine 2A receptor on the intestinal mobility in post-infectious irritable bowel syndrome mouse

Group	First black stool time (min)	Bristol stool grade
Control (n = 6)	407 ± 10.33	1.00 ± 0.00
PI-IBS (n = 6)	132 ± 12.59[a]	2.67 ± 0.52[a]
IBS + SCH58261 (n = 6)	246 ± 14.20[c]	1.33 ± 0.51[c]
IBS + CGS21680 (n = 6)	168 ± 11.38	2.66 ± 0.54

[a]P < 0.05 *vs* the control group.
[c]P < 0.05 *vs* the PI-IBS group.
PI-IBS: Post-infectious irritable bowel syndrome.

levels in PI-IBS mice rose considerably (P < 0.01, Figure 2A) as did A2AR protein expression (P < 0.01, Figure 2B-D). Intestinal ATP levels and A2AR expression were further enhanced when the PI-IBS mice were treated with the A2AR agonist CGS21680 (P < 0.05, Figure 2A-D). At the same time, the levels of inflammatory factors such as IL-1, IL-6, IL-17, and IFN-α were also further boosted compared to the PI-IBS model group (Figure 2E-G). Interestingly, when SCH58261, an antagonist of A2AR, was administered in PI-IBS mice, the significant increase in ATP levels and the up-regulation of A2AR expression triggered by PI-IBS was reversed (Figure 2A-D), followed by the drop of inflammatory factors' expression compared with the PI-IBS group, including IL-1, IL-6, IL-17 and IFN-α (Figure 2E-G).

Intestinal epithelial tight junctions (TJs) proteins, such as ZO-1, Occludin, and Claudin-1, play a vital role in maintaining the epithelial barrier function to restrict the paracellular movement of harmful substances across intestinal mucosa[29]. The disrup- tion of the TJs barrier could increase dysregulated immune reactions, such as the activation of mucosal immune response and the permeation of noxious molecules, and thus inducing gut inflammation[30,31]. Thus, we next tested the change of ZO-1, occludin, and claudin-1 expression. As we can see, the expression of TJ proteins ZO-1, Occludin, and Claudin-1 was sharply reduced in PI-IBS mice compared to the control, while agonism of A2AR further inhibited the expression of the proteins mentioned above. In line with the results in Figure 2A-D, treatment with the antagonism of A2AR SCH58261 also reversed the decreased expression of ZO-1, Occludin, and Claudin-1 in the PI-IBS group (Figure 2H-I). The results of the experiment found clear support for the hypothesis that A2AR is crucial to the pathophysiology of PI-IBS.

The upregulated A2AR in γδ T cells attributes to PI-IBS progression

It has been previously reported that the intestinal γδ T cells could exert an important role in a PI-IBS mouse model[32]. However, we wanted to further corroborate whether it is the altered A2AR expression in γδ T cells that directly influences the pathogenesis of PI-IBS. Before starting the exploration, we first purified γδ T cells. Figure 3A-C depicts the extraction and purification of γδ T cells from the spleen of PI-IBS mice for subsequent *in vitro* functional assessment through FACS sorting. Presently, we examined the A2AR expression in unpurified γδ T cells (the control group) and purified γδ T cells (the γδ T cell group) by immunohistochemical staining, respectively. The results were presented in Figure 3D and E. Notably, the A2AR expression level of γδ T cells was significantly higher than that in the control group, suggesting that A2AR was mainly highly expressed in γδ T cells. Furthermore, we treated γδ T cells with A2AR agonist CGS21680 and A2AR antagonist SCH58261, respectively, and we can visualize through Figure 3F and G that the A2AR expression level was further

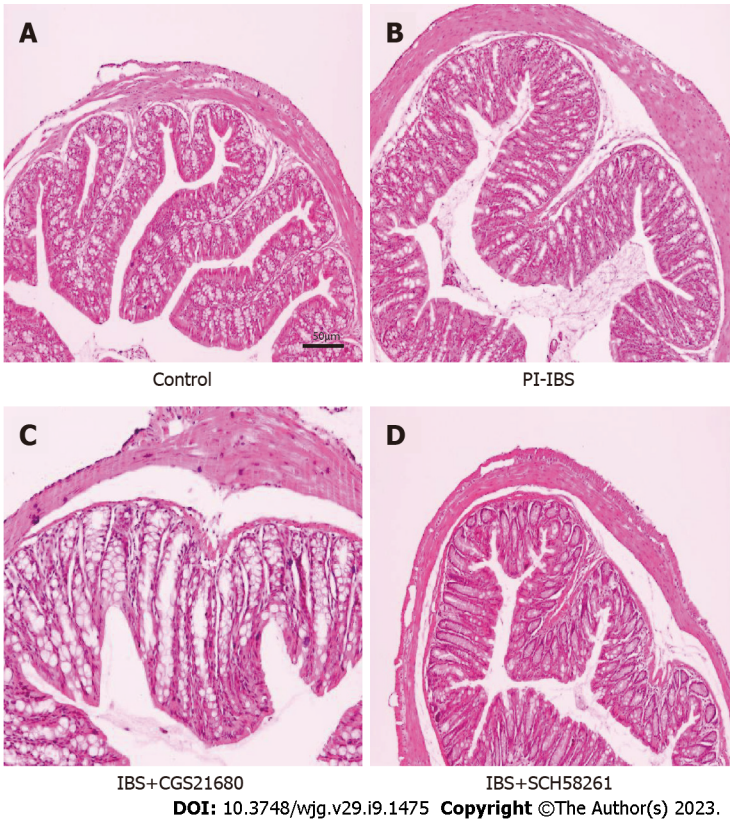

DOI: 10.3748/wjg.v29.i9.1475

Figure 1 The effect of adenosine 2A receptor on the histopathological changes in post-infectious irritable bowel syndrome mouse. A and B: The Post-infectious irritable bowel syndrome (PI-IBS) model (B) exhibits no substantial inflammatory alterations in its colon tissue compared to the control animal (A); C: Adenosine 2A receptor (A2AR) agonist CGS21680 leads to some inflammatory alterations in the colon tissue of the PI-IBS model mice, including the infiltration of certain inflammatory cells; D: A2AR antagonist SCH58261 relieves inflammation in the colon tissue of the PI-IBS model mice. A2AR: Adenosine 2A receptor; PI-IBS: Post-infectious irritable bowel syndrome. Scale bars, 50 μm.

enhanced in T cells treated with A2AR agonists, while the A2AR expression in T cells was significantly downregulated after the administration of SCH58261 to inhibit A2AR.

Besides, western blot and reverse transcription PCR results further confirmed the immunohistochemical findings: the agonist significantly increased both A2AR protein and mRNA level in γδ T cells, whereas the antagonist did the opposite (Figure 3H-J). Taken together, these results revealed that γδ T cells were the main immune cell subtype mediating the upregulation of A2AR expression in the intestinal immune microenvironment. By interfering with A2AR expression within γδ T cells, the function of γδ T cells might be affected, which could in turn interfere with disease progression throughout PI-IBS.

The viability and function maintenance of γδ T cells is closely related to A2AR

To verify the conjecture of the previous chapter, we would like to further unveil the effect of A2AR on γδ T-cells' viability and function. First, we assessed the correlation between A2AR and γδ T-cell viability by the measurement of altered ATP content in γδ T cells and the percentage of proliferating γδ T cells. The results are shown in Figure 4A and B. When we treated γδ T cells with the A2AR agonist CGS21680, both the intracellular ATP content and the percentage of proliferating cells increased compared with the control γδ T cells, suggesting that A2AR activation could enhance the cell viability of γδ T cells; whereas the intracellular ATP content and proliferating percentage both decreased when the antagonist of cellular A2AR, SCH58261, was given. Subsequently, we further evaluated whether the apoptosis of γδ T cells was affected by A2AR, and the results demonstrated that inhibition of A2AR promoted the apoptosis of γδ T cells, while activation of A2AR greatly inhibited the apoptosis process (Figure 4C and D). Finally, we examined the function of γδ T cells. To be specific, we reinfused γδ T cells that have been treated differently into PI-IBS mice. A similar pattern of results was obtained in the expression of inflammatory factors, including IL-1β, IL-6, IL-17A and IFN-α in γδ T cells. Virtually, the addition of A2AR agonist CGS21680 promoted the expression of IL-1β, IL-6, IL-17A and IFN-α, while A2AR antagonist SCH58261 inhibited the expression of the above-mentioned inflammatory factors ($P < 0.05$, Figure 4E). The above results suggest that A2AR has an important effect on the viability and function of γδ T cells, especially on the secretion of inflammatory factors.

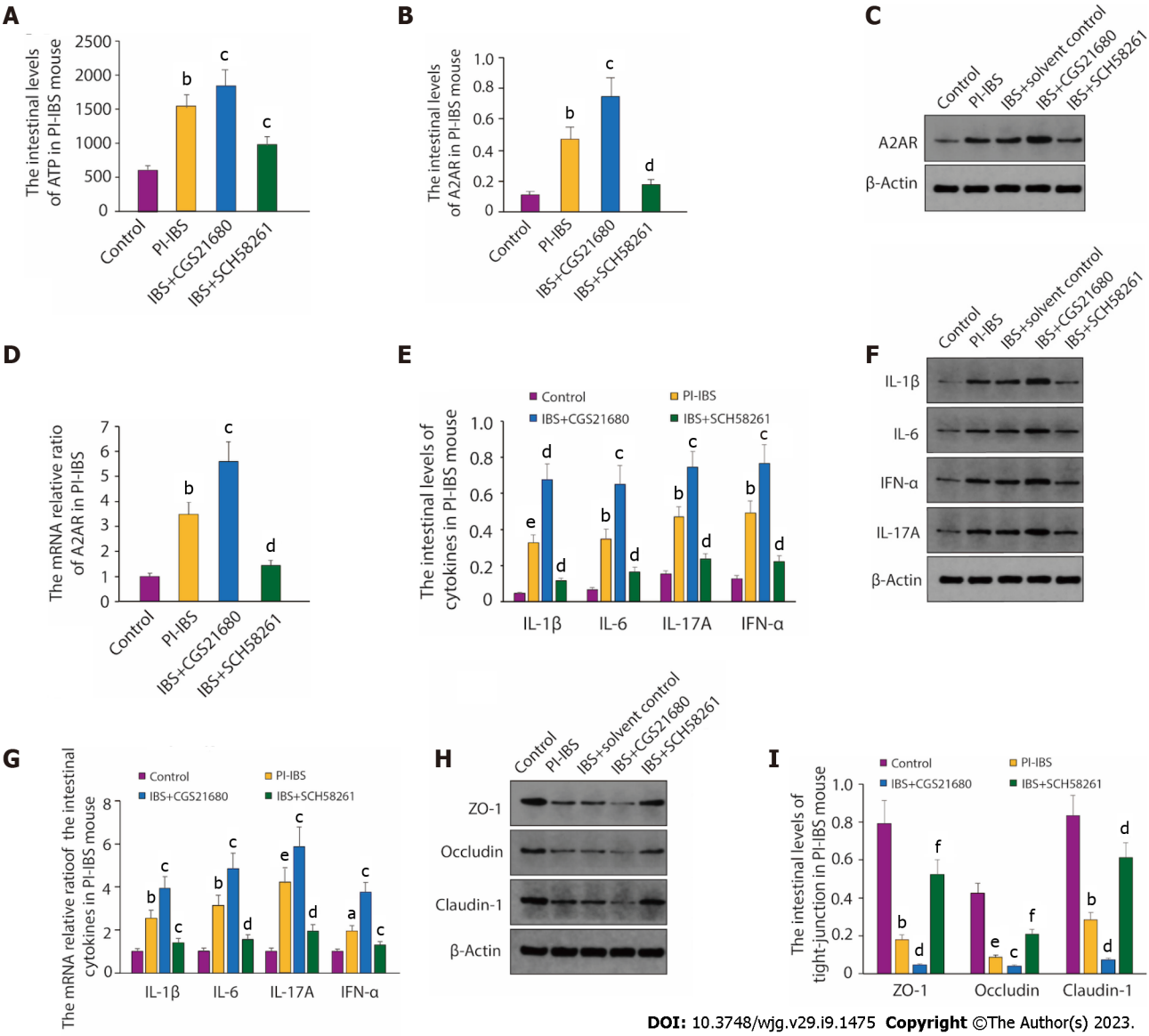

DOI: 10.3748/wjg.v29.i9.1475

Figure 2 The intestinal ATP and adenosine 2A receptor expression in post-infectious irritable bowel syndrome mouse. A: The level of ATP in post-infectious irritable bowel syndrome (PI-IBS) mouse. The results were independently repeated three times; B and C: The intestinal levels of adenosine 2A receptor (A2AR) in PI-IBS mouse; D: The mRNA relative ratio of A2AR in PI-IBS mouse. The results were independently repeated three times; E and F: The intestinal levels of the inflammatory cytokines in PI-IBS mice were measured by ELISA and western blot, respectively. The ELISA results were obtained from six mice; G: The mRNA relative ratio of the intestinal cytokines in PI-IBS mouse. The samples were from mice mentioned in E and F. The results were independently repeated three times; H and I: The intestinal levels of tight junction proteins in PI-IBS mice were tested through western blot and quantified by image J software. β-Actin is used as the loading control for both western blot and reverse transcription polymerase chain reaction. $^{a}P < 0.05$, $^{b}P < 0.01$, $^{e}P < 0.001$ *vs* the Control group; $^{c}P < 0.05$, $^{d}P < 0.01$, $^{f}P < 0.001$ *vs* the PI-IBS group.

The regulation of A2AR on γδ T cells relies on the PKA/CREB/NF-κB signaling pathway

As ADO binds to A2AR, A2AR then interacts with Gs family proteins to increase intracellular cAMP levels and activate downstream PKA/CREB-related pathways[33], we next investigated the activation of signaling pathways in γδ T cells by western blot. The change of PKA/p-PKA, CREB/p-CREB, NF-κB/p-NF-κB protein level, and quantitative results elucidated that compared to control γδ T cells, treatment of γδ T cells with the A2AR antagonist SCH58261 significantly decreased the expression of PKA/CREB/NF-κB and reduced the phosphorylation levels of the above proteins; whereas the introduction of A2AR agonist CGS21680 further promoted the protein expression of PKA/CREB/NF-κB as well as the phosphorylation activation level of the above proteins (Figure 5A-D). Therefore, given the above results, we can safely draw the conclusion that the PKA/CREB/NF-κB pathway is the key downstream signaling pathway for γδ T cells to regulate the relevant clinical manifestations *via* A2AR during PI-IBS disease progression.

A2AR knockdown inhibits the inflammatory response

To further clarify the effect of A2AR on the expression of inflammatory factors, we constructed A2AR-

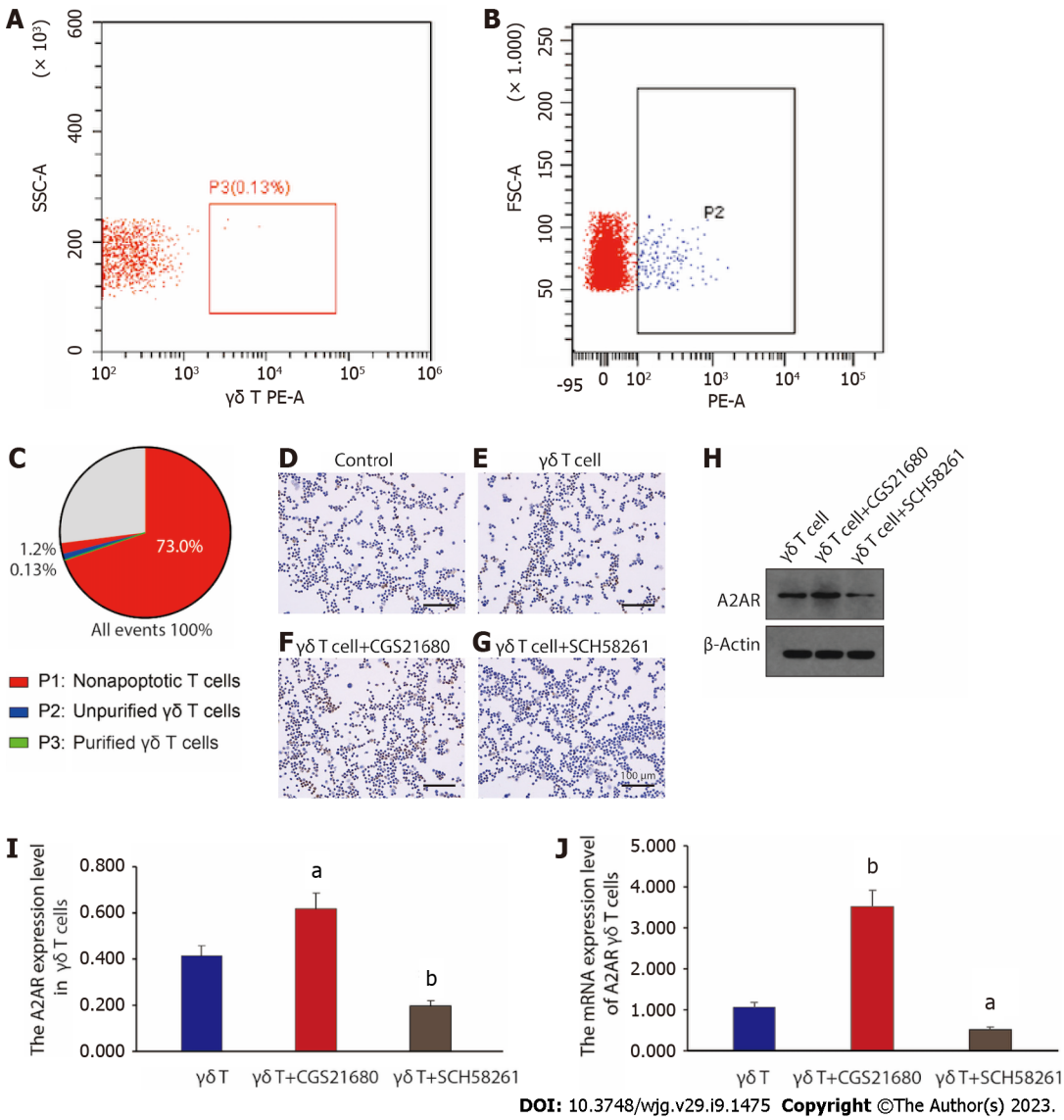

DOI: 10.3748/wjg.v29.i9.1475

Figure 3 γδ T cells' isolation and functional evaluation. A-C: Based on the results of fluorescence-activated cell sorting, γδ T cells were effectively extracted and purified. P2, unpurified γδ T cells; P3, purified γδ T cells; D-G: Immunohistochemistry labeling of adenosine 2A receptor (A2AR) expression in γδT cells. Scale bars, 100 μm; H: Western blot analysis of A2AR expression levels in γδ T cells. β-Actin is used as the loading control; I: The quantitive result of A2AR expression level in γδ T cells was analyzed from data shown in H. Results from three times of independently repeated experiments were analysed; J: Reverse transcription polymerase chain reaction analysis of the expression level of A2AR mRNA in γδ T cells. The results were independently repeated three times. A2AR: Adenosine 2A receptor. $^{a}P < 0.05$, $^{b}P < 0.01$ *vs* the γδ T cell group.

shRNA and inhibited the expression of A2AR by plasmid transfection. The results illustrated that A2AR expression was greatly boosted in the PI-IBS group compared with the control group; when transfected with shRNA, A2AR expression was significantly reduced in the IBS + shRNA group. Moreover, when IBS tissue cells were co-incubated with γδ T cells, the A2AR expression level was further increased. Meanwhile, silencing A2AR downregulated A2AR expression in the IBS + shRNA + γδ T cells group compared with the IBS + γδ T cells group (Figure 6A). After clarifying the silencing efficiency, we examined the effect of silencing A2AR on the expression level of inflammatory factors. From the results in Figure 6B, we can clearly see that the inflammatory factor levels, which were originally higher in the PI-IBS model group, were dramatically reduced due to A2AR knockdown. At the same time, given that the reduced expression of TJ proteins leads to increased intestinal permeability, we also evaluated the altered expression levels of TJ proteins and found that the originally suppressed TJ protein expression in PI-IBS mice was significantly reversed after A2AR silencing (Figure 6C). Taken together, the above findings demonstrate that downregulation of A2AR can reduce γδ T cell-induced inflammatory cytokine production and release.

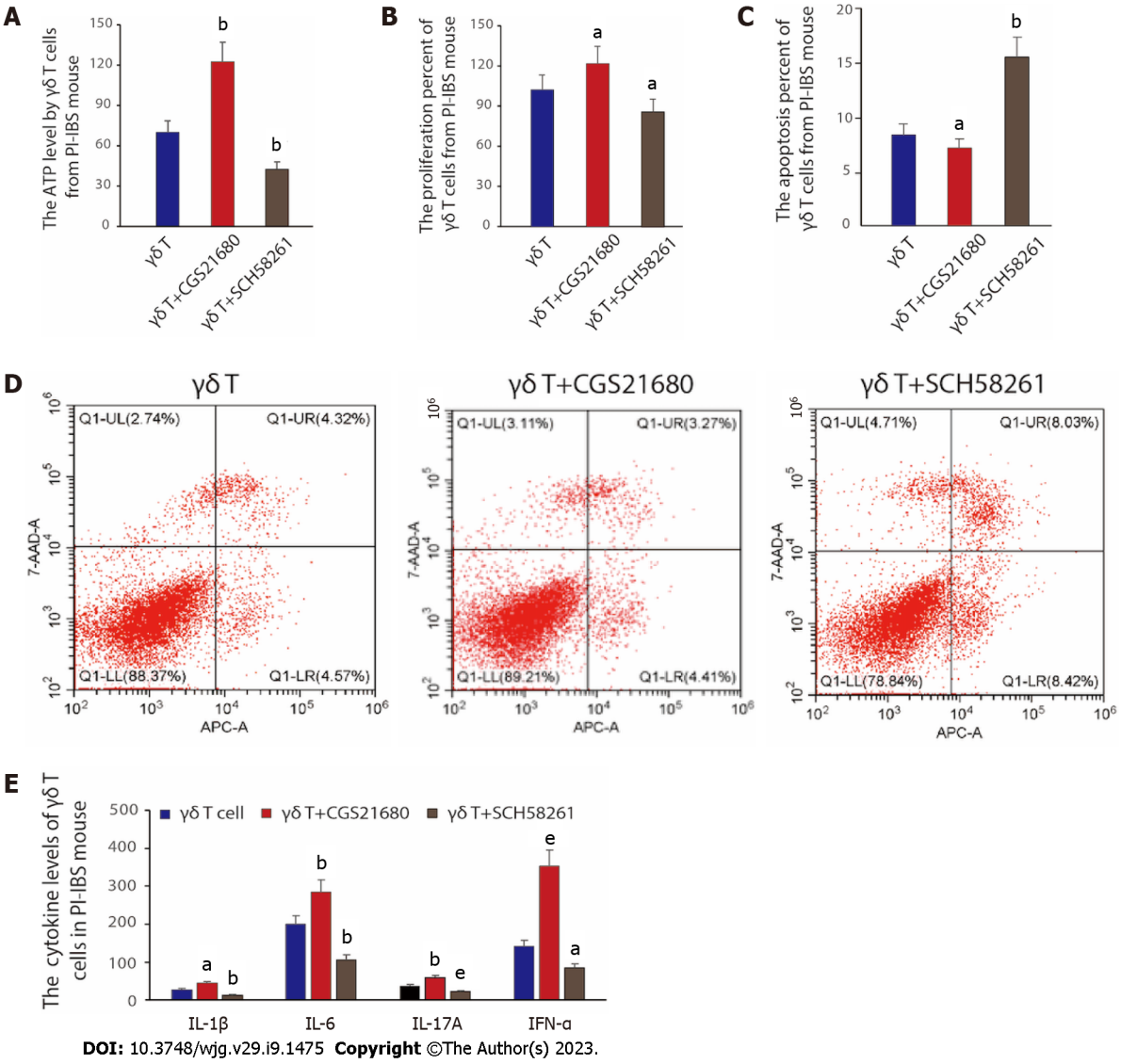

DOI: 10.3748/wjg.v29.i9.1475

Figure 4 Functional evaluation of γδ T cells *in vitro*. A: The ATP level changed by differently treated γδ T cells from post-infectious irritable bowel syndrome (PI-IBS) mice. The data was obtained from six mice in each group; B: The proliferation percent of γδ T cells from PI-IBS mouse was analysed through CCK8 assay. The samples were taken from six mice in each group; C: The apoptosis percent of γδ T cells from PI-IBS mouse measured by fluorescence-activated cell sorting. The γδ T cells were taken from six mice in each group; D: Apoptosis rates were detected according to Annexin V and PI double-staining method; E: The cytokines level of IL-1β, IL-6, IL-17A and IFN-α from PI-IBS mice after reinfusing control γδ T cells and γδ T cells treated with CGS21680 or SCH58261, respectively. The data was obtained from six mice in each group. PI-IBS: Post-infectious irritable bowel syndrome. $^{a}P < 0.05$, $^{b}P < 0.01$, $^{e}P < 0.001$ *vs* the γδ T cell group.

DISCUSSION

Persistent intestinal low-degree inflammation occurs in IBS due to complex disorders in the immune system, especially in PI-IBS, leading to minor biochemical and pathological changes but continuous clinical symptoms in patients[34]. Nevertheless, the precise immune regulatory mechanism in PI-IBS remains unknown. We have previously reported that γδ T cells could alleviate PI-IBS through promoting Th17 polarization *via* HSP70 receptor[12]. This study is a follow-up study on the pathogenesis of PI-IBS with the aim of finding new immunomodulatory proteins that directly regulate the intestinal microenvironment and interfere with PI-IBS disease progression.

Few literatures have been reported the relationship between adenosine receptor and PI-IBS. According to our research, an increase in intestinal ATP level is followed by the upregulation of intestinal A2AR in PI-IBS, suggesting that ATP and A2AR may be involved in the pathophysiology of PI-IBS. It is unclear if the quantitative alterations of intestinal A2AR originated from PI-IBS could lead to exacerbated PI-IBS. After being administered with the A2AR antagonist, the digestive tissue of the animals remained unchanged, but their clinical symptoms improved. This discovery contradicted earlier notions that A2AR antagonist exhibits a protective function in inflammation[35]. Moreover, an A2AR antagonist may activate an unidentified pathway to control the equilibrium, and an extended persistence of elevated adenosine levels can be deleterious, contributing to the formation of an immunosuppressed niche that is conducive to the initiation and development of neoplasia[36]. These

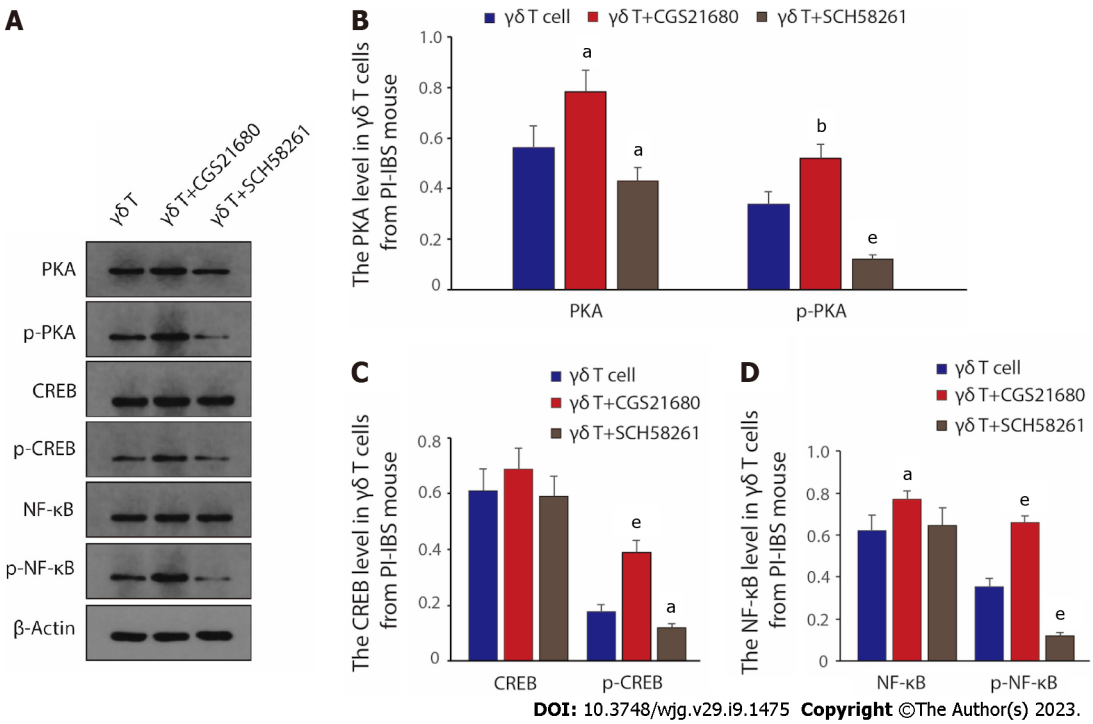

DOI: 10.3748/wjg.v29.i9.1475

Figure 5 Adenosine 2A receptor mediated signaling pathway that could regulate the function of γδ T cells. A: The PKA/p-PKA, CREB/p-CREB, NF-κB/p-NF-κB protein levels in γδ T cells of post-infectious irritable bowel syndrome (PI-IBS) mice. β-Actin is used as the loading control; B: The relative PKA level in γδ T cells from mice with PI-IBS; C: The relative CREB level in γδ T cells from PI-IBS mice; D: The relative NF-κB level in γδ T cells from mice with PI-IBS. The results from three times of independently repeated experiments were gathered and analyzed. PI-IBS: Post-infectious irritable bowel syndrome. $^{a}P < 0.05$, $^{b}P < 0.01$, $^{e}P < 0.001$ *vs* the γδ T cell group.

findings also indicate the complexity of PI-IBS.

IL-6, IL-17A, and IFN-α are important pro-inflammatory factors. IL-17A can increase the permeability of cells by binding to specific receptors and can stimulate various types of cells to produce chemokines, IFN-α, and IL-1β to stimulate inflammatory reactions. IFN-α can interrupt the function of intestinal epithelial cells, leading to intestinal epithelial barrier dysfunction[37]. IL-6 is mainly manifested in maintaining regulatory T cells and effector T cells and inhibiting the apoptosis of CD4+ T cells in the inflammatory response[38]. Our study suggested that the levels of pro-inflammatory factors IL-6, IL-17A, and IFN-α were significantly elevated in PI-IBS mice. This indicated that there was a low-grade inflammatory response in the intestinal mucosa, resulting in a defect in the epithelial barrier. The epithelial barrier dysfunction can lead to an increase in intestinal permeability, which further promotes the increase and activation of immune cells[39]. TJ proteins such as ZO-1, Claudin-1, and Occludin form a tight junction structure between adjacent intestinal epithelial cells as the structural basis of the mechanical intestinal barrier, thereby defending against external damaging factors and maintaining intestinal mucosal homeostasis[40,41]. Under the stimulation of severe infection and surgical blows, the tight junction structure between the intestinal epithelium can be destructed, The damaged mechanical barrier and the translocation of intestinal flora into the blood then cause bacteremia and sepsis to stimulate the release of systemic inflammatory factors, leading to systemic inflammatory response syndrome and multiple organ dysfunction[42]. In this study, the expression of ZO-1, Claudin-1, and Occludin was reduced substantially, suggesting that PI-IBS mice had impaired intestinal epithelial barrier function, and were susceptible to stimulation by various etiologies to activate the intestinal epithelial immune system and lead to intestinal inflammatory responses.

The uneven distribution of γδ T cells in normal and inflammatory tissues plays an important role in autoimmunity[43]. In some patients with autoimmune diseases, the proportion of γδ T cells in infiltrating T cells is abnormally increased. γδ T cells are the main source of proinflammatory cytokines IL-17, IL-23, IFN-α, and TGF-β. These inflammatory molecules are responsible for creating an inflammatory environment that enhances disease progression through different pathways[44]. The relationship between different disease phenotypes and γδT cells can be clearly discerned. γδT cells acquire the ability to produce IL-17 during embryonic thymus development, and T cells expressing γδT cell receptors are an important innate source of the pro-inflammatory cytokine IL-17. The potent inflammatory effects of IL-17 are mainly related to its ability to recruit immune cells and synergistic effects with other pro-inflammatory cytokines[45]. Hence, it is no exaggeration to say that γδ T cells play a crucial role in regulating inflammation and the immune response. In our results, we firstly found that the number of γδ T cells markedly increased, accompanied by the increased A2AR expressed on their

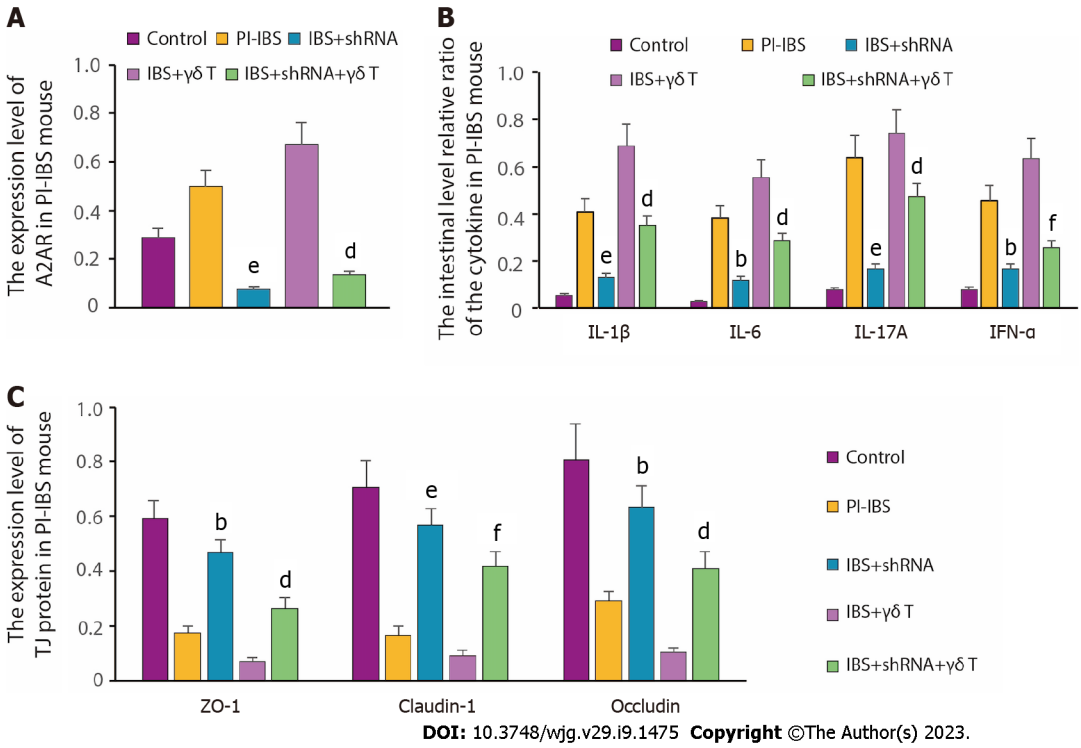

DOI: 10.3748/wjg.v29.i9.1475

Figure 6 The inflammatory response alteration after adenosine 2A receptor knockdown. A: The altered level of adenosine 2A receptor (A2AR) expression after A2AR-shRNA transfection or γδ T cell reinfusion in post-infectious irritable bowel syndrome (PI-IBS) mice was assessed. The results were obtained from three times of independently repeated experiments; B: The relative ratio of the intestinal cytokine level in PI-IBS mice (n = 6, per group); C: The degree of TJ (tight junction protein) protein expression in PI-IBS mice (n = 6, per group). $^{a}P < 0.05$, $^{b}P < 0.01$, $^{e}P < 0.001$ *vs* the PI-IBS group; $^{c}P < 0.05$, $^{d}P < 0.01$, $^{f}P < 0.001$ *vs* the IBS + γδ T group.

surfaces. Secondly, the agonist of A2AR boosted the quantity of γδ T cells together with upregulated A2AR expression. Thirdly, the A2AR antagonist reduced γδ T cells' number and impaired their function. These findings demonstrated that γδ T cells participated in intestinal inflammation mediated by A2AR.

At present, the anti-inflammatory mechanism of A2AR mainly includes: (1) Inhibition of neutrophils and release of peroxidase[46,47]; (2) promotion of the production of IL-10 by monocytes and macrophages; (3) inhibition of the release of IL-12 and TNF-α[48]; and (4) phosphorylation of cAMP response element-binding (CREB) protein by activating the cAMP-PKA pathway, in which phosphorylated CREB competes with the p65 subunit of NF-κB and the NF-κB coactivator CREB-binding protein combined to inhibit the transcriptional regulation of NF-κB on target genes, thereby blocking the production of inflammatory mediators[49,50]. Excessive release of inflammatory mediators is the main mechanism that causes uncontrolled inflammatory responses in the body. Therefore, the A2AR-cAMP-PKA-CREB-NF-κB signaling pathway is the main mechanism and classical pathway for A2AR mediated function of γδ T cells to inhibit inflammation. Furthermore, we revealed that the A2AR agonist CGS21680 could increase both protein and mRNA expression levels of PKA, CREB and NF-κB, and their phosphorylation activation levels were elevated as well in γδ T cells from PI-IBS mice. Apart from that, we also observed the opposite effects after the treatment of A2AR antagonist SCH58261 in γδ T cells compared with results in A2AR agonist CGS21680 treatment group. Thus, we illustrated that the A2AR-PKA-CREB-NF-κB pathway is the crucial intracellular signaling pathway for A2AR-induced γδ T cells' role in PI-IBS. However, whether there are other signaling pathways at play still needs to be studied.

Furthermore, we decreased the A2AR expression with LV-A2AR-shRNA, which alleviated the symptoms of PI-IBS in model mice. Meanwhile, we then reinfused the γδ T cell to PI-IBS mice, the disease became severer. Interestingly, when the PI-IBS mice reinfused with sh-A2AR γδ T cells, the severity of their clinical symptoms was lessened. Besides, we also observed the alterations in the cytokines and TJ protein expression, and the results were in accordance with the changes in the clinical symptoms. These data suggested that γδ T cells participated in PI-IBS *via* the A2AR mediated signaling pathway.

Our study included a few drawbacks as well. The type of visceral hypersensitivity was not investigated in PI-IBS mice, and the water content from the feces of mice was not examined. Due to the difficulties of isolating T cells directly from the gut, we utilized spleen-isolated T cells, likely resulting in a greater degree of variety than their intestinal counterparts.

CONCLUSION

In the present study, we found higher expression of A2AR in PI-IBS mice than normal mice, which initially suggested the relevance of A2AR to PI-IBS disease development. Further mechanistic studies demonstrated that A2AR, which located on the surface of γδ T cells, could regulate the function of γδ T cells. Notably, A2AR regulated T cell viability and increased the secretion of inflammatory factors, mainly through the PKA/CREB/NF-κB signaling pathway, which followed by the progression of PI-IBS. Fortunately, the application of A2AR antagonists could markedly reduce the inflammatory response and improve PI-IBS symptoms by regulating the function of γδ T cells.

In summary, through our study, we identified A2AR, a key protein that promotes disease progression in PI-IBS, and demonstrated the feasibility of antagonizing A2AR to intervene in PI-IBS, thus providing a new therapeutic target for PI-IBS treatment.

ARTICLE HIGHLIGHTS

Research background

Persistent low level of inflammation due to immune dysfunction is regarded as one of the prime pathogenic mechanisms of post-infectious irritable bowel syndrome (PI-IBS). γδ T cells play a key role in innate and adaptive immunity. Adenosine and its receptors expressed on γδ T cells are involved in intestinal inflammation and immune regulation.

Research motivation

To unveil the role of γδ T cells regulated by adenosine 2A receptor (A2AR) in the pathogenesis of PI-IBS.

Research objectives

This study aims to investigate the role of A2AR in γδ T cells and γδ T cells in PI-IBS.

Research methods

A PI-IBS mouse model was established with Trichinella spiralis (*T. spiralis*) infection. Intestinal A2AR and A2AR in γδ T cells were detected through immunohistochemistry, and inflammatory cytokines were detected through western blot. The role of A2AR on isolated γδ T cells, including γδ T cell proliferation, apoptosis and γδ T cell-mediated cytokine secretion, was assessed *in vitro*. A2AR expression in γδ T cells was determined by western blot and reverse transcription polymerase chain reaction (RT-PCR). Mice were injected with A2AR agonist or A2AR antagonist and cultured γδ T cells were also reinfused into the animals, and then the above parameters and clinical features were examined again. In addition, alterations in A2AR-related signaling pathway molecules were detected by western blot and RT-PCR.

Research results

The expression levels of ATP and A2AR were increased in PI-IBS mice ($P < 0.01$), and inhibition of A2AR further enhanced the clinical features of PI-IBS, as reflected by the abdominal withdrawal reflex and colonic transport test results. The development of PI-IBS was associated with an increase in intestinal γδ T cells and cytokines including interleukin-1 (IL-1), IL-6, IL-17A and interferon-α (IFN-α). In addition, γδ T cells obtained by purification *in vitro* could express A2AR and promote IL-1, IL-6, IL-17A and IFN-α secretion, which is also regulated by A2AR agonists and antagonists. We also found that A2AR antagonists improved γδ T cell function through the PKA/CREB/NF-κB signaling pathway.

Research conclusions

Our results suggested that A2AR contributes to the development of PI-IBS after *T. spiralis* infection *via* the PKA/CREB/NF-κB signaling pathway by γδ T cells.

Research perspectives

Hypo-inflammation caused by immune dysfunction is considered to be one of the main pathogenic mechanisms of PI-IBS. In this study, we discovered that A2AR on the surface of γδ T cells can regulate the function of γδ T cell, thereby increasing inflammatory factor secretion and promoting PI-IBS progression. Luckily, the utilization of A2AR antagonists can improve PI-IBS symptoms by promoting γδ T cells' function. Through our study, we identified A2AR, a key protein that promotes PI-IBS disease progression, and demonstrated the feasibility of antagonizing A2AR to intervene in PI-IBS, thus providing a novel therapeutic target and an effective intervention strategy for PI-IBS treatment.

FOOTNOTES

Author contributions: Dong LW, Chen YY, and Chen CC contributed equally to this manuscript and should be as the co-first authors. Lan C, Sun DM, Dong LW, Chen YY, and Chen CC contributed to the conception and design; Lan C, Dong LW, Chen YY, and Chen CC contributed to development of methodology; Dong LW, Chen YY, Chen CC, Ma ZC, Fu J, Huang BL, and Liu FJ contributed to acquisition of data (provided animals, acquired and managed patients, provided facilities, *etc.*), analysis and interpretation of data (*e.g.*, statistical analysis, biostatistics, computational analysis); Dong LW, Liang DC, and Sun DM contributed to writing, review, and/or revision of the manuscript; Chen YY, Chen CC, and Liang DC contributed to the administrative, technical, or material support (*i.e.*, reporting or organizing data, constructing databases); Lan C supervised the study; all authors have read and approved the final version of the manuscript.

Supported by National Natural Science Foundation of China, No. 81160057, No. 81860102, and No. 82060102; Natural Science Foundation of Hainan Province, High-level Personnel Program, No. 821RC1116; Research Project of Health Industry in Hainan Province, No. 20A200066; and Hainan Provincial Clinical Medical Center.

Institutional animal care and use committee statement: The experimental protocol was approved by the Animal Care and Use Committee of Hainan General Hospital.

Conflict-of-interest statement: All the authors report no relevant conflicts of interest for this article.

Data sharing statement: No additional data are available.

ARRIVE guidelines statement: The authors have read the ARRIVE guidelines, and the manuscript was prepared and revised according to the ARRIVE guidelines.

Country/Territory of origin: China

ORCID number: Cheng Lan 0000-0002-1435-5510.

S-Editor: Gong ZM
L-Editor: A
P-Editor: Yuan YY

REFERENCES

1 **Camilleri M**. Diagnosis and Treatment of Irritable Bowel Syndrome: A Review. *JAMA* 2021; **325**: 865-877 [PMID: 33651094 DOI: 10.1001/jama.2020.22532]
2 **Berumen A**, Edwinson AL, Grover M. Post-infection Irritable Bowel Syndrome. *Gastroenterol Clin North Am* 2021; **50**: 445-461 [PMID: 34024451 DOI: 10.1016/j.gtc.2021.02.007]
3 **Bonetto S**, Fagoonee S, Battaglia E, Grassini M, Saracco GM, Pellicano R. Recent advances in the treatment of irritable bowel syndrome. *Pol Arch Intern Med* 2021; **131**: 709-715 [PMID: 34463082 DOI: 10.20452/pamw.16067]
4 **Ng QX**, Soh AYS, Loke W, Lim DY, Yeo WS. The role of inflammation in irritable bowel syndrome (IBS). *J Inflamm Res* 2018; **11**: 345-349 [PMID: 30288077 DOI: 10.2147/JIR.S174982]
5 **Aguilera-Lizarraga J**, Hussein H, Boeckxstaens GE. Immune activation in irritable bowel syndrome: what is the evidence? *Nat Rev Immunol* 2022; **22**: 674-686 [PMID: 35296814 DOI: 10.1038/s41577-022-00700-9]
6 **Zeng L**, Li K, Wei H, Hu J, Jiao L, Yu S, Xiong Y. A Novel EphA2 Inhibitor Exerts Beneficial Effects in PI-IBS in Vivo and in Vitro Models *via* Nrf2 and NF-κB Signaling Pathways. *Front Pharmacol* 2018; **9**: 272 [PMID: 29662452 DOI: 10.3389/fphar.2018.00272]
7 **Zhang Y**, Wu X, Wu J, Li S, Han S, Lin Z, Ding S, Jia X, Gong W. Decreased expression of microRNA-510 in intestinal tissue contributes to post-infectious irritable bowel syndrome *via* targeting PRDX1. *Am J Transl Res* 2019; **11**: 7385-7397 [PMID: 31934286]
8 **Kobayashi H**, Tanaka Y. γδ T Cell Immunotherapy-A Review. *Pharmaceuticals (Basel)* 2015; **8**: 40-61 [PMID: 25686210 DOI: 10.3390/ph8010040]
9 **Ribot JC**, Lopes N, Silva-Santos B. γδ T cells in tissue physiology and surveillance. *Nat Rev Immunol* 2021; **21**: 221-232 [PMID: 33057185 DOI: 10.1038/s41577-020-00452-4]
10 **Ramstead AG**, Jutila MA. Complex role of γδ T-cell-derived cytokines and growth factors in cancer. *J Interferon Cytokine Res* 2012; **32**: 563-569 [PMID: 23078623 DOI: 10.1089/jir.2012.0073]
11 **Su D**, Shen M, Li X, Sun L. Roles of γδ T cells in the pathogenesis of autoimmune diseases. *Clin Dev Immunol* 2013; **2013**: 985753 [PMID: 23533458 DOI: 10.1155/2013/985753]
12 **He Z**, Sun X, Ma Z, Fu J, Huang B, Liu F, Chen Y, Deng T, Han X, Sun D, Lan C. Heat shock protein 70 protects mouse

against post-infection irritable bowel syndrome *via* up-regulating intestinal γδ T cell's Th17 response. *Cell Biosci* 2018; **8**: 38 [PMID: 29928498 DOI: 10.1186/s13578-018-0237-z]

13 **Layland J**, Carrick D, Lee M, Oldroyd K, Berry C. Adenosine: physiology, pharmacology, and clinical applications. *JACC Cardiovasc Interv* 2014; **7**: 581-591 [PMID: 24835328 DOI: 10.1016/j.jcin.2014.02.009]

14 **Borea PA**, Gessi S, Merighi S, Vincenzi F, Varani K. Pharmacology of Adenosine Receptors: The State of the Art. *Physiol Rev* 2018; **98**: 1591-1625 [PMID: 29848236 DOI: 10.1152/physrev.00049.2017]

15 **Pelleg A**, Porter RS. The pharmacology of adenosine. *Pharmacotherapy* 1990; **10**: 157-174 [PMID: 2196534]

16 **Kumar V**, Sharma A. Adenosine: an endogenous modulator of innate immune system with therapeutic potential. *Eur J Pharmacol* 2009; **616**: 7-15 [PMID: 19464286 DOI: 10.1016/j.ejphar.2009.05.005]

17 **Antonioli L**, Fornai M, Colucci R, Ghisu N, Tuccori M, Del Tacca M, Blandizzi C. Regulation of enteric functions by adenosine: pathophysiological and pharmacological implications. *Pharmacol Ther* 2008; **120**: 233-253 [PMID: 18848843 DOI: 10.1016/j.pharmthera.2008.08.010]

18 **Belikoff B**, Hatfield S, Sitkovsky M, Remick DG. Adenosine negative feedback on A2A adenosine receptors mediates hyporesponsiveness in chronically septic mice. *Shock* 2011; **35**: 382-387 [PMID: 21192284 DOI: 10.1097/SHK.0b013e3182085f12]

19 **Hou T**, Xiang H, Yu L, Su W, Shu Y, Li H, Zhu H, Lin L, Hu X, Liang S, Zhang H, Li M. Electroacupuncture inhibits visceral pain *via* adenosine receptors in mice with inflammatory bowel disease. *Purinergic Signal* 2019; **15**: 193-204 [PMID: 31187350 DOI: 10.1007/s11302-019-09655-4]

20 **Sun L**, Li X, Guan H, Chen S, Fan X, Zhou C, Yang H, Xiao W. A Novel Role of A(2A)R in the Maintenance of Intestinal Barrier Function of Enteric Glia from Hypoxia-Induced Injury by Combining with mGluR5. *Front Pharmacol* 2021; **12**: 633403 [PMID: 34093180 DOI: 10.3389/fphar.2021.633403]

21 **Long SR**, Wang ZQ, Liu RD, Liu LN, Li LG, Jiang P, Zhang X, Zhang ZF, Shi HN, Cui J. Molecular identification of Trichinella spiralis nudix hydrolase and its induced protective immunity against trichinellosis in BALB/c mice. *Parasit Vectors* 2014; **7**: 600 [PMID: 25522912 DOI: 10.1186/s13071-014-0600-9]

22 **Yang B**, Zhou X, Lan C. Changes of cytokine levels in a mouse model of post-infectious irritable bowel syndrome. *BMC Gastroenterol* 2015; **15**: 43 [PMID: 25886744 DOI: 10.1186/s12876-015-0272-8]

23 **Suzuki R**, Kohno H, Sugie S, Tanaka T. Dose-dependent promoting effect of dextran sodium sulfate on mouse colon carcinogenesis initiated with azoxymethane. *Histol Histopathol* 2005; **20**: 483-492 [PMID: 15736053 DOI: 10.14670/HH-20.483]

24 **Lan C**, Sun XN, Zhou XC, Yang B, Huang BL, Deng TZ, He ZT, Han XY. Preinduced intestinal HSP70 improves visceral hypersensitivity and abnormal intestinal motility in PI-IBS mouse model. *Asian Pac J Trop Med* 2016; **9**: 302-305 [PMID: 26972407 DOI: 10.1016/j.apjtm.2016.01.022]

25 **Vork L**, Wilms E, Penders J, Jonkers DMAE. Stool Consistency: Looking Beyond the Bristol Stool Form Scale. *J Neurogastroenterol Motil* 2019; **25**: 625 [PMID: 31587553 DOI: 10.5056/jnm19086]

26 **Wu Z**, Yang L, Shi L, Song H, Shi P, Yang T, Fan R, Jiang T, Song J. Prognostic Impact of Adenosine Receptor 2 (A2aR) and Programmed Cell Death Ligand 1 (PD-L1) Expression in Colorectal Cancer. *Biomed Res Int* 2019; **2019**: 8014627 [PMID: 31275983 DOI: 10.1155/2019/8014627]

27 **Sauer KA**, Scholtes P, Karwot R, Finotto S. Isolation of CD4+ T cells from murine lungs: a method to analyze ongoing immune responses in the lung. *Nat Protoc* 2006; **1**: 2870-2875 [PMID: 17406546 DOI: 10.1038/nprot.2006.435]

28 **Williams L**, Dery KJ, Lee WH, Li H, Shively JE, Kujawski M. Isolation and expansion of murine γδ T cells from mouse splenocytes. *J Immunol Methods* 2022; **508**: 113322 [PMID: 35843266 DOI: 10.1016/j.jim.2022.113322]

29 **Turner JR**. Intestinal mucosal barrier function in health and disease. *Nat Rev Immunol* 2009; **9**: 799-809 [PMID: 19855405 DOI: 10.1038/nri2653]

30 **Li B**, Lee C, Chuslip S, Lee D, Biouss G, Wu R, Koike Y, Miyake H, Ip W, Gonska T, Pierro A. Intestinal epithelial tight junctions and permeability can be rescued through the regulation of endoplasmic reticulum stress by amniotic fluid stem cells during necrotizing enterocolitis. *FASEB J* 2021; **35**: e21265 [PMID: 33373067 DOI: 10.1096/fj.202001426R]

31 **Suzuki T**. Regulation of intestinal epithelial permeability by tight junctions. *Cell Mol Life Sci* 2013; **70**: 631-659 [PMID: 22782113 DOI: 10.1007/s00018-012-1070-x]

32 **Mangan BA**, Dunne MR, O'Reilly VP, Dunne PJ, Exley MA, O'Shea D, Scotet E, Hogan AE, Doherty DG. Cutting edge: CD1d restriction and Th1/Th2/Th17 cytokine secretion by human Vδ3 T cells. *J Immunol* 2013; **191**: 30-34 [PMID: 23740951 DOI: 10.4049/jimmunol.1300121]

33 **Mastelic-Gavillet B**, Navarro Rodrigo B, Décombaz L, Wang H, Ercolano G, Ahmed R, Lozano LE, Ianaro A, Derré L, Valerio M, Tawadros T, Jichlinski P, Nguyen-Ngoc T, Speiser DE, Verdeil G, Gestermann N, Dormond O, Kandalaft L, Coukos G, Jandus C, Ménétrier-Caux C, Caux C, Ho PC, Romero P, Harari A, Vigano S. Adenosine mediates functional and metabolic suppression of peripheral and tumor-infiltrating CD8(+) T cells. *J Immunother Cancer* 2019; **7**: 257 [PMID: 31601268 DOI: 10.1186/s40425-019-0719-5]

34 **El-Salhy M**, Gundersen D, Hatlebakk JG, Hausken T. Low-grade inflammation in the rectum of patients with sporadic irritable bowel syndrome. *Mol Med Rep* 2013; **7**: 1081-1085 [PMID: 23417076 DOI: 10.3892/mmr.2013.1320]

35 **Leone RD**, Lo YC, Powell JD. A2aR antagonists: Next generation checkpoint blockade for cancer immunotherapy. *Comput Struct Biotechnol J* 2015; **13**: 265-272 [PMID: 25941561 DOI: 10.1016/j.csbj.2015.03.008]

36 **D'Antongiovanni V**, Fornai M, Pellegrini C, Benvenuti L, Blandizzi C, Antonioli L. The Adenosine System at the Crossroads of Intestinal Inflammation and Neoplasia. *Int J Mol Sci* 2020; **21** [PMID: 32708507 DOI: 10.3390/ijms21145089]

37 **Yang S**, Yu M, Sun L, Xiao W, Yang X, Zhang C, Ma Y, Yang H, Liu Y, Lu D, Teitelbaum DH. Interferon-γ-induced intestinal epithelial barrier dysfunction by NF-κB/HIF-1α pathway. *J Interferon Cytokine Res* 2014; **34**: 195-203 [PMID: 24237301 DOI: 10.1089/jir.2013.0044]

38 **Hovhannisyan Z**, Treatman J, Littman DR, Mayer L. Characterization of interleukin-17-producing regulatory T cells in inflamed intestinal mucosa from patients with inflammatory bowel diseases. *Gastroenterology* 2011; **140**: 957-965 [PMID:

21147109 DOI: 10.1053/j.gastro.2010.12.002]

39 **González-Castro AM**, Martínez C, Salvo-Romero E, Fortea M, Pardo-Camacho C, Pérez-Berezo T, Alonso-Cotoner C, Santos J, Vicario M. Mucosal pathobiology and molecular signature of epithelial barrier dysfunction in the small intestine in irritable bowel syndrome. *J Gastroenterol Hepatol* 2017; **32**: 53-63 [PMID: 27087165 DOI: 10.1111/jgh.13417]

40 **Xiao W**, Wang W, Chen W, Sun L, Li X, Zhang C, Yang H. GDNF is involved in the barrier-inducing effect of enteric glial cells on intestinal epithelial cells under acute ischemia reperfusion stimulation. *Mol Neurobiol* 2014; **50**: 274-289 [PMID: 24878766 DOI: 10.1007/s12035-014-8730-9]

41 **Xiao W**, Feng Y, Holst JJ, Hartmann B, Yang H, Teitelbaum DH. Glutamate prevents intestinal atrophy *via* luminal nutrient sensing in a mouse model of total parenteral nutrition. *FASEB J* 2014; **28**: 2073-2087 [PMID: 24497581 DOI: 10.1096/fj.13-238311]

42 **Lu YZ**, Wu CC, Huang YC, Huang CY, Yang CY, Lee TC, Chen CF, Yu LC. Neutrophil priming by hypoxic preconditioning protects against epithelial barrier damage and enteric bacterial translocation in intestinal ischemia/reperfusion. *Lab Invest* 2012; **92**: 783-796 [PMID: 22370946 DOI: 10.1038/labinvest.2012.11]

43 **Paul S**, Shilpi, Lal G. Role of gamma-delta (γδ) T cells in autoimmunity. *J Leukoc Biol* 2015; **97**: 259-271 [PMID: 25502468 DOI: 10.1189/jlb.3RU0914-443R]

44 **Huang Y**, Getahun A, Heiser RA, Detanico TO, Aviszus K, Kirchenbaum GA, Casper TL, Huang C, Aydintug MK, Carding SR, Ikuta K, Huang H, Wysocki LJ, Cambier JC, O'Brien RL, Born WK. γδ T Cells Shape Preimmune Peripheral B Cell Populations. *J Immunol* 2016; **196**: 217-231 [PMID: 26582947 DOI: 10.4049/jimmunol.1501064]

45 **Bao K**, Reinhardt RL. The differential expression of IL-4 and IL-13 and its impact on type-2 immunity. *Cytokine* 2015; **75**: 25-37 [PMID: 26073683 DOI: 10.1016/j.cyto.2015.05.008]

46 **Gonzales JN**, Gorshkov B, Varn MN, Zemskova MA, Zemskov EA, Sridhar S, Lucas R, Verin AD. Protective effect of adenosine receptors against lipopolysaccharide-induced acute lung injury. *Am J Physiol Lung Cell Mol Physiol* 2014; **306**: L497-L507 [PMID: 24414256 DOI: 10.1152/ajplung.00086.2013]

47 **Koizumi S**, Odashima M, Otaka M, Jin M, Linden J, Watanabe S, Ohnishi H. Attenuation of gastric mucosal inflammation induced by indomethacin through activation of the A2A adenosine receptor in rats. *J Gastroenterol* 2009; **44**: 419-425 [PMID: 19333545 DOI: 10.1007/s00535-009-0028-8]

48 **Nowak M**, Lynch L, Yue S, Ohta A, Sitkovsky M, Balk SP, Exley MA. The A2aR adenosine receptor controls cytokine production in iNKT cells. *Eur J Immunol* 2010; **40**: 682-687 [PMID: 20039304 DOI: 10.1002/eji.200939897]

49 **Milne GR**, Palmer TM. Anti-inflammatory and immunosuppressive effects of the A2A adenosine receptor. *ScientificWorldJournal* 2011; **11**: 320-339 [PMID: 21298223 DOI: 10.1100/tsw.2011.22]

50 **Lin G**, Field JJ, Yu JC, Ken R, Neuberg D, Nathan DG, Linden J. NF-κB is activated in CD4+ iNKT cells by sickle cell disease and mediates rapid induction of adenosine A2A receptors. *PLoS One* 2013; **8**: e74664 [PMID: 24124453 DOI: 10.1371/journal.pone.0074664]

World Journal of Gastroenterology

Submit a Manuscript: https://www.f6publishing.com

World J Gastroenterol 2023 March 7; 29(9): 1492-1508

DOI: 10.3748/wjg.v29.i9.1492

ISSN 1007-9327 (print) ISSN 2219-2840 (online)

ORIGINAL ARTICLE

Retrospective Cohort Study

Supply and quality of colonoscopy according to the characteristics of gastroenterologists in the French population-based colorectal-cancer screening program

Akoï Koïvogui, Catherine Vincelet, Gaëlle Abihsera, Hamou Ait-Hadad, Hélène Delattre, Tu Le Trung, Agnès Bernoux, Rachel Carroll, Jérôme Nicolet

Specialty type: Gastroenterology and hepatology

Provenance and peer review: Invited article; Externally peer reviewed.

Peer-review model: Single blind

Peer-review report's scientific quality classification

Grade A (Excellent): 0
Grade B (Very good): B, B
Grade C (Good): C, C
Grade D (Fair): 0
Grade E (Poor): 0

P-Reviewer: Bustamante-Balen M, Spain; Gencdal G, Turkey; Muguruma N, Japan; Teramoto-Matsubara OT, Mexico

Received: November 17, 2022
Peer-review started: November 17, 2022
First decision: January 23, 2023
Revised: February 7, 2023
Accepted: February 27, 2023
Article in press: February 27, 2023
Published online: March 7, 2023

Akoï Koïvogui, Site de Seine-Saint-Denis, Centre Régional de Coordination des Dépistages des Cancers en Ile-de-France (CRCDC-IDF), Bondy 93146, France

Catherine Vincelet, Site des Yvelines, Centre Régional de Coordination des Dépistages des Cancers en Ile-de-France (CRCDC-IDF), Le Chesnay Cedex 78153, France

Gaëlle Abihsera, Rachel Carroll, Site du Val-de-Marne, Centre Régional de Coordination des Dépistages des Cancers en Ile-de-France (CRCDC-IDF), Joinville-le-Pont 94340, France

Hamou Ait-Hadad, Site de Seine-et-Marne, Centre Régional de Coordination des Dépistages des Cancers en Ile-de-France (CRCDC-IDF), Lieusaint 77763, France

Hélène Delattre, Site des Hauts-de-Seine, Centre Régional de Coordination des Dépistages des Cancers en Ile-de-France (CRCDC-IDF), Nanterre 92000, France

Tu Le Trung, site du Val-d'Oise, Centre Régional de Coordination des Dépistages des Cancers en Ile-de-France (CRCDC-IDF), Cergy Saint-Christophe 95800, France

Agnès Bernoux, Site de l'Essonne, Centre Régional de Coordination des Dépistages des Cancers en Ile-de-France (CRCDC-IDF), Fontenay-Les-Briis 91640, France

Jérôme Nicolet, Siège Paris, Centre Régional de Coordination des Dépistages des Cancers en Ile-de-France (CRCDC-IDF), Paris 75015, France

Corresponding author: Akoï Koïvogui, MD, MHSc, MSc, Doctor, Site de Seine-Saint-Denis, Centre Régional de Coordination des Dépistages des Cancers en Ile-de-France (CRCDC-IDF), 41 Avenue de Verdun, Bondy 93146, France. aakoivogui@live.fr

Abstract

BACKGROUND

Since its complete roll-out in 2009, the French colorectal cancer screening program (CRCSP) experienced 3 major constraints [use of a less efficient Guaiac-test (gFOBT), stopping the supply of Fecal-Immunochemical-Test kits (FIT), and suspension of the program due to the coronavirus disease 2019 (COVID-19)] affecting its effectiveness.

AIM
To describe the impact of the constraints in terms of changes in the quality of screening-colonoscopy (Quali-Colo).

METHODS
This retrospective cohort study included screening-colonoscopies performed by gastroenterologists between Jan-2010 and Dec-2020 in people aged 50-74 living in Ile-de-France (France). The changes in Quali-colo (Proportion of colonoscopies performed beyond 7 mo (Colo_7 mo), Frequency of serious adverse events (SAE) and Colonoscopy detection rate) were described in a cohort of Gastroenterologists who performed at least one colonoscopy over each of the four periods defined according to the chronology of the constraints [gFOBT: Normal progress of the CRCSP using gFOBT (2010-2014); FIT: Normal progress of the CRCSP using FIT (2015-2018); STOP-FIT: Year (2019) during which the CRCSP experienced the cessation of the supply of test kits; COVID: Program suspension due to the COVID-19 health crisis (2020)]. The link between each dependent variable (Colo_7 mo; SAE occurrence, neoplasm detection rate) and the predictive factors was analyzed in a two-level multivariate hierarchical model.

RESULTS
The 533 gastroenterologists (cohort) achieved 21509 screening colonoscopies over gFOBT period, 38352 over FIT, 7342 over STOP-FIT and 7995 over COVID period. The frequency of SAE did not change between periods (gFOBT: 0.3%; FIT: 0.3%; STOP-FIT: 0.3%; and COVID: 0.2%; $P = 0.10$). The risk of Colo_7 mo doubled between FIT [adjusted odds ratio (aOR): 1.2 (1.1; 1.2)] and STOP-FIT [aOR: 2.4 (2.1; 2.6)]; then, decreased by 40% between STOP-FIT and COVID [aOR: 2.0 (1.8; 2.2)]. Regardless of the period, this Colo_7 mo's risk was twice as high for screening colonoscopy performed in a public hospital [aOR: 2.1 (1.3; 3.6)] compared to screening-colonoscopy performed in a private clinic. The neoplasm detection, which increased by 60% between gFOBT and FIT [aOR: 1.6 (1.5; 1.7)], decreased by 40% between FIT and COVID [aOR: 1.1 (1.0; 1.3)].

CONCLUSION
The constraints likely affected the time-to-colonoscopy as well as the colonoscopy detection rate without impacting the SAE's occurrence, highlighting the need for a respectable reference time-to-colonoscopy in CRCSP.

Key Words: Colorectal cancer screening; Screening colonoscopy; Faecal immunochemical test; Guaiac faecal occult blood test; Quality of colonoscopy; Severity of tumor lesions

Core Tip: The study showed that the detection rate of colonoscopy dropped significantly in France during the years 2019 and 2020, probably due to the coronavirus disease health crisis. The risk of a long delay (> 7 mo) in performing the colonoscopy was twice as high in a public hospital compared to colonoscopies performed in a private endoscopy practice. The constraints likely affected the time to colonoscopy as well as the colonoscopy detection rate without impacting the occurrence of serious adverse events.

Citation: Koïvogui A, Vincelet C, Abihsera G, Ait-Hadad H, Delattre H, Le Trung T, Bernoux A, Carroll R, Nicolet J. Supply and quality of colonoscopy according to the characteristics of gastroenterologists in the French population-based colorectal-cancer screening program. *World J Gastroenterol* 2023; 29(9): 1492-1508
URL: https://www.wjgnet.com/1007-9327/full/v29/i9/1492.htm
DOI: https://dx.doi.org/10.3748/wjg.v29.i9.1492

INTRODUCTION

The impact of the Screening program on controlling colorectal cancer (CRC) morbidity and mortality has been widely proved[1-4]. But since its complete roll-out in France in 2009, the population-based colorectal cancer screening program (CRCSP) has continued to face constraints affecting its effectiveness. Despite the existence of the fecal immunochemical test (FIT) in certain European programs (*i.e.*, Italy, Czech Republic) when the program roll-out was completed in France[5], the health authority chose the Guaiac Hemoccult II test® (gFOBT). It later turned out that gFOBT only identified 50% of colorectal cancer (CRC) lesions and a third of adenomas[6], which led some GPs to be wary of it, at the

risk of seeing some of their patients fall through the cracks[6,7].

To consider this first constraint induced using a low sensitivity/specificity screening test, the health authority decided to replace gFOBT in 2015, with the FIT (Threshold set at 150 ng hemoglobin/mL of stool, "Institut National du Cancer", www.e-cancer.fr). While admitting an improvement in participation with FIT compared to gFOBT, most studies published in France have confirmed the high sensitivity (detection of advanced adenomas and CRC) of FIT and its better acceptability by the population and GPs[8-12]. This performance of the FIT inevitably leads to an increase in colonoscopy requests in the screened population and subsequently to an extension of the time to colonoscopy after a positive FIT result[13]. However, these analyses of the time to colonoscopy only considered the characteristics of the target population without any adjustment to the characteristics of the colonoscopy supply.

On April 25, 2018, the Paris Administrative Court cancelled, during an appeal session, the contract concluded in 2014 between the Health Insurance Agency and the Cerba-Daklapack® consortium (www.slbc.fr). This contract, which related to the supply of screening test kits and the laboratory analysis of the tests carried out, had thus been cancelled only three years after the introduction of the FIT in CRCSP. This legal and administrative confusion led to a market shutdown between March and September 2019. In the Ile-de-France (IDF) region, this shutdown led to a drastic decrease in the number of tests carried out in 2019, compared to forecasts (annual activity report 2019).

Only a few months after the resumption of the test kits' market, the World Health Organization (WHO) announced the pandemic of COVID-19[14]. This pandemic constraint required a relocation of health care resources to control this global health crisis. Screening programs, in particular the CRCSP, were suspended in many countries. The aim of this study was to describe the impact of the constraints listed above in terms of changes to the quality of screening colonoscopies (Quali-colo) in a cohort of gastroenterologists (GEs) practicing in IDF.

MATERIALS AND METHODS

This retrospective cohort study included all screening colonoscopies, performed between 01/01/2010 and 31/12/2020 by GEs in the IDF region and collected by the eight sites (Paris, Seine-et-Marne, Yvelines, Essonne, Hauts-de-Seine, Seine-Saint-Denis, Val-de-Marne and Val-d'Oise) of the IDF CRCSP Coordination Centre (CRCDC-IDF). These screening colonoscopies were performed following a positive screening test in people aged 50-74, living in IDF, France.

Considering the chronology of the constraints in the CRCSP, four periods for carrying out the colonoscopy were distinguished (Figure 1). The first period (gFOBT) corresponded to the five years (2010-2014) of normal progress of the CRCSP using gFOBT. The second period (FIT) corresponded to the four years (2015-2018) of normal progress of the CRCSP using FIT. The third (FIT-STOP) corresponded to the year (2019) during which the CRCSP experienced the cessation of the supply of test kits and the fourth (COVID) corresponded to the program suspension due to the COVID-19 health crisis (2020).

The supply of screening colonoscopy was described by the number and type of practice of GEs practicing in IDF and having performed a screening colonoscopy in a person living in IDF. The Quali-colo was described in terms of time to colonoscopy, yield of colonoscopy and frequency of undesirable events (incidents/accidents, incomplete colonoscopy, refusal of 2nd colonoscopy).

Descriptive and evolutive analyses (supply and Quali-colo) were carried out between the periods (gFOBT, FIT, FIT-STOP, and COVID). These changes were first described according to the characteristics of the GEs who performed the screening colonoscopies. Secondly, the impact of constraints was described in terms of changes in Quali-colo indicators between the four periods, in a cohort of GEs (Cohort-GE) who performed at least one colonoscopy in each of the four periods.

Screening organization and study data collection

The National Council of the Order of Physicians (Research and Statistics Study Department) provided the medical demographic data. Screening data were extracted from CRCDC-IDF departmental databases. Over the study period, the CRCSP campaigns were organized following the CRCSP specifications[15,16]. As a preliminary to each campaign in each study department, an update of the files of eligible people was made after the transmission of individual data by the partners (Health Insurance plans, Medical Information Services of hospitals, Pathologists, GEs, Surgeons, GPs, patients). Anyone who had a screening test did not need a screening colonoscopy if the test result was negative. In case of a positive test result, the person was subsequently invited five years after a normal colonoscopy or excluded from the CRCSP after a positive colonoscopy result (polyp or CRC).

Definition of variables

The screening colonoscopy (complete or incomplete) was considered completed only if the result was provided with or without a completion date. When the completion date was provided, the time to screening colonoscopy was expressed as the number of months between the date of completion of the screening test and the date of completion of the colonoscopy. In the cases where several colonoscopies

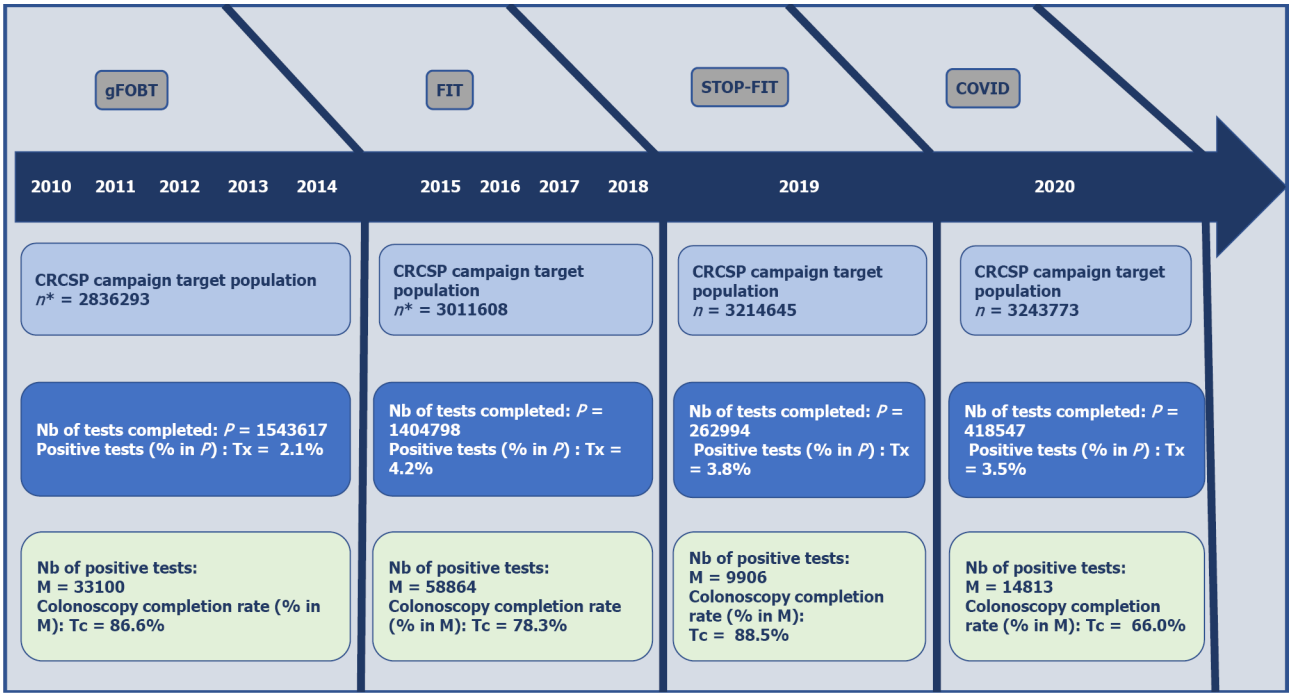

DOI: 10.3748/wjg.v29.i9.1492

Figure 1 Evolution of the colorectal cancer screening program indicators (target population of the campaigns, number of tests carried out, number and proportion of positive tests, rate of completion of colonoscopy) over the 4 study periods (guaiac fecal occult blood test, fecal immunochemical test, STOP-fecal immunochemical test, and COVID). The asterisk (*) is the target population at the start of the period. The colonoscopy completion rate was estimated based on data extraction as of January 31, 2022. gFOBT: Guaiac fecal occult blood test; COVID: Coronavirus disease; FIT: Fecal immunochemical test; Nb: Number; CRCSP: Colorectal cancer screening program.

were carried out to investigate the same positive test, the time to screening colonoscopy was that related to the first colonoscopy. The proportion of screening colonoscopies with an abnormally long time to access colonoscopy (Long-delay-colo) was estimated by the frequency of colonoscopies performed beyond a 7-mo delay among the screening colonoscopies for which the completion date was provided. This delay threshold considers the fact that the risk of colorectal cancer is increased by about 40% for any colonoscopy performed after a waiting period of 7-12 mo[17].

The screening colonoscopy was complete when the colon was examined until crossing the Bauhin valve. The reasons for an incomplete colonoscopy were: Insufficient preparation, Anatomical (dolichocolon, Presence of an obstructive lesion requiring a second colonoscopy or surgery). The accidents related to screening colonoscopy were: exterior hemorrhage with or without transfusion, perforation, death. Incidents related to anesthesia or general condition (cardiorespiratory disorders) were distinguished from those related to endoscopy (*i.e.*, difficulty crossing a cul-de-sac, placement of clips to stop bleeding after a polypectomy). The proportion of serious adverse events (SAEs) was estimated by the frequency of screening colonoscopies during which an incident/accident was notified.

The screening colonoscopy was classified as positive when a neoplasm (Polyp/adenoma/CRC) was discovered, negative if not. The screening colonoscopy detection rate (yield of colonoscopy) was estimated by the proportion of positive colonoscopies among the screening colonoscopies performed. The CRC and polyps/adenomas diagnoses were those coded C18-C20 and D12 according to the 10th version of the WHO International Classification of Diseases (ICD10)[18]. The CRC was considered "seen at colonoscopy" when an ulcerative-budding/ulcerative-necrotizing lesion was described by the GE. The high-risk polyps were adenomatous or scalloped polyps with a diameter of ≥ 10 mm (except hyperplastic polyps), high-grade dysplasia adenomas, villous or tubulo-villous adenomas. The TNM classification[19] has been used to define CRC severity. Any CRC ≥ T3 (subserous invaded) or ≥ N1 (at least one regional node invaded) or M1 (with metastasis) was considered severe CRC.

For each GE practicing in IDF region, having performed at least one screening colonoscopy, the factors studied were: (1) The existence of a gastroenterology consultation carried out before the screening colonoscopy completion date; (2) the annual number of screening colonoscopies performed (1, 2-30, 31-100, and > 100 colonoscopies); (3) the place of performance of the screening colonoscopy (1-Private clinic in the IDF; 2-Private hospitals in the IDF; 3-Public hospital in the IDF including: The Public Assistance of Paris hospitals -APHP-, Other public hospitals in the IDF including army hospitals and municipal health centers). The colonoscopies performed by GEs practicing in ≥ 2 locations, the locations of which had not been specified (n = 2), were attributed to the locations most frequented by these GEs over the period. Similarly, Colo for which the location was specified but for which the GEs were not

specified (n = 6), were attributed to the GEs who performed the greatest number of colonoscopies on the location and over the period. Colo performed in a country other than France were classified as "Place Unspecified". Colonoscopies performed in another region of France were classified "Outside-IDF"; (4) the annual number of colonoscopy locations (1 Location, ≥ 2 Locations); (5) the density of GEs in the municipality where the GE performed the screening colonoscopy. The density (D) of GEs was estimated as number of GEs/100000 inhabitants. Each colonoscopy year, with reference to a regional average density (M) and standard deviation (SD). Low density of GE was: D < M-SD, average-density of GE was: D in M ± SD, high density of GE was: D > M + SD; (6) the seniority of the GE (for any year "A", the GE having no screening colonoscopy in the years prior to "A" was considered a new GE); (7) the residence of the CRCSP target patient treated by the GE (1-the Colonoscopy's supply municipality, 2-other municipality in the Colonoscopy's supply department, 3-other IDF departments). As a reminder, in 2018, The National Institute of Statistics and Economic Studies (INSEE) counted 1267 municipalities in IDF in addition to the city of Paris; and (8) the age of the CRCSP target patient treated by the GE (50-54, 55-59, 60-64, 65-69, and ≥ 70 years).

Statistical analysis

The proportions (Colo performed within one month or after a waiting delay > 7 mo, incomplete and redone Colo, incidents/accidents, positive Colo, high_risk_polyp, CRC seen at Colo, CRC with provided status, severe CRC) were described and compared between periods (gFOBT, FIT, FIT-STOP, and COVID) by the Pearson' Chi-2 test. In the strata defined according to the characteristics of the cohort-GE, the time to perform the screening colonoscopy (in months) was analyzed in terms of average and confidence interval (CI) then, an analysis of variance (ANOVA on repeated measures) was used to compare the average delays between periods (gFOBT, FIT, FIT-STOP *vs* COVID). In the strata defined according to the characteristics of the cohort-GE, the proportions (colonoscopies performed after > 7 mo delay, proportion of SAEs, yield of screening colonoscopy) were compared between periods (gFOBT, FIT, FIT-STOP *vs* COVID) by Cochran's Q test.

The link between each dependent variable (binary variables 0/1: Long-delay-colo; SAEs, Yield of screening colonoscopy) and the predictive factors (annual number of screening colonoscopies performed, Place of performance of the screening colonoscopy, Annual number of colonoscopy locations, Density of GE, Residence of the patient, Age of the patient) was analyzed in a multivariate and two level (colonoscopy and GE) hierarchical regression model. The generalized linear model (family: Bernoulli, link: Logit) with mixed effect was preferred. This multivariate analysis was performed using a model with all covariates regardless of their relationship in univariate analysis. In addition, a strong correlation existed between several covariates (*i.e.*, annual number of screening colonoscopies and Place of performance, Annual number of screening colonoscopies and Municipal density of GEs, Annual number of screening colonoscopies and Period), the model was extended to these terms of interaction between covariates. Only the significant interaction terms (P < 0.05 in univariate analysis) were kept in the final model evaluated by the likelihood ratio test. A biomedical statistician performed the statistical review. All the analyses were carried out at the 5% threshold with version 13 of the STATA software (College Station, TX, United States).

Regulatory issues

Before analysis, all data were anonymized. The screening database had a favourable opinion from the institution that oversees the ethics of data collection ("Commission *nationale de l'informatique et des libertés*": CNIL)[20]. According to the current French legislation, a study that does not change the care of patients did not require the opinion of the Clinical Research Centre's Ethics Committee.

RESULTS

Descriptive and evolutive analyses

Out of a total of 1267 municipalities listed in the IDF region, only 155 municipalities had at least one GE in 2010. This number of municipalities having at least one GE falling from 155 in 2010 to 142 in 2020. In the municipalities having at least one GE, the average annual density of GEs fluctuated between a minimum of 6.3 (in 2014) and a maximum of 6.5 GE/100000 inhabitants over the study period (Table 1).

The gap between the number of GEs registered in the medical demographic database and the number of GEs having performed at least one screening colonoscopy, increased from 134 in 2010 (761 registered *vs* 627 having performed ≥ 1 screening colonoscopy), to 206 in 2015 (776 *vs* 570) before being reduced to 123 in 2019 (798 *vs* 675). The proportion of GEs performing screening colonoscopies at two or more locations varied from 20.6% in 2010 to 13.9% in 2015, then 21.8% in 2019. The proportion of new GEs decreased from 12.6% in 2011 to 7.7% in 2015, then increased to 13.5% in 2016 and further decreased to 4.7% in 2019. In 2016, a total of 727 GEs performed at least one colonoscopy. Among them, 97 GE performed only one screening colonoscopy and 8 GEs exceeded an annual number of 100 screening colonoscopies (Table 1).

Table 1 Evolution of the regional offer in number of gastroenterologists and the number of gastroenterologists having performed at least one colonoscopy, by year of performance of the screening colonoscopy

Year of colonoscopy	Nb of GE in IDF[1]		Number of gastroenterologists who performed a screening colonoscopy[2]												
			Number of GE by seniority		Number of GE by density of GE in the municipality of practice of the GE			Number of GE by place of performance of the colonoscopy			Number of GE by annual number (A) of colonoscopies performed				Total (*n*) of GE in IDF (% GE ≥ 2 location)
	Nb of GE (density)[3]	Nb of municipalities with GE	Senior	New (% in *n*)	Low	Average	High	Private clinic	Private Hop.	Public Hop.	A = 1	A = 2-30	A = 30-100	A > 100	
2010	761 (6.5)	155	627	-	134	85	493	415	114	214	119	473	35	-	627 (20.6)
2011	756 (6.4)	156	534	77 (12.6)	140	71	474	408	117	201	106	465	40	-	611 (17.2)
2012	759 (6.4)	155	538	57 (9.6)	116	79	473	383	112	206	117	454	24	-	595 (16.8)
2013	761 (6.4)	154	539	30 (5.3)	98	92	442	378	115	181	107	448	14	-	569 (16.5)
2014	757 (6.3)	155	522	63 (10.8)	129	75	451	384	106	193	123	448	14	-	585 (17.4)
2015	776 (6.4)	154	526	44 (7.7)	117	53	449	379	103	178	140	419	11	-	570 (13.9)
2016	784 (6.5)	154	629	98 (13.5)	128	65	628	432	143	312	97	447	175	8	727 (18.8)
2017	793 (6.5)	152	642	72 (10.1)	142	56	603	418	142	312	93	486	134	1	714 (19.9)
2018	799 (6.5)	149	665	64 (8.8)	141	51	626	424	151	312	100	488	139	2	729 (20.7)
2019	798 (6.5)	147	643	32 (4.7)	123	63	574	388	152	287	92	512	71	-	675 (21.8)
2020	802 (6.5)	142	619	76 (10.9)	147	50	582	412	162	265	124	475	96	-	695 (19.7)

[1]Number of gastroenterologists (GE) registered in the region (source: National Council of the Order of Physicians).
[2]Number of gastroenterologists who performed a screening colonoscopy during the calendar year (regardless of the type of test and regardless of the date of the screening test).
[3]Density in Number of GE/100000 inhabitants: Regional average density (5.5 à 7.5 GE/100000 inhabitants) Low density of GE (< 5.5 GE/100000 habitants) and high density of GE (> 7.5 GE/100000 inhabitants).
GE: Gastroenterologist; Hop: Hospital; IDF: Ile-de-France; Nb: Number.

In 2011, out of a total of 6428 colonoscopies performed in IDF, the proportion of colonoscopies performed by new GEs was 2.0%, the proportion of colonoscopies performed in a municipality with a high density of GEs was 62.2%, the proportion of colonoscopies performed in a public hospital was 12.5%. In 2016, 1041 screening colonoscopies were performed by the GEs having an annual volume of > 100 screening colonoscopies and 9148 (58.9%) screening colonoscopies were performed by the GEs having an annual volume of 30-100 screening colonoscopies. Compared to 2010 (1.7%), the proportion of screening colonoscopies performed outside the IDF region was significantly higher in 2020 (2.5%; $P < 0.0001$). Similarly, compared to 2019 (16.8%), the proportion of screening colonoscopies performed in public hospitals decreased significantly in 2020 (13.0%, $P < 0.0001$) (Table 2).

Table 2 Evolution of the number of colonoscopies performed according to the characteristics of the gastroenterologist, by year of performance of the screening colonoscopy, *n* (%)

Year of colonoscopy	Number of colonoscopies performed according to GE characteristics														
	Number of colonoscopies by seniority of GE		Number of colonoscopies by density of GE in the municipality of practice of the GE[1]			Number of colonoscopies by place of performance of the colonoscopy			Number of colonoscopies by GE's annual number (A) of colonoscopies performed				Total		
	Senior	New	Low	Average	High	Clinic	Private Hop.	Public Hop.	A = 1	A = 2-30	A = 31-100	A > 100	Nb (*n*) of Colo performed in IDF (average Nb of Colo by GE)	Nb of Colo with place specified (% outside IDF)	Nb of Colo (% Place unspecified)
2010	6059	-	1535	900 (14.9)	3624 (59.8)	4507	830 (13.7)	722 (11.9)	119	4493 (74.2)	1447 (23.9)	-	6059 (11)	6161 (1.7)	6441 (4.4)
2011	6300	128 (2.0)	1684	712 (11.1)	4032 (62.7)	4677	946 (14.7)	805 (12.5)	106	4578 (71.2)	1744 (27.1)	-	6428 (12)	6543 (1.8)	6928 (5.6)
2012	5355	76 (1.4)	1186	766 (14.1)	3479 (64.1)	3818	830 (15.3)	783 (14.4)	117	4284 (78.9)	1030 (19.0)	-	5431 (11)	5533 (1.8)	5852 (5.5)
2013	4309	47 (1.1)	1045	737 (16.9)	2574 (59.1)	3156	660 (15.2)	540 (12.4)	107	3725 (85.5)	524 (12.0)	-	4356 (9)	4409 (1.2)	4712 (6.4)
2014	4320	132 (3.0)	1104	611 (13.7)	2737 (61.5)	3199	650 (14.6)	603 (13.5)	123	3718(83.5)	611 (13.7)	-	4452 (9)	4515 (1.4)	4746 (4.9)
2015	3712	63 (1.7)	879	446 (11.8)	2450 (64.9)	2692	604 (16.0)	479 (12.7)	140	3198 (84.7)	437 (11.6)	-	3775 (8)	3818 (1.1)	4034 (5.4)
2016	15196	333 (2.1)	3406	1862 (12.0)	10261 (66.1)	10886	2527 (16.3)	2116 (13.6)	97	5243 (33.8)	9148 (58.9)	1041	15529 (25)	15811 (1.8)	16651 (5.0)
2017	11519	192 (1.6)	2876	1262 (10.8)	7573 (64.7)	7919	1937 (16.5)	1855 (15.8)	93	5370 (45.9)	6137(52.4)	111	11711 (18)	11920 (1.8)	12345 (3.4)
2018	12181	164 (1.3)	2758	1190 (9.6)	8397 (68.0)	8233	2300 (18.6)	1812 (14.7)	100	5331 (43.2)	6684 (54.1)	230	12345 (19)	12602 (2.0)	13057 (3.5)
2019	8189	98 (1.2)	1582	932 (11.3)	5773 (69.7)	5365	1532 (18.5)	1390 (16.8)	92	5261 (63.5)	2934 (35.4)	-	8287 (13)	8487 (2.4)	8767 (3.2)
2020	9103	158 (1.7)	2088	755 (8.2)	6418 (69.3)	6654	1900 (20.5)	1199 (13.0)	124	5049 (54.5)	4088 (44.1)	-	9261 (15)	9501 (2.5)	9793 (3.0)

[1]Density in Number of GE/100000 inhabitants: Regional average density (5.5 à 7.5 GE/100000 inhabitants), low density of GE (< 5.5 GE/100000 habitants) et High density of GE (> 7.5 GE/100000 inhabitants).
Colo: Screening colonoscopy; GE: Gastroenterologist; Hop.: Hospital; IDF: Ile-de-France; Nb: Number.

Overall, the time to screening colonoscopy was significantly longer over STOP-FIT (gFOBT: 2.6 ± 2.9 *vs* FIT: 3.0 ± 3.0; STOP-FIT: 3.9 ± 3.9, COVID: 3.5 ± 3.9, $P < 0.0001$). Over the gFOBT period, 3.1% of the 28679 colonoscopies performed were incomplete (20.7% were redone) for reasons: Anatomical (60.6%), insufficient preparation (16.1%). The proportion of incomplete and redone colonoscopies was significantly higher over FIT ($P < 0.001$). Although one case of death was reported during the gFOBT period, the proportion of adverse events was not significantly related to the period (0.05). The proportion of cancers seen at colonoscopy was lower over FIT (gFOBT: 61.4%, *vs* FIT: 55.2% or STOP-FIT: 57.5% or COVID: 56.1%; $P < 0.0001$) (Table 3).

Table 3 Quality indicators and results of colonoscopies by period of performance of colonoscopy in people aged 50-74, residing in Ile-de-France, *n* (%)

Quality indicator	Period				
	gFOBT	FIT	STOP-FIT	COVID	*P* value[1]
Total number (*n*) of colonoscopies	28679	46087	8767	9783	
Existence of a GE consultation before colonoscopy					
Nb (A) colonoscopies with date of consultation	5267 (18.4)	1517 (3.3)	406 (4.6)	198 (2.0)	$< 10^{-3}$
Date of consultation ≠ Date of colonoscopy					
Nb colonoscopies of which date of consultation ≠ colon date (% in A)	298.4 (56.7)	883 (58.2)	402 (99.0)	191 (96.5)	$< 10^{-3}$
Time to colonoscopy					
Average (in mean ± SD)	2.6 ± 2.9	3.0 ± 3.0	3.9 ± 3.9	3.5 ± 2.9	$< 10^{-3*}$
Number of colonoscopies performed within one month	4957 (17.3)	4572 (9.9)	458 (5.2)	726 (7.4)	$< 10^{-3}$
Number of colonoscopies performed beyond 7 mo	1520 (5.3)	2949 (6.4)	1034 (11.8)	933 (9.5)	$< 10^{-3}$
Complete colonoscopy					$< 10^{-3}$
Nb colonoscopies without information on performance	1263 (4.4)	2360 (5.1)	410 (4.7)	432 (4.4)	
Number of complete colonoscopies	26530 (92.5)	41695(90.5)	8004 (91.3)	8981 (91.8)	
Nb (B) of incomplete colonoscopies	886 (3.1)	2032 (4.4)	357 (4.1)	376 (3.8)	
Reasons for incomplete colonoscopies					$< 10^{-3}$
Unspecified: *n* (% in B)	206 (23.3)	617 (30.4)	109 (30.5)	114 (30.3)	
Anatomical reason/Obstruction by lesion: *n* (% in B)	537 (60.6)	845 (41.6)	150 (42.0)	161 (42.8)	
Insufficient preparation: *n* (% in B)	143 (16.1)	570 (28.1)	98 (27.5)	101 (26.9)	
Redone incomplete colonoscopy					
Number of redone colonoscopies (% B)	183 (20.7)	960 (47.2)	158 (44.3)	163 (43.3)	$< 10^{-3}$
Frequency of incidents					0.14
No incidents reported: *n*	28873 (99.6)	45947 (99.7)	8740 (99.7)	9763 (99.8)	
Related to anaesthesia/general condition: *n*	18 (0.06)	24 (0.05)	3 (0.03)	2 (0.02)	
Related to endoscopy: *n*	88 (0.3)	116 (0.3)	22 (0.3)	18 (0.2)	
Frequency of accidents					0.17
No accidents reported: *n*	28589 (99.7)	45970 (99.8)	8749 (99.8)	9763 (99.8)	
Suspected complication: *n*	24 (0.08)	23 (0.05)	5 (0.04)	3 (0.03)	
Exterior bleeding: *n*	57 (0.2)	66 (0.1)	14 (0.2)	12 (0.1)	
Perforation: *n*	8 (0.03)	28 (0.06)	3 (0.03)	4 (0.04)	
Deaths: *n*	1 (0.0)	0	0	0	
Colonoscopies results					
Detection rate: Nb of lesions	14857 (51.8)	29843 (64.8)	5565 (63.5)	5967 (60.1)	$< 10^{-3}$
Nb Polyps (% HRP)	12947 (44.2)	26624 (56.4)	5040 (53.3)	5425 (51.8)	$< 10^{-3}$
Nb of CRC (% CRC seen at colonoscopy)	1910 (61.4)	3219 (55.2)	525 (57.3)	542 (56.1)	$< 10^{-3}$
% CRC with severity stage specified among Nb CRC[2]	90.3	80.5	74.3	72.3	$< 10^{-3}$
Nb CRC with severity stage specified (% severe CRC)[2]	1724 (50.7)	2592 (40.9)	390 (39.5)	392 (39.5)	$< 10^{-3}$

[1]Pearson's χ^2/Fisher's exact test of proportion or Fisher's *F* test (ANOVA).
[2]Any CRC ≥ T3 (subserous invaded) or ≥ N1 (at least one regional node invaded) or M1 (with metastasis) was considered severe colorectal cancer.
CRC: Colorectal cancer; FIT: Fecal immunochemical test; GE: Gastroenterologist; gFOBT: Guaiac fecal occult blood test; HRP: High risk polyps (advanced adenoma); Nb: Number.

Changes in Quali-colo indicators between the four periods, in a cohort of GEs

The cohort of 533 GE achieved 21509 Screening colonoscopies over the gFOBT period, 38352 over FIT, 7342 over STOP-FIT and 7995 over the COVID period. In this cohort, the difference in time (months) to screening colonoscopy between periods was globally significant [gFOBT: 2.6 (2.5; 2.6) *vs* FIT: 3.0 (2.9; 3.0); STOP-FIT: 3.9 (3.8; 4.0) and COVID: 3.5 (3.4; 3.6); $P < 0.0001$]. The average time to colonoscopy was longer in public hospitals compared to clinics or private hospital, regardless of the period. This average time was paradoxically shorter over the COVID period compared to the STOP-FIT period, regardless of the type of establishment [in STOP-FIT clinic: 3.7 (3.6; 3.7) *vs* COVID: 3.4 (3.3-3.5) in public hospitals STOP-FIT: 5.1 (4.7-5.9) *vs* COVID: 4.2 (3.8; 4.7)]. The average time to colonoscopy was significantly lower among GEs practicing in low-density areas of GEs compared to those practicing in high-density areas of GEs, over the gFOBT and FIT periods, conversely, depending on the density area the confidence intervals were not significant over the STOP-FIT and COVID periods (Table 4).

Regardless of the GE's characteristics, the proportion of screening colonoscopy performed in > 7 mo delay was significantly higher over STOP-FIT ($P < 0.001$). The proportion of colonoscopies performed in > 7 mo delay was higher in public hospitals compared to clinics and private hospitals, regardless of the period ($P < 0.001$ in each period). This proportion of colonoscopies performed in > 7 mo delay decreased during the COVID period compared to the STOP-FIT period, regardless of the place of colonoscopy $P < 0.001$ for each place). The proportion of colonoscopies performed in > 7 mo delay was higher in the 50-54 age group, regardless of the period $P < 0.001$ in each period) (Table 5).

Whatever the characteristics of the Cohort-GE, the decline in colonoscopy detection rate was significant between the FIT and COVID period (Table 6). The risk of having a long delay to colonoscopy was twice as high for screening-colonoscopy performed in a public hospital [adjusted odds ratio (aOR): 2.1 (1.3; 3.6)] compared to screening colonoscopy performed in a private IDF clinic. Except for the patient's age, the risk of adverse events was not related to any other predictive factor. Compared to patients aged 50-54, patients aged 70 had a 70% increased risk of neoplasm detection. The risk of neoplasm detection decreased by about 40% between the periods FIT [aOR: 1.6 (1.5; 1.7)] and COVID [aOR: 1.1 (1.0; 1.3)] (Table 7).

DISCUSSION

The European guide for quality assurance of colorectal cancer screening recommends performing a colonoscopy within 31 d following a positive test result[21]. In our Cohort-GE, if the increase in the time to screening colonoscopy between the first and the second period was attributable to the introduction of FIT, its increase after the second period was attributable to the malfunction of the program due to the slowdown of the kit market and the COVID-19 health crisis. There is certainly no relationship between the kit market and the colonoscopy offer, but the unexplained increase in the time to perform colonoscopy during a year that saw a market slowdown can be explained factually by this market crisis. The hypothesis would be that general practitioners reacted to the market crisis by relaxing the program, in particular the follow-up of people who had a positive test. Indeed, in France, in addition to the distribution of the test kit, the training doctors are real facilitators of access to colonoscopy (helping the patient to make an appointment with a gastroenterologist, motivating the patient to have the colonoscopy). This hypothesis is confirmed by the slight decrease in the time to colonoscopy in 2020 compared to 2019, despite the COVID-19 health crisis. The year 2020 was moreover affected by this kit market crisis than by the COVID-19 health crisis. Indeed, after the resumption of the kit market in September 2019, several people who had a positive test during the last quarter of 2019 were inevitably the first to be affected by colonoscopy postponements at the start of the first confinement in March 2020. However, the improvement in the time to colonoscopy during the pandemic (compared to the STOP-FIT period) could also be linked to the fact that people have refocused their concerns on their health. Regardless of the characteristics of the Cohort-GE, the screening colonoscopy detection rate dropped significantly between the STOP-FIT and COVID periods, while the proportions of SAEs stayed unchanged.

The long delay to access colonoscopy observed on the gFOBT and FIT periods converges with the results of another French study[22], although it is clearly higher than those observed elsewhere[23,24]. The definition of a reference delay and the obligation of compliance with it by all GEs taking part in CRCSP would effectively reduce the delay in France. This reframing is necessary, especially since the number of GEs is large, but with an increased disparity in terms of the number of screening colonoscopies performed by GEs.

Despite this longer waiting time to colonoscopy, the proportion of colonoscopies during which a SAE was reported did not change between periods. Although high, the frequency of perforations remains lower than that (1.1%) found in Alsace[25]. In the program, there was no nationally standardized forms for collecting screening colonoscopy data. Information concerning the date of consultation before the colonoscopy, or the progress of the examination can sometimes be missed or be considered irrelevant during this collection. Therefore, the low frequency of SAEs reported in this study could be the consequence of under-reporting.

Table 4 Average time (in months) to colonoscopy according to the characteristics of the cohort of gastroenterologists who performed at least one colonoscopy over each of the four periods (guaiac fecal occult blood test, fecal immunochemical test, STOP-fecal immunochemical test, and COVID)

Characteristics of the cohort of gastroenterologists	Nb of GE	Average time (in months) to colonoscopy, by period								P^1
		gFOBT		FIT		STOP-FIT		COVID		
		Nb of Colo	Average, 95%CI	Nb of Colo	Average, 95%CI	Nb of Colo	Average, 95%CI	Nb of Colo	Average, 95%CI	
Overall	533	21509	2.6 [2.5; 2.6]	38352	3.0 [2.9; 3.0]	7342	3.9 [3.8; 4.0]	7995	3.5 [3.4; 3.6]	$< 10^{-3}$
Annual Nb of Colo										
1	201[2]	304	3.1 [2.8; 3.5]	150	3.3 [2.7; 3.8]	38	4.3 [3.1; 4.8]	51	4.0 [3.5; 4.6]	0.08
2-30	481[2]	16819	2.6 [2.5; 2.6]	15970	3.0 [3.0; 3.1]	4887	3.9 [3.8; 4.0]	4211	3.5 [3.4; 3.6]	$< 10^{-3}$
31-100	44[2]	4386	2.4 [2.3; 2.5]	21137	3.0 [2.9; 3.0]	2817	3.8 [3.6; 3.9]	3733	3.5 [3.4; 3.6]	$< 10^{-3}$
> 100	0	0		1095	2.5 [2.3; 2.6]	0		0		
Place of S-colo performance										
Clinic	355[2]	15745	2.4 [2.4; 2.5]	27003	2.9 [2.8; 2.9]	5039	3.7 [3.6; 3.7]	5560	3.4 [3.3; 3.5]	$< 10^{-3}$
Private hospital	125[2]	3041	2.5 [2.4; 2.6]	6500	2.9 [2.8; 3.0]	1359	3.6 [3.5; 3.7]	1621	3.4 [3.3; 3.5]	$< 10^{-3}$
Public hospital	235[2]	2723	3.3 [3.2; 3.4]	4849	3.8 [3.7; 3.9]	940	5.1 [4.7; 5.9]	795	4.2 [3.8; 4.7]	$< 10^{-3}$
Average density of GE (GE/100000iHbts)										
Low	127[2]	4643	2.4 [2.3; 2.5]	8419	2.9 [2.8; 2.9]	1519	3.9 [3.8; 4.1]	1800	3.4 [3.3; 3.5]	$< 10^{-3}$
Average	108[2]	3245	2.5 [2.4; 2.5]	4314	2.9 [2.8; 2.9]	810	4.1 [3.8; 4.4]	781	3.6 [3.4; 3.9]	$< 10^{-3}$
High	467[2]	13621	2.6 [2.6; 2.7]	25619	3.0 [3.0; 3.1]	5009	3.8 [3.7; 3.9]	5395	3.5 [3.4; 3.6]	$< 10^{-3}$
Annual Nb of Colo locations										
1 location	483[2]	14437	2.6 [2.6; 2.7]	24851	3.0 [3.0; 3.1]	4763	3.8 [3.7; 3.9]	5160	3.5 [3.4; 3.6]	$< 10^{-3}$
≥ 2 locations	153[2]	7072	2.4 [2.4; 2.5]	13501	2.9 [2.9; 3.0]	2575	4.0 [3.9; 4.1]	2816	3.5 [3.4; 3.7]	$< 10^{-3}$
Residence of the patient										
Colonoscopy's supply municipality	338[2]	4947	2.5 [2.4; 2.5]	7775	2.9 [2.9; 3.0]	1502	3.9 [3.7; 4.1]	1530	3.5 [3.3; 3.6]	$< 10^{-3}$
Other municipality in Colonoscopy's supply department	480[2]	13259	2.5 [2.5; 2.6]	23754	3.0 [3.0; 3.1]	4401	3.9 [3.8; 4.0]	4982	3.5 [3.4; 3.6]	$< 10^{-3}$
Other departments in IDF	419[2]	3303	2.7 [2.6; 2.8]	6823	2.9[2.9; 3.0]	1435	3.8 [3.6; 4.0]	1464	3.6 [3.5; 3.8]	$< 10^{-3}$
Age (in yr) of the patients										
50-54	485[2]	4995	2.7 [2.6; 2.8]	8018	3.1 [3.0; 3.2]	1695	4.1 [3.9; 4.2]	1616	3.8 [3.7; 4.0]	$< 10^{-3}$
55-59	452[2]	4669	2.6 [2.5; 2.7]	7355	3.1 [3.0; 3.1]	1446	3.9 [3.7; 4.1]	1560	3.6 [3.4; 3.7]	$< 10^{-3}$
60-64	466[2]	4889	2.5 [2.4; 2.6]	7851	3.0 [2.9; 3.0]	1478	3.7 [3.5; 3.9]	1531	3.5 [3.4; 3.7]	$< 10^{-3}$
65-69	464[2]	3766	2.5 [2.4; 2.5]	8511	2.9 [2.8; 2.9]	1403	3.8 [3.6; 4.0]	1590	3.3 [3.1; 3.5]	$< 10^{-3}$
≥ 70	431[2]	3190	2.4 [2.3; 2.5]	6617	2.9 [2.8; 3.0]	1316	3.7 [3.5; 3.8]	1679	3.4 [3.3; 3.6]	$< 10^{-3}$

[1](Prob > F) ANOVA.

[2]This is the number of gastroenterologists (GEs) having performed a colonoscopy over the guaiac fecal occult blood test period, the same GE can be present in all of the modalities, for example the same GE having performed colonoscopies at 3 different sites corresponding to each of the density zones (low average high).

95%CI: 95% confidence interval; Colo: Screening colonoscopy; FIT: Fecal immunochemical test; GE: Gastroenterologist; gFOBT: Guaiac fecal occult blood test; iHbts: Inhabitants; IDF: Ile-De-France; Nb: Number.

The high proportion of incomplete colonoscopies due to insufficient preparation should alert to the need to set up a specific preparation protocol for screening colonoscopy. To date, it is impossible to evaluate with relevance the preparation of a colonoscopy in outpatients, who are not hospitalized at the time of the preparation. Similarly, there is no standard preparation scheme imposed in the French

Table 5 Proportion of colonoscopies performed beyond 7 mo and proportion of serious adverse events, according to the characteristics of the cohort of gastroenterologists who performed at least one colonoscopy in each of the three periods (guaiac fecal occult blood test, fecal immunochemical test, STOP-fecal immunochemical test, and COVID)

Characteristics of the cohort of gastroenterologists	Proportion of colonoscopies performed beyond 7 mo by period					Proportion of serious adverse events by period				
	gFOBT	FIT	STOP-FIT	COVID		gFOBT	FIT	STOP-FIT	COVID	
	Nb of Colo (% > 7 mo)	Nb of Colo (% > 7 mo)	Nb of Colo (% > 7mo)	Nb of Colo (% > 7 mo)	P^1	%EI	%EI		%EI	P^1
Overall	21509 (5.3)	38352 (6.2)	7342 (11.3)	7995 (9.2)	$< 10^{-3}$	0.3	0.3	0.3	0.2	0.10
Annual Nb of Colo										
1	304 (10.1)	150 (11.8)	38 (18.4)	51 (12.0)	$< 10^{-3}$	0.3	0	0	0	0.67
2-30	16819 (5.5)	15970 (6.9)	4887 (11.8)	4211 (9.4)	$< 10^{-3}$	0.3	0.4	0.3	0.1	0.09
31-100	4386 (4.1)	21137 (5.7)	2817 (10.6)	3733 (9.0)	$< 10^{-3}$	0.4	0.2	0.3	0.2	0.25
> 100		1095 (3.7)					0.2			
Place of Colo performance										
Clinic	15745 (4.8)	27003 (5.4)	5039 (10.4)	5560 (8.3)	$< 10^{-3}$	0.3	0.3	0.3	0.1	0.16
Private hospital	3041 (5.1)	6500 (5.9)	1359 (9.6)	1621 (9.5)	$< 10^{-3}$	0.3	0.2	0.2	0.2	0.71
Public hospital	2723 (8.5)	4849 (10.6)	940 (18.8)	795 (15.1)	$< 10^{-3}$	0.6	0.6	0.2	0.4	0.48
Average density of GE (GE/100000 iHbts)										
Low	4643 (5.1)	8419 (5.8)	1519 (11.5)	1800 (9.1)	$< 10^{-3}$	0.3	0.2	0.3	0.1	0.59
Average	3245 (4.9)	4314 (6.5)	810 (11.0)	781 (9.9)	$< 10^{-3}$	0.2	0.3	0.1	0.5	0.48
High	13621 (5.5)	25619 (6.2)	5009 (11.3)	5395 (9.2)	$< 10^{-3}$	0.4	0.3	0.3	0.1	0.04
Annual Nb of Colo locations										
1 location	14437 (5.6)	24851 (6.3)	4763 (10.6)	5160 (9.5)	$< 10^{-3}$	0.4	0.3	0.3	0.2	0.17
≥ 2 location	7072 (4.8)	13501 (6.0)	2575 (12.7)	2816 (8.7)	$< 10^{-3}$	0.2	0.2	0.2	0.1	0.80
Residence of the patient										
Colonoscopy's supply municipality	4947 (4.9)	7775 (5.9)	1502 (11.6)	1530 (8.0)	$< 10^{-3}$	0.2	0.3	0.3	0.0	0.18
Other municipality in Colonoscopy's supply department	13259 (5.1)	23754 (6.0)	4401 (11.0)	4982 (9.6)	$< 10^{-3}$	0.4	0.3	0.2	0.2	0.02
Other departments in IDF	3303 (6.6)	6823 (6.9)	1435 (12.1)	1464 (9.2)	$< 10^{-3}$	0.3	0.4	0.4	0.3	0.80
Age (in yr) of the patients										
50-54	4995 (6.7)	8018 (7.0)	1695 (12.2)	1616 (11.0)	$< 10^{-3}$	0.2	0.2	0.1	0.1	0.43
55-59	4669 (5.7)	7355 (6.6)	1446 (11.8)	1560 (9.9)	$< 10^{-3}$	0.3	0.3	0.4	0.2	0.79
60-64	4889 (4.7)	7851 (5.9)	1478 (10.3)	1531 (8.9)	$< 10^{-3}$	0.4	0.3	0.5	0.3	0.76
65-69	3766 (4.4)	8511 (5.5)	1403 (11.7)	1590 (8.2)	$< 10^{-3}$	0.4	0.3	0.3	0.1	0.20
≥ 70	3190 (4.6)	6617 (5.7)	1316 (10.6)	1679 (8.2)	$< 10^{-3}$	0.5	0.4	0.2	0.2	0.49

[1]Cochran *Q* test.

Colo: Screening colonoscopy; Colo+: Positive screening colonoscopy; FIT: Fecal immunochemical test; GE: Gastroenterologist; gFOBT: Guaiac fecal occult blood test; iHbts: Inhabitants; IDF: Ile-De-France; Nb: Number.

screening program, each GE proposing the method of his choice to the patient. However, although a non-superiority of a preparation scheme (Enema *vs* Oral preparation) was argued[21], studies admitted that a short time (1-6 h *vs* > 8 h) between the colic preparation and colonoscopy is associated with a

Table 6 Neoplasm detection rate at colonoscopy, according to the characteristics of the cohort of gastroenterologists who performed at least one colonoscopy in each of the three periods (guaiac fecal occult blood test, fecal immunochemical test, STOP-fecal immunochemical test, and COVID)

Characteristics of the cohort of gastroenterologists	Neoplasm detection rate at colonoscopy by period				
	gFOBT	FIT-1	STOP-FIT	COVID	
	Nb of Colo (% Colo+)	Nb of Colo (% Colo+)	Nb of Colo (% Colo+)	Nb of Colo (% Colo+)	*P*[1]
Overall	21509 (52.3)	38352 (65.0)	7342 (63.3)	7995 (60.1)	$< 10^{-3}$
Annual Nb of Colo					
1	304 (50.7)	150 (62.0)	38 (71.1)	51 (51.0)	0.02
2-30	16819 (53.6)	15970 (64.5)	4887 (63.7)	4211 (59.6)	$< 10^{-3}$
31-100	4386 (47.6)	21137 (65.8)	2817 (62.5)	3733 (61.8)	$< 10^{-3}$
> 100		1095 (58.6)	0	0	
Place of S-colo performance					
Clinic	15745 (52.4)	27 003 (64.9)	5039 (62.8)	5560 (60.1)	$< 10^{-3}$
Private hospital	3041 (54.3)	6500 (65.0)	1359 (64.8)	1621 (62.7)	$< 10^{-3}$
Public hospital	2723 (49.8)	4849 (65.6)	940 (63.7)	795 (59.5)	$< 10^{-3}$
Average Density of GE (GE/100000iHbts)					
Low	4643 (53.0)	8419 (64.5)	1519 (61.7)	1800 (58.4)	$< 10^{-3}$
Average	3245 (53.1)	4314 (64.1)	810 (65.2)	781 (61.1)	$< 10^{-3}$
High	13621 (51.9)	25619 (65.4)	5009 (63.4)	5395 (61.2)	$< 10^{-3}$
Annual Nb of S-colo locations					
1 location	14437 (52.8)	24851 (64.8)	4763 (63.0)	5160 (60.8)	$< 10^{-3}$
≥ 2 locations	7072 (51.3)	13501 (65.6)	2575 (63.8)	2816 (60.2)	$< 10^{-3}$
Residence of the patient					
Colonoscopy's supply municipality	4947 (53.4)	7775 (65.3)	1502 (61.1)	1530 (59.5)	$< 10^{-3}$
Other municipality in Colonoscopy's supply department	13259 (51.7)	23754 (65.0)	4401 (64.2)	4982 (61.2)	$< 10^{-3}$
Other departments in IDF	3303 (53.1)	6823 (64.9)	1435 (62.8)	1464 (59.6)	$< 10^{-3}$
Age (in yrs) of the patients					
50-54	4995 (44.9)	8018 (56.5)	1695 (55.2)	1616 (52.9)	$< 10^{-3}$
55-59	4669 (50.8)	7355 (63.1)	1446 (61.3)	1560 (58.9)	$< 10^{-3}$
60-64	4889 (54.2)	7851 (67.9)	1478 (65.5)	1531 (63.1)	$< 10^{-3}$
65-69	3766 (57.1)	8511 (68.9)	1403 (68.3)	1590 (65.3)	$< 10^{-3}$
≥ 70	3190 (57.5)	6617 (69.2)	1316 (67.9)	1679 (62.8)	$< 10^{-3}$

[1]Cochran *Q* test.

Colo: Screening colonoscopy; Colo+: Positive screening colonoscopy; FIT: Fecal immunochemical test; GE: Gastroenterologist; gFOBT: Guaiac fecal occult blood test; iHbts: Inhabitants; IDF: Ile-De-France; Nb: Number.

better quality of colonic preparation[26].

Compared to gFOBT, the high proportion of 2nd colonoscopies over the FIT period would confirm the literature on the performance of FIT in screening for precancerous lesions[27], which most often only require endoscopic resection. However, in addition to a high proportion of obstructive lesions, the proportion of severe cancers was significantly higher over the gFOBT period.

Several study results converge on a link between the long delay in access to colonoscopy and the CRC risk. Forbes *et al*[28] propose that wherever possible, colonoscopy should not be delayed beyond 6 mo of positive fecal testing as an aspirational target (with 9 mo as an upper limit). In the Kaiser Permanente (California) health plan members, the risk of CRC was increased by about 40% for any colonoscopy

Table 7 Multivariate analysis of the relationship between each dependent variable (binary variables 0/1: Screening colonoscopy performed beyond 7-mo; Serious adverse events, Yield of neoplasm at screening colonoscopy) and the predictive factors

Characteristics of the cohort of gastroenterologists	Colo performed beyond a 7-mo risk analysis		Serious adverse events risk analysis		Neoplasms risk analysis	
	OR_a, 95%CI	P^1	OR_a, 95%CI	P^1	OR_a, 95%CI	P^1
Annual Nb of Colo (Ref: 1 Colo)						
2-30	0.7 [0.6; 1.0]	0.002	2.5 [0.3; 18.2]	0.37	0.9 [0.7; 1.1]	0.41
> 30	0.7 [0.3; 0.9]	0.008	2.9 [0.9; 23.0]	0.05	0.8 [0.6; 1.1]	0.32
Place of S-colo performance (Ref: Clinic)						
Private hospital	1.2 [0.9; 1.6]	0.18	0.7 [0.3; 1.8]	0.47	1.1 [0.9; 1.3]	0.41
Public hospital	2.1 [1.3; 3.6]	0.001	1.6 [0.3; 8.7]	0.60	1.1 [0.8; 1.4]	0.20
Density of GE (Ref: Low)						
Average	0.9 [0.8; 1.0]	0.05	1.2 [0.6; 2.2]	0.59	1.0 [0.9; 1.1]	0.76
High	1.0 [1.0; 1.2]	0.28	1.2 [0.6; 2.3]	0.65	0.9 [0.8; 1.0]	0.04
Annual Nb of S-colo locations (Ref: 1 location)						
≥ 2 locations	1.1 [0.8; 1.5]	0.11	1.6 [0.5; 4;4]	0.41	1.0 [0.8; 1.3]	0.84
Residence of the patient (Ref: Colonoscopy's supply municipality)						
Other municipality in Colonoscopy's supply department	1.0 [0.9; 1.0]	0.30	1.0 [0.5; 2.1]	0.97	1.0 [0.9; 1.0]	0.31
Other departments in IDF	1.2 [1.1; 1.3]	$< 10^{-3}$	1.2 [0.3; 5.2]	0.81	0.9 [0.8; 1.0]	0.13
Age (yrs) of the patients (Ref: 50-54 yr)						
55-59	0.9 [0.8; 1.0]	0.03	1.6 [1.0; 2.6]	0.04	1.3 [1.2; 1.4]	$< 10^{-3}$
60-64	0.8 [0.7; 0.9]	0.001	2.0 [1.2; 3.1]	0.006	1.6 [1.5; 1.6]	$< 10^{-3}$
65-69	0.7 [0.7; 0.8]	$< 10^{-3}$	1.9 [1.2; 3.0]	0.01	1.7 [1.6; 1.8]	$< 10^{-3}$
≥ 70	0.7 [0.6; 0.8]	0.003	2.1 [1.3; 3.4]	0.002	1.7 [1.6; 1.8]	$< 10^{-3}$
Period (Ref.: gFOBT)						
FIT	1.2 [1.1; 1.2]	$< 10^{-3}$	0.8 [0.4; 1.5]	0.11	1.6 [1.5; 1.7]	$< 10^{-3}$
STOP-FIT	2.4 [2.1; 2.6]	$< 10^{-3}$	0.8 [0.5; 1.3]	0.27	1.3 [1.1; 1.5]	$< 10^{-3}$
COVID	2.0 [1.8; 2.2]	$< 10^{-3}$	0.5 [0.3; 0.9]	0.02	1.1 [1.0; 1.3]	0.08

[1]$P > |z|$.

95%CI: 95% confidence interval; Colo: Screening colonoscopy; FIT: Fecal immunochemical test; GE: Gastroenterologist; gFOBT: Guaiac fecal occult blood test; IDF: Ile-De-France; OR_a: Adjusted odds-ratio.

performed after a waiting period of 7-12 mo[17]. A recent meta-analysis shows that the risk of colorectal cancer is increased by 42%, and that the risk of cancer at an advanced stage was multiplied by 2 or even more, when colonoscopy was performed more than 6 mo after a positive test[29]. In this study, the time to access colonoscopy as well as its lengthening, induced first by the change of the test and then by the health crisis, had no impact in terms of the CRC severity, probably because of the discriminatory approach prioritizing patients with already existing symptoms. As a reminder, the French Society of Digestive Endoscopy had made, in mid-April 2020, the specific recommendation to postpone by 6 wk any colonoscopy following a positive screening test result, if there was no clinical nor biological sign of CCR[30]. In addition, since FIT was introduced in 2015 in a population screened biannually with gFOBT, the severe CRC screened by FIT are likely to be those not detected at an early stage by gFOBT. This hypothesis is confirmed by the drop in the colonoscopy detection rate and by the proportion of severe CRC over STOP-FIT and COVID periods.

To celebrate the tenth anniversary of the first atlas of medical demography, the National Council of the Order of Physicians focused on the gradual transfer from liberal activity to salaried activity. The focus also mentioned the widening of territorial inequalities to the detriment of regions and departments already in difficulty in terms of medical density[31]. Although the number of GEs is unevenly distributed over the 1268 IDF municipalities, the density of GEs in the IDF region was well

above the range (4.2 to 4.9) of the national average observed in 2017[31].

Each GE participating in a CRCSP must perform at least 300 colonoscopies per year[21]. Despite the superiority of the regional offer compared to the national average, the annual number of colonoscopies per GE stays very disparate and below 300, especially for GEs in public hospitals. The main limitation of this study is the fact that it only gives an opinion on screening colonoscopies. Indeed, screening colonoscopies only represented 5.5% of all colonoscopies performed in France in 2012 (gFOBT-period) and about 10% in 2016 (FIT-period)[32]. Since the patient base of a GE is not limited to the population of the region of practice, several GEs in the IDF region could reach or exceed this recommended annual number, in particular GEs practicing in a private clinic. The other limit of the study would come from the fact that the measurements of the indicators cannot be generalized over the whole of France. Indeed, the density of gastroenterologists and the types of practice (clinical hospital, *etc.*) may vary from one municipality (or department or region) to another. Only access to databases for the reimbursement of colonoscopy procedures could allow the exhaustive evaluation of such a quality indicator.

CONCLUSION

Although GEs are unevenly distributed over the municipalities of the IDF region, the supply of colonoscopies has remained almost constant between 2010 and 2020. The increase in colonoscopy requests induced by the change of the test kit has led to an increase in the average annual number of colonoscopies performed by GEs at the start of the FIT period. This very disparate annual average number between GEs fell over the STOP-FIT and COVID periods, due to the decrease in demand induced by the shutdown of the test kit market and the COVID-19 health crisis. The definition of a reference time and the obligation to respect it by all GEs would effectively reduce the time to access screening colonoscopy in France. The increase in the time to colonoscopy between the first and the second period was attributable to the introduction of the FIT, its increase after the second period was probably attributable to the malfunction of the program due to the slowdown of the kit market and the COVID-19 health crisis. Regardless of the characteristics of the GEs, the colonoscopy detection rate dropped significantly between the STOP-FIT and COVID periods, while the proportions of SAEs remained unchanged. However, the time to colonoscopy as well as its lengthening induced by the constraints had no impact in terms of CRC severity, probably because of a discriminatory approach prioritizing patients with existing symptoms.

ARTICLE HIGHLIGHTS

Research background

The impact of the Screening program on controlling the colorectal cancer (CRC) morbidity and mortality has been proved. But since its complete roll-out in 2009, the French population-based colorectal cancer screening program (CRCSP) experienced 3 major constraints [use of a less efficient Guaiac-test (gFOBT), Stopping the supply of Faecal-Immunochemical-Test kits (FIT), Suspension of the program due to the coronavirus disease 2019 (COVID-19)] affecting its effectiveness.

Research motivation

At this time when all the spotlights are focused on the impact of the health crisis linked to COVID-19, our motivation was to warn of the continued deterioration in the quality of screening colonoscopies in France.

Research objectives

To describe the impact of the constraints in terms of changes to the quality of screening colonoscopies.

Research methods

This retrospective cohort study included screening colonoscopies performed by the gastroenterologists between January 2010 and December 2020 in people aged 50-74 Living in Ile-de-France (France). The changes to the quality of screening colonoscopy (proportion of colonoscopies performed beyond 7 mo, Frequency of serious adverse events and the colonoscopy detection rate) were described in a cohort of Gastroenterologists who performed at least one colonoscopy over each of the four periods defined according to the chronology of the constraints [gFOBT: Normal progress of the CRCSP using gFOBT (2010-2014); FIT: Normal progress of the CRCSP using FIT(2015-2018); STOP-FIT: Year (2019) during which the CRCSP experienced the cessation of the supply of test kits; COVID: program suspension due to the COVID-19 health crisis (2020)]. The link between each dependent variable (Colo_7 mo; SAE Occurrence, Neoplasm detection rate) and the predictive factors was analyzed in a two-level multivariate hierarchical model.

Research results

The retrospective cohort was made up of 533 gastroenterologists. These 533 gastroenterologists achieved 21509 screening colonoscopies over the gFOBT period, 38,352 over FIT, 7342 over STOP-FIT and 7995 over the COVID period. The frequency of serious adverse events did not change between periods (gFOBT: 0.3%; FIT: 0.3%; STOP-FIT: 0.3%, and COVID: 0.2%; P = 0.10). The risk of colonoscopies performed beyond 7 mo doubled between FIT [adjusted-odds-ratio (aOR): 1.2 (1.1; 1.2)] and STOP-FIT [aOR: 2.4 (2.1; 2.6)], then decreased by 40% between STOP-FIT and COVID [aOR: 2.0 (1.8; 2.2)]. Regardless of the period, this Colo_7 mo's risk was twice as high for screening colonoscopy performed in a public hospital [aOR: 2.1 (1.3; 3.6)] compared to screening-colonoscopy performed in a private clinic. The neoplasm detection, which increased by 60% between gFOBT and FIT [aOR: 1.6 (1.5; 1.7)], decreased by 40% between FIT and COVID [aOR: 1.1 (1.0; 1.3)].

Research conclusions

The study showed that the constraints likely affected the time-to-colonoscopy as well as the colonoscopy detection rate without impacting the occurrence of the serious adverse events, highlighting the need for a respectable reference time-to-colonoscopy in CRCSP.

Research perspectives

At the end of this study, we initially aim to develop, evaluate, and validate a standard form for collecting data from screening colonoscopies in France. In a second step, we will evaluate the impact of the patient's motivation by the attending physician on the time taken to perform the colonoscopy.

ACKNOWLEDGEMENTS

The authors would like to thank the staff of the CRCDC-IDF. The authors would like to thank Stéphanie RASSE (National Council of the Order of Physicians, Research and Statistics Study Department) who facilitated access to medical demographic data. The authors are grateful to all contributors who participated in the final revisions.

FOOTNOTES

Author contributions: Koïvogui A, Vincelet C, Abihsera G, Ait-Hadad H, Delattre H, Le Trung T, and Bernoux A are the doctors in charge of coordinating the screening program in each department; Nicolet J is the medical director of the CRCDC-IDF; Koïvogui A conceptualized and designed the project; all doctors in charge of coordinating the screening program collected the field data; Koïvogui A, Vincelet C, and Abihsera G analyzed the data, interpreted the results, and drafted the manuscript; all the authors revised the manuscript, read, and approved the final version of this manuscript.

Institutional review board statement: This study is co-signed by the heads of the structures involved, as such, no further Institutional Review Board was required.

Informed consent statement: Patients were not required to give informed consent to the study because the analysis used anonymous data that was obtained after each patient agreed to participate in screening campaigns.

Conflict-of-interest statement: The authors declare that they have no conflict of interest.

Data sharing statement: Data and materials are available when requested by e-mail. However, each request will be processed following French legislation on the availability of research data.

STROBE statement: The authors have read the STROBE Statement—checklist of items, and the manuscript was prepared and revised according to the STROBE Statement—checklist of items.

Country/Territory of origin: France

ORCID number: Akoï Koïvogui 0000-0001-9097-3006.

S-Editor: Chen YL

L-Editor: A
P-Editor: Chen YL

REFERENCES

1 **Faivre J**, Dancourt V, Lejeune C, Tazi MA, Lamour J, Gerard D, Dassonville F, Bonithon-Kopp C. Reduction in colorectal cancer mortality by fecal occult blood screening in a French controlled study. *Gastroenterology* 2004; **126**: 1674-1680 [PMID: 15188160 DOI: 10.1053/j.gastro.2004.02.018]
2 **Hardcastle JD**, Chamberlain JO, Robinson MH, Moss SM, Amar SS, Balfour TW, James PD, Mangham CM. Randomised controlled trial of faecal-occult-blood screening for colorectal cancer. *Lancet* 1996; **348**: 1472-1477 [PMID: 8942775 DOI: 10.1016/S0140-6736(96)03386-7]
3 **Kronborg O**, Jørgensen OD, Fenger C, Rasmussen M. Randomized study of biennial screening with a faecal occult blood test: results after nine screening rounds. *Scand J Gastroenterol* 2004; **39**: 846-851 [PMID: 15513382 DOI: 10.1080/00365520410003182]
4 **Faivre J**, Lepage C, Viguier J. [Colorectal cancer: from diagnosis to screening]. *Gastroenterol Clin Biol* 2009; **33**: 660-671 [PMID: 19709833 DOI: 10.1016/j.gcb.2009.07.008]
5 **Cardoso R**, Guo F, Heisser T, Hoffmeister M, Brenner H. Utilisation of Colorectal Cancer Screening Tests in European Countries by Type of Screening Offer: Results from the European Health Interview Survey. *Cancers (Basel)* 2020; **12** [PMID: 32486077 DOI: 10.3390/cancers12061409]
6 **Guignot C**. Cancer colorectal. Vers un dépistage mieux accepté. Science et Santé. [cited 20 January 2023]. Available from: https://www.ipubli.inserm.fr/bitstream/handle/10608/9439/2015_26_36.pdf?sequence=1
7 **Le Pimpec F**, Moutel G, Piette C, Lièvre A, Bretagne JF. Fecal immunological blood test is more appealing than the guaiac-based test for colorectal cancer screening. *Dig Liver Dis* 2017; **49**: 1267-1272 [PMID: 28867474 DOI: 10.1016/j.dld.2017.08.018]
8 **Koïvogui A**, Mab GL, Benamouzig R. Detection of Colorectal Neoplasia in a Cohort Before and After the Change of Fecal Occult Blood Test in a French Colorectal Cancer Screening Program. *Am J Gastroenterol* 2018; **113**: 1891-1899 [PMID: 30337703 DOI: 10.1038/s41395-018-0367-2]
9 **Vitellius C**, Laly M, Banaszuk AS, Deherce I, Cornet N, Bertrais S, Saulnier P, Caroli-Bosc FX. Contribution of the OC Sensor(®) immunoassay in comparison to the Hemoccult II(®) guaiac-test in organized colorectal cancer screening. *Eur J Epidemiol* 2019; **34**: 163-172 [PMID: 30536183 DOI: 10.1007/s10654-018-0471-z]
10 **Senore C**, Basu P, Anttila A, Ponti A, Tomatis M, Vale DB, Ronco G, Soerjomataram I, Primic-Žakelj M, Riggi E, Dillner J, Elfström MK, Lönnberg S, Sankaranarayanan R, Segnan N. Performance of colorectal cancer screening in the European Union Member States: data from the second European screening report. *Gut* 2019; **68**: 1232-1244 [PMID: 30530530 DOI: 10.1136/gutjnl-2018-317293]
11 **Bretagne JF**, Piette C, Cosson M, Durand G, Lièvre A. Switching from guaiac to immunochemical faecal occult blood test increases participation and diagnostic yield of colorectal cancer screening. *Dig Liver Dis* 2019; **51**: 1461-1469 [PMID: 31151896 DOI: 10.1016/j.dld.2019.05.004]
12 **Bretagne JF**, Carlo A, Piette C, Rousseau C, Cosson M, Lièvre A. Significant decrease in interval colorectal cancer incidence after implementing immunochemical testing in a multiple-round guaiac-based screening programme. *Br J Cancer* 2021; **125**: 1494-1502 [PMID: 34511603 DOI: 10.1038/s41416-021-01546-z]
13 **Kaufmanis A**, Vincelet C, Koivogui A, Ait Hadad H, Bercier S, Brixi Z, Delattre-Massy H, Deyra J, Le Mab G, Le Trung T, Liautaud A. Dépistage organisé du cancer colorectal en Ile-de-France: état des lieux du délai de réalisation de la coloscopie avant et après l'introduction du test immunologique. Journées Francophones d'Hépato-Gastroentérolgie et d'Oncologie Digestive (JFHOD) de la Société Nationale Française de Gastro-Entérologie (SNFGE). March 22, 2018. [cited 20 January 2023]. Available from: https://www.snfge.org/content/depistage-organise-du-cancer-colorectal-en-ile-de-france-etat-des-lieux-du-delai-de
14 **Mazidimoradi A**, Tiznobaik A, Salehiniya H. Impact of the COVID-19 Pandemic on Colorectal Cancer Screening: a Systematic Review. *J Gastrointest Cancer* 2022; **53**: 730-744 [PMID: 34406626 DOI: 10.1007/s12029-021-00679-x]
15 **Goulard H**, Boussac-Zarebska M, Bloch J. Epidemiological assessment of the pilot programme for organized colorectal cancer screening. 2009. [cited 20 January 2023]. Available from: https://www.semanticscholar.org/paper/Epidemiological-assessment-of-the-pilot-programme-Goulard-Boussac-Zarebska/6ba13198a01d64068277b9249d6ef9d42d417d7f
16 **Leuraud K**, Jezewski-Serra D, Viguier J, Salines E. Colorectal cancer screening by guaiac faecal occult blood test in France: Evaluation of the programme two years after launching. *Cancer Epidemiol* 2013; **37**: 959-967 [PMID: 24035240 DOI: 10.1016/j.canep.2013.07.008]
17 **Corley DA**, Jensen CD, Quinn VP, Doubeni CA, Zauber AG, Lee JK, Schottinger JE, Marks AR, Zhao WK, Ghai NR, Lee AT, Contreras R, Quesenberry CP, Fireman BH, Levin TR. Association Between Time to Colonoscopy After a Positive Fecal Test Result and Risk of Colorectal Cancer and Cancer Stage at Diagnosis. *JAMA* 2017; **317**: 1631-1641 [PMID: 28444278 DOI: 10.1001/jama.2017.3634]
18 World Health Oorganization. ICD-10 Version: 2008. 10th International Classification of Diseases. [cited 20 January 2023]. Available from: https://icd.who.int/browse10/2008/fr
19 **Amin MB**, Edge S, Greene F, Byrd DR, Brookland RK, Washington MK, Gershenwald JE, Compton CC, Hess KR, Sullivan DC, Jessup JM, Brierley JD, Gaspar LE, Schilsky RL, Balch CM, Winchester DP, Asare EA, Madera M, Gress DM, Meyer LR. AJCC Cancer Staging Manual. 8th ed. New York: Springer, 2017
20 **Journal Officiel de la République Française**. Délibération n 2017-215 du 13 juillet 2017 portant adoption d'une norme destinée à simplifier l'obligation de déclaration des traitements de données à caractère personnel ayant pour finalité le dépistage organisé du cancer du sein, du cancer colorectal et du cancer du col de l'utérus mis en œuvre par les structures de

gestion conventionnées, et abrogeant la délibération n 2015-175 du 11 juin 2015 (décision d'autorisation unique n AU-043) (NS-059). [cited 20 January 2023]. Available from: https://www.legifrance.gouv.fr/affichTexte.do?cidTexte=JORFTEXT000035484848&categorieLien=id

21 **Valori R**, Rey JF, Atkin WS, Bretthauer M, Senore C, Hoff G, Kuipers EJ, Altenhofen L, Lambert R, Minoli G; International Agency for Research on Cancer. European guidelines for quality assurance in colorectal cancer screening and diagnosis. First Edition--Quality assurance in endoscopy in colorectal cancer screening and diagnosis. *Endoscopy* 2012; **44** Suppl 3: SE88-S105 [PMID: 23012124 DOI: 10.1055/s-0032-1309795]

22 **Cariou M**, El Fettouhi A, Kermarrec T, Bommelaere F, Foll Y, Nousbaum JB, Robaszkiewicz M, Quénéhervé L. Comparative evaluation of two colorectal cancer screening campaigns using different faecal occult blood tests in a French area. *Cancer Epidemiol* 2020; **69**: 101839 [PMID: 33096500 DOI: 10.1016/j.canep.2020.101839]

23 **Beshara A**, Ahoroni M, Comanester D, Vilkin A, Boltin D, Dotan I, Niv Y, Cohen AD, Levi Z. Association between time to colonoscopy after a positive guaiac fecal test result and risk of colorectal cancer and advanced stage disease at diagnosis. *Int J Cancer* 2020; **146**: 1532-1540 [PMID: 31173655 DOI: 10.1002/ijc.32497]

24 **Demb J**, Liu L, Bustamante R, Dominitz JA, Earles A, Shah SC, Gawron AJ, Martinez ME, Gupta S. COVID-19 Pandemic Had Minimal Impact on Colonoscopy Completion After Colorectal Cancer Red Flag Sign or Symptoms in US Veterans. *Dig Dis Sci* 2022; 1-10 [PMID: 36169748 DOI: 10.1007/s10620-022-07685-4]

25 **Denis B**, Gendre I, Weber S, Perrin P. Adverse events of colonoscopy in a colorectal cancer screening program with fecal immunochemical testing: a population-based observational study. *Endosc Int Open* 2021; **9**: E224-E232 [PMID: 33553585 DOI: 10.1055/a-1324-2763]

26 Colonoscopy Outcomes by Duration of NPO Status Prior to Colonoscopy with Moderate or Deep Sedation [Internet]. Washington (DC): Department of Veterans Affairs (US); 2015 Jan- [PMID: 26312369]

27 **van Rossum LG**, van Rijn AF, Laheij RJ, van Oijen MG, Fockens P, van Krieken HH, Verbeek AL, Jansen JB, Dekker E. Random comparison of guaiac and immunochemical fecal occult blood tests for colorectal cancer in a screening population. *Gastroenterology* 2008; **135**: 82-90 [PMID: 18482589 DOI: 10.1053/j.gastro.2008.03.040]

28 **Forbes N**, Hilsden RJ, Martel M, Ruan Y, Dube C, Rostom A, Shorr R, Menard C, Brenner DR, Barkun AN, Heitman SJ. Association Between Time to Colonoscopy After Positive Fecal Testing and Colorectal Cancer Outcomes: A Systematic Review. *Clin Gastroenterol Hepatol* 2021; **19**: 1344-1354.e8 [PMID: 33010414 DOI: 10.1016/j.cgh.2020.09.048]

29 **Mutneja HR**, Bhurwal A, Arora S, Vohra I, Attar BM. A delay in colonoscopy after positive fecal tests leads to higher incidence of colorectal cancer: A systematic review and meta-analysis. *J Gastroenterol Hepatol* 2021; **36**: 1479-1486 [PMID: 33351959 DOI: 10.1111/jgh.15381]

30 **Société Française d'Endoscopie Digestive**. Epidémie de COVID-19-Recommandations en endoscopie digestive 11 mars 2020. Société Française d'Endoscopie Digestive (SFED). Mar 11, 2020. [cited 20 January 2023]. Available from: https://www.sfed.org/sites/www.sfed.org/files/2021-10/covid19endo_reco.pdf

31 **Conseil National de l'Ordre des Médecins**. Atlas de la démographie médicale en france 2017. Profils comparés : 2007/2017-les territoires au cœur de la réflexion. Paris, France: Conseil National de l'Ordre des Médecins (CNOM). 2018. [cited 20 January 2023]. Available from: https://www.conseil-national.medecin.fr/sites/default/files/external-package/analyse_etude/1sogkeq/atlas_de_la_demographie_medicale_2017.pdf

32 **Denis B**, Gendre I, Perrin P. Colorectal cancer screening: a disappointing performance needs improvement. *Rev Prat* 2018; **68**: 839-846 [PMID: 30869446]

World Journal of Gastroenterology

Submit a Manuscript: https://www.f6publishing.com

World J Gastroenterol 2023 March 7; 29(9): 1509-1522

DOI: 10.3748/wjg.v29.i9.1509

ISSN 1007-9327 (print) ISSN 2219-2840 (online)

ORIGINAL ARTICLE

Retrospective Cohort Study

Comprehensively evaluate the short outcome of small bowel obstruction: A novel medical-economic score system

Wei-Xuan Xu, Qi-Hong Zhong, Yong Cai, Can-Hong Zhan, Shuai Chen, Hui Wang, Peng-Sheng Tu, Wen-Xuan Chen, Xian-Qiang Chen, Jun-Rong Zhang

Specialty type: Gastroenterology and hepatology

Provenance and peer review: Unsolicited article; Externally peer reviewed.

Peer-review model: Single blind

Peer-review report's scientific quality classification

Grade A (Excellent): A
Grade B (Very good): B
Grade C (Good): 0
Grade D (Fair): 0
Grade E (Poor): 0

P-Reviewer: Papazafiropoulou A, Greece; Zharikov YO, Russia

Received: November 27, 2022
Peer-review started: November 27, 2022
First decision: December 27, 2022
Revised: January 1, 2023
Accepted: February 15, 2023
Article in press: February 15, 2023
Published online: March 7, 2023

Wei-Xuan Xu, Qi-Hong Zhong, Yong Cai, Can-Hong Zhan, Shengli Clinical Medical College, Fujian Medical University, Fuzhou 350122, Fujian Province, China

Shuai Chen, Hui Wang, Peng-Sheng Tu, Wen-Xuan Chen, Xian-Qiang Chen, Jun-Rong Zhang, Department of General Surgery (Emergency Surgery), Fujian Medical University Union Hospital, Fuzhou 350001, Fujian Province, China

Corresponding author: Jun-Rong Zhang, MD, Attending Doctor, Chief Doctor, Surgeon, Surgical Oncologist, Department of General Surgery (Emergency Surgery), Fujian Medical University Union Hospital, No. 29 Xinquan Road, Fuzhou 350001, Fujian Province, China. junrongzhang@fjmu.edu.cn

Abstract

BACKGROUND

Small bowel obstruction (SBO) still imposes a substantial burden on the health care system. Traditional evaluation systems for SBO outcomes only focus on a single element. The comprehensive evaluation of outcomes for patients with SBO remains poorly studied. Early intensive clinical care would effectively improve the short-term outcomes for SBO, however, the full spectrum of the potential risk status regarding the high complication-cost burden is undetermined.

AIM

We aim to construct a novel system for the evaluation of SBO outcomes and the identification of potential risk status.

METHODS

Patients who were diagnosed with SBO were enrolled and stratified into the simple SBO (SiBO) group and the strangulated SBO (StBO) group. A principal component (PC) analysis was applied for data simplification and the extraction of patient characteristics, followed by separation of the high PC score group and the low PC score group. We identified independent risk status on admission *via* a binary logistic regression and then constructed predictive models for worsened management outcomes. Receiver operating characteristic curves were drawn, and the areas under the curve (AUCs) were calculated to assess the effectiveness of the predictive models.

RESULTS

Of the 281 patients, 45 patients (16.0%) were found to have StBO, whereas 236 patients (84.0%) had SiBO. Regarding standardized length of stay (LOS), total hospital cost and the presence of severe adverse events (SAEs), a novel principal component was extracted (PC score = 0.429 × LOS + 0.444 × total hospital cost + 0.291 × SAE). In the multivariate analysis, risk statuses related to poor results for SiBO patients, including a low lymphocyte to monocyte ratio (OR = 0.656), radiological features of a lack of small bowel feces signs (OR = 0.316) and mural thickening (OR = 1.338), were identified as risk factors. For the StBO group, higher BUN levels (OR = 1.478) and lower lymphocytes levels (OR = 0.071) were observed. The AUCs of the predictive models for poor outcomes were 0.715 (95%CI: 0.635-0.795) and 0.874 (95%CI: 0.762-0.986) for SiBO and StBO stratification, respectively.

CONCLUSION

The novel PC indicator provided a comprehensive scoring system for evaluating SBO outcomes on the foundation of complication-cost burden. According to the relative risk factors, early tailored intervention would improve the short-term outcomes.

Key Words: Principal component analysis; Small bowel obstruction; Outcome evaluation system; Risk factors; Intensive clinical care; Radiomics

Core Tip: A novel outcome indicator based on the standardized length of stay, total hospital cost and the presence of severe adverse events provided a comprehensive system for evaluating small bowel obstruction (SBO) outcomes. Furthermore, risk statuses associated with poor results were identified; specifically, for simple SBO patients, a low lymphocyte to monocyte ratio, as well as radiological features of a lack of small bowel feces signs and mural thickening, should be noticeable. For the strangulated SBO group, higher blood urea nitrogen levels and lower lymphocytes levels were recognized. Accordingly, early clinical intensive care was applicable for outcome improvement.

Citation: Xu WX, Zhong QH, Cai Y, Zhan CH, Chen S, Wang H, Tu PS, Chen WX, Chen XQ, Zhang JR. Comprehensively evaluate the short outcome of small bowel obstruction: A novel medical-economic score system. *World J Gastroenterol* 2023; 29(9): 1509-1522
URL: https://www.wjgnet.com/1007-9327/full/v29/i9/1509.htm
DOI: https://dx.doi.org/10.3748/wjg.v29.i9.1509

INTRODUCTION

Small bowel obstructions (SBO) result in over 300000 hospitalizations *per* year in the United States[1]. With the increasing public health burden, the average cost for SBOs ranges from $30000-$38000 individually, and the total cost for SBOs is estimated to be approximately 9-11.4 billion dollars[2,3]. Recently, the short outcomes of SBO were evaluated by using in-hospital mortality, major complications and the length of hospital stay[3-6]. There is still lack of an integrative medical-economic system to evaluate the overall outcomes for SBO, even though previous studies have confirmed the relationship between worse outcomes and higher hospital costs[7,8]. Furthermore, the question of how to comprehensively evaluate outcomes for patients with SBO remains uncharted.

Principal component analysis (PCA) is commonly used for dimension reduction[9,10], linear correlation resolution and data simplification. By summarizing and maximizing the information encoding a set of outcome variables, a novel principal component for evaluating the clinical and economic effects on SBO is available. For SBO, patients' statuses on admission, including longer pain duration, acute kidney injury and malnutrition, were found to be closely correlated with severe adverse events (SAEs), based on previous studies[3,5,7,11]. However, the risk factors for the integrative scoring system, including clinical and economic adverse events, have not been extensively evaluated. The method of how to fully evaluate the potential risk status regarding the high complication-cost burden is urgently needed.

As an urgent life-threatening problem, the physical status of strangulated SBO is considerably deteriorating[12-14]. To control this confounding factor[15,16] and to further identify the risk admission status, we divided patients into a simple bowel obstruction group and a strangulated bowel obstruction group for the stratification analysis. We also constructed a novel indicator combining standardized SAEs, length of stay (LOS) and total hospital cost for defining outcomes of SBO. Furthermore, we

established a representative model to distinguish high-risk statuses for both the simple small bowel obstruction (SiBO) and strangulated small bowel obstruction (StBO) groups to guide clinical intensive care for SBO.

MATERIALS AND METHODS

Patient population

From October 2016 to February 2021, 479 patients diagnosed with intestinal obstructions at Fujian Medical University Union Hospital were included in the study. After excluding 180 cases with large bowel obstructions, 4 cases with missing computed tomography (CT) images and 13 cases with incomplete clinical data, 281 patients were recruited for the final study (shown in Figure 1). The following stratification was made according to the pathological confirmation of intestinal ischemia: A simple bowel obstruction (SiBO, n = 236) group and a strangulated bowel obstruction (StBO, n = 45) group. For patients without acute peritonitis, conservative treatment was applied. Once patients with highly suspect of bowel ischemia or failure to conservative treatment, laparoscopy as well as laparotomy was adopted for SBO patients according to different intrabdominal pressures (shown in Table 1). The study protocol was approved by the Institutional Review Board of Fujian Medical University Union Hospital (Approval No. 2021YF005-02), and all of the patients provided written informed consent for the procedure.

CT findings

All of the patients with suspected SBO underwent CT scans before receiving treatment. The features of the CT scans that were recorded in this study were separated into mesenteric fluid, ascites, spiral signs, concentric circle signs, small bowel feces signs and edema of the bowel wall categories[17-20]. All of the CT scan images were cross-reviewed and evaluated by two senior general surgeons (Chen XQ and Zhang JR, and both surgeons had abundant experience in abdominal emergency surgery. The definitions of CT characteristics are shown in Supplementary Figure 1 and supplied in Supplementary Table 1[21-25].

Clinical characteristics and laboratory tests

Baseline demographics consisted of sex, age, body mass index (BMI), comorbidity, temperature, pain duration and history of abdominal pain. Biochemical parameters, including white blood cell count, neutrophil percentage, lymphocyte concentration, monocyte concentration, hemoglobin concentration, platelet concentration, albumin, alanine aminotransferase, aspartate aminotransferase (AST), calcium concentration, chloride concentration, potassium concentration, sodium concentration, blood urea nitrogen (BUN), serum creatinine, glucose, prothrombin time (PT), activated partial thromboplastin time (APTT), D-dimer (DDI) and fibrinogen, were collected within 24 h of admission. Combinations of inflammatory parameters, such as the neutrophil to lymphocyte ratio and lymphocyte to monocyte ratio (LMR), were calculated and recorded accordingly.

Outcome definition

Posttreatment outcomes were both clinically and economically evaluated.

Postoperative complications were defined as any deviation from the normal postoperative course during the index admission for SBO treatment, which was guided by the European Perioperative Clinical Outcome definitions[7,26]. The severity of complications was graded according to the Clavien-Dindo (CD) system[27], which is a validated classification system that categorizes complication severity based on the level of required treatment. Grade I was defined as complications without the need for pharmacological treatment or surgical, endoscopic and radiological interventions, as well as only minor interventions such as vomiting; grade II was defined as complications requiring pharmacological or other treatments, such as blood transfusions and total parenteral nutrition; grade III was defined as complications requiring surgical interventions or other interventional treatments; grade IV was defined as life-threatening complications, including central nervous system, cardiac and pulmonary complications, as well as renal failure and those interventions requiring intensive care unit (ICU) management; and grade V was defined as death. CD grade I to grade III were classified as non-SAE, and CD grade IV to grade V were classified as SAE.

The LOS was defined as the number of days from admission to discharge. Total hospital cost was defined as the total expenditure for medical resource utilization during hospitalizations, which included fees for operations (materials and occupancy of the operating room), medications, radiology, laboratory tests, microbiology tests, ward stay, ICU days, feeding and blood products[28].

PCA

PCA was used to achieve data simplification by expressing multivariate outcome indicators with fewer dimensions. With standardized LOS, total hospital cost and the presence of SAEs, a novel principal

Table 1 Compared the clinical and laboratory characteristics of the patients with low or high principal component score

Characteristics	Simple obstruction (*n* = 236)		*P* value	Strangulated obstruction (*n* = 45)		*P* value
	Low PC score	High PC score		Low PC score	High PC score	
Baseline data						
Gender, *n* (%)			1.000[1]			0.421[2]
Male	117 (69.2%)	39 (69.6%)		18 (52.9%)	8 (72.7%)	
Female	52 (30.8%)	17 (30.4%)		16 (47.1%)	3 (27.3%)	
Age (yr)	60 (47, 69)	65 (53, 71)	0.081	63 (52.25, 70.00)	(61.0, 71.5)	0.321
BMI (kg/m^2)	20.70 (18.83, 22.98)	20.94 (18.21, 22.65)	0.196	20.20 (18.16, 22.00)	18.75 (17.72, 19.81)	0.228
Comorbidity, *n* (%)			0.245[1]			1.000[2]
None	128 (75.7%)	38 (67.9%)		27 (79.4%)	9 (81.8%)	
Yes	41 (24.3%)	18 (32.1%)		7 (20.6%)	2 (18.2%)	
Pain duration (d)	2 (1, 5)	6 (3, 12.5)	< 0.000	2.00 (1.00, 3.75)	2.0 (1.0, 4.0)	0.989
History of abdominal operation, *n* (%)			0.471[1]			0.603[2]
None	43 (25.4%)	17 (30.4%)		11 (32.4%)	2 (18.2%)	
Yes	126 (74.6)	39 (69.6%)		23 (67.6%)	9 (81.8%)	
Temperature (degrees Celsius)	36.6 (36.5, 36.8)	36.6 (36.5, 36.8)	0.401	36.6 (36.5, 36.8)	36.60 (36.50, 36.75)	0.956
CT characteristics						
Mesenteric fluid (%)			0.430			0.985[2]
None	32 (18.9%)	8 (14.3%)		1 (2.9%)	1 (9.1%)	
Yes	137 (81.1%)	48 (85.7%)		33 (97.1%)	10 (90.9%)	
Ascites (%)			0.849			1.000[2]
None	58 (34.3%)	20 (35.7%)		4 (11.8%)	1 (9.1%)	
Yes	111 (65.7%)	36 (64.3%)		30 (88.2%)	10 (90.9%)	
Spiral signs (%)			0.612[2]			0.436[2]
None	151 (89.3%)	52 (92.9%)		22 (64.7%)	5 (45.5%)	
Yes	18 (10.7%)	4 (7.1%)		12 (35.3%)	6 (54.5%)	
Concentric circle sign (%)			0.132[2]			0.745[2]
None	164 (97.0%)	51 (91.1%)		31 (91.2%)	11 (100%)	
Yes	5 (3.0%)	5 (8.9%)		3 (8.8%)	0 (0%)	
Small bowel feces sign (%)			0.006			1.000[2]
None	70 (41.4%)	35 (62.5%)		17 (50.0%)	5 (45.5%)	
Yes	99 (58.6%)	21 (37.5%)		17 (50.0%)	5 (54.5%)	
Mural thickness (median)	3.28 (2.30, 3.75)	3.63 (2.97, 4.53)	0.002	3.51 (3.16, 4.12)	3.42 (2.67, 4.07)	0.634
Laboratory data						
WBC (10^9/L)	6.770 (4.89, 9.52)	7.345 (4.87, 11.18)	0.387	8.70 (5.89, 12.23)	6.83 (10.01, 18.25)	0.384
NE%	75.50 (65.9, 83.3)	77.45 (68.5, 84.03)	0.422	83.60 (69.05, 86.90)	77.50 (73.30, 90.25)	0.853
Lymphocyte (10^9/L)	1.01 (0.74, 1.42)	0.94 (0.64, 1.34)	0.240	0.96 (0.65, 1.34)	0.60 (0.42, 0.76)	0.020
Monocyte (10^9/L)	0.420 (0.30, 0.58)	0.565 (0.34, 0.73)	0.011	0.570 (0.407, 0.735)	0.540 (0.33, 0.760)	0.721
NLR (ratio)	4.650 (3.03, 8.07)	6.115 (3.74, 9.30)	0.159	7.750 (4.085, 12.922)	9.030 (4.990, 15.565)	0.491
LMR (ratio)	2.286 (1.67, 3.42)	1.591 (1.13, 2.84)	0.002	1.681 (2.131, 1.141)	1.482 (0.957, 1.933)	0.459

Hb (g/L)	128.0 (115, 142)	120.5 (108, 133)	0.016	131.0 (110.0, 137.7)	129.0 (120.5, 145.0)	0.587
PLT (10^9/L)	205.5 (162.50, 250.75)	250.5 (180.25, 307.25)	0.002	213 (163, 260)	180.0 (152.0, 242.5)	0.256
Albumin (g/L)	35.9 (32.30, 40.45)	36.1 (31.80, 39.45)	0.403	34.6 (31.7, 39.6)	37.1 (28.6, 42.0)	0.977
ALT (U/L)	16 (11, 24)	16 (11, 22)	0.727	15.00 (12.00, 21.75)	15.00 (13.25, 27.75)	0.612
AST (U/L)	20 (16, 26)	21 (17, 25.5)	0.619	19.50 (17.00, 23.75)	36.50 (20.75, 45.25)	0.022
Ca (mmol/L)	2.19 (2.04,2.32)	2.15 (2.02,2.26)	0.152	2.19 (2.09, 2.31)	2.05 (1.95, 2.20)	0.062
Cl (mmol/L)	102.30 (100.0, 104.1)	100.15 (96.85, 104.03)	0.015	100.85 (98.13, 103.85)	102.00 (101.35, 104.15)	0.296
K (mmol/L)	4.035 (3.78, 4.34)	3.985 (3.74, 4.43)	0.957	4.00 (3.56, 4.31)	4.36 (3.62, 5.07)	0.290
Na (mmol/L)	138.40 (136.68, 140.48)	138.15 (135.50, 141.23)	0.533	138.05 (134.13, 140.30)	135.60 (134.75, 137.75)	0.334
BUN (mmol/L)	5.5 (4.3, 7.2)	5.4 (3.68, 8.23)	0.872	6.45 (4.00, 8.57)	10.6 (7.3, 15.3)	0.002
Glu (mmol/L)	6.78 (5.30, 8.67)	6.59 (5.16, 9.51)	0.515	8.165 (6.963, 9.300)	8.66 (6.78, 11.04)	0.428
PT (s)	13.6 (13.1, 14.3)	13.6 (13.28, 14.43)	0.825	13.45 (12.90, 13.90)	15.40 (14.20, 16.65)	0.004
APTT (s)	35.6 (33.3, 38.3)	36.1 (34.0, 40.9)	0.184	35.15 (32.18, 37.10)	41.6 (36.1, 45.0)	0.012
DDI (mg/L)	1.45 (0.71, 2.52)	1.94 (0.79, 4.67)	0.151	1.64 (0.88, 3.50)	5.75 (2.39, 6.72)	0.024
Fib (g/L)	3.49 (2.92, 4.37)	3.78 (3.25, 4.59)	0.150	3.69 (2.71, 4.60)	3.89 (3.17, 4.82)	0.548
Creatinine (umol/L)	70.0 (56, 81)	70.5 (54.75, 88.00)	0.512	67 (57, 76)	93 (80, 147)	0.003
Management			< 0.000[2]			0.215[2]
Conservative treatment	155 (91.7%)	17 (30.4%)		1 (2.9%)	0 (0%)	
Laparoscopy	11 (6.5%)	8 (14.3%)		8 (23.5%)	0 (0%)	
Laparotomy	3 (1.8%)	31 (55.4%)		25 (73.5%)	11 (100%)	
CD, *n* (%)			< 0.000[2]			< 0.000[2]
Grade I	141 (83.4%)	20 (35.7%)		5 (14.7%)	0 (0%)	
Grade II	28 (16.6%)	32 (57.1%)		28 (82.4%)	2 (18.2%)	
Grade III	0 (0%)	1 (1.8%)		1 (2.9%)	0 (0%)	
Grade IV	0 (0%)	3 (5.4%)		0 (0%)	9 (81.8%)	
Grade V	0 (0%)	0 (0%)		0 (0%)	0 (0%)	
SAE, *n* (%)			0.018[2]			< 0.000[2]
None	169 (100%)	53 (94.6%)		34 (100%)	2 (18.2%)	
Yes	0 (0%)	3 (5.4%)		0 (0%)	9 (81.8%)	
Fee (¥)	12070 (8830, 19935)	54322 (41370, 74623)	< 0.000	51828 (33575, 66954)	83553.0 (74146.0, 142409.5)	< 0.000
Length of stay (d)	5 (4, 8)	16 (13.75, 22.50)	< 0.000	14.00 (10.25, 17.00)	28.0 (18.5, 35.5)	< 0.000

[1]were compared using the χ^2 test.
[2]were adjusted *P* values or Fisher's exact test.
SiBO: Simple small bowel obstruction; StBO: Strangulated small bowel obstruction; PC score: Principle component score; BMI: Body mass index; WBC: White blood cell; NE%: Neutrophil percentage; NLR: Neutrophil to lymphocyte ratio; LMR: Lymphocyte to monocyte ratio; Hb: Hemoglobi; PLT: Platelet; ALT: Alanine aminotransferase, AST: Aspartate aminotransferase; Ca: Calcium; Cl: Chloride; K: Potassiun; Na: Sodium; BUN: Blood urea nitrogen; Glu: Glucose; PT: Prothrombin time; APTT: Activated partial thromboplastin time; DDI: D-dimer; Fib: Fibrinogen; CD: Clavien-Dindo; SAE: Severe adverse event.

component was extracted: PC score = 0.429 × LOS + 0.444 × total hospital cost + 0.291 × SAE. Furthermore, the patient population was classified in the following manner according to the quartile PC score: The low PC score group (below the 75% quartile) and the high PC score group (in the upper 75% quartile). This analysis was performed in R V.4.1.3 (R Foundation for Statistical Programming, Vienna, Austria) by using the psych packages.

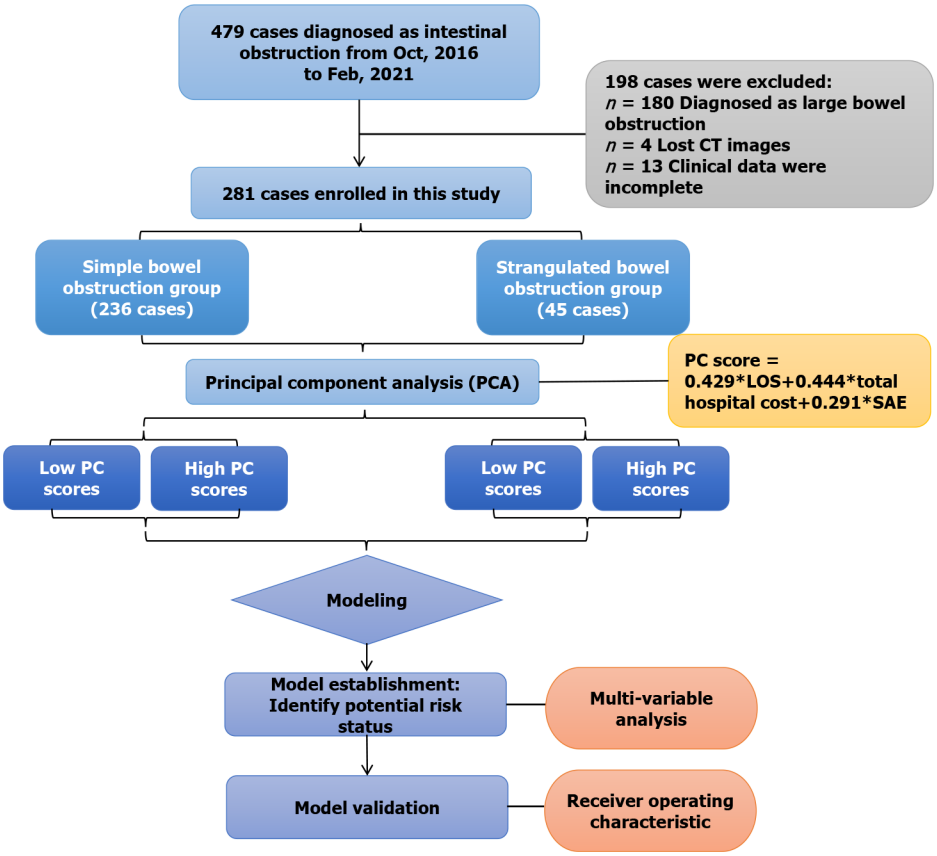

DOI: 10.3748/wjg.v29.i9.1509

Figure 1 Workflow of this study. CT: Computed tomography; PC: Principal component; LOS: Length of stay; SAE: Severe adverse event.

Statistical analysis

Categorical variables were compared by using the χ^2 test or Fisher's exact test between the two groups. Data are presented as the mean ± SD or median for continuous variables. Independent t tests or Kruskal-Wallis tests were applied according to the characteristics of the variables. The association of admission status with higher PC scores was evaluated by using univariate logistic regression and summarized with an odds ratio (OR) and 95% confidence interval (CI). After setting the variables with a significance level of $P < 0.05$ and variance inflation factors < 5, a multivariate logistic regression with "binomial" method was performed, and independent risk factors were determined. We extracted the following risk score formulas based on these independent risk factors: Risk score 1 (RS1) = [0.291 × (bowel wall thickness) - 1.150 × (small bowel feces sign) - 0.421 × (LMR)] and RS2 = [-2.632 × (lymphocyte concentration) + 0.391 × (BUN concentration)] for the SiBO group and StBO group, respectively. Receiver operating characteristic curves and the area under the curve were calculated to assess the accuracy of the models. All of the statistical analyses were performed in R Version.4.1.3. The statistical methods of this study were reviewed by Yin YR.

RESULTS

Outcome analysis

For 281 patients with SBO who were included in this study, posttreatment outcomes were evaluated by LOS, total hospital cost and the presence of SAEs. *Via* the univariate analysis, admission risk status, including lower LMR ($P = 0.005$), higher BUN concentration ($P = 0.022$), higher glucose concentration ($P = 0.007$) and higher DDI concentration ($P = 0.001$), was significantly associated with higher hospital costs. Patients with SAE had lower levels of lymphocyte concentration ($P = 0.003$), higher levels of AST ($P = 0.027$), higher levels of potassium ($P < 0.000$), higher levels of BUN ($P < 0.000$), higher levels of serum creatinine ($P < 0.000$) and coagulation and fibrinolysis disturbances, including longer PT ($P = 0.001$), APTT ($P = 0.012$) and higher levels of DDI ($P < 0.000$). Furthermore, at admission, lower LMR ($P = 0.003$), higher monocyte concentration ($P = 0.003$), lower hemoglobin concentration ($P = 0.038$), higher level of glucose ($P = 0.049$), higher level of DDI ($P = 0.004$) and abnormal electrolyte and metabolic changes, such as lower calcium concentration ($P = 0.042$), lower chloride concentration ($P = 0.003$) and lower sodium concentration ($P = 0.043$), were closely related to a longer LOS (Figure 2 and Supplemen-

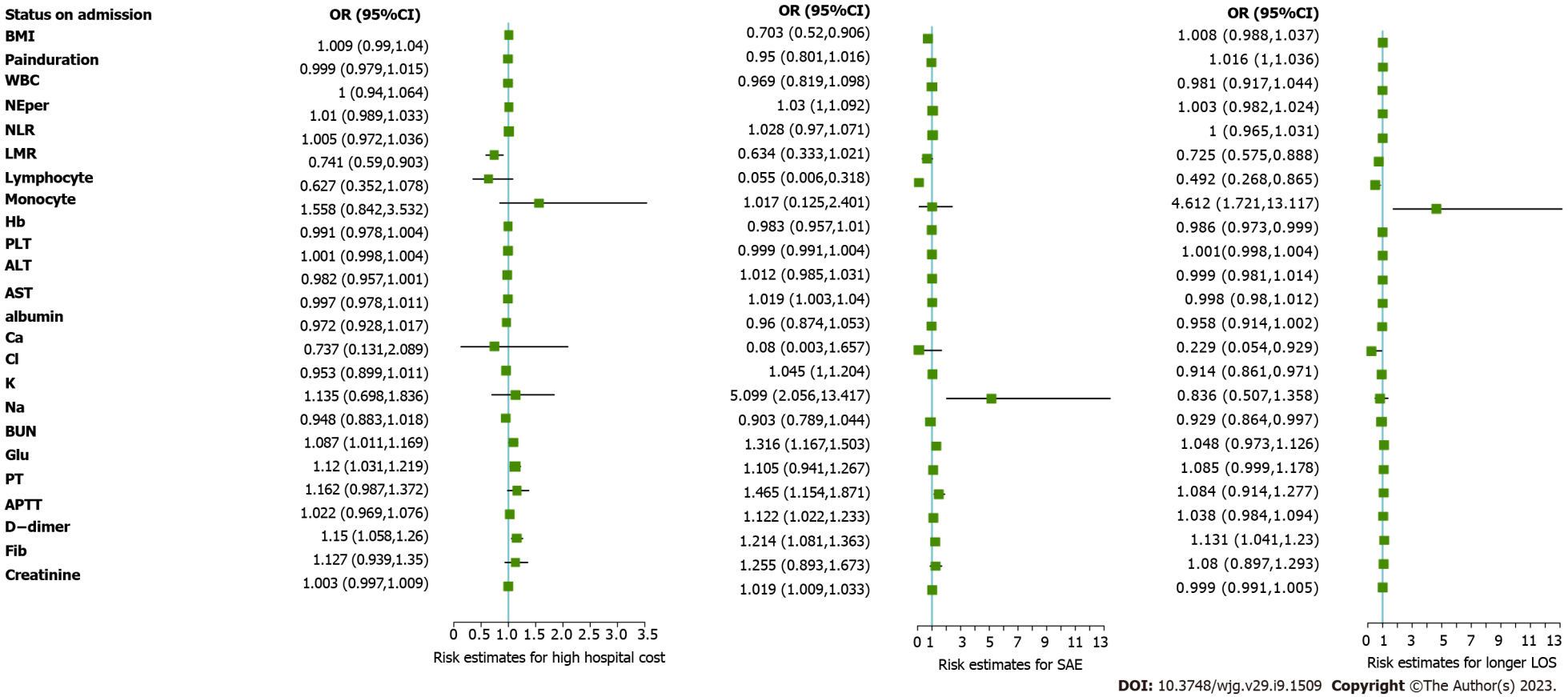

DOI: 10.3748/wjg.v29.i9.1509

Figure 2 Risk factors for worse outcome of small bowel obstruction. Risk estimates for high hospital cost; Risk estimates for severe adverse event; Risk estimates for longer length of stay. OR: Odds ratio; CI: Confidence interval; BMI: Body mass index; WBC: White blood cell; NE%: Neutrophil percentage; NLR: Neutrophil to lymphocyte ratio; LMR: Lymphocyte to monocyte ratio; Hb: Hemoglobin; PLT: Platelet, ALT: Alanine aminotransferase; AST: Aspartate aminotransferase; Ca: Calcium; Cl: Chloride; K: Potassiun; Na: Sodium; BUN: Blood urea nitrogen; Glu: Glucose; PT: Prothrombin time; APTT: Activated partial thromboplastin time; DDI: D-dimer; Fib: Fibrinogen; SAE: Severe adverse event; LOS: Length of stay.

tary Table 2).

PCA

After maximizing the possible information and variation of the above-mentioned outcome indicators, including total hospital cost, LOS and SAEs, data simplification was performed. *Via* PCA, one principal component was extracted (Supplementary Figure 2). The PC score was calculated according to weights given to each outcome indicator: PC score = 0.429 × LOS + 0.444 × total hospital cost + 0.291 × SAE (Figure 1).

Of the 281 patients with SBO who were included in this study, 45 patients (16.0%) were found to have StBO, whereas 236 patients (84.0%) were found to have SiBO. The low PC score group (< 75% quartile) and high PC score group (> 75% quartile) were identified according to the quartile PC score. For both the SiBO and StBO groups, no significant difference was observed between the two PC score groups for sex, age, BMI, comorbidity status, temperature or history of abdominal operation (all *P* values > 0.05, Table 1). For patients with SiBO, a higher PC score was significantly related to longer pain duration (*P* < 0.000), higher monocyte concentration (*P* = 0.011), lower LMR (*P* = 0.002), lower hemoglobin concentration (*P* = 0.016), lower platelet count (*P* = 0.002) and low level of chloride (*P* = 0.015). Through the univariate analysis of radiological characteristics, we determined that a lack of small bowel feces signs and mural thickening were risk factors for a high PC score. In contrast, in the StBO group, low levels of lymphocytes (*P* = 0.020), high levels of AST (*P* = 0.022), high levels of BUN (*P* = 0.002) and coagulation and fibrinolysis disturbances, including abnormal DDI concentrations (*P* = 0.024), PTs (*P* = 0.004) and APTTs (*P* = 0.012), were significantly associated with higher PC scores. None of the risk radiological characteristics were observed in this stratification.

Univariate and multivariate analyses of risk statuses

Via the univariate analysis of the admission clinical-laboratory features, we determined potential risk status, including longer pain duration (*P* = 0.048), higher monocyte concentration (*P* = 0.003), lower LMR (*P* = 0.006), lower hemoglobin concentration (*P* = 0.033), lower platelet count (*P* = 0.036) and low level of chloride (*P* = 0.031), as well as radiological characteristics of mural thickening (*P* = 0.033) and lack of small bowel feces sign (*P* = 0.006), for high PC scores in the SiBO stratification. *Via* the multivariate analysis, independent risk factors consisting of radiological findings of small bowel feces sign (OR = 0.316), mural thickening (OR = 1.338) and LMR (OR = 0.656) were identified (all *P* values < 0.05, Table 2 and Figure 3). For StBO stratification, low levels of lymphocytes (*P* = 0.038), high levels of AST (*P* = 0.027), longer PTs (*P* = 0.015), high levels of BUN (*P* = 0.004) and creatinine (*P* = 0.022) seemed to be related to high PC scores. Finally, we found that only lymphocytes (OR = 0.071) and BUN (OR=1.478) were independent risk factors for high PC scores (all *P* values < 0.05, Table 2 and Figure 3).

Based on the regression coefficient for each factor, we calculated risk scores and built prediction models for worse outcomes: RS1 = [0.291 × (bowel wall thickness) - 1.150 × (small bowel feces sign) - 0.421 × (LMR)] for the SiBO group and RS2 = [-2.632 × (lymphocyte concentration) + 0.391 × (BUN concentration)] for the StBO group. Furthermore, receiver operating characteristic curves were drawn with areas under the curve of 0.715 (95%CI: 0.635-0.795) and 0.874 (95%CI: 0.762-0.986) for the SiBO and StBO stratifications, respectively (Figure 4).

DISCUSSION

Given that approximately 9-11.4 billion dollars are the costs *per* year in the United States, SBO still imposes a substantial burden on the health care system[2]. In contrast to the traditional evaluation systems that only focus on a single element[3-6], in this study, the standardized LOS, total hospital cost and the presence of SAEs were considered as integrative systems to evaluate the clinical-economic outcomes of SBO *via* PCA[9]. Previous studies have confirmed the close relationship between patients' statuses on admission (including longer pain duration, acute kidney injury and malnutrition) and adverse outcomes, which provides a potential target for improving outcomes[3,5,7,11]. Commonly, severe statuses, including severe inflammatory reactions, electrolyte disturbances and hemostatic abnormalities, tend to occur in strangulated bowel obstruction[22]. Following the formula that assigned weights to each component, we determined PC score = 0.429 × LOS + 0.444 × total hospital cost + 0.291 × SAE; thus, the posttreatment outcome of SBO could be calculated and precisely evaluated (Figure 1).

For people with SiBO, only low LMR is observed, as radiological features (such as a lack of small bowel feces signs and mural thickening) were independent risk factors for high PC scores *via* the multivariate analysis. The area under the curve (AUC) of the predictive model based on the comprehensive scores for SiBO was 0.715 (95%CI: 0.635-0.795). As acute intestinal failure accompanies the obstructive bowel[26], when mechanical obstruction develops, the bowel lumen dilates along with the accumulation of air and intestinal fluid; thus, enteric stasis initiates bacterial proliferation with the intestinal gas produced by the fermentation of ingested food[22]. Conversely, when obstruction is incomplete or mild, the lasting bowel absorptive function can allow for fluid reabsorption across the bowel wall, thus leading to the small bowel feces sign as an independent protective factor for SBO[18,29]. Furthermore, progressive bowel dilation accompanied by compromised venous reflux increases intramural tension, which causes mural edema, secondary intestinal absorptive dysfunction and the loss of mucosal integrity (both functionally and physically)[22,30]. Similarly, as a potential effect on decreasing mural edema, the use of gastrografin challenge has been identified as the standardized management for SBO[31,32]. Moreover, in this study, the LMR was much lower in the high PC group, which may be due to the immune system becoming weakened as a result of the underlying malnutrition, as well as an excessive compensatory anti-inflammatory response[33-37].

Table 2 Univariate and multivariate analyses of risk factors for high principal component score

Characteristics	Simple obstruction (*n* = 236)				Strangulated obstruction (*n* = 45)			
	Univariate		Multivariate		Univariate		Multivariate	
	OR (95%CI)	*P* value	OR (95%CI)	*P* value	OR (95%CI)	*P* value	OR (95%CI)	*P* value
Pain duration (d)	1.019 (1.002, 1.041)	0.048[1]						
Small bowel feces sign (+)/(-)	0.424 (0.225, 0.783)	0.006[1]	0.316 (0.158, 0.612)	< 0.000[1]				
Mural thickening (cm)	2.119 (1.084, 4.375)	0.033[1]	1.338 (1.098, 1.664)	0.003[1]				
Lymphocyte (10^9/L)					0.097 (0.007, 0.665)	0.038[1]	0.071 (0.003, 0.539)	0.033[1]
Monocyte (10^9/L)	5.472 (1.809, 17.780)	0.003[1]						
LMR (ratio)	0.708 (0.541, 0.891)	0.006[1]	0.656 (0.496, 0.836)	0.001[1]				
Hb (g/L)	0.983 (0.969, 0.998)	0.033[1]						
PLT (10^9/L)	1.003 (1.001, 1.007)	0.036[1]						
AST (U/L)					1.075 (1.018, 1.156)	0.027[1]		
Cl (mmol/L)	0.931 (0.871, 0.993)	0.031[1]						
BUN (mmol/L)					1.383 (1.133, 1.786)	0.004[1]	1.478 (1.169, 2.061)	0.004[1]
PT (s)					1.568 (1.141, 2.418)	0.015[1]		
APTT (s)					1.109 (0.999, 1.264)	0.076		
DDI (mg/L)					1.196 (1.006, 1.513)	0.067		
Creatinine (umol/L)					1.034 (1.011, 1.071)	0.022[1]		

[1]indicates that the parameters have statistical difference ($P < 0.05$).

SiBO: Simple small bowel obstruction; StBO: Strangulated small bowel obstruction; OR: Odds ratio; CI: Confidence interval; LMR: Lymphocyte to monocyte ratio; Hb: Hemoglobin; PLT: Platelet; AST: Aspartate aminotransferase; Cl: Chloride; BUN: Blood urea nitrogen; PT: Prothrombin time; APTT: Activated partial thromboplastin time; DDI: D-dimer.

Once SiBO deteriorated into StBO, the risk factors were dynamically changed. None of the radiological characteristics were found to be related to the outcomes. In particular, coagulation and fibrinolysis disturbances (including abnormal DDI, PT and APTT), kidney injury (such as increasing BUN and creatinine levels) and relevant lymphocytes were confirmed as being risk factors. Finally, only BUN and lower lymphocyte counts were identified as being independent risk factors for high PC. Partially due to the impaired mucosal barriers[22,38], lactic acid from intestinal anaerobic glycolysis gradually accumulates, which adversely deteriorates renal function with increasing levels of BUN in the peripheral blood[39]. Similarly, it is difficult to correct conventional enteral interventions and intestinal mucosal malnutrition due to the weakened immune status[33,40], which may explain why a lower level

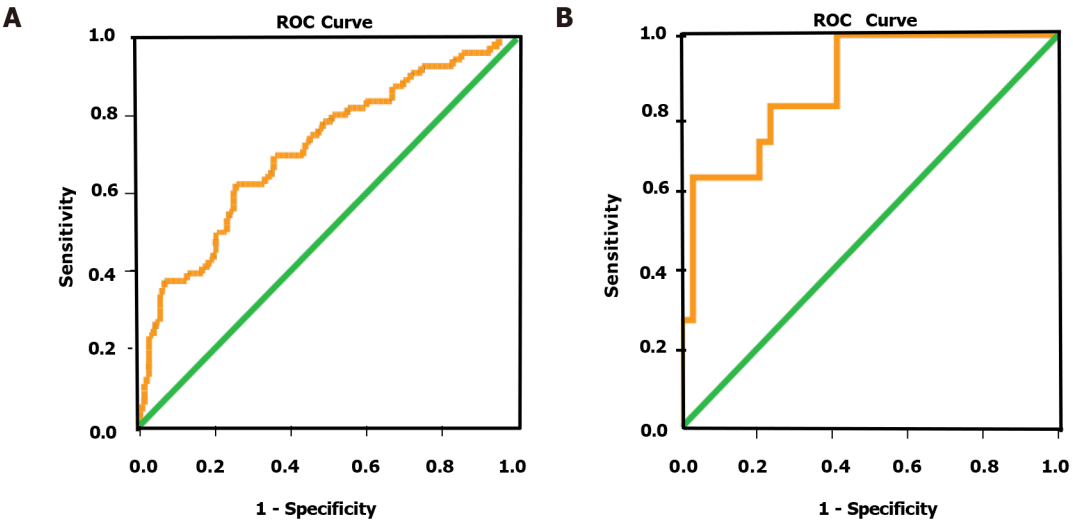

DOI: 10.3748/wjg.v29.i9.1509

Figure 3 Receiver operating characteristic curve for high principal component score prediction. The areas under the curve were 0.715 (95%CI: 0.635-0.795), 0.874 (95%CI: 0.762-0.986), respectively. A: Receiver operating characteristic curve of simple small bowel obstruction group for high principal component score prediction. B: Receiver operating characteristic curve of strangulated small bowel obstruction group for high principal component score prediction. ROC: Receiver operating characteristic.

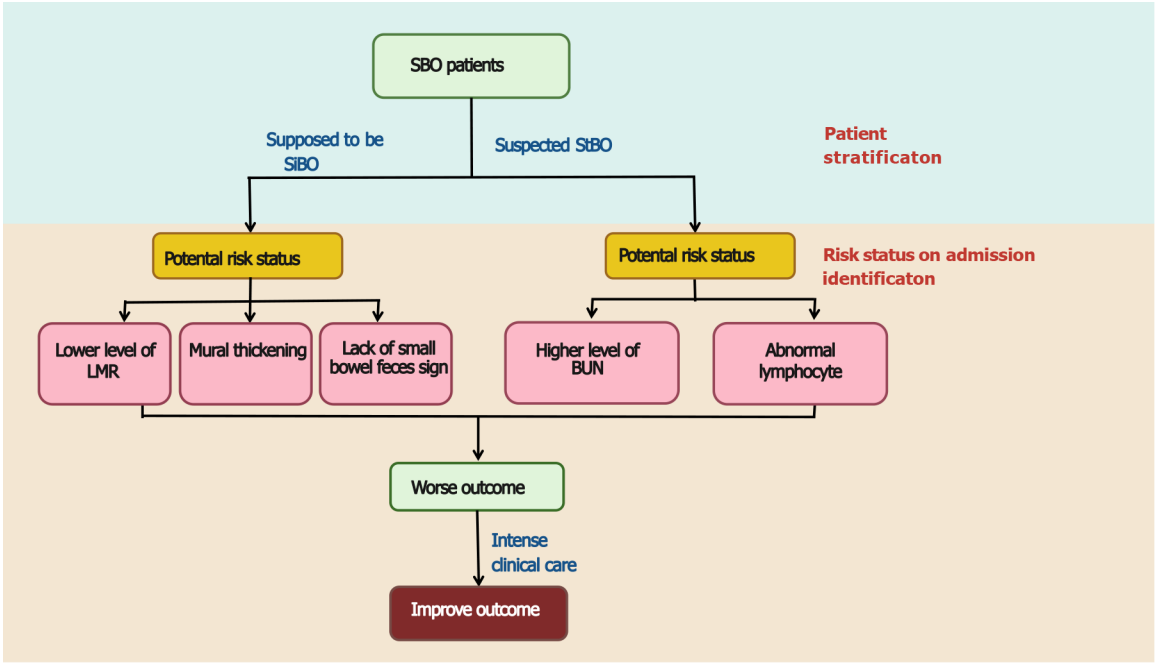

DOI: 10.3748/wjg.v29.i9.1509

Figure 4 Proposal early clinical intensive care for small bowel obstruction patients on admission. SBO: Small bowel obstruction; SiBO: simple small bowel obstruction; StBO: Strangulated small bowel obstruction; LMR: Lymphocyte to monocyte ratio; BUN: Blood urea nitrogen.

of lymphocytes is a risk factor for poorer outcomes. The predictive model for StBO yielded an AUC of 0.874 (95%CI: 0.762-0.986), which provided an excellent differentiating ability.

There were a few limitations to the present study. Primarily, this was a retrospective study conducted in a single center. In addition, the sample size of the initial models was relatively small. However, in both group (SiBO or StBO) the patients evaluated were consecutively enrolled and this could reproduce a real-world situation. Adequately powered and well-designed studies are required to confirm these findings and to establish causality.

CONCLUSION

The novel PC indicator provided a comprehensive scoring system for evaluating SBO outcomes on the foundation of complication-cost burden. According to the relative risk factors, early tailored intervention would improve the short-term outcomes.

ARTICLE HIGHLIGHTS

Research background

Small bowel obstruction (SBO) still imposes a substantial burden on the health care system. Traditional evaluation systems for SBO outcomes only focus on a single element. There is still lack of an integrative medical-economic system to evaluate the overall outcomes for SBO. Moreover, patients' statuses on admission, including longer pain duration, acute kidney injury and malnutrition, were found to be closely correlated with severe adverse events (SAEs). However, the risk factors for the integrative scoring system, including clinical and economic adverse events, have not been extensively evaluated.

Research motivation

SBO still imposes a substantial burden on the health care system. Traditional evaluation systems for SBO outcomes only focus on a single element. The comprehensive evaluation of outcomes for patients with SBO remains poorly studied. Early intensive clinical care would effectively improve the short-term outcomes for SBO, however, the full spectrum of the potential risk status regarding the high complication-cost burden is undetermined.

Research objectives

In this study, we aim to construct a novel indicator combining standardized SAEs, length of stay (LOS) and total hospital cost for defining outcomes of SBO. Furthermore, we established a representative model for distinguishing high-risk statuses on admission for the simple SBO (SiBO) or strangulated SBO (StBO) groups. Given that SBO still imposes a substantial burden on the health care system, we believe our findings will provide a new insight for comprehensively evaluation outcomes of SBO as well as a guideline for early intervention.

Research methods

In this study, we evaluated posttreatment outcomes of SBO both clinically and economically. Principal component analysis (PCA) was used to achieve data simplification by expressing multivariate outcome indicators with fewer dimensions. By summarizing and maximizing the information encoding in standardized LOS, total hospital cost and the presence of SAEs, a novel principal component was extracted: PC score = 0.429 × LOS + 0.444 × total hospital cost + 0.291 × SAE. Furthermore, the patient population was classified in the following manner according to the quartile PC score: The low PC score group (below the 75% quartile) and the high PC score group (in the upper 75% quartile).

Research results

In this study, a novel outcome indicator based on the standardized LOS, total hospital cost and the presence of SAEs provided a comprehensive system for evaluating SBO outcomes (PC score = 0.429 × LOS + 0.444 × total hospital cost + 0.291 × SAE). Furthermore, risk statuses associated with poor results were identified; specifically, for SiBO patients, a low LMR, as well as radiological features of a lack of small bowel feces signs and mural thickening, should be noticeable. For the StBO group, higher blood urea nitrogen levels and lower lymphocytes levels were recognized. Accordingly, early clinical intensive care was applicable for outcome improvement. In the future, adequately powered and well-designed studies are required to confirm these findings and to establish causality.

Research conclusions

In this study, PCA was innovatively used for dimension reduction, linear correlation resolution and data simplification. Furthermore, a novel comprehensive system for the evaluation of SBO outcomes was constructed and the potential risk status associated with poor results were identified.

Research perspectives

Large-scale and prospective studies are going to be designed to confirm these findings and to establish causality.

ACKNOWLEDGEMENTS

The authors thank the staff of the Department of General surgery (Emergency surgery) of Fujian Medical University Union Hospital, for their guidance and support.

FOOTNOTES

Author contributions: Xu WX designed and performed the research and drafted the manuscript; Zhang JR designed the research and supervised and reviewed the report; Chen XQ supervised the report and provided funding acquisition; Zhong QH, Cai Y, Zhan CH, designed the research and contributed to the analysis; Chen WX, Chen S, Wang H, Tu PS collected data and provided methodology.

Supported by Joint Funds for the innovation of science and Technology, Fujian Province, No. 2018Y9054; Young and Middle-Aged Talents Backbone Program of Fujian Province, No. 2020GGA034; The Construction Project of Fujian Province Minimally Invasive Medical Center, No. [2021]76.

Institutional review board statement: The study protocol was approved by the Institutional Review Board of Fujian Medical University Union Hospital (Approval No. 2021YF005-02).

Informed consent statement: Patients were not required to give informed consent to the study because the analysis used anonymous clinical data that were obtained after each patient agreed to treatment by written consent.

Conflict-of-interest statement: All authors read and approved the final manuscript and declared no conflicts of interest.

Data sharing statement: The original anonymous dataset is available on request from the corresponding author at junrongzhang@fjmu.edu.cn.

STROBE statement: The authors have read the STROBE Statement—checklist of items, and the manuscript was prepared and revised according to the STROBE Statement—checklist of items.

Country/Territory of origin: China

ORCID number: Wei-Xuan Xu 0000-0002-4876-3678; Qi-Hong Zhong 0000-0002-5490-5855; Yong Cai 0000-0003-2741-6682; Can-Hong Zhan 0000-0003-1807-094X; Shuai Chen 0000-0002-6278-896X; Hui Wang 0000-0002-2080-0166; Peng-Sheng Tu 0000-0001-6795-0156; Wen-Xuan Chen 0000-0002-3450-1255; Xian-Qiang Chen 0000-0001-5503-9840; Jun-Rong Zhang 0000-0001-8073-7405.

S-Editor: Liu GL
L-Editor: A
P-Editor: Liu GL

REFERENCES

1 **Sikirica V**, Bapat B, Candrilli SD, Davis KL, Wilson M, Johns A. The inpatient burden of abdominal and gynecological adhesiolysis in the US. *BMC Surg* 2011; **11**: 13 [PMID: 21658255 DOI: 10.1186/1471-2482-11-13]
2 **Bilderback PA**, Massman JD 3rd, Smith RK, La Selva D, Helton WS. Small Bowel Obstruction Is a Surgical Disease: Patients with Adhesive Small Bowel Obstruction Requiring Operation Have More Cost-Effective Care When Admitted to a Surgical Service. *J Am Coll Surg* 2015; **221**: 7-13 [PMID: 26095546 DOI: 10.1016/j.jamcollsurg.2015.03.054]
3 **Brandt WS**, Wood J, Bhattacharya B, Pei K, Davis KA, Schuster K. Relationship between duration of preoperative symptoms and postoperative ileus for small bowel obstruction. *J Surg Res* 2018; **225**: 40-44 [PMID: 29605033 DOI: 10.1016/j.jss.2017.12.031]
4 **Oyasiji T**, Angelo S, Kyriakides TC, Helton SW. Small bowel obstruction: outcome and cost implications of admitting service. *Am Surg* 2010; **76**: 687-691 [PMID: 20698371]
5 **Lee MJ**, Sayers AE, Drake TM, Marriott PJ, Anderson ID, Bach SP, Bradburn M, Hind D, Verjee A, Fearnhead NS; NASBO steering group and NASBO collaborators. National prospective cohort study of the burden of acute small bowel obstruction. *BJS Open* 2019; **3**: 354-366 [PMID: 31183452 DOI: 10.1002/bjs5.50136]
6 **Byrne J**, Saleh F, Ambrosini L, Quereshy F, Jackson TD, Okrainec A. Laparoscopic versus open surgical management of

adhesive small bowel obstruction: a comparison of outcomes. *Surg Endosc* 2015; **29**: 2525-2532 [PMID: 25480627 DOI: 10.1007/s00464-014-4015-7]

7 **Lee DK**, Frye A, Louis M, Koshy AN, Tosif S, Yii M, Ma R, Nikfarjam M, Perini MV, Bellomo R, Weinberg L. Postoperative complications and hospital costs following small bowel resection surgery. *PLoS One* 2020; **15**: e0241020 [PMID: 33085700 DOI: 10.1371/journal.pone.0241020]

8 **Straatman J**, Cuesta MA, de Lange-de Klerk ES, van der Peet DL. Hospital cost-analysis of complications after major abdominal surgery. *Dig Surg* 2015; **32**: 150-156 [PMID: 25791798 DOI: 10.1159/000371861]

9 **Alavi M**, Visentin DC, Thapa DK, Hunt GE, Watson R, Cleary M. Exploratory factor analysis and principal component analysis in clinical studies: Which one should you use? *J Adv Nurs* 2020 [PMID: 32255218 DOI: 10.1111/jan.14377]

10 **Zhang JJ**, Cao YY, Tan G, Dong X, Wang BC, Lin J, Yan YQ, Liu GH, Akdis M, Akdis CA, Gao YD. Clinical, radiological, and laboratory characteristics and risk factors for severity and mortality of 289 hospitalized COVID-19 patients. *Allergy* 2021; **76**: 533-550 [PMID: 32662525 DOI: 10.1111/all.14496]

11 **Soressa U**, Mamo A, Hiko D, Fentahun N. Prevalence, causes and management outcome of intestinal obstruction in Adama Hospital, Ethiopia. *BMC Surg* 2016; **16**: 38 [PMID: 27259287 DOI: 10.1186/s12893-016-0150-5]

12 **Schwenter F**, Poletti PA, Platon A, Perneger T, Morel P, Gervaz P. Clinicoradiological score for predicting the risk of strangulated small bowel obstruction. *Br J Surg* 2010; **97**: 1119-1125 [PMID: 20632281 DOI: 10.1002/bjs.7037]

13 **Xu WX**, Zhong QH, Cai Y, Zhan CH, Chen S, Wang H, Lin L, Geng YQ, Hou P, Chen XQ, Zhang JR. Prediction and management of strangulated bowel obstruction: a multi-dimensional model analysis. *BMC Gastroenterol* 2022; **22**: 304 [PMID: 35733109 DOI: 10.1186/s12876-022-02363-1]

14 **Huang X**, Fang G, Lin J, Xu K, Shi H, Zhuang L. A Prediction Model for Recognizing Strangulated Small Bowel Obstruction. *Gastroenterol Res Pract* 2018; **2018**: 7164648 [PMID: 29780412 DOI: 10.1155/2018/7164648]

15 **Hajibandeh S**, Hajibandeh S, Panda N, Khan RMA, Bandyopadhyay SK, Dalmia S, Malik S, Huq Z, Mansour M. Operative versus non-operative management of adhesive small bowel obstruction: A systematic review and meta-analysis. *Int J Surg* 2017; **45**: 58-66 [PMID: 28728984 DOI: 10.1016/j.ijsu.2017.07.073]

16 **Hernandez MC**, Finnesgard EJ, Shariq OA, Knight A, Stephens D, Aho JM, Kim BD, Schiller HJ, Zielinski MD. Disease Severity and Cost in Adhesive Small Bowel Obstruction. *World J Surg* 2019; **43**: 3027-3034 [PMID: 31555867 DOI: 10.1007/s00268-019-05148-y]

17 **Chang WC**, Ko KH, Lin CS, Hsu HH, Tsai SH, Fan HL, Tung HJ, Huang GS, Chen RC. Features on MDCT that predict surgery in patients with adhesive-related small bowel obstruction. *PLoS One* 2014; **9**: e89804 [PMID: 24587047 DOI: 10.1371/journal.pone.0089804]

18 **Zielinski MD**, Eiken PW, Bannon MP, Heller SF, Lohse CM, Huebner M, Sarr MG. Small bowel obstruction-who needs an operation? *World J Surg* 2010; **34**: 910-919 [PMID: 20217412 DOI: 10.1007/s00268-010-0479-3]

19 **Kim J**, Lee Y, Yoon JH, Lee HJ, Lim YJ, Yi J, Jung WB. Non-strangulated adhesive small bowel obstruction: CT findings predicting outcome of conservative treatment. *Eur Radiol* 2021; **31**: 1597-1607 [PMID: 33128599 DOI: 10.1007/s00330-020-07406-3]

20 **Ofer A**, Abadi S, Nitecki S, Karram T, Kogan I, Leiderman M, Shmulevsky P, Israelit S, Engel A. Multidetector CT angiography in the evaluation of acute mesenteric ischemia. *Eur Radiol* 2009; **19**: 24-30 [PMID: 18690454 DOI: 10.1007/s00330-008-1124-5]

21 **Ishikawa E**, Kudo M, Minami Y, Ueshima K, Kitai S, Ueda K. Cecal intussusception in an adult with Cronkhite-Canada syndrome relieved by colonoscopy. *Intern Med* 2010; **49**: 1123-1126 [PMID: 20558928 DOI: 10.2169/internalmedicine.49.2813]

22 **Rami Reddy SR**, Cappell MS. A Systematic Review of the Clinical Presentation, Diagnosis, and Treatment of Small Bowel Obstruction. *Curr Gastroenterol Rep* 2017; **19**: 28 [PMID: 28439845 DOI: 10.1007/s11894-017-0566-9]

23 **Millet I**, Taourel P, Ruyer A, Molinari N. Value of CT findings to predict surgical ischemia in small bowel obstruction: A systematic review and meta-analysis. *Eur Radiol* 2015; **25**: 1823-1835 [PMID: 25850889 DOI: 10.1007/s00330-014-3440-2]

24 **Scaglione M**, Galluzzo M, Santucci D, Trinci M, Messina L, Laccetti E, Faiella E, Beomonte Zobel B. Small bowel obstruction and intestinal ischemia: emphasizing the role of MDCT in the management decision process. *Abdom Radiol (NY)* 2022; **47**: 1541-1555 [PMID: 33057806 DOI: 10.1007/s00261-020-02800-3]

25 **Paulson EK**, Thompson WM. Review of small-bowel obstruction: the diagnosis and when to worry. *Radiology* 2015; **275**: 332-342 [PMID: 25906301 DOI: 10.1148/radiol.15131519]

26 **Jammer I**, Wickboldt N, Sander M, Smith A, Schultz MJ, Pelosi P, Leva B, Rhodes A, Hoeft A, Walder B, Chew MS, Pearse RM; European Society of Anaesthesiology (ESA) and the European Society of Intensive Care Medicine (ESICM); European Society of Anaesthesiology; European Society of Intensive Care Medicine. Standards for definitions and use of outcome measures for clinical effectiveness research in perioperative medicine: European Perioperative Clinical Outcome (EPCO) definitions: a statement from the ESA-ESICM joint taskforce on perioperative outcome measures. *Eur J Anaesthesiol* 2015; **32**: 88-105 [PMID: 25058504 DOI: 10.1097/EJA.0000000000000118]

27 **Dindo D**, Demartines N, Clavien PA. Classification of surgical complications: a new proposal with evaluation in a cohort of 6336 patients and results of a survey. *Ann Surg* 2004; **240**: 205-213 [PMID: 15273542 DOI: 10.1097/01.sla.0000133083.54934.ae]

28 **Krielen P**, van den Beukel BA, Stommel MWJ, van Goor H, Strik C, Ten Broek RPG. In-hospital costs of an admission for adhesive small bowel obstruction. *World J Emerg Surg* 2016; **11**: 49 [PMID: 27713763 DOI: 10.1186/s13017-016-0109-y]

29 **Yamamoto Y**, Miyagawa Y, Kitazawa M, Tanaka H, Kuroiwa M, Hondo N, Koyama M, Nakamura S, Tokumaru S, Muranaka F, Soejima Y. Association of feces sign with prognosis of non-emergency adhesive small bowel obstruction. *Asian J Surg* 2021; **44**: 292-297 [PMID: 32732062 DOI: 10.1016/j.asjsur.2020.07.012]

30 **Grootjans J**, Lenaerts K, Buurman WA, Dejong CH, Derikx JP. Life and death at the mucosal-luminal interface: New perspectives on human intestinal ischemia-reperfusion. *World J Gastroenterol* 2016; **22**: 2760-2770 [PMID: 26973414 DOI: 10.3748/wjg.v22.i9.2760]

31 **Zielinski MD**, Haddad NN, Cullinane DC, Inaba K, Yeh DD, Wydo S, Turay D, Pakula A, Duane TM, Watras J, Widom

KA, Cull J, Rodriguez CJ, Toschlog EA, Sams VG, Hazelton JP, Graybill JC, Skinner R, Yune JM; EAST SBO Workgroup: Martin D. Zielinski, MD; Nadeem N. Haddad, MD; Asad J. Choudhry, MBBS; Daniel C. Cullinane, MD; Kenji Inaba, MD; Agustin Escalante; D. Dante Yeh, MD; Salina Wydo, MD; David Turay, MD; Andrea Pakula, MD; Therese M. Duane, MD; Jill Watras, MD; Kenneth A. Widom, MD; John Cull, MD; Carlos J. Rodriguez, DO; Eric A. Toschlog, MD; Valerie G. Sams, MD; Joshua P. Hazelton, DO; John Christopher Graybill, MD, Ruby Skinner, MD, Ji-Ming Yune, MD. Multi-institutional, prospective, observational study comparing the Gastrografin challenge versus standard treatment in adhesive small bowel obstruction. *J Trauma Acute Care Surg* 2017; **83**: 47-54 [PMID: 28422909 DOI: 10.1097/TA.0000000000001499]

32 **Mahony CR**, Traynor MD Jr, Knight AW, Hughes JD, Hernandez MC, Finnesgard EJ, Musa J, Selby SL, Rivera M, Kim BD, Heller SF, Zielinski MD. Small bowel obstruction managed without hospital admission: A safe way to reduce both cost and time in the hospital? *Surgery* 2022; **171**: 1665-1670 [PMID: 34815095 DOI: 10.1016/j.surg.2021.10.041]

33 **Lee MJ**, Sayers AE, Drake TM, Singh P, Bradburn M, Wilson TR, Murugananthan A, Walsh CJ, Fearnhead NS; NASBO Steering Group and NASBO Collaborators. Malnutrition, nutritional interventions and clinical outcomes of patients with acute small bowel obstruction: results from a national, multicentre, prospective audit. *BMJ Open* 2019; **9**: e029235 [PMID: 31352419 DOI: 10.1136/bmjopen-2019-029235]

34 **Vural V**, Ozozan OV. The Usefulness of Inflammation-based Prognostic Scores for the Prediction of Postoperative Mortality in Patients Who Underwent Intestinal Resection for Acute Intestinal Ischemia. *Cureus* 2019; **11**: e6372 [PMID: 31886096 DOI: 10.7759/cureus.6372]

35 **Gentile LF**, Cuenca AG, Efron PA, Ang D, Bihorac A, McKinley BA, Moldawer LL, Moore FA. Persistent inflammation and immunosuppression: a common syndrome and new horizon for surgical intensive care. *J Trauma Acute Care Surg* 2012; **72**: 1491-1501 [PMID: 22695412 DOI: 10.1097/TA.0b013e318256e000]

36 **Christou NV**, Meakins JL, Gordon J, Yee J, Hassan-Zahraee M, Nohr CW, Shizgal HM, MacLean LD. The delayed hypersensitivity response and host resistance in surgical patients. 20 years later. *Ann Surg* 1995; **222**: 534-46; discussion 546 [PMID: 7574933 DOI: 10.1097/00000658-199522240-00011]

37 **Xiao W**, Mindrinos MN, Seok J, Cuschieri J, Cuenca AG, Gao H, Hayden DL, Hennessy L, Moore EE, Minei JP, Bankey PE, Johnson JL, Sperry J, Nathens AB, Billiar TR, West MA, Brownstein BH, Mason PH, Baker HV, Finnerty CC, Jeschke MG, López MC, Klein MB, Gamelli RL, Gibran NS, Arnoldo B, Xu W, Zhang Y, Calvano SE, McDonald-Smith GP, Schoenfeld DA, Storey JD, Cobb JP, Warren HS, Moldawer LL, Herndon DN, Lowry SF, Maier RV, Davis RW, Tompkins RG; Inflammation and Host Response to Injury Large-Scale Collaborative Research Program. A genomic storm in critically injured humans. *J Exp Med* 2011; **208**: 2581-2590 [PMID: 22110166 DOI: 10.1084/jem.20111354]

38 **Wright HK**, O'Brien JJ, Tilson MD. Water absorption in experimental closed segment obstruction of the ileum in man. *Am J Surg* 1971; **121**: 96-99 [PMID: 5540839 DOI: 10.1016/0002-9610(71)90083-3]

39 **Baum N**, Dichoso CC, Carlton CE. Blood urea nitrogen and serum creatinine. Physiology and interpretations. *Urology* 1975; **5**: 583-588 [PMID: 1093306 DOI: 10.1016/0090-4295(75)90105-3]

40 **Clumeck N**, George C. Immunological aspects to severe bacterial sepsis. *Intensive Care Med* 1981; **7**: 109-114 [PMID: 7012215 DOI: 10.1007/BF01738612]

World Journal of Gastroenterology

Submit a Manuscript: https://www.f6publishing.com

World J Gastroenterol 2023 March 7; 29(9): 1523-1535

DOI: 10.3748/wjg.v29.i9.1523

ISSN 1007-9327 (print) ISSN 2219-2840 (online)

SCIENTOMETRICS

Global trend and future landscape of intestinal microcirculation research from 2000 to 2021: A scientometric study

Sun-Jing Fu, Meng-Ting Xu, Bing Wang, Bing-Wei Li, Hao Ling, Yuan Li, Qin Wang, Xue-Ting Liu, Xiao-Yan Zhang, Ai-Ling Li, Ming-Ming Liu

Specialty type: Gastroenterology and hepatology

Provenance and peer review: Unsolicited article; Externally peer reviewed.

Peer-review model: Single blind

Peer-review report's scientific quality classification

Grade A (Excellent): 0
Grade B (Very good): 0
Grade C (Good): C, C
Grade D (Fair): 0
Grade E (Poor): 0

P-Reviewer: Huan C, United States; Tai X, China

Received: November 18, 2022
Peer-review started: November 18, 2022
First decision: January 23, 2023
Revised: February 1, 2023
Accepted: February 24, 2023
Article in press: February 24, 2023
Published online: March 7, 2023

Sun-Jing Fu, Meng-Ting Xu, Bing Wang, Bing-Wei Li, Yuan Li, Qin Wang, Xue-Ting Liu, Xiao-Yan Zhang, Ai-Ling Li, Ming-Ming Liu, Institute of Microcirculation, Key Laboratory of Microcirculation, Ministry of Health, Chinese Academy of Medical Sciences & Peking Union Medical College, Beijing 100005, China

Hao Ling, Department of Radiology, The Affiliated Changsha Central Hospital, Hengyang Medical School, University of South China, Changsha 410004, Hunan Province, China

Ming-Ming Liu, Diabetes Research Center, Chinese Academy of Medical Sciences & Peking Union Medical College, Beijing 100005, China

Corresponding author: Ming-Ming Liu, PhD, Research Scientist, Institute of Microcirculation, Key Laboratory of Microcirculation, Ministry of Health, Chinese Academy of Medical Sciences & Peking Union Medical College, No. 5 Dong Dan Third Alley, Dongcheng District, Beijing 100005, China. mingmingliu@imc.pumc.edu.cn

Abstract

BACKGROUND

The intestinal microcirculation functions in food absorption and metabolic substance exchanges. Accumulating evidence indicates that intestinal microcirculatory dysfunction is a significant source of multiple gastrointestinal diseases. To date, there has not been a scientometric analysis of intestinal microcirculatory research.

AIM

To investigate the current status, development trends, and frontiers of intestinal microcirculatory research based on bibliometric analysis.

METHODS

VOSviewer and CiteSpace 6.1.R2 were used to identify the overall characteristics and knowledge map of intestinal microcirculatory research based on the core literature published from 2000 to 2021 in the Web of Science database. The characteristics of each article, country of origin, institution, journal, cocitations, and other information were analyzed and visualized.

RESULTS

There were 1364 publications enrolled in the bibliometric analysis, exhibiting an upward trend from 2000 to 2021 with increased participation worldwide. The

United States and Dalhousie University took the lead among countries and institutions, respectively. *Shock* was the most prolific journal, and *Nature Reviews Microbiology Clinical* had the most citations. The topical hotspots and frontiers in intestinal microcirculatory research were centered on the pathological processes of functional impairment of intestinal microvessels, diverse intestinal illnesses, and clinical treatment.

CONCLUSION

Our study highlights insights into trends of the published research on the intestinal microcirculation and offers serviceable guidance to researchers by summarizing the prolific areas in intestinal disease research to date.

Key Words: Intestinal microcirculation; Bibliometric analysis; CiteSpace; VOSviewer; Visualization

Core Tip: This bibliometric analysis of the research directions and important literature related to the intestinal microcirculation over the last 22 years documents the current status, development trends, and frontiers of intestinal microcirculatory research and provides information that may guide future research efforts.

Citation: Fu SJ, Xu MT, Wang B, Li BW, Ling H, Li Y, Wang Q, Liu XT, Zhang XY, Li AL, Liu MM. Global trend and future landscape of intestinal microcirculation research from 2000 to 2021: A scientometric study. *World J Gastroenterol* 2023; 29(9): 1523-1535

URL: https://www.wjgnet.com/1007-9327/full/v29/i9/1523.htm

DOI: https://dx.doi.org/10.3748/wjg.v29.i9.1523

INTRODUCTION

The intestines function in food absorption and metabolic substance exchange. Approximately 20%-25% of cardiac output is directed toward the digestive tract under physiological conditions. Among them, about 60%-80% flow to the submucosal and mucosal layers[1], providing the highly metabolically active epithelial, immune with nutrients and oxygen. Intestinal microvessels and lymph capillaries serve as an integrated system (so-called intestinal microcirculation) providing multiple bidirectional transport processes while defending the lumen against the threat of chemicals and bacteria. The intestinal microcirculation regulates a variety of metabolic and physiological processes involved in diseases such as shock, sepsis[2,3], gastrointestinal diseases[4], and diabetes mellitus[5].

Recent studies have shown that intestinal microcirculatory dysfunction is characterized by nutritive perfusion failure, inflammatory cell responses, surges in proinflammatory mediators, and breakdown of epithelial barrier function, as well as bacterial translocation and the development of systemic inflammatory responses[6-8]. Notably, there is widespread consensus that ischemic injury and severe microcirculatory dysfunction in the highly vascularized gut are significant sources of multiple organ dysfunction and even death[9,10]. Moreover, the intestinal microcirculation behaves as an isolated area in patients with postoperative abdominal sepsis[11], suggesting that the intestinal microcirculation does not always correlate with systemic hemodynamic variables (for example, blood pressure)[12] in gastrointestinal diseases. Therefore, it is rational to have a comprehensive scenario that depicting the functional status of intestinal microcirculation in discussing the specific issues. However, there have been few attempts to systematically assess the scientific findings and current networks in this field from a worldwide perspective.

Bibliometrics analyzes the quantitative relationships, distribution structure, and cocitation patterns of publications using mathematical and statistical methods, revealing the disciplinary development direction and research dynamics of related fields and illustrating the key paths and knowledge nodes of disciplinary field evolution[13]. This study provided a bibliometric analysis of the research process and important literature related to the intestinal microcirculation over the last 22 years to provide information for future research on the intestinal microcirculation.

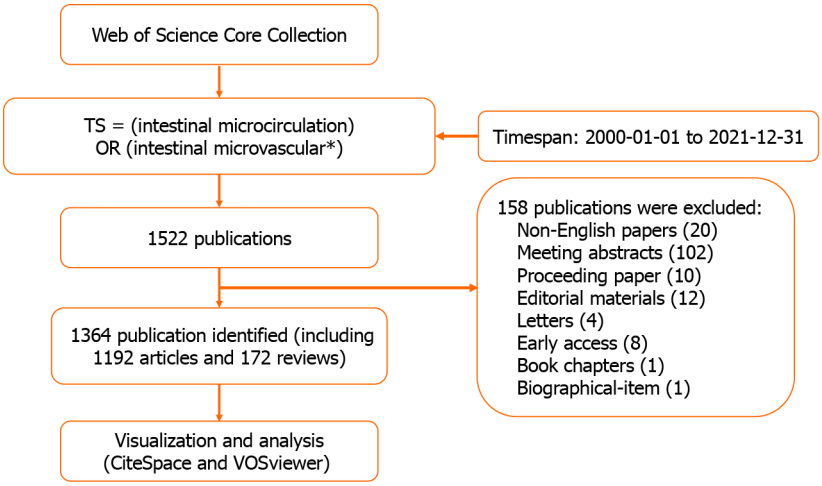

DOI: 10.3748/wjg.v29.i9.1523

Figure 1 The flow chart for the search and selection strategy of the study.

MATERIALS AND METHODS

Search strategies

The literature data for this study were retrieved from Clarivate Analytics' Web of Science Core Collection (WOSCC). The key topic for retrieval was TS = (intestinal microcirculation) OR (intestinal microvascular*). The timespan was limited from January 1, 2000 to December 31, 2021. The data were obtained within one day to avoid any potential discrepancies due to daily updates of the database. Only English-language original articles and reviews were selected. Consequently, a total of 1364 publications, comprising 1192 articles and 172 reviews, were retrieved, and each literature record included relevant information such as title, author, keywords, abstract, year, organization, and citation. A summary of the search and selection methodology for the study can be found in Figure 1.

Data analysis and visualization

In this current study, CiteSpace 6.1.R2 (https://citespace.podia.com) was adopted to map cooperation networks (institutions) and document cocitation clustering, and keyword clustering. The set of parameters was as follows: The time slice was set to one year for articles published from 2000 to 2021, and the node types were "institution", "reference", and "keyword", with a g-index k value of 25. Different parameters were set following different node types, and the visualization map was drawn.

VOSviewer (1.6.18) (www.vosviewer.com) was used to identify and illustrate the co-occurring countries/regions, cocitation analysis of journals and references, and analysis of keyword co-occurrence. The screening condition and thresholds were as follows: The counting method was set as "Full counting" with a minimum number of 5 and a maximum of 1000 items.

RESULTS

Characteristics and trends of publications

The annual publication trend reflects the development level of intestinal microcirculatory research[14]. From 2000 to 2021, a total of 1364 intestinal microcirculation-related articles met the retrieval standard. Subsequently, we illustrated the article counts per year with a histogram. According to Figure 2, the annual number of relevant publications was rather consistent, with a mean of 65 publications, indicating sustained attention from 2000-2021. Although articles accounted for most of the literature, there was a considerable increase in reviews from 2019-2021, indicating a growing interest in the intestinal microcirculation.

Contributions by countries/regions and institutions

The number of papers published by research groups according to country/region and institution can reflect the distribution of research forces in the field of intestinal microcirculatory research. In Table 1, the top 10 countries and institutions were ranked based on the number of publications related to the intestinal microcirculation. With 420 publications accounting for 30.79% of the total, the United States was the top-producing nation, followed by Germany (231, 16.94%) and China (164, 12.02%). The co-occurrence map demonstrated that the United States attached great importance to cooperation and worked closely with Germany, England, Canada, and other European countries (Figure 3). In addition,

Table 1 The top 10 countries and institutions contributed to publications on intestinal microcirculation

Rank	Country	Count	Institution	Count
1	United States	420	Dalhousie Univ	41
2	Germany	231	Univ Szeged	35
3	China	164	Univ Amsterdam	33
4	Japan	113	Louisiana State Univ	31
5	England	77	Med Coll Wisconsin	29
6	Canada	69	Univ Louisville	29
7	Italy	67	Univ Munster	23
8	Netherlands	63	Univ Sao Paulo	23
9	France	51	China Agr Univ	20
10	Sweden	47	Lund Univ	20

Table 2 The top 10 journals and cited journals of intestinal microcirculation research

Rank	Journal	Count	Cited-journal	Count
1	*Shock*	53	*Nature Reviews Microbiology*	2930
2	*Journal of Surgical Research*	37	*Clinical Microbiology Reviews*	1533
3	*World Journal of Gastroenterology*	36	*Journal of Pathology*	1520
4	*American Journal of Physiology-Gastrointestinal and Liver Physiology*	34	*Critical Care Medicine*	1499
5	*Critical Care Medicine*	34	*Gastroenterology*	1372
6	*Clinical Hemorheology and Microcirculation*	27	*American Journal of Physiology-Gastrointestinal and Liver Physiology*	1175
7	*Microcirculation*	20	*World Journal of Gastroenterology*	1126
8	*Microvascular Research*	95	*Science*	968
9	*Plos One*	73	*Shock*	965
10	*American Journal of Physiology-Heart and Circulatory Physiology*	70	*Journal of Immunology*	937

colleges and universities were the major sources of intestinal microcirculatory research. Dalhousie University was identified as the most productive scientific institution, with the most papers (41), followed by the University of Szeged (35) and the University of Amsterdam (33). These findings highlighted useful information on prominent research teams and established collaborative ties.

Analysis of journals and cited journals

Table 2 lists the top 10 most prolific journals and most-cited journals. *Shock* (53) published the most papers about the intestinal microcirculation, followed by the *Journal of Pathology* (37), and the *World Journal of Gastroenterology* (36). *Nature Reviews Microbiology* had the highest number of local citations (2930 local citations) in the field, *Clinical Microbiology Reviews* was the second-cited journal (1533 local citations) and the *Journal of Pathology* (1520 local citations) was the third. Additionally, a dual-map overlay of journals with four colored pathways was established to reflect the disciplinary distribution of academic journals (Figure 4). Most clusters of citing and cited journals are located in medicine, clinical, molecular, biology, and immunology.

Analysis of co-cited references

The landmark literature and the rapid development of this field can be clarified through the cocitation analysis of relevant publications[15]. We then established the co-cited reference network map (Figure 5A), and through cluster analysis, similar references were categorized into knowledge units (Figure 5B). Additionally, the modularity value (Q value) and the mean silhouette value (S value) were used to evaluate the effect of the literature cocitation mapping.

With more than 5000 references cited in the last 22 years, the top 10 most cited articles about the intestinal microcirculation are listed in Table 3. (Binion DG, 1997), which had a citation count of 65, was

Table 3 Top 10 highly cited publications in intestinal microcirculation

Rank	Title	Citations	Journal	First author	Published year
1	Enhanced Leukocyte Binding by Intestinal Microvascular Endothelial Cells in Inflammatory Bowel Disease	65	*Gastroenterology*	David G. Binion	1997
2	Intestinal mucosal lesion in low-flow states	62	*Archives of Surgery*	Chu-Jeng Chiu	1970
3	The microcirculation is the motor of sepsis	49	*Critical care*	Can Ince	2005
4	Microvascular Blood Flow Is Altered in Patients with Sepsis	46	*American Journal of Respiratory and Critical Care Medicine*	Daniel De Backer	2002
5	How to evaluate the microcirculation: report of a round table conference	45	*Critical care*	Daniel De Backer	2007
6	Preparation of rat intestinal muscle and mucosa for quantitative microcirculatory studies	43	*Microcirculation research*	H.Glenn Bohlen	1976
7	Persistent microcirculatory alterations are associated with organ failure and death in patients with septic shock	42	*Critical care medicine*	Yasser Sakr	2004
8	Microcirculatory oxygenation and shunting in sepsis and shock	34	*Critical care medicine*	Can Ince	1999
9	Angiogenesis as a Novel Component of Inflammatory Bowel Disease Pathogenesis	32	*Gastroenterology*	Silvio Danese	2006
10	Ischemia–Reperfusion Injury of the Intestine and Protective Strategies Against Injury	32	*Digestive Diseases and Sciences*	Ismail Hameed Mallick	2004

Table 4 Top 10 keywords in terms of frequency

Rank	Frequency	Centrality	Keywords
1	136	0.05	Expression
2	136	0.04	Nitric oxide
3	134	0.06	Blood flow
4	109	0.05	Rat
5	106	0.03	Injury
6	100	0.04	Microvascular endothelial cell
7	100	0.08	Inflammatory bowel disease
8	92	0.06	Microcirculation
9	85	0.08	Sepsis
10	85	0.05	Septic shock

the top-ranked article. (Chiu CJ, 1970), with 62 citations, and (Ince C, 2005), with 49 citations, followed. Moreover, 9 clusters were identified for mitochondrial respiration, sepsis, tissue oxygen tension, ischemia-reperfusion injury, hemorrhagic shock, endothelium, adenosine 5-triphosphate, gut, and no-reflow. The Q value of the clustering map was 0.9342, and the S value was 0.9579, confirming that the structured network was well mapped and that the clustering results were effective and reliable.

Analysis of keywords

Keywords refer to a high-level overview and refinement of the study topic and article content[16]. In terms of frequency, the top 10 keywords in the intestinal microcirculatory research from 2000 to 2021 were determined by creating a graphical map of keyword co-occurrence (Figure 6A and Table 4). The top keywords were "expression", "nitric oxide", "blood flow", "rat", "injury", "microvascular endothelial cell", "inflammatory bowel disease", "microcirculation", "sepsis" and "sepsis shock". Clustering analysis was carried out based on the above results and the following 10 clusters were identified (Figure 6B), which represented the key research areas. Specifically, the clusters "nitric oxide", "Shiga toxin" and "alkaline phosphatase" explored the mechanisms and pathological basis of damage to the intestinal microcirculation; the clusters "septic shock" and "inflammatory bowel disease" were diseases related to the intestinal microcirculation; the cluster "intravital microscopy" represented an effective measurement technique; and the clusters "cytokine therapy" and "negative pressure wound

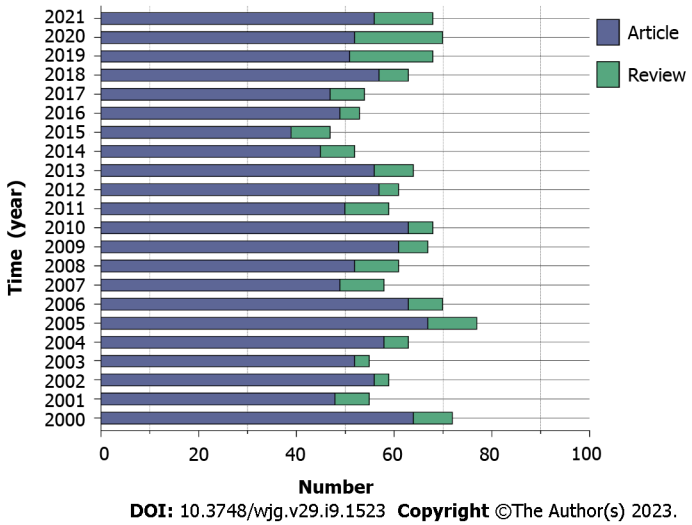

DOI: 10.3748/wjg.v29.i9.1523 **Copyright** ©The Author(s) 2023.

Figure 2 Distribution of articles published in the intestinal microcirculatory research from 2000 to 2021. The chart showed trends in annual publishing during the previous 22 years. Purple bars represent the number of articles related to intestinal microcirculation per year, while green bars represent the number of reviews.

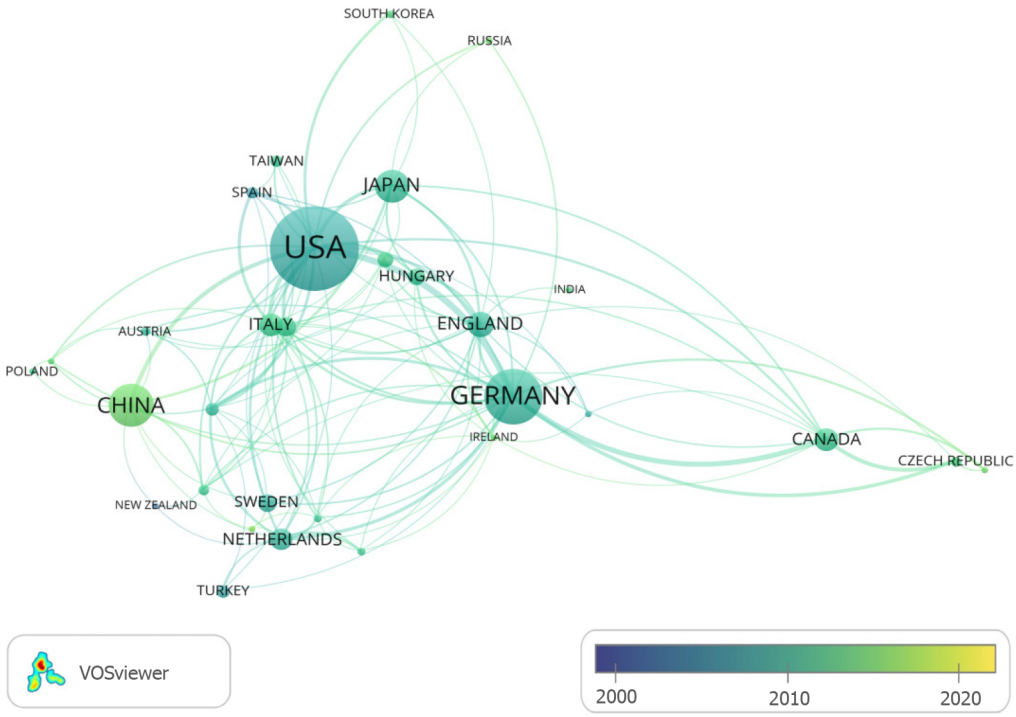

DOI: 10.3748/wjg.v29.i9.1523 **Copyright** ©The Author(s) 2023.

Figure 3 The network of countries/regions engaged in the intestinal microcirculatory research. The collaborations were generated after a minimum of five publications per country. Of the 62 countries active in this field, 32 countries meet this criterion. The size of the node represents the number of posts, and the links between the nodes represent the connection or cooperation between the countries. The transition from blue to yellow in the color bar depicts the years 2000 to 2021.

therapy" involve effective and reliable countermeasures for intestinal microcirculatory dysfunction.

Burst keywords also highlight hotspots and developing trends; hence, the detection of keywords with the fastest increase in citations (citation bursts) denotes the emerging focus in dynamic domains[17]. Our analysis revealed the top 25 keywords for the strongest citation bursts from 2000 to 2021 (Figure 7). Among them, the highest burst strength (10.34) was found for "multiple organ failure" since 2000, and also the longest-lasting burst term was "endothelial growth factor" (2007-2019). From 2000 to 2005, the mechanism tended to be more actively researched based on the main keywords "neutrophil", "adhesion", "free radical", and "platelet-activating factor". Since 2006, researchers have begun to investigate the potential correlation between clinical gut illnesses and microcirculation, with the main

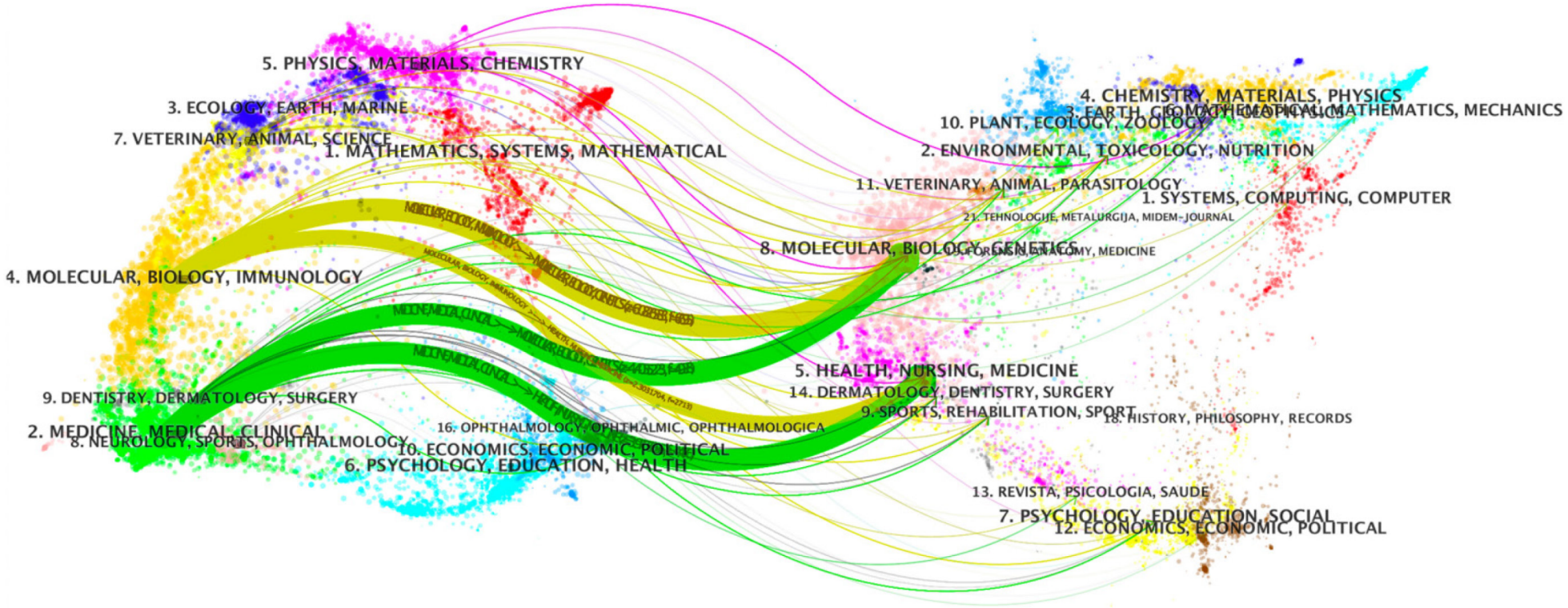

DOI: 10.3748/wjg.v29.i9.1523

Figure 4 The dual-map overlay of journals in the intestinal microcirculatory research. The left panel shows the map of citing journals while the right panel represents the map of the cited journals. The labels represent the scientific subject covered by the journals. Colored paths indicate the citation relationships, with the thicker lines representing the main pathways.

keywords being "ulcerative colitis", "Crohn's disease", and "necrotizing enterocolitis". In addition, the keyword for the most recent burst was "gut microbiota" (2019), suggesting it has been in the spotlight so far.

DISCUSSION

This study performed a scientometric analysis of publications on the intestinal microcirculation published from 2000 to 2021 using CiteSpace and VOSviewer. The findings provided insight into recent developments in global research collaborations, the most active journals, the core research areas, and emerging research areas.

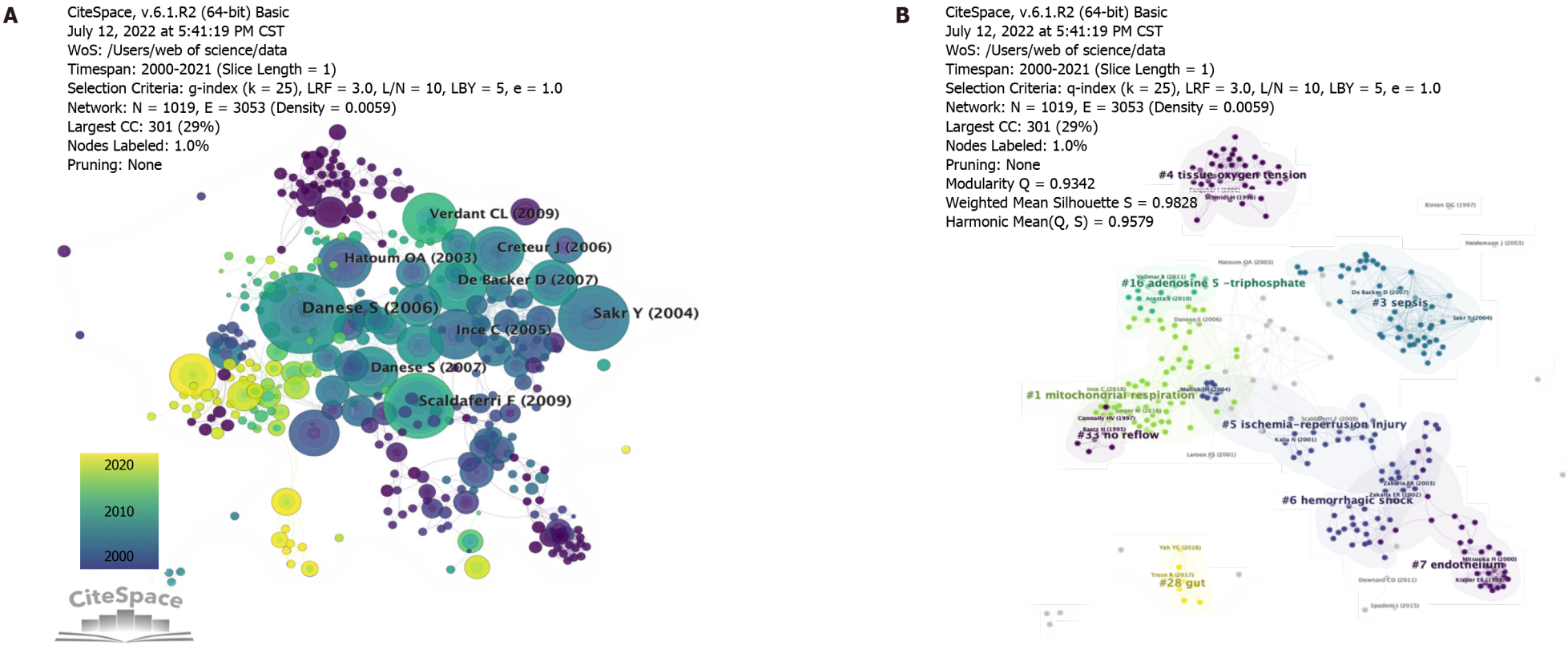

DOI: 10.3748/wjg.v29.i9.1523

Figure 5 The network map of co-cited references in the intestinal microcirculatory research. A: The network map of co-cited references. Nodes in the visualized network represent co-cited references and lines between nodes represent co-cited links; B: The network map of co-cited clusters. 9 clusters with diversified research themes were formed and illustrated in different colors. Silhouette = 0.9828. Modularity Q = 0.9342.

In total, 1364 publications about the intestinal microcirculation were extracted from WOSCC. Although the trend of annual publications from 2000 to 2021 reflected the continued interest of scholars in intestinal microcirculatory research, in comparison to research on the microcirculation of other tissues and organs, the annual number of papers on the intestinal microcirculation is relatively low, which may be associated with the technical and clinical challenges involved in the research. The United States and Germany are thriving hubs of intestinal microcirculatory research due to increased collaborations and strengthened citation links between several European countries, suggesting that a strong level of collaboration promotes academic influence.

Notably, journals focusing on clinical practice and published reviews and articles on the crucial role of the intestinal microcirculation in the progression of gastrointestinal diseases. Additionally, a dual-

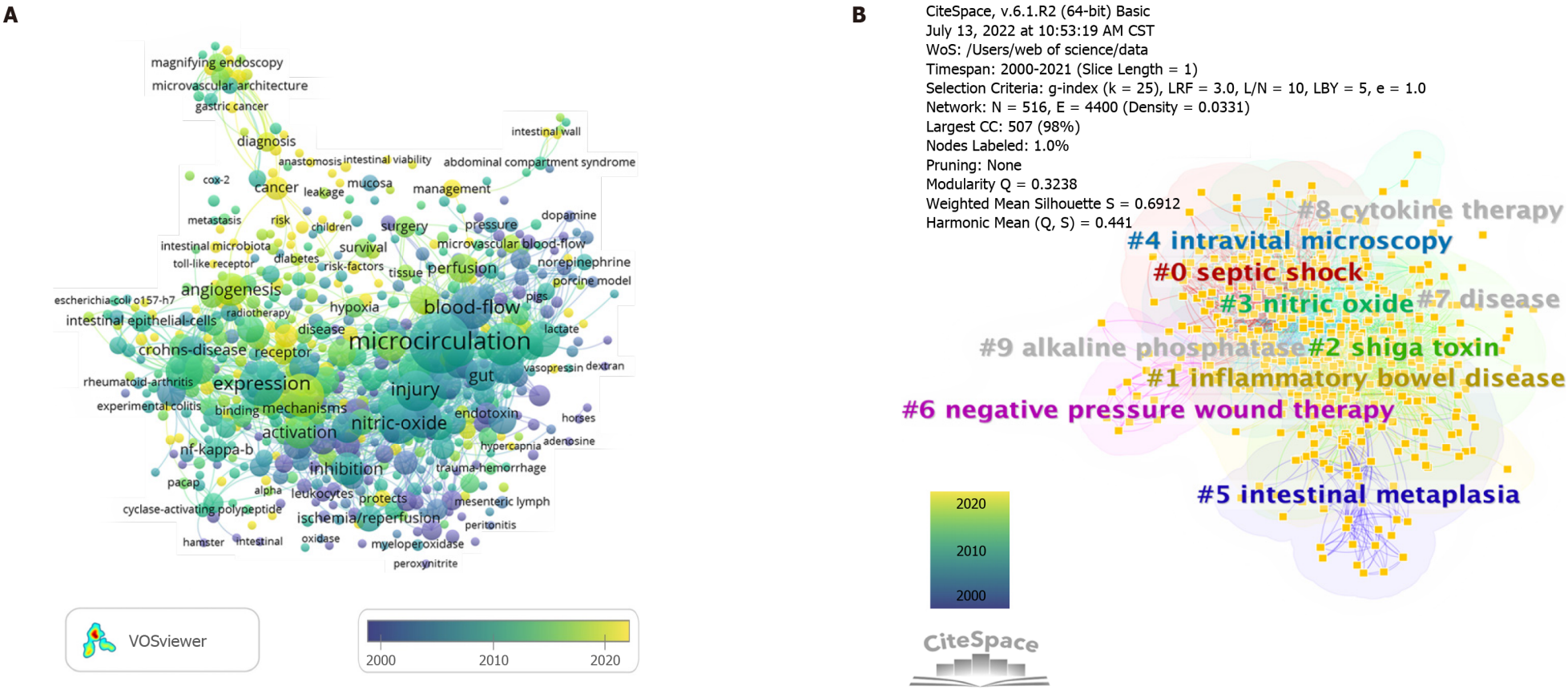

DOI: 10.3748/wjg.v29.i9.1523

Figure 6 The network map of keywords in the intestinal microcirculatory research. A: The co-occurrence map of keywords in the intestinal microcirculatory research. The graphical mapping of terms was created when setting the minimum number of keyword occurrences to 5. Of the 6607 keywords in the field, 572 reached this threshold. Each node represents a keyword, and the sizes of the node denote the number of occurrences of the keywords map. The transition from blue to yellow in the color bar depicts the years 2000 to 2021; B: The clustering map of keywords in the intestinal microcirculatory research. 10 clusters with diversified themes were formed and illustrated in different colors. Colors represent clusters of the close-working network. Silhouette = 0.3238. Modularity Q = 0.6912.

map overlay of journals demonstrated that the research was focused on basic and clinical medicine, thus, multidisciplinary efforts are needed to support the development of the intestinal microcirculatory field. Co-cited references revealed that (Binion DG, 1997), with the highest frequency of citations, was a representative reference that laid the foundation for intestinal microcirculatory mechanisms in inflammatory bowel disease. Other landmark publications such as (Ince C, 2005) and (Daniel DB, 2002), outlined mechanisms of interaction between sepsis and microcirculation. In addition, (Daniel DB, 2007)

Top 25 keywords with the strongest citation bursts

Keywords	Year	Strength	Begin	End	2000-2021
Multiple organ failure	2000	10.34	**2000**	2005	
Neutrophil	2000	8.55	**2000**	2003	
Adhesion	2000	6.77	**2000**	2003	
Intestinal ischemia reperfusion	2000	6.4	**2000**	2004	
Tumor necrosis factor	2000	4.89	**2000**	2007	
Free radical	2000	4.85	**2000**	2005	
Microvascular permeability	2000	4.85	**2000**	2005	
Platelet activating factor	2000	4.58	**2000**	2005	
P selectin	2000	4.96	**2002**	2004	
Small intestine	2000	4.35	**2003**	2005	
Endothelial cell dysfunction	2000	4.68	**2004**	2005	
Ulcerative coliti	2000	5.3	**2006**	2011	
Severe sepsis	2000	6.31	**2007**	2012	
Endothelial growth factor	2000	4.38	**2007**	2019	
Crohns disease	2000	5.29	**2008**	2011	
Intestinal metaplasia	2000	4.63	**2008**	2012	
Pathogenesis	2000	4.66	**2009**	2011	
Necrotizing enterocoliti	2000	6.62	**2011**	2019	
Management	2000	5.41	**2012**	2021	
Survival	2000	5.25	**2013**	2015	
Perfusion	2000	6.51	**2014**	2018	
Intestinal microcirculation	2000	5.35	**2015**	2021	
Cell	2000	5.75	**2017**	2021	
Inflammation	2000	5.2	**2018**	2021	
Gut microbiota	2000	5.74	**2019**	2021	

DOI: 10.3748/wjg.v29.i9.1523

Figure 7 Top 25 keywords with the strongest citation bursts. Keywords bursts identify as indicators of emerging trends in the intestinal microcirculatory field to a published article. In the burst detection, "begin" represented the year the reference began to have a citation burst, and "end" represented the year ended the citation burst. The red line is the time of duration and the "strength" is the intensity of the citation burst.

reported the results of a roundtable organized in Amsterdam, reaching a formal consensus on the acquisition and analysis of microcirculatory images. These references provided a solid theoretical foundation for future research.

Based on the analysis of keywords, we sought to identify research interests and focus related to the intestinal microcirculation. Keywords revealed by the co-occurrence map were classified into two categories: Pathophysiology-related research and clinical disease-related research, which is also consistent with the clustering of the cocitation references. The keywords "expression", "blood flow", "microvascular endothelial cell" and "nitric oxide" were associated with the pathophysiology of the intestinal microcirculation. Endothelial cell activation, hemorheological alterations, and altered vasoreactivity were just a few examples of functional and structural modifications[18-20]. Additionally, pathological situations significantly disrupted the nitric oxide (NO) system, which is essential to the autoregulatory control of microcirculatory patency and could result in pathological flow shunting. These conspicuous keywords indicated that further research on microcirculatory mechanisms is needed.

Previous research has revealed that intestinal microcirculatory dysfunction can occur early in patients with shock and sepsis[21]. Necrotizing enterocolitis and inflammatory bowel disease are included as examples resulting from the pathologic changes in the intestinal microcirculation[22]. Several studies have shown that microvascular remodeling and angiogenesis, vasodilatation microvascular dysfunction, and infiltration of immune cells play a role in the pathogenesis of inflammatory bowel disease and necrotizing enterocolitis[23-25]. Additionally, the imbalance among vascular mediators such as NO, catecholamines, and endothelin regulates neonatal intestinal vascular resistance and may influence the pathophysiology of these gut diseases[26,27]. Thus, the intestinal microcirculation as a new therapeutic target offers possibilities for treating these diseases.

Largely ignored throughout history, the intestinal microcirculation has recently been identified as the center of various pathophysiological processes. The determinants of oxygen delivery, tissue oxygen tension, blood flow regulation, and mitochondrial well-being have yet to be fully understood. The origin of intestinal microcirculatory failure in necrotizing enterocolitis and inflammatory bowel disease that is not responsive to therapy is represented by the dysfunction of the integrated intestinal microcirculation rather than systemic hemodynamic variables. Therefore, a new area of outcomes and the potential for discovering novel therapeutic targets has been made possible by introducing improved tools into clinical practice that permit the examination of integrated intestinal microcirculation. Small-molecule drugs (melatonin[28], L-citrulline[29], heparin[30], and potential vasoactive Chinese traditional medicines such as Weiqi decoction[31]), as well as novel therapeutic approaches such as remote ischemic conditioning[32] are recommended. Furthermore, research that determines whether these medicines are effective at enhancing the outcome of patients by ameliorating the intestinal microcircu-

lation should be investigated in the future.

However, our study also has certain limitations. First, this analysis was restricted to English papers in the WOSCC database which may contain fewer established articles than other databases, future research may consider embedding expanded literature databases, such as Scopus. Second, non-English literature was not included in the database or analysis, possibly resulting in linguistic source bias. Finally, bibliometric data that change over time might lead to a different conclusion. In an updated analysis, it will be necessary to follow the most recent primary studies and non-English investigations dynamically.

CONCLUSION

The intestinal microcirculation has important academic value and clinical application prospects in health and diseases. We illustrated the global developing trends, influential articles, thematic keywords, and research frontiers from 2000 to 2021 in this field. In coauthorship analyses, the patterns of scientific cooperation were found across countries/regions, institutions, and journals. Moreover, the current state and potential future directions were detected by the reference cocitation analysis, burst references, and keyword identification. We now have a deeper grasp of the pathophysiologic mechanisms underlying the intestinal microcirculation, and optimal diagnosis, prognosis assessment, and clinical therapies are the features and trends of the field. Multidisciplinary collaborations will be critical to advancing intestinal microcirculatory research.

ARTICLE HIGHLIGHTS

Research background

The intestinal microcirculation plays an important role in food absorption and metabolic substance exchange. And it is beneficial to comprehensively describe the progress of intestinal microcirculation research and provide information that may guide future research efforts.

Research motivation

Few attempts have been made to systematically assess scientific findings and current networks in the field of intestinal microcirculation. It is difficult to identify potential research hotspots or emerging research frontiers.

Research objectives

To investigate the research status, development trend, and frontier dynamics of intestinal microcirculation in the past 22 years (2000-2021).

Research methods

Based on the core literature published in the Web of Science database from 2000-2021, VOSviewer and CiteSpace 6.1.R2 were used to analyze and visualize the overall characteristics, source countries, institutions, journals, and citation frequencies of intestinal microcirculatory research.

Research results

A total of 1364 publications were included in the bibliometric analysis, showing an upward trend from 2000 to 2021. The United States and Dalhousie University ranked first among all countries and institutions. Most of the publications were released in Shock, and the most cited journal was Nature Reviews Microbiology Clinical. The topical hotspots and frontiers of intestinal microcirculation focused on the pathological processes of functional impairment on intestinal micro-vessels, diverse intestinal illnesses, and clinical treatment.

Research conclusions

Our study reveals research trends in the field of intestinal microcirculation and offers serviceable guidance to researchers by providing the prolific areas for intestinal disease research to date.

Research perspectives

Our analysis systematically assesses the scientific findings and current networks in this study of intestinal microcirculation from a worldwide perspective. Optimization of diagnosis, prognostic assessment, and clinical treatment are features and trends in this field. Multidisciplinary collaboration is essential to facilitate intestinal microcirculation research.

FOOTNOTES

Author contributions: Liu MM designed the scientometric analysis strategy; Fu SJ, Xu MT, Wang B, Li BW, Ling H, Wang Q, Liu XT, Zhang XY, and Li AL downloaded and analyzed the data; Fu SJ and Liu MM wrote the manuscript; Liu MM made critical revisions to the article for important intellectual content; All authors discussed the results and approved the final version of the manuscript.

Supported by the Beijing Municipal Natural Science Foundation, No. 7212068; and the National Natural Science Foundation of China, No. 81900747.

Conflict-of-interest statement: All the authors report no relevant conflicts of interest for this article.

PRISMA 2009 Checklist statement: The authors have read the PRISMA 2009 Checklist, and the manuscript was prepared and revised according to the PRISMA 2009 Checklist.

Country/Territory of origin: China

ORCID number: Sun-Jing Fu 0000-0002-2064-0537; Meng-Ting Xu 0000-0002-4430-1302; Bing Wang 0000-0002-7287-0852; Bing-Wei Li 0000-0002-0373-446X; Hao Ling 0000-0003-4786-6787; Yuan Li 0000-0002-0065-9038; Qin Wang 0000-0003-4575-0457; Xue-Ting Liu 0000-0002-4281-4462; Xiao-Yan Zhang 0000-0002-4725-1849; Ai-Ling Li 0000-0003-4937-4700; Ming-Ming Liu 0000-0002-6750-5068.

S-Editor: Zhang H
L-Editor: A
P-Editor: Yuan YY

REFERENCES

1 **Hasibeder W**. Gastrointestinal microcirculation: still a mystery? *Br J Anaesth* 2010; **105**: 393-396 [PMID: 20837720 DOI: 10.1093/bja/aeq236]
2 **Tang AL**, Shen MJ, Zhang GQ. Intestinal microcirculation dysfunction in sepsis: pathophysiology, clinical monitoring, and therapeutic interventions. *World J Emerg Med* 2022; **13**: 343-348 [PMID: 36119779 DOI: 10.5847/wjem.j.1920-8642.2022.031]
3 **Assimakopoulos SF**, Triantos C, Thomopoulos K, Fligou F, Maroulis I, Marangos M, Gogos CA. Gut-origin sepsis in the critically ill patient: pathophysiology and treatment. *Infection* 2018; **46**: 751-760 [PMID: 30003491 DOI: 10.1007/s15010-018-1178-5]
4 **Zhang HY**, Wang F, Feng JX. Intestinal microcirculatory dysfunction and neonatal necrotizing enterocolitis. *Chin Med J (Engl)* 2013; **126**: 1771-1778 [PMID: 23652066]
5 **Nerup N**, Ambrus R, Lindhe J, Achiam MP, Jeppesen PB, Svendsen LB. The effect of glucagon-like peptide-1 and glucagon-like peptide-2 on microcirculation: A systematic review. *Microcirculation* 2019; **26**: e12367 [PMID: 28266749 DOI: 10.1111/micc.12367]
6 **Thorburn T**, Aali M, Lehmann C. Immune response to systemic inflammation in the intestinal microcirculation. *Front Biosci (Landmark Ed)* 2018; **23**: 782-795 [PMID: 28930572 DOI: 10.2741/4616]
7 **Han JY**, Li Q, Ma ZZ, Fan JY. Effects and mechanisms of compound Chinese medicine and major ingredients on microcirculatory dysfunction and organ injury induced by ischemia/reperfusion. *Pharmacol Ther* 2017; **177**: 146-173 [PMID: 28322971 DOI: 10.1016/j.pharmthera.2017.03.005]
8 **Fan CN**, Yang SJ, Shih PY, Wang MJ, Fan SZ, Tsai JC, Sun WZ, Liu CM, Yeh YC. Comparing effects of intraoperative fluid and vasopressor infusion on intestinal microcirculation. *Sci Rep* 2020; **10**: 19856 [PMID: 33199828 DOI: 10.1038/s41598-020-76983-6]
9 **Czabanka M**, Peter C, Martin E, Walther A. Microcirculatory endothelial dysfunction during endotoxemia--insights into pathophysiology, pathologic mechanisms and clinical relevance. *Curr Vasc Pharmacol* 2007; **5**: 266-275 [PMID: 17979793 DOI: 10.2174/157016107782023389]
10 **Haussner F**, Chakraborty S, Halbgebauer R, Huber-Lang M. Challenge to the Intestinal Mucosa During Sepsis. *Front Immunol* 2019; **10**: 891 [PMID: 31114571 DOI: 10.3389/fimmu.2019.00891]
11 **Edul VS**, Ince C, Navarro N, Previgliano L, Risso-Vazquez A, Rubatto PN, Dubin A. Dissociation between sublingual and gut microcirculation in the response to a fluid challenge in postoperative patients with abdominal sepsis. *Ann Intensive Care* 2014; **4**: 39 [PMID: 25625013 DOI: 10.1186/s13613-014-0039-3]
12 **Tavy AL**, de Bruin AF, Boerma EC, Ince C, Hilty MP, Noordzij PG, Boerma D, van Iterson M. Association between serosal intestinal microcirculation and blood pressure during major abdominal surgery. *J Intensive Med* 2021; **1**: 59-64 [PMID: 36789277 DOI: 10.1016/j.jointm.2021.03.003]
13 **Cooper ID**. Bibliometrics basics. *J Med Libr Assoc* 2015; **103**: 217-218 [PMID: 26512226 DOI:

10.3163/1536-5050.103.4.013]
14 **Qin Y**, Zhang Q, Liu Y. Analysis of knowledge bases and research focuses of cerebral ischemia-reperfusion from the perspective of mapping knowledge domain. *Brain Res Bull* 2020; **156**: 15-24 [PMID: 31843561 DOI: 10.1016/j.brainresbull.2019.12.004]
15 **Zhang X**, Zhou Y, Wei N, Shou X, Fan S, You Y, Li Y, Hu Y. A Bibliometric Analysis of Heart Failure with Preserved Ejection Fraction From 2000 to 2021. *Curr Probl Cardiol* 2022; **47**: 101243 [PMID: 35545178 DOI: 10.1016/j.cpcardiol.2022.101243]
16 **Liang YD**, Li Y, Zhao J, Wang XY, Zhu HZ, Chen XH. Study of acupuncture for low back pain in recent 20 years: a bibliometric analysis *via* CiteSpace. *J Pain Res* 2017; **10**: 951-964 [PMID: 28479858 DOI: 10.2147/JPR.S132808]
17 **Luo H**, Cai Z, Huang Y, Song J, Ma Q, Yang X, Song Y. Study on Pain Catastrophizing From 2010 to 2020: A Bibliometric Analysis *via* CiteSpace. *Front Psychol* 2021; **12**: 759347 [PMID: 34975649 DOI: 10.3389/fpsyg.2021.759347]
18 **Chen Y**, Pu W, Maswikiti EP, Tao P, Li X, Wang D, Gu B, Yu Y, Gao L, Zhao C, Chen H. Intestinal congestion and reperfusion injury: damage caused to the intestinal tract and distal organs. *Biosci Rep* 2021; **41** [PMID: 34369557 DOI: 10.1042/BSR20211560]
19 **Dickson K**, Malitan H, Lehmann C. Imaging of the Intestinal Microcirculation during Acute and Chronic Inflammation. *Biology (Basel)* 2020; **9** [PMID: 33255906 DOI: 10.3390/biology9120418]
20 **Colbert JF**, Schmidt EP. Endothelial and Microcirculatory Function and Dysfunction in Sepsis. *Clin Chest Med* 2016; **37**: 263-275 [PMID: 27229643 DOI: 10.1016/j.ccm.2016.01.009]
21 **Hiltebrand LB**, Krejci V, tenHoevel ME, Banic A, Sigurdsson GH. Redistribution of microcirculatory blood flow within the intestinal wall during sepsis and general anesthesia. *Anesthesiology* 2003; **98**: 658-669 [PMID: 12606910 DOI: 10.1097/00000542-200303000-00014]
22 **Hatoum OA**, Heidemann J, Binion DG. The intestinal microvasculature as a therapeutic target in inflammatory bowel disease. *Ann N Y Acad Sci* 2006; **1072**: 78-97 [PMID: 17057192 DOI: 10.1196/annals.1326.003]
23 **Deban L**, Correale C, Vetrano S, Malesci A, Danese S. Multiple pathogenic roles of microvasculature in inflammatory bowel disease: a Jack of all trades. *Am J Pathol* 2008; **172**: 1457-1466 [PMID: 18458096 DOI: 10.2353/ajpath.2008.070593]
24 **Alkim C**, Alkim H, Koksal AR, Boga S, Sen I. Angiogenesis in Inflammatory Bowel Disease. *Int J Inflam* 2015; **2015**: 970890 [PMID: 26839731 DOI: 10.1155/2015/970890]
25 **Bowker RM**, Yan X, De Plaen IG. Intestinal microcirculation and necrotizing enterocolitis: The vascular endothelial growth factor system. *Semin Fetal Neonatal Med* 2018; **23**: 411-415 [PMID: 30213591 DOI: 10.1016/j.siny.2018.08.008]
26 **Watkins DJ**, Besner GE. The role of the intestinal microcirculation in necrotizing enterocolitis. *Semin Pediatr Surg* 2013; **22**: 83-87 [PMID: 23611611 DOI: 10.1053/j.sempedsurg.2013.01.004]
27 **Nair J**, Lakshminrusimha S. Role of NO and other vascular mediators in the etiopathogenesis of necrotizing enterocolitis. *Front Biosci (Schol Ed)* 2019; **11**: 9-28 [PMID: 30844734 DOI: 10.2741/S524]
28 **Lansink MO**, Patyk V, de Groot H, Effenberger-Neidnicht K. Melatonin reduces changes to small intestinal microvasculature during systemic inflammation. *J Surg Res* 2017; **211**: 114-125 [PMID: 28501107 DOI: 10.1016/j.jss.2016.11.055]
29 **Wijnands KA**, Vink H, Briedé JJ, van Faassen EE, Lamers WH, Buurman WA, Poeze M. Citrulline a more suitable substrate than arginine to restore NO production and the microcirculation during endotoxemia. *PLoS One* 2012; **7**: e37439 [PMID: 22666356 DOI: 10.1371/journal.pone.0037439]
30 **Zhu C**, Liang Y, Liu Y, Shu W, Luan Z, Ma X. Unfractionated Heparin Protects Microcirculation in Endotoxemic Rats by Antagonizing Histones. *J Surg Res* 2023; **282**: 84-92 [PMID: 36257167 DOI: 10.1016/j.jss.2022.09.019]
31 **Yin J**, Yi J, Yang C, Xu B, Lin J, Hu H, Wu X, Shi H, Fei X. Weiqi Decoction Attenuated Chronic Atrophic Gastritis with Precancerous Lesion through Regulating Microcirculation Disturbance and HIF-1α Signaling Pathway. *Evid Based Complement Alternat Med* 2019; **2019**: 2651037 [PMID: 31320912 DOI: 10.1155/2019/2651037]
32 **Koike Y**, Li B, Ganji N, Zhu H, Miyake H, Chen Y, Lee C, Janssen Lok M, Zozaya C, Lau E, Lee D, Chusilp S, Zhang Z, Yamoto M, Wu RY, Inoue M, Uchida K, Kusunoki M, Delgado-Olguin P, Mertens L, Daneman A, Eaton S, Sherman PM, Pierro A. Remote ischemic conditioning counteracts the intestinal damage of necrotizing enterocolitis by improving intestinal microcirculation. *Nat Commun* 2020; **11**: 4950 [PMID: 33009377 DOI: 10.1038/s41467-020-18750-9]

World Journal of Gastroenterology

Submit a Manuscript: https://www.f6publishing.com

World J Gastroenterol 2023 March 7; 29(9): 1536-1538

DOI: 10.3748/wjg.v29.i9.1536

ISSN 1007-9327 (print) ISSN 2219-2840 (online)

LETTER TO THE EDITOR

Thiopurines are an independent risk factor for active tuberculosis in inflammatory bowel disease patients

Flora Maria Lorenzo Fortes, Raquel Rocha, Genoile Oliveira Santana

Specialty type: Gastroenterology and hepatology

Provenance and peer review: Unsolicited article; Externally peer reviewed.

Peer-review model: Single blind

Peer-review report's scientific quality classification

Grade A (Excellent): 0
Grade B (Very good): 0
Grade C (Good): C, C, C
Grade D (Fair): 0
Grade E (Poor): 0

P-Reviewer: Oley MH, Indonesia; Wang LH, China; Zharikov YO, Russia

Received: November 21, 2022
Peer-review started: November 21, 2022
First decision: December 10, 2022
Revised: January 5, 2023
Accepted: February 22, 2023
Article in press: February 22, 2023
Published online: March 7, 2023

Flora Maria Lorenzo Fortes, Genoile Oliveira Santana, Ciências da Vida, Universidade do Estado da Bahia, Salvador 41150000, Brazil, and Programa de Pós-Graduação em Medicina e Saúde, Universidade Federal da Bahia, Salvador 40110060, Brazil

Raquel Rocha, Ciência da Nutrição, Universidade Federal da Bahia, Salvador 40110160, Brazil

Corresponding author: Raquel Rocha, DSc, Adjunct Associate Professor, Ciência da Nutrição, Universidade Federal da Bahia, Av Araujo Pinho, Salvador 40110160, Brazil.
raquelrocha2@yahoo.com.br

Abstract

The use of thiopurines is an independent risk factor for active tuberculosis in patients with inflammatory bowel disease.

Key Words: Tuberculosis; Inflammatory bowel disease; Thiopurines; Therapy; Risk

Core Tip: Inflammatory bowel disease (IBD) patients recommended for anti-tumor necrosis factor (anti-TNF) therapy need to be tested for latent tuberculosis (TB) prior to treatment. Azathioprine monotherapy is also an independent risk factor for active TB in patients with IBD. However, the recommendations of the Brazilian Public Health Guideline for Tuberculosis Prevention do not include patients who are receiving immunosuppressive therapy in the risk group for screening for latent TB. We evaluated 301 patients with IBD, and the use of azathioprine treatment increased the risk by 6.87-fold compared to patients without this treatment. The use of anti-TNF therapy had a 10.34-fold increased risk of TB, and the combination of both increased the risk by 17.81-fold.

Citation: Fortes FML, Rocha R, Santana GO. Thiopurines are an independent risk factor for active tuberculosis in inflammatory bowel disease patients. *World J Gastroenterol* 2023; 29(9): 1536-1538
URL: https://www.wjgnet.com/1007-9327/full/v29/i9/1536.htm
DOI: https://dx.doi.org/10.3748/wjg.v29.i9.1536

TO THE EDITOR

It is known that immunosuppression increases the risk of tuberculosis, especially in countries with a high frequency of active tuberculosis. We read with interest the article published by Fortes *et al*[1], who performed a retrospective cohort study among Inflammatory bowel disease (IBD) patients at a reference center in Brazil, which is a country with a moderate incidence of TB. A total of 301 IBD patients were evaluated; 61.8% had ulcerative colitis, and 38.2% had Crohn's disease. Twenty-seven (9.0%) patients received anti-tumor necrosis factor (anti-TNFα) as a monotherapy, 31 (10.3%) patients received anti-TNF α associated with azathioprine, 3 (1.0%) patients received anti-TNFα treatment associated with methotrexate, and 70 (23.3%) patients received only azathioprine. The use of azathioprine treatment increased the risk by 6.87-fold in comparison to patients without this treatment. The use of anti-TNF therapy showed a 10.34-fold increased risk of TB in this sample, and the association of both increased the risk to 17.81.

Advances in the treatment of IBD have been adopted worldwide. Some post marketing adverse events have been reported, including active tuberculosis (TB) during anti-TNF therapy. It has already been established that the incidence of active TB in this scenario is associated with the TB burden in the geographic region of the study. Brazil is one of the 20 countries in which TB presents a high incidence along with countries from Africa and Asia[2].

IBD patients with a recommendation for anti-TNF therapy need to test for latent TB before treatment. The TNF alpha blocking mechanism, which is critical in stabilizing granulomas during TB infection, would explain this increase in risk. An unanswered question is whether azathioprine in monotherapy is an independent risk factor for active TB in IBD patients[1,3]. A case report published by van Wijngaarden *et al*[4] already drew attention to the development of pleural tuberculosis in a patient with Crohn's disease while receiving azathioprine as the sole immunosuppressive treatment.

Considering that transplant recipients need substantial immunosuppression and azathioprine is one of the drugs used, studies among transplant recipients receiving immunosuppressive therapy helped guide physicians in the care of IBD patients. A Spanish group evaluated the risk factors for active TB after lung transplantation and concluded that the use of azathioprine was identified as an independent risk factor[5].

The recommendations of the Brazilian Public Health Guideline for Tuberculosis Prevention, reviewed in 2020, did not include patients receiving immunosuppressive therapy in the risk group for screening of latent TB[6]. However, consensus from endemic countries suggests investigation and treatment of latent TB before starting immunosuppressive therapy[7-9].

These findings suggest that in areas with a high burden of TB, the use of thiopurines is an independent risk factor for active TB in IBD patients. This evidence needs to be considered when using this therapy for these patients, especially those from countries with a high TB burden. We suggest giving attention to and treating patients with latent tuberculosis and guiding prevention with possible contacts with active tuberculosis. New studies reporting the risk of active TB among IBD patients receiving immunosuppressive therapy from countries with different incidence rates of TB are needed.

FOOTNOTES

Author contributions: Fortes FML designed the study and performed the data analysis; Rocha R reviewed the manuscript and provided technical and material support; and Santana GO contributed to the study design, manuscript revision, supervision of the study, had full access to all of the data in the study and was responsible for the integrity of the data.

Conflict-of-interest statement: Genoile O Santana is on the Advisory Board for Janssen; has received speaking fees from Abbvie, Ferring, Janssen, Takeda, Pfizer and UCB Pharma; and has received research grants from Janssen, Lilly, Pfizer, Roche and Takeda. The other authors declare that they have no conflicts of interest.

Country/Territory of origin: Brazil

ORCID number: Flora Maria Lorenzo Fortes 0000-0002-9897-5337; Raquel Rocha 0000-0002-2687-2080; Genoile Oliveira Santana 0000-0001-5936-9791.

S-Editor: Liu GL
L-Editor: A
P-Editor: Liu GL

REFERENCES

1 **Fortes FML**, Sorte NB, Mariano VD, Andrade LD, Oliveira FA, Santos MC, Dos Santos CIN, Passos CA, Pacheco MP, Surlo VC, de Almeida NP, Fontes JA, Pimentel AM, Rocha R, Santana GO. Active tuberculosis in inflammatory bowel disease patients under treatment from an endemic area in Latin America. *World J Gastroenterol* 2020; **26**: 6993-7004 [PMID: 33311945 DOI: 10.3748/wjg.v26.i44.6993]

2 **Kedia S**, Mouli VP, Kamat N, Sankar J, Ananthakrishnan A, Makharia G, Ahuja V. Risk of Tuberculosis in Patients With Inflammatory Bowel Disease on Infliximab or Adalimumab Is Dependent on the Local Disease Burden of Tuberculosis: A Systematic Review and Meta-Analysis. *Am J Gastroenterol* 2020; **115**: 340-349 [PMID: 32032073 DOI: 10.14309/ajg.0000000000000527]

3 **Banerjee R**, Ali RAR, Wei SC, Adsul S. Biologics for the Management of Inflammatory Bowel Disease: A Review in Tuberculosis-Endemic Countries. *Gut Liver* 2020; **14**: 685-698 [PMID: 33191310 DOI: 10.5009/gnl19209]

4 **van Wijngaarden P**, Meijssen MA. Tuberculous pleurisy: an unusual complication during treatment of Crohn disease with azathioprine. *Scand J Gastroenterol* 2001; **36**: 1004-1007 [PMID: 11521975 DOI: 10.1080/003655201750305567]

5 **Guirao-Arrabal E**, Santos F, Redel-Montero J, Vaquero JM, Cantisán S, Vidal E, Torre-Giménez Á, Rivero A, Torre-Cisneros J. Risk of tuberculosis after lung transplantation: the value of pretransplant chest computed tomography and the impact of mTOR inhibitors and azathioprine use. *Transpl Infect Dis* 2016; **18**: 512-519 [PMID: 27224905 DOI: 10.1111/tid.12555]

6 **Brazil**. Ministry of Health. Secretary of Health Surveillance. Department of Communicable Disease Surveillance. Epidemiological Bulletin Special Number -Tuberculosis 2020. Available from: https://www.gov.br/saude/pt-br/centrais-de-conteudo/publicacoes/boletins/epidemiologicos/especiais/2020/boletim-tuberculose-2020-marcas-1.pdf/view

7 **Kucharzik T**, Ellul P, Greuter T, Rahier JF, Verstockt B, Abreu C, Albuquerque A, Allocca M, Esteve M, Farraye FA, Gordon H, Karmiris K, Kopylov U, Kirchgesner J, MacMahon E, Magro F, Maaser C, de Ridder L, Taxonera C, Toruner M, Tremblay L, Scharl M, Viget N, Zabana Y, Vavricka S. ECCO Guidelines on the Prevention, Diagnosis, and Management of Infections in Inflammatory Bowel Disease. *J Crohns Colitis* 2021; **15**: 879-913 [PMID: 33730753 DOI: 10.1093/ecco-jcc/jjab052]

8 **Park DI**, Hisamatsu T, Chen M, Ng SC, Ooi CJ, Wei SC, Banerjee R, Hilmi IN, Jeen YT, Han DS, Kim HJ, Ran Z, Wu K, Qian J, Hu PJ, Matsuoka K, Andoh A, Suzuki Y, Sugano K, Watanabe M, Hibi T, Puri AS, Yang SK. Asian Organization for Crohn's and Colitis and Asia Pacific Association of Gastroenterology consensus on tuberculosis infection in patients with inflammatory bowel disease receiving anti-tumor necrosis factor treatment. Part 1: risk assessment. *Intest Res* 2018; **16**: 4-16 [PMID: 29422793 DOI: 10.5217/ir.2018.16.1.4]

9 **Ran Z**, Wu K, Matsuoka K, Jeen YT, Wei SC, Ahuja V, Chen M, Hu PJ, Andoh A, Kim HJ, Yang SK, Watanabe M, Ng SC, Hibi T, Hilmi IN, Suzuki Y, Han DS, Leung WK, Sollano J, Ooi CJ, Qian J. Asian Organization for Crohn's and Colitis and Asia Pacific Association of Gastroenterology practice recommendations for medical management and monitoring of inflammatory bowel disease in Asia. *J Gastroenterol Hepatol* 2021; **36**: 637-645 [PMID: 32672839 DOI: 10.1111/jgh.15185]

Published by **Baishideng Publishing Group Inc**
7041 Koll Center Parkway, Suite 160, Pleasanton, CA 94566, USA
Telephone: +1-925-3991568
E-mail: bpgoffice@wjgnet.com
Help Desk: https://www.f6publishing.com/helpdesk
https://www.wjgnet.com